

Design and Synthesis of Selective Estrogen Receptor β Agonists and Their Pharmacology

K. L. Iresha Sampathi Perera
Marquette University

Recommended Citation

Perera, K. L. Iresha Sampathi, "Design and Synthesis of Selective Estrogen Receptor β Agonists and Their Pharmacology" (2017).
Dissertations (2009 -). 735.
https://epublications.marquette.edu/dissertations_mu/735

**DESIGN AND SYNTHESIS OF SELECTIVE ESTROGEN RECEPTOR β
AGONISTS AND THEIR PHARMACOLOGY**

by

K. L. Iresha Sampathi Perera, B.Sc. (Hons), M.Sc.

A Dissertation Submitted to the Faculty of the Graduate School,
Marquette University,
in Partial Fulfillment of the Requirements for
the Degree of Doctor of Philosophy

Milwaukee, Wisconsin

August 2017

ABSTRACT
DESIGN AND SYNTHESIS OF SELECTIVE ESTROGEN RECEPTOR β
AGONISTS AND THEIR PHARMACOLOGY

K. L. Iresha Sampathi Perera, B.Sc. (Hons), M.Sc.

Marquette University, 2017

Estrogens (17 β -estradiol, E2) have garnered considerable attention in influencing cognitive process in relation to phases of the menstrual cycle, aging and menopausal symptoms. However, hormone replacement therapy can have deleterious effects leading to breast and endometrial cancer, predominantly mediated by estrogen receptor-alpha (ER α) the major isoform present in the mammary gland and uterus. Further evidence supports a dominant role of estrogen receptor-beta (ER β) for improved cognitive effects such as enhanced hippocampal signaling and memory consolidation via estrogen activated signaling cascades.

Creation of the ER β selective ligands is challenging due to high structural similarity of both receptors. Thus far, several ER β selective agonists have been developed, however, none of these have made it to clinical use due to their lower selectivity or considerable side effects. The research in this dissertation involved the design of non-steroidal ER β selective agonists for hippocampal memory consolidation. The step-wise process to achieve the ultimate goal of this research includes: (1) design and synthesis of (4-hydroxyphenyl)cyclohexyl or cycloheptyl derivatives, (2) *in vitro* biological evaluation of synthesized compounds to identify highly potent and selective candidates, and (3) *in vivo* biological evaluation of selected candidates for hippocampal memory consolidation.

Several (4-hydroxyphenyl)cyclohexyl or cycloheptyl derivatives were synthesized having structural alterations on both aromatic and cyclohexyl/heptyl ring scaffolds. ER β agonist potency was initially evaluated in TR-FRET ER β ligand binding assay and compounds having high potency were re-evaluated in functional cell based assays for potency and ER β vs. ER α selectivity. Two compounds from each series, ISP 163-PK4 and ISP 358-2 were identified as most selective ER β agonists. Both compounds revealed high metabolic stability, solubility and no cross reactivity towards other nuclear receptors. *In vivo* efficiency of ISP 358-2 was evaluated in ovariectomized mice (C57BL/6) with object recognition (OR) and object placement (OP) tasks. The results indicate improved memory consolidation at 100 pg/ hemisphere and 0.5 mg/Kg via DH infusion and IP injection respectively. The information learned from this project serves as a foundation for development of other cycloheptyl/hexyl based ER β agonists or antagonists having acceptable pharmacological profiles.

ACKNOWLEDGMENTS

K. L. Iresha Sampathi Perera, B.Sc. (Hons), M.Sc.

Since my journey as a PhD candidate is coming to an end, it is time to reminisce the people who stood by me along the way. This is my sincere gratitude to those wonderful souls, who helped in making my story a success.

I am ever grateful to my advisor Professor William A. Donaldson for the wonderful opportunity he gave me to join his research group. I can't thank him enough for his valuable guidance and input during the whole course my research which improved me as a researcher in leaps and bounds. The most special aspect was the faith he showed in me during my research to achieve the results and the kind motivating words whenever I found myself challenged. I haven't got enough words to thank him for being the motivator and mentor in bringing my research to a high-quality level. I could not have imagined having a better advisor for my Ph.D. study. Thank you again for your amazing support.

I would like to thank the rest of my dissertation committee: Prof. Daniel Sem, Prof. James Kincaid and Dr. Christopher Dockendorff for their valuable time and effort in reviewing my dissertation. Further, their insightful comments during the committee meetings incited me to widen my research from various perspectives. Additionally, Dr. Christopher Dockendorff deserves a special mention on granting me access to their laboratory facilities which helped me immensely throughout my research.

I am also very much thankful to Professor Daniel Sem, Professor Karyn Frick for the fantastic opportunity to work with them on an interesting project. I gained invaluable research experience from the monthly meetings I attended and the insightful suggestions and comments undoubtedly helped me to improve my research work. I also would like to mention Alicia Schulz and Jaekyoon Kim for their support during the collaboration. Thank you for giving me the opportunity to be a part of a fantastic team of researchers.

I am also grateful to Department of Chemistry for providing me unrestricted facilities during my stay as a graduate student. I would like to convey my sincere gratitude to Dr. Sergey Lindeman and Dr. Sheng Cai for helping me with X-ray crystallographic and NMR studies. I would like to mention, Dr. Sandra Lukaszewski-Rose for the support she rendered to me during my tenure as a teaching assistant. I will always fondly remember the numerous functions you organized for students and the enjoyment I had. My acknowledgement would be incomplete without a word on Mr. Mark Bartelt. I am utterly grateful to him for all the technical supports on my research work.

A very special mention to Prof. Isiah Warner at Louisiana State University for helping me in during my masters. I can't thank you enough for the support you gave me during my time at Louisiana State University. Your encouraging words made me stronger to believe in myself and pursue my goals. Also, I would like to thank Prof. Chieu D. Tran, who was my first advisor at Marquette for his valuable guidance and help. I would also like to pay gratitude to the Chemistry department at University of Colombo where I took first steps as a researcher during my bachelors. I should specially thank my undergraduate thesis advisor Prof. Ramani Wijesekara for her immense help and guidance.

I thank all past and present members of Donaldson and Dockendorff groups for their invaluable support. The groups have been a source of friendship as well as good advice. I wish all of you success in all your endeavors.

Many thanks to Dr. Ajith Wijenayake and his family who helped me immensely when I moved to Milwaukee and my friends in Milwaukee for supporting me at all times. Further, to all my friends in Sri Lanka, U.S. and all around the world; I appreciate your encouragement and love I received. I love you all.

Most importantly, my family was with me at every step of the way in this long journey. My Father Ariyasena Perera and My mother Hema Jayakody were the two pillars of strength whenever I was challenged. Their unconditional love made me stronger to thrive in what I do. I thank to my in-laws, especially my father in-law Mr. Jinadasa Nanayakkara for his encouragement. My brother and his family, my aunties, and my relatives for their lovely support. Finally, my loving husband Muditha Nanayakkara who listened, believed and taught me to be strong and being there for me whenever I needed the most. I love you so much.

DEDICATION

*This dissertation is dedicated
with love to*

*My parents Hema and Ariyasena Perera
My brother Erandha Perera
My aunt Buddhi Jayakody*

and

My loving husband Muditha Nanayakkara

for supporting, encouraging and believing me in all endeavors.....

TABLE OF CONTENTS

ACKNOWLEDGEMENT.....	i
DEDICATION.....	iv
LIST OF TABLES.....	viii
LIST OF FIGURES.....	ix
LIST OF SCHEMES	xii
LIST OF ABBREVIATIONS AND SYMBOLS.....	xiv
CHAPTER 1. Background and Goals of Research.....	1
1.1 Discovery of Estrogen Receptors.....	1
1.2 Estrogen Receptors and Human Disease.....	2
1.2.1 Estradiol, the Hippocampus and Memory.....	5
1.2.2 Estrogen Decrease in Menopause and Hormone Replacement Therapy.....	9
1.3 Estrogen Receptor Structure and Mechanism of Action.....	11
1.4 Important Interactions within the Ligand Binding Domain.....	15
1.5 Estrogen Receptor – Agonists, Antagonist and Selective Estrogen Receptor Modulators.....	17
1.6 Review of ER β Subtype Selective Ligands.....	23
1.6.1 Design of Non-Steroidal ER β Selective Agonists.....	24
1.7 Design of 4-Cyclohexyl or Cycloheptyl Phenolic Derivatives as Selective ER β Agonists.....	31

CHAPTER 2. Development of 4-(4-hydroxyphenyl)cycloheptanemethanol and Analogues.....	35
2.1 Background and 1 st Generation Synthesis of 4-(4-(hydroxyphenyl)cycloheptanemethanol.....	35
2.2 2 nd Generation Synthesis of 4-(4-hydroxyphenyl)cycloheptanemethanol.....	36
2.3 3 rd Generation Synthesis of 4-(4-hydroxyphenyl)cycloheptanemethanol.....	43
2.4 4 th Generation Synthesis of 4-(4-hydroxyphenyl)cycloheptanemethanol.....	46
2.5 Separation of Stereoisomers of 4-(4-(hydroxyphenyl)cycloheptane methanol.....	47
2.6 Synthesis of Other 4-Cycloheptylphenol Analogues for SAR Studies.....	54
CHAPTER 3. Development of 4-(4-(Hydroxymethyl)cyclohexyl)phenol and Analogues.....	60
3.1 Synthesis of 4-[4-(hydroxymethyl)cyclohexyl]phenol.....	60
3.2 Synthesis of 4-Cyclohexylphenol Analogs.....	66
3.3 Synthesis of Fluorine Containing 4-Cyclohexylphenol Analogs.....	71
CHAPTER 4. Biological Evaluation of ER β Selective Compounds.....	77
4.1 <i>In vitro</i> and <i>In vivo</i> Biological Evaluation –Assay Summary.....	77
4.2 Description of <i>In vitro</i> Assays and Results.....	78
4.2.1 TR-FRET ER β Binding Assay.....	78
4.2.2 ER α and ER β Cell-Based Assay.....	79
4.2.3 TR-FRET Results for 4-[4-(hydroxymethyl)cyclohexyl]phenol and its Analogs.....	81
4.2.4 Cell-based Functional Assay Results for Selected 4-[4-(hydroxymethyl)cyclohexyl]phenol Analogs.....	85
4.2.5 TR-FRET and Cell-based Assay Results for 4-[4-(hydroxymethyl)cycloheptyl]phenol and Analogs.....	87
4.2.6 TR-FRET and Cell-based Assay of the Stereoisomers of 4-[4-(hydroxymethyl)-cycloheptyl]phenol.....	90

4.2.7 CYP450 Assay and Results for ISP358-2 and ISP163.....	92
4.2.8 hERG Assay results for ISP358-2.....	94
4.2.9 Nuclear Receptor Panel Screening.....	95
4.3 Description of <i>In vivo</i> Assays and Results.....	96
4.3.1 Assessment of Memory Consolidation in Ovariectomized Mice...96	
4.3.2 Assessment of Memory Consolidation by Dorsal Hippocampal Infusion.....	98
4.3.3 Assessment of Memory Consolidation by Intraperitoneal Administration.....	99
CHAPTER 5. Conclusion and Outlook.....	101
5.1 Summary.....	101
5.2 Conclusion.....	104
5.3 Outlook.....	104
CHAPTER 6. Synthesis and Characterization.....	107
6.1 Chemicals and General Methods.....	107
6.2 Experimental Details.....	107
REFERENCES.....	183
APPENDIX.....	195
VITA.....	219

LIST OF TABLES

Table 1.1:	Classification of SERMs (Adapted from Selective Estrogen Receptor Modulators, Cano, et. al, Springer, 2006, pg 51).....	21
Table 4.1:	TR-FRET ER β binding data for six-membered analogs.....	83
Table 4.2:	Cell-based assay data for selected six-membered analogs and comparison to TR-FRET assay.....	86
Table 4.3:	TR-FRET ER β binding data for seven-membered analogs.....	88
Table 4.4:	TR-FRET and cell-based assay data for selected seven-and five-membered analogs.....	89
Table 4.5:	TR-FRET and cell-based assay data for ISP163 stereoisomers.....	91
Table 4.6:	CYP450 assay data for ISP358-2 and ISP163.....	94
Table 4.7:	Nuclear receptor panel screen data for ISP358-2.....	96
Table 4.8:	Nuclear receptor panel screen data for ISP163-PK4.....	96

LIST OF FIGURES

Figure 1.1: Structure of 17 β -estradiol (E2).....	2
Figure 1.2: Schematic illustration of non-classical mechanisms required for E2 and ERs to enhance hippocampal memory consolidation.....	7
Figure 1.3: Structure of ER α and ER β selective agonists.....	9
Figure 1.4: Schematic representation of structural domain of human ER α and ER β	11
Figure 1.5: Formation of Zinc fingers in DNA binding domain. (Adapted from Selective Estrogen Receptor Modulators, A. Cano, et al., Springer, 2006, pg 20).....	12
Figure 1.6: Classical mechanism action of estrogen receptor.....	14
Figure 1.7: a) classical mechanism of action. b,c,d) indirect effects of estrogen receptors on transcription activation.....	15
Figure 1.8: Principal interactions of estradiol with ER α and ER β conserved and nonconserved residues.....	16
Figure 1.9: a) The conformation of H12 of ER α due to diethylstilbestrol (agonist) binding (yellow) and tamoxifen (antagonist) binding (magenta) b) Ligand-dependent structural deviation between agonists (red) and antagonists (white) conformations.....	18
Figure 1.10: a) The binding interactions in the ER α for agonists (red) and antagonists (white) b) binding interactions in ER β for agonist (blue) and antagonist (green).....	20
Figure 1.11: Selected chemical structures of SERMs	22
Figure 1.12: Examples of natural ER β -selective agonists.....	23
Figure 1.13: a) Schematic representations of hER β -GEN complex. Helices are depicted as rods and H12 is colored in green. b) Comparison of ligand-binding mode of GEN (protein- light blue; ligand, green) in hER β -LBD and E2 (protein-red; ligand-purple) in hER α -LBD (PDB code: 1ERE) within the cavity. The ligands are viewed looking down from the β -face of the cavity and only those side chains that interact with the bound ligand or exhibit different orientations are shown. Hydrogen bonds are depicted as broken lines.....	24

Figure 1.14: Crossed stereo view of S-DPN (Panel A) and R-DPN (Panel B) docked and minimized in the ER and ER LBD Pockets, respectively. DPN and the ER β pocket residues are shown with standard atom colors, whereas in the ER α complex, DPN and the pocket residues are shown in orange.....	26
Figure 1.15: Examples of ER β selective agonists from Wyeth library.....	27
Figure 1.16: Schematic representation of ERB-041 complexed with ER α and ER β , showing key interactions within the ligand binding domain.....	28
Figure 1.17: ERB-041 binding interactions with ER α and ER β	28
Figure 1.18: Racemic unadorned and racemic all <i>cis</i> - 3,4-cyclofused- (n = 1-3) benzopyrans.....	28
Figure 1.19: Surface diagram of the X-ray structure of SERBA-1 complexed to ER α (1A) and ER β (1B).....	30
Figure 1.20: SERBA-1 binding interactions with ER α and ER β	30
Figure 1.21: Design of ACD-pseudosteroids as ER β selective agonists.....	31
Figure 1.22: Predicted binding orientation of the lead compound A) in ER β agonist conformation B) in antagonist conformation C) overlay of estradiol (black) and lead compound (yellow).....	33
Figure 2.1: Diastereomers of compound 2.5a (I and II).....	40
Figure 2.2: Identification of presence of four isomers of ISP163.....	47
Figure 2.3: Prep Chromatogram of ISP163 for a single injection (courtesy of Phenomenex).....	48
Figure 2.4: Implemented Stacked Injections for ISP163 (courtesy of Phenomenex)...	49
Figure 2.5: Analytical QC chromatograms of all four isomers of ISP163 (courtesy of Phenomenex).....	50
Figure 2.6: ¹ H NMR analysis of all four isomers of ISP163.....	51
Figure 2.7: a) ORTEP projections of the stereoisomers of trans- 4-(4-(hydroxyphenyl)cycloheptanemethanol; a) peak 3 (7R, 10S); b) peak 4 (7S, 10R); c) 3D-crystal packing of peaks 3 and 4 (identical) in solvent.....	52

Figure 2.8: a) and b) Two possible X-ray crystal structure of pk1 isomer c) 3D-crystal packing in solvent.....	53
Figure 3.1: ¹ H NMR spectra of 4-[4-(hydroxymethyl)cyclohexyl]phenol from a) produced using 9-BBN b) produced using BH ₃ .THF as hydroboration reagent (solvent = CD ₃ OD).....	64
Figure 3.2: a) X-ray crystal structure of compound 3.4b (ISP358-2) b) Crystal packing nature of compound 3.4b in solution.....	65
Figure 4.1: Simplified schematic for TR-FRET ERβ binding assay (http://slideplayer.com/slide/8532001/26/images/32/Receptor+binding+assay.jpg).....	78
Figure 4.2: TR-FRET ERβ binding profile of ISP163 isomers.....	79
Figure 4.3: Schematic representation of ERα and ERβ cell-based assay (https://www.caymanchem.com/pdfs/15739.pdf).....	80
Figure 4.4: ERβ cell-based agonist assay profile of IS163 isomers.....	80
Figure 4.5: Reported ERβ agonist 4-adamantyl phenol (AdP).....	82
Figure 4.6: ERβ cell-based assay profiles for individual ISP163 stereoisomers.....	91
Figure 4.7: Schematic diagram for basis of CYP450 assay (http://www.lumflu.com/A_Info.asp?id=36).....	92
Figure 4.8: CYP2C9 assay profile for ISP358-2.....	93
Figure 4.9: hERG profile of ISP358-2.....	95
Figure 4.10: Illustration of object placement (OP) and object recognition (OR) protocols.....	97
Figure 4.11: a) Amount of time (of 30 sec total) spent with the novel object in OR assay; b) Amount of time (of 30 sec total) spent with the novel in OP assay [DH infusion].....	99
Figure 4.12: a) Amount of time (of 30 sec total) spent with the novel object in OR assay; b) Amount of time (of 30 sec total) spent with the novel in OP assay [IP injection].....	100

LIST OF SCHEMES

Scheme 1.1: The major metabolic pathway involves initial conversion of tamoxifen to N-desmethyl-tamoxifen and 4-hydroxy-tamoxifen followed by conversion to endoxifen via CYP450s.....	3
Scheme 1.2: Mechanism of quinone formation and DNA adduction.....	10
Scheme 1.3: 1 st generation synthesis of cis-4-(4hydroxyphenyl)cycloheptane methanol [reagents: a, vinylmagnesium chloride/THF/CH ₂ Cl ₂ (57%); b, 4-acetoxystyrene (2 eq), 5% Grubbs' 1st generation catalyst (64%); c, H ₂ O ₂ /HO ⁻ , d, LiAlH ₄ , then 140°C (32%); e, H ₂ , 10% Pd/C (50%)].	32
Scheme 2.1: 1 st Generation synthesis of 4-(4-hydroxyphenyl)cycloheptanemethanol from organoiron methodology.....	36
Scheme 2.2: Retrosynthetic analysis for preparation of 4-(4-hydroxyphenyl)-1-hydroxymethylcycloheptane.....	37
Scheme 2.3: Preparation of tertiary alcohol intermediate 2.3a	38
Scheme 2.4: Mechanism of formation of compound 2.3b	38
Scheme 2.5: Ring closing metathesis and ionic reduction.....	39
Scheme 2.6: Possible mechanism for generation of 2.7 and aldehydic by-product.....	40
Scheme 2.7: Transformation of olefin 2.5 into cycloheptanone 2.7	41
Scheme 2.8: Conversion of 2.7 into 4-(4-(hydroxyphenyl)cycloheptanemethanol.....	42
Scheme 2.9: 9-Step, 2nd generation synthesis of 4-(4-(hydroxyphenyl)cycloheptanemethanol (2.1% yield).....	44
Scheme 2.10: 3 rd Generation synthesis of 4-(4-(hydroxyphenyl)cycloheptanemethanol (10.7% yield).....	45
Scheme 2.11: Preparation of 4-(4-(hydroxyphenyl)cycloheptanone intermediate by ring expansion.....	47
Scheme 2.12: Synthesis of analog 2.23	54
Scheme 2.13: Synthesis of analogs 2.24 , 2.25 and 2.26	55
Scheme 2.14: Synthesis of 4-(2-hydroxyethyl)cycloheptylphenol.....	56

Scheme 2.15: Synthesis of 4-(4-hydroxy-3-methylphenyl)cycloheptan-1-ol.....	57
Scheme 2.16: Oxidative cyclization of 2.10 to generate tricyclic ether 2.39	58
Scheme 2.17: Synthesis of 3-(4-(hydroxyphenyl)cyclopentanemethanol.....	59
Scheme 3.1: 1 st Generation synthesis of 4-(4-(hydroxymethyl)cyclohexyl)phenol.....	62
Scheme 3.2: 2 nd Generation synthesis of 4-(4-(hydroxymethyl)cyclohexyl)phenol.....	63
Scheme 3.3: Mechanistic rationale for bicyclic ether formation of <i>cis</i> -isomer over <i>trans</i> -isomer.....	66
Scheme 3.4: Synthesis of analogs 3.9 , 3.10 , and 3.11	67
Scheme 3.5: Synthesis of analogs 3.12 , 3.13 , 3.15 , 3.16 and 3.17	68
Scheme 3.6: Synthesis of analogs 3.18 , 3.19 and 3.20	70
Scheme 3.7: Synthesis of 4-(4-(2-hydroxyethyl)cyclohexyl)phenol.....	71
Scheme 3.8: Synthesis of analog 3.25b	72
Scheme 3.9: Synthesis of analogs 3.26a and 3.26b	72
Scheme 3.10: Attempted synthesis towards analogs 3.27 and 3.28	73
Scheme 3.11: Synthesis of intermediate 3.33	74
Scheme 3.12: Synthesis of 3.38 and proposed routes to 3.39a and 3.39b	75
Scheme 5.1: Proposed synthetic protocol for <i>cis</i> - and <i>trans</i> - ISP171	106

ABBREVIATIONS

ER	Estrogen Receptor
E2	Estrogen
ER β	Estrogen Receptor beta
ER α	Estrogen Receptor alpha
SERMs	Selective Estrogen Receptor Modulators
4-OHT	4-hydroxytamoxifen
RBA	Relative Binding Affinity
PI3K	Phosphatidy-Inositol 3-Kinase
PTEN	Phosphatase and Tension homolog
FOXO3	Forkhead bOX O3 protein
CDKN1A	Cyclin-Dependent Kinase Inhibitor1
α ERKO	Estrogen Receptor α Knock-Out
β ERKO	Estrogen Receptor β Knock-Out
MCA	Middle Cerebral Artery
NMDA	N-methyl-D-Aspartate
CREB	cAMP Response Element Binding protein
LP	Long term Potentiation
mGluR1	metabotropic Glutamate Receptor 1
ERK	Extracellular Signal Regulated Kinase
GPER	G-Protein coupled Estrogen Receptor
JNK	c-Jun N-terminal Kinase

MAPK	Mitogen Activated Protein Kinase
pCREB	Phosphorylated cAMP Response Element Binding protein
HRT	Hormone Replacement Therapy
CYP450	Cytochrome 450
NTD	N-Terminal Domain
DBD	DNA Binding Domain
LBD	Ligand Binding Domain
AF1	Activation Function 1
AF2	Activation Function 2
ERE	Estrogen Response Element
Hsp	Heat-shock protein
TF	Transcription Factor
AP1	Activating Protein 1
Sp1	Specificity protein 1
NF κ β	Nuclear Factor κ β
IL-6	Interleukin-6
EGFR	Epidermal Growth Factor Receptor
IGF1R	Insulin-like Growth Factor 1 Receptor
NOS3	Nitric Oxide Synthase 3 enzyme
HER2	Human Epidermal growth factor 2
LPB	Ligand Binding Pocket
DPN	2,3-bis(4-hydroxyphenyl)propionitrile

IC ₅₀	Concentration of drug required for 50% of inhibition
ORTEP	Oak Ridge Thermal Ellipsoid Plot
TR-FRET	Time Resolved Fluorescence Resonance Energy Transfer
hERG	human Ether-à-go-go-Related Gene
AR	Androgen Receptor
GR	Glucocorticoid Receptor
MR	Mineralocorticoid Receptor
PPAR-Δ	Peroxisome Proliferator-Activator Receptor delta
PR	Progesterone Receptor
TR-β	Thyroid hormone Receptor beta
VDR	Vitamin D Receptor
OP	Object Placement
OR	Object Recognition
DH infusion	Dorsal Hippocampal infusion
IP injection	Intra-Peritoneal injection
BBB	Blood Brain Barrier
CNS	Central Nervous System
NMR	Nuclear Magnetic Resonance
ppm	parts-per-million
RCM	Ring Closing Metathesis
CM	Cross Metathesis
THF	Tetrahydrofuran

DMSO	Dimethyl Sulfoxide
DMF	Dimethylformamide
HPLC	High-Performance Liquid Chromatography
TFA	Trifluoroacetic acid
mCPBA	meta-Chloroperoxybenzoic acid
PCC	Pyridinium chlorochromate
DMP	Dess–Martin periodinane
TBDMSCl	tert-Butyldimethylsilyl chloride
TBAF	Tetrabutylammonium fluoride
DDQ	2,3-Dichloro-5,6-dicyano-1,4-benzoquinone
DIBAL	Diisobutylaluminum hydride
TBDPSCI	tert-Butyldiphenylsilyl chloride
9-BBN	9-Borabicyclo[3.3.1]nonane
DAST	Diethylaminosulfur trifluoride
NFSI	N-Fluorobenzenesulfonimide

CHAPTER 1

BACKGROUND AND GOALS OF RESEARCH

The goal of this research is the design, synthesis and biological evaluation of estrogen receptor β (ER β) selective agonists for hippocampal memory consolidation for potential use by postmenopausal women.

1.1 Discovery of Estrogen Receptors

Estrogens, such as 17 β -estradiol (E2, Figure 1.1), play an important role in the growth, development and maintenance of a variety of tissues which are mainly mediated by the estrogen receptor (ER), a ligand-activated transcription factor.¹⁻² There are two distinct subtypes of estrogen receptors, ER α and ER β , which are found to diverge with respect to their transcriptional activities and tissue distribution.²⁻⁴ Since the first observations by Jensen and co-workers in 1968⁵ that exogenous estrogen binds to a specific receptor protein in the rat uterus, this estrogen receptor protein (ER α) has been extensively studied. The gene which encodes for ER α (ESR1 located on chromosome 6) was successfully cloned in 1986.⁴ Until 1995, it was believed that there was a single ER which was responsible for facilitating all the biological effects of estrogens. Thus, it was a surprise when, in 1995, a second distinct estrogen receptor from rat prostate was reported by the Gustafson's group. This later estrogen receptor is known as ER β and the gene which encodes for ER β is located on chromosome 14.^{4,6-8}

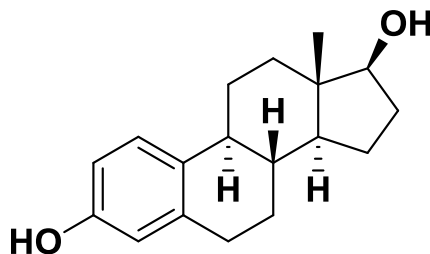


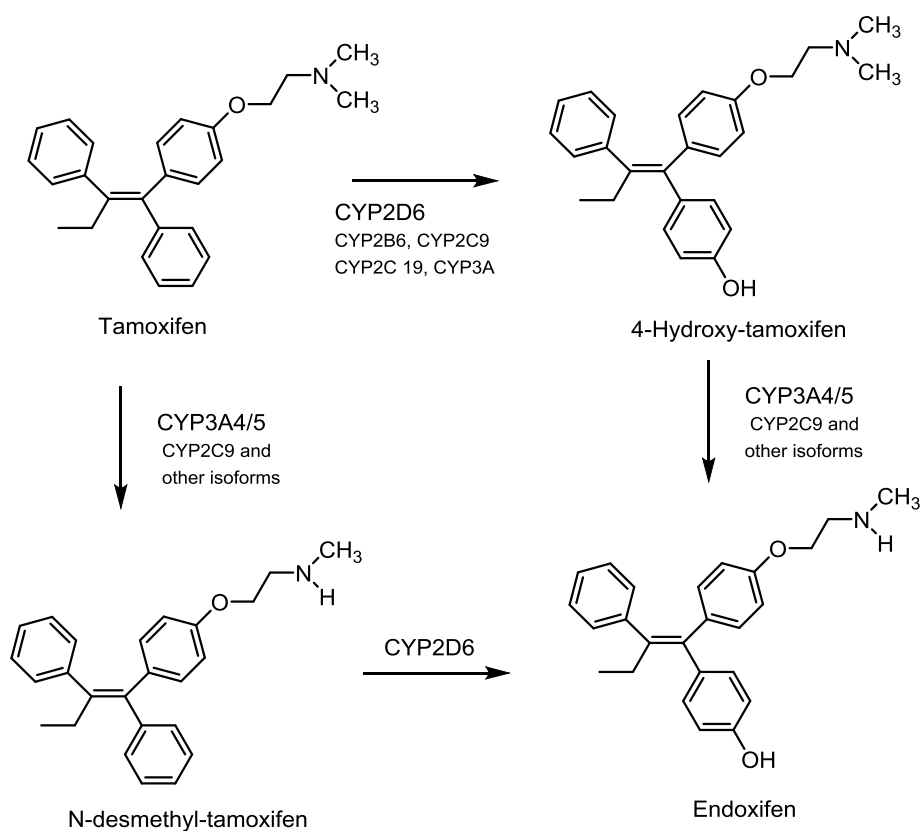
Figure 1.1: Structure of 17 β -estradiol (E2)

The two receptors, ER α and ER β , display overlapping but distinct patterns of tissue distributions as well as different types of transcriptional regulation.⁹⁻¹⁰ ER α is highly expressed in the breast, liver and uterus and contributes to the malignant growth in these tissues, whereas ER β has counteractive anti-proliferative effects on breast cancer cell lines.¹¹⁻¹³ In addition, ER β is expressed in the lungs, prostate, colon, brain and gastrointestinal tract and upon binding of estradiol, it exerts beneficial effects in these organs/ tissues without the risk of breast cancer.^{9, 11, 14} These differential effects prompted researchers to develop novel ER β selective ligands (agonists / antagonists)⁹

1.2 Estrogen Receptors and Human Disease

The prevalence of breast cancer remains highest among all the cancers in women and it is the leading cause of cancer-related mortality within the United States.¹⁵⁻¹⁶ While initiation and progression of breast cancer involves several environmental and genetic factors, estrogen and ERs plays a vital role in the progression and treatment of this disease. Approximately 70% of breast cancers are ER α positive and respond to the selective estrogen receptor modulator (SERMs) prodrug tamoxifen as part of anti-estrogen therapy.^{4, 17-18} While, tamoxifen has relatively low binding to either ER α or ER β (7% and 6% relative binding affinity (RBA) compared to estradiol), it is metabolized by cytochrome P450 enzymes into 4-hydroxytamoxifen (4-OHT) which has greatly increased binding

affinity (178% and 338% RBA compared to estradiol)(Scheme 1.1).¹⁹ Competitive binding of 4-OHT to ER α effects a decrease in expression of cyclin D1 (important for cell progression through the G1 phase), and c-myc (which regulates cell growth). These changes eventually lead to repression of Bcl2, which regulates anti-apoptosis, thus leading to increased cell death.^{4, 20} In estrogen-sensitive malignancies ER α usually act as an oncogene whereas ER β is a tumor suppressor which clearly reveals a divergent relationship (yin/yang relation) between the ER subtypes.⁴



Scheme 1.1: The major metabolic pathway involves initial conversion of tamoxifen to N-desmethyl-tamoxifen and 4-hydroxy-tamoxifen followed by conversion to endoxifen via CYP450s²¹

Estrogen and its receptors are essential for the development and branching morphogenesis of the prostate. ER β is predominantly expressed in both human and rodent

prostate in comparison to ER α . So far, ER β shows anti-proliferative effects for certain prostate cancer cell lines (DU145) by repressing key oncogenes such as **phosphatidylinositol 3-kinase (PI3K)**, **c-myc**, **cyclin E** (which is involved in promotion of cells from the S phase to the G1 phase) and stimulating the expressions of anti-proliferative genes such as the **phosphatase and tension homolog (PTEN)**, **Forkhead box O3 protein (FOXO3)** which functions as a trigger for apoptosis, and **cyclin-dependent kinase inhibitor 1 (CDKN1A)** which regulates cell cycle progression at the G1 and S phases.^{4, 22-23}

Osteoporosis is defined as the loss of bone mass and strength, mainly due to increased bone resorption and this condition is associated with estrogen deficiency.³ In ER α knock-out (α ERKO) mice, shorter bone lengths and reduced mineral density were observed in comparison to wild type mice.^{3, 24} Conversely, adult female ER β knock-out (β ERKO) mice were found to have slightly higher bone mineral density, signifying a regulatory role for ER β in bone growth.^{3, 25} Similarly, male mice deficient in ER α , or both ER α and ER β , (due to knock-out) exhibited reduced bone mineral density, bone diameter and length, while male mice with only ER β knockout did not exhibit these reductions.^{3, 26} These observations suggest the significance of ER α in bone mass regulation.

ERs also have profound effects in the brain, mainly in brain injury, neurodegeneration and cognitive decline.²⁷ Both ERs are distributed in numerous regions of the brain such as the hypothalamus, hippocampus, cerebral cortex, forebrain and midbrain.²³ Dubal, *et al.*, demonstrated that the removal of ER α completely abolished the protective role in brain injury, whereas the protection is preserved in the absence of ER β in ovariectomized / ischemia mice models.^{23, 27} Another study, where stroke was induced from reversible **m**iddle **c**erebral **a**rtery (MCA) occlusion, found that no enhanced tissue

damage was observed in female α ERKNO mice.²⁸ This indicates the subtype independent nature of estrogen action towards brain injury prevention. Impressively, Gustafsson, *et al.* showed an abundance of morphological abnormalities such as neuronal loss and proliferation of astroglial cells in the brains of β ERKO mice and no changes were observed in α ERKO mice.²⁹ Moreover, several researchers conclude that ER β is crucial for neuron survival and its valuable influence on treatment of neurodegenerative diseases including Alzheimer disease, Parkinson disease, and schizophrenia.^{7, 23, 30}

1.2.1 Estradiol, the Hippocampus and Memory

A plethora of literature accumulated over last twenty years has demonstrated that 17 β -estradiol (E2) is an important trophic factor that mediates the function of cognitive regions of the brain.³¹ “The importance of estrogen in cognitive function has been highlighted by examining cognition in relation to phases of the menstrual cycle, menopausal symptoms, circulating hormone levels and aging.”³² The decline in E2 production as a result of menopause is linked with etiology of dementia, depression and cognitive decline in women, as well as rapid memory decline in animal models.³¹

According to recent studies, it is evident that E2 governs the dendritic length in the basal forebrain and neuronal dendritic spine density in the somatosensory cortex, the amygdala, and the prefrontal cortex of the brain.³³ Similarly, estradiol controls morphology and synaptic plasticity in the hippocampus; the major brain region responsible for cognitive activity. So far, several mechanisms of action for the effects of estradiol on cognitive functions of the hippocampus have been recognized through several distinct pathways. E2 promotes the formation of new dendritic spines and excitatory synapses, and stimulates the expression of *N*-methyl-D-aspartate (NMDA) mediated synaptic activity.

Moreover, E2 increases the phosphorylation of the **cAMP response element binding protein (CREB)** and long term potentiation (LP) which are highly responsible for the learning and long-term memory.³²⁻³⁴

ER α and ER β are confined in several compartments in hippocampal neurons, such as the nucleus, axon terminals and dendritic spine synapses. In the nucleus, ERs mediate the estrogen effects on the classical genomic pathway leading to the gene transcription. However, the localization of ERs at distal sites, such as dendritic spines and axon terminals, proposed the possibility of a “non-genomic” or “non-classical” mechanism of estrogen receptors. Indeed, binding of both ERs to the **metabotropic glutamate receptor 1 (mGluR1)** triggers the hippocampal **extracellular signal-regulated kinase (ERK)** signaling and promotes CREB phosphorylation. The interaction of E2 with NMDA receptor also triggers ERK signaling as well as local protein synthesis. Both ERK and CREB play pivotal role in hippocampal memory consolidation. Besides intracellular ERs, several putative membrane bound ERs have been identified (e.g. GPER, ER-X and Gq-ER). E2 binds to these receptors and enhances the memory consolidation by activating the **c-Jun N-terminal kinase (JNK)** cascade, which eventually facilitates gene transcription and protein translation (Figure 1.2)^{31,33}

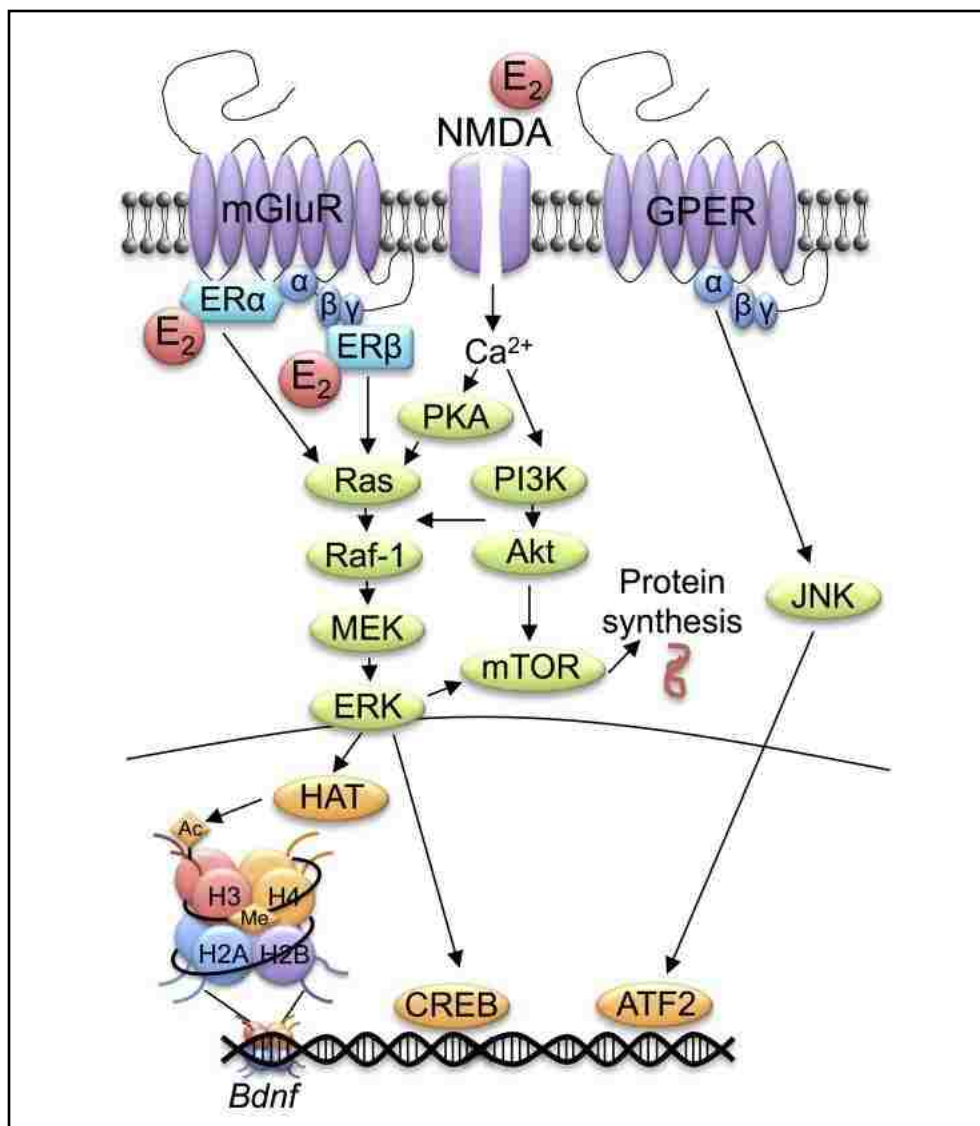


Figure: 1.2: Schematic illustration of non-classical mechanisms required for E₂ and ERs to enhance hippocampal memory consolidation³³

Though estrogen has been involved in influencing cognitive functions, the sub type of estrogen receptor responsible for these effects remain unclear. However, accumulating biochemical, pharmacological and behavioral studies support the key role of ERβ for hippocampal memory and synaptic plasticity. A few selected examples are discussed here.³²⁻³³

In general, hippocampal memory in rodents have been primarily evaluated in spatial tasks, including object placement, the Morris water maze and the radial arm maze, as well as through object recognition tasks.³³ In 2002, Gustafsson and coworkers, demonstrated that removal of either receptor (by ER α or ER β knockouts) impairs the spatial memory in the Morris water maze^{31, 35-36} Semple-Rewland, *et al.*, showed that spatial memory deficit induced by ER α knockouts can be restored by viral vector-mediated delivery of the ER α gene to the hippocampus. However, the same delivery of the ER α gene to the hippocampus did not restore memory deficit in ER β knockout mice.^{31, 37} Moreover, both Walf, *et al.*^{31, 38-39} and Brandon, *et al.*³² showed that exogenously administered E2 did not enhanced the hippocampal memory in female ER β knockout mice.

Besides the memory related studies, Brandon and coworkers examined the molecular events driven by ER β in the hippocampus.³² Since estrogen exerts effects on synaptic physiology by activating non-genomic signaling cascades (MAPK), the abundance of pCREB levels were monitored in ovariectomized rats. Dosing ovariectomized rats with ER β selective agonist (WAY-200070) and estradiol significantly increased the phosphorylated cAMP response element binding (pCREB) levels; there were not pCREB level increases observed with administration of the ER α selective agonist PPT (Figure 1.3).³²

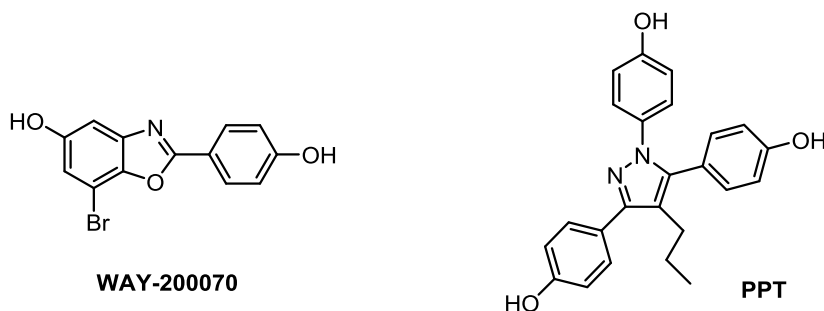
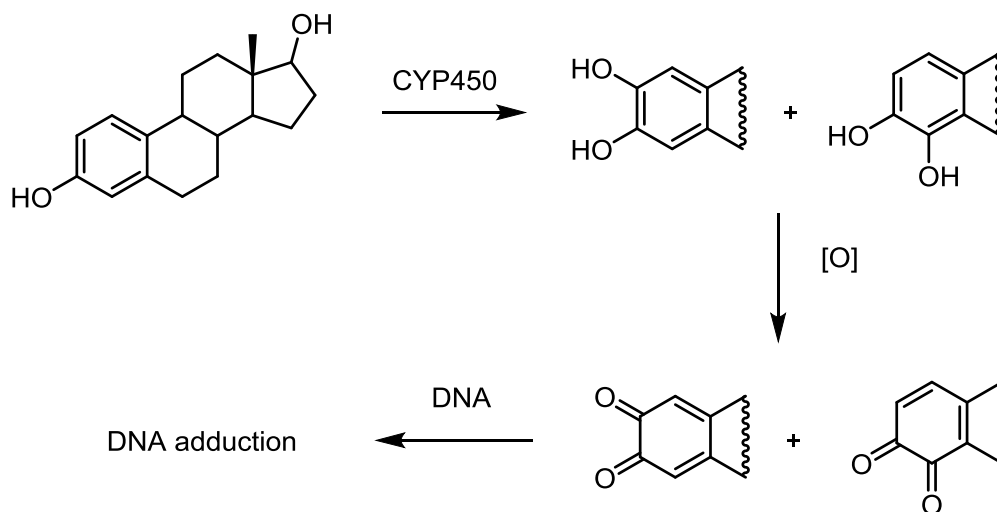


Figure 1.3: Structure of ER α and ER β selective agonists

1.2.2 Estrogen Decrease in Menopause and Hormone Replacement Therapy

Estrogen levels decrease in both sexes as humans age, but drop more precipitously in women during the menopausal transition. Lower estrogen levels during menopause is correlated with “diseases of the skeleton (osteoporosis), cardiovascular system (coronary heart disease) and central nervous system (Alzheimer’s disease).”¹ Hormone replacement therapy (HRT), the prolonged administration of estrogen and progesterone supplements, was initially developed to address the lower production of these important mediators. HRT reduced the risk of dementia, mild cognitive impairment and prevented the spine and hip fracture in postmenopausal women. However, the safety of continuous administration of estrogen supplements in HRT is currently under scrutiny due an increased risk of breast and endometrial cancer.⁴⁰⁻⁴³ The etiology of HRT carcinogenicity is complex, but an increasing amount of evidence supports the formation of catecholic estrogens via CYP450 and their subsequent oxidation to tumor-initiative quinones (Scheme 1.2).⁴⁴⁻⁴⁸



Scheme 1.2: Mechanism of quinone formation and DNA adduction

Nevertheless, estradiol has garnered considerable attention over the past decades in influencing cognitive processes in relation to phases of the menstrual cycle, aging and menopausal symptoms. Accumulating evidence supports the dominant role of estrogen receptor-beta ($ER\beta$); the predominant isoform in the hippocampus for improved cognitive effects.³² $ER\beta$ mediates estradiol's effects on neural plasticity, neuroprotection, enhanced hippocampal signaling and memory consolidation via estrogen activated signaling cascades, via the extracellular signal-regulated kinase/mitogen-activated protein kinase pathway (ERK/MAPK).⁴⁹⁻⁵⁰ Due to the deleterious effects of activating $ER\alpha$ compared to beneficial effects of activating $ER\beta$, selective $ER\beta$ agonists are an exciting new direction in drug discovery for the treatment of cognitive deficits in postmenopausal women.

1.3 Estrogen Receptor Structure and Mechanism of Action

“ER α and ER β belong to the nuclear hormone receptor family whose members are ligand-controlled transcription factors.”⁷ ER α is a 66 kDa, 595-residue protein whereas ER β is a 62 kDa, 530-residue protein.² Both ERs exhibit similar architecture, having six regions of the primary amino acid sequence (A-F) and composed of three major functional domains: the N-terminal or A/B domain (NTD), the DNA-binding domain (DBD), and the C-terminal D/E/F or ligand-binding domain (LBD) (Figure 1.4). The two human ERs share ~ 97% similarity between the DBD domains, 59% similarity in the LBD domains, but only 16% similarity in the NTD domain. The two receptors are functionally not interchangeable.^{2, 4, 6}

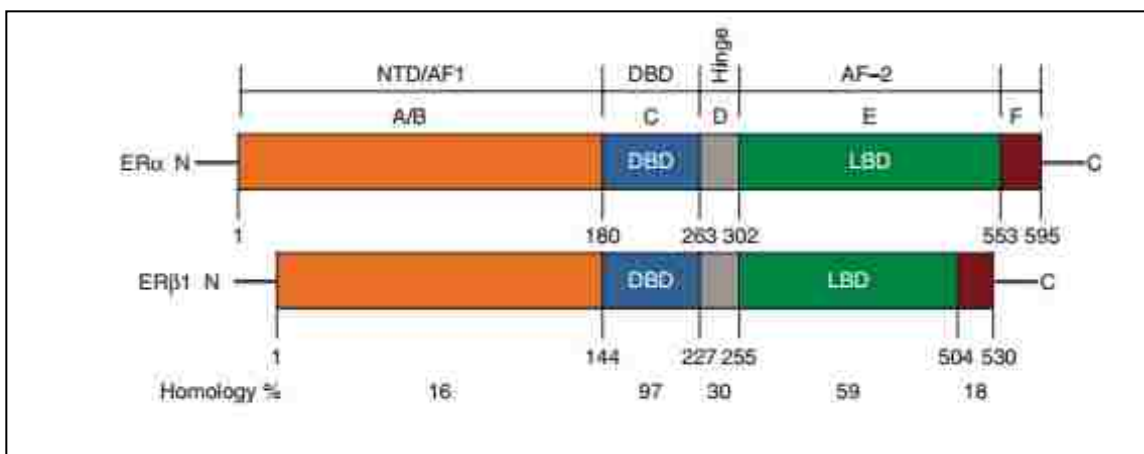


Figure 1.4: Schematic representation of structural domain of human ER α and ER β ⁴

The N-terminal domain (NTD) of ER consists of ligand-independent activation function (AF1) where it involves the protein-protein interactions and transcriptional activation. In ER α , the AF1 domain shows higher activity in stimulation of reporter gene expression via estrogen response element (ERE) whereas AF1 activity of ER β appeared to

be diminished under the same conditions. This dissimilarity in N-terminal region accounts for the difference in activity of ER α and ER β towards various exogenous ligands.⁶⁻⁷

The DNA binding domain (DBD) of both receptors shares a high degree of sequence homology and each contains a zone called “zinc fingers”. This region is rich in cysteine residues and four cysteine residues are coordinated to the zinc atom to form the finger structure, having a loop of 15 to 22 aminoacids.⁵¹ Zinc fingers are common to transcription factors and there are two zinc fingers for each receptor. These play an integral role in receptor- DNA binding in that they offer “an optimum architecture for the mutual recognition between specific sequences of amino acids and nucleotides”⁵¹. This eventually establishes the hydrogen bridges (via H-bonding) in order to form the stable ER-DNA complex.^{8, 51}

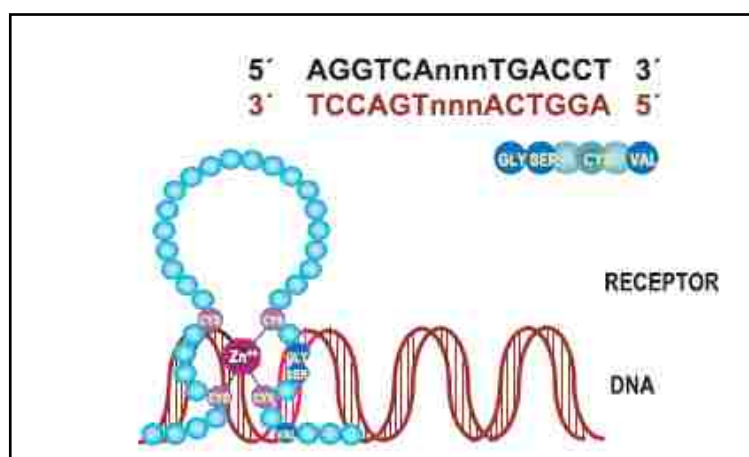


Figure 1.5: Formation of Zinc fingers in DNA binding domain. (Adapted from Selective Estrogen Receptor Modulators, A. Cano, *et al.*, Springer, 2006, pg 20)⁵¹

The C-terminal ligand binding domain (LBD) governs the target gene expression via ligand binding, receptor dimerization and subsequent dimer-nuclear translocation. The LBDs of both receptors have higher homology with respect to their amino acid sequences and have similar tertiary architecture. LBD usually comprises of 12 helices (H1-H12) in

three anti parallel layers. It incorporates an **activation function 2** segment (AF2), whose structure and function are mainly mediated by incoming ligands. AF2 interaction surface is composed of amino acids in helix 3, 4, 5, and 12 and the positioning of helix 12 is effected by incoming ligands based on their agonist or antagonist nature. Overall, the ligand-binding domains of ERs have a net hydrophobic character, which is an essential prerequisite for attachment of low molecular weight organic molecules.^{2, 6-7} Small differences between the LBDs of ER α and ER β influence the shape of their ligand binding pockets there by engendering unique affinities for ligands.⁶ These differences in the LBD will be discussed in more detail in Section 1.4.

The ERs are mostly localized in the cytoplasm in complex with heat-shock proteins (Hsp) 50, 70 and 90 which stabilize the receptors in an inactive state.⁴ “The action of ERs is tripartite, as it involves the receptor, ligands (natural or synthetic) and coregulatory proteins.”⁵² In the classical mode of action, binding of estrogen to the LBD of ER induces receptor conformational changes (mainly dissociation of ER-Hsp chaperone complex), leading to receptor dimerization (ER₂). This dimer binds to a specific sequence of DNA in the promoter region known as the estrogen response element (ERE). This binding promotes the recruitment and interaction with coregulators from the nucleus, and formation of a pre-initiation complex. Finally, the receptor-DNA-coregulator complex undergoes DNA transcription to form mRNA and thereby desired proteins which lead to an alteration in cell function (Figure 1.6).^{4, 8, 51}

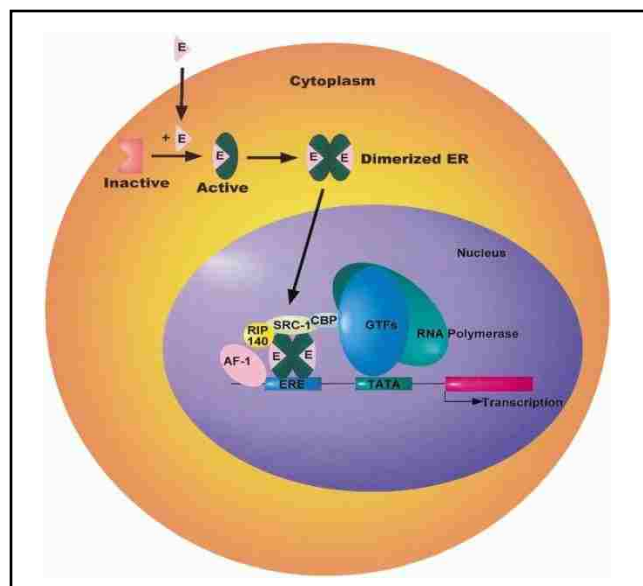


Figure 1.6: Classical mechanism action of estrogen receptor⁵³

In addition to its classical mode of action, it is now accepted that ERs can mediate gene expression without directly binding to DNA. One possible pathway is transcriptional cross-talk, where the E2-receptor complex is tethered to a transcription factor (TF) that interacts with the DNA, thus avoiding a direct ER-DNA interactions (Figure 1.7).^{4, 6, 8, 54} Examples for transcriptional cross talk include interaction of ERs at activating protein 1 (AP1), specificity protein 1 (Sp1), cAMP response element-binding protein (CREB), nuclear factor κ B (NF κ B), p53 binding sites. Interaction of ER with the nuclear factor κ B (NF κ B) prevents the NF κ B binding to interleukin-6 (IL-6) promoter leading to repression of cytokine IL-6 protein. ERs regulate several genes by this mechanism and both AP1 and Sp1 mediated gene expression vary with the ligand, cell and receptor subtype.^{4, 6, 54-55}

Furthermore, “ERs stimulate transcriptional responses in the absence of estradiol. Epidermal growth factor receptor (EGFR) and insulin-like growth factor 1 receptor (IGF1R) can initiate the protein kinase cascade, thus phosphorylation and activation of ERs in the absence of the ligand.”⁸

18

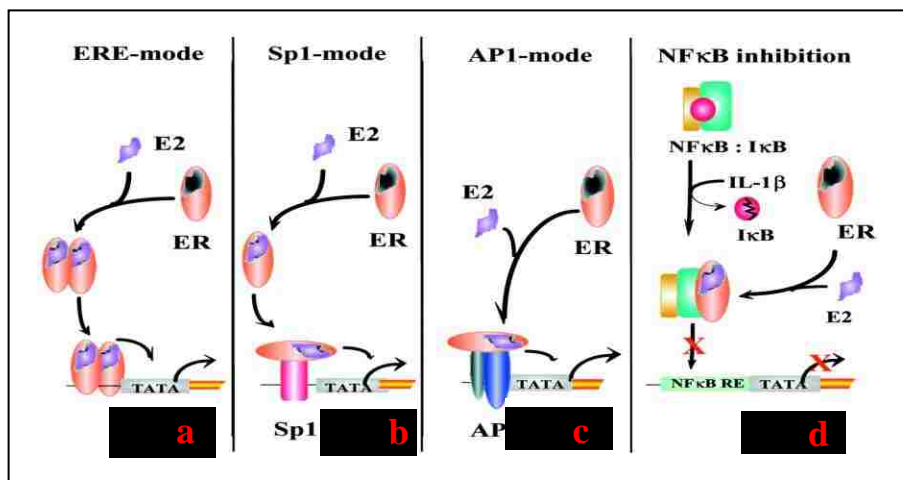


Figure 1.7: a) classical mechanism of action. b,c,d) “indirect effects of estrogen receptors on transcriptional activation”⁶

Likewise, accumulating evidence supports for the rapid and non-genomic effects of membrane bound and cytoplasmic ERs where binding of estradiol activates the following proteins: **mitogen-activated protein kinase (MAPK)**, **phosphatidylinositol 3-kinase (PI3K)**, **nitric oxide synthase 3 (NOS3)**, **human epidermal growth factor receptor 2 (HER2)** and **G proteins (GP)**. Finally, these proteins can signal to regulate the gene expression via activation of other transcriptional factors.^{6, 8}

1.4 Important Interactions within the Ligand Binding Domain

While the ligand binding domains (LBDs) of ERs share less than 60% of amino acid sequence, the ligand binding pockets (LBP) of the two isoforms have only minute variations in structure and composition.¹¹ The crystal structure of estradiol bound to ER α revealed a hydrogen bonding network between the endogenous ligand and surrounding amino acid residues.⁵⁶ The phenolic OH group interacts with a bound water molecule and two amino acid residues of the ER LBP (Glu353 and Arg394 in ER α , Glu305 and Arg346 in ER β , Figure.1.8) and the 17 β -hydroxy group is involved in an additional hydrogen bond

interaction to His524 (ER α) or His475 (ER β).⁵⁷ The two LBPs are composed of 23 amino acid residues, 21 of which are conserved and only two of which are variant. The residues Leu384 and Met421 in ER α are replaced with Met 336 and Ile373 in ER β respectively. Furthermore, the interchanged Leu384/ Met336 residues are positioned above the B- and C-rings of estradiol whereas the interchanged Met421/Ile373 residues are positioned below the estradiol D-ring within the LBP. These minute alterations in amino acid sequence plus other small variations in tertiary structure make the ER β LBP smaller in volume (279 Å³) in comparison to the LBP of ER α (379 Å³). However, the creation of ER β selective ligands seems to be a real challenge due to higher structural similarity of LBP of both receptors.^{11,}

47, 57-60

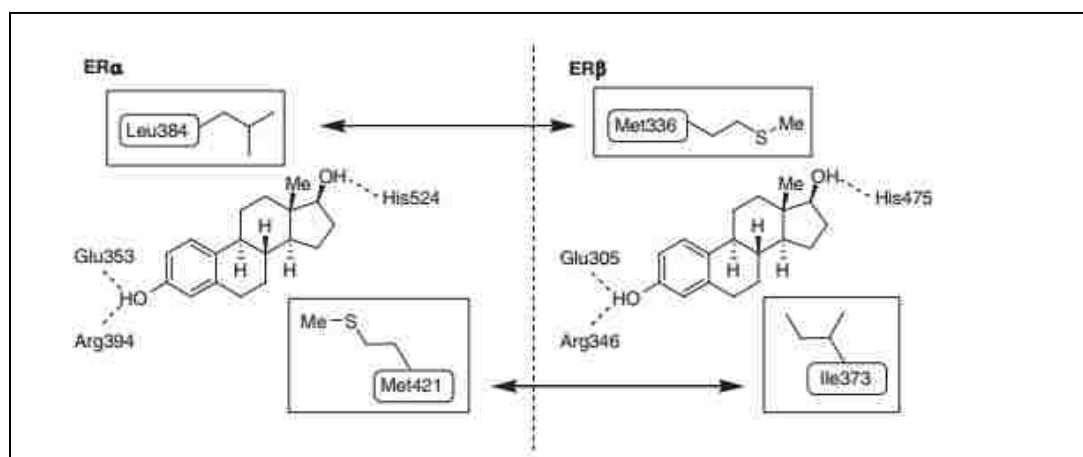


Figure 1.8: “Principal interactions of estradiol with ER α and ER β conserved and nonconserved residues”⁶⁰

1.5 Estrogen Receptor – Agonists, Antagonist and Selective Estrogen Receptor Modulators

The molecules that bind to ERs possess significant variations in the process of uptake, binding, and/or recruitment of coregulator(s) leading to different transcriptional responses. The conformational changes that occur at the LBD upon formation of ER-molecular complex determine its transcriptional responses relative to the native estrogen.⁶¹

Natural and synthetic ligands may be classified as agonists, antagonists or selective estrogen receptor modulators (SERMs). Ligands that form complexes in a similar but not identical manner to those formed by estradiol are known as ER agonists. They recruit a similar set of cofactors and eventually produce similar but not identical transcriptional responses.^{51, 61} On the contrary, ligands that form complexes at the LBD, but create different conformational changes compared to estradiol, are termed as ER-antagonists or antiestrogens. These complexes fail to dimerize or recruit the same set of cofactors as estradiol or recruit different cofactors leading to a blocking of transcriptional responses.^{51,}

⁶¹

ER agonists and antagonists bind at the same site of the LBD with different binding orientations or modes. For this reason, agonist or antagonist activity is mainly due to the spatial repositioning of helix 12 (H12) after binding; the location of this helix is a key factor for the subsequent recruitment of the transcription cofactors.^{2, 62} Indeed, the binding of an agonist restructures the ligand binding domain, making helix 12 rotate in a way that it is positioned over the ligand binding pocket. This facilitates the movement of coactivators while removing the corepressors from their original site. In contrast, antagonist ligands lodge into the hydrophobic groove conferred by helices 3, 4, and 5 and disrupts helix 12 conformation for coactivator interaction. Figure 1.9 depicts the difference in positioning

of H12 of ER α upon binding of agonist (diethylstilbestrol) and antagonist (4-hydroxytamoxifen) to the LBD.

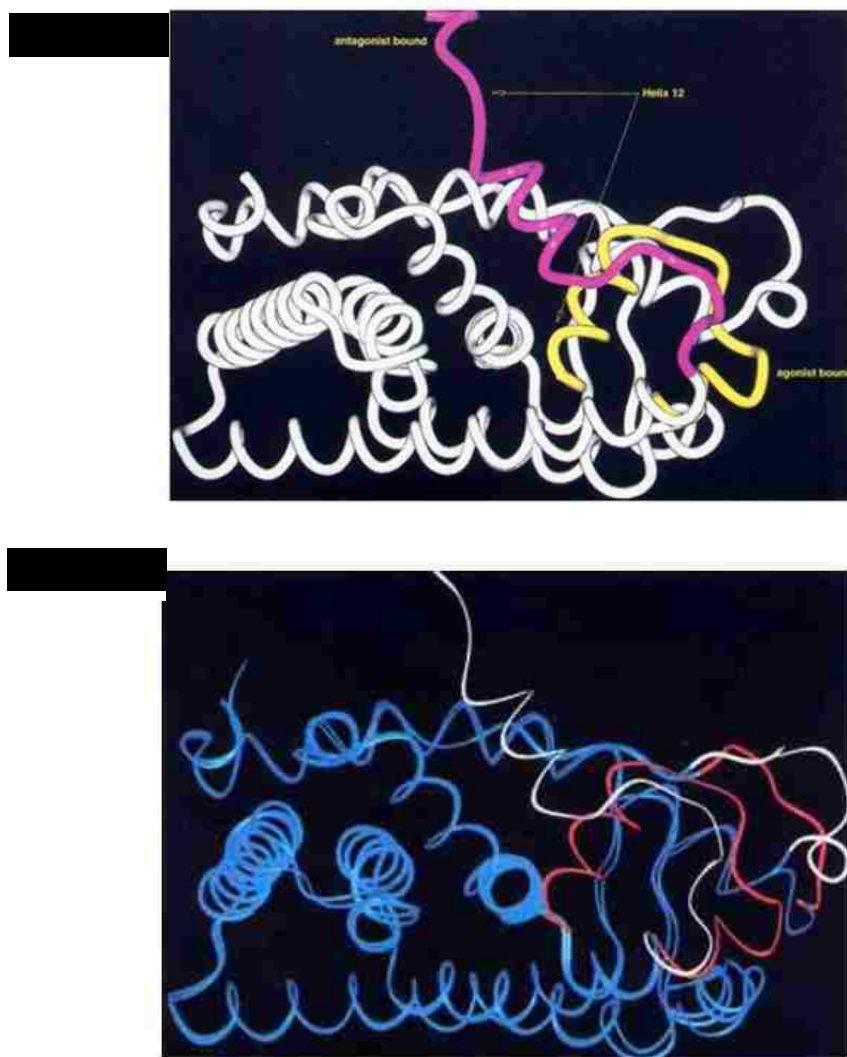


Figure 1.9: a) The conformation of H12 of ER α due to diethylstilbestrol (agonist) binding (yellow) and tamoxifen (antagonist) binding (magenta) b) Ligand-dependent structural deviation between agonists (red) and antagonists (white) conformations.²

The folded yellow and extended pink portions represent the H12 helix in agonist and antagonist mode respectively and are readily discernable. Moreover, the superposition of both agonist and antagonist forms of LBD without any modification clearly reveal the

conformationally conservative nature of the LBD (blue colored) aside from the H12 orientation.^{2, 6, 62}

ER α agonists (red in Figure 1.10a) primarily interact with Glu353, Arg394 and His524, whereas ER α antagonists (white) have an additional interaction with Asp351 (upper left corner of Figure 1.10a). This additional interaction is responsible for the antagonism which prevents the conformational change of helix 12. Similar amino acid residues in ER β are engaged in these interactions (Figure 1.10b); these differ only in residue numbering (Glu305, Arg346, His475, Asp303).²

Selective estrogen receptor modulators (SERMs) are a structurally diverse class of therapeutic agents that interact with estrogen receptors but that exhibit a selective ER agonist vs antagonist profile which is tissue/organ specific.⁶³ To date several SERMs drugs are developed and some are approved for clinical use. For an example, tamoxifen is used as an antagonist for the treatment of breast cancer, but shows agonist effects on bone mineral density and serum lipids on postmenopausal women. Raloxifene, is used for treatment of osteoporosis and vertebral fractures, even though it is a failed breast cancer drug.^{17, 51, 63} Table 1.1 shows the classification of SERMs and Figure 1.11 shows some of their chemical structures.⁵¹

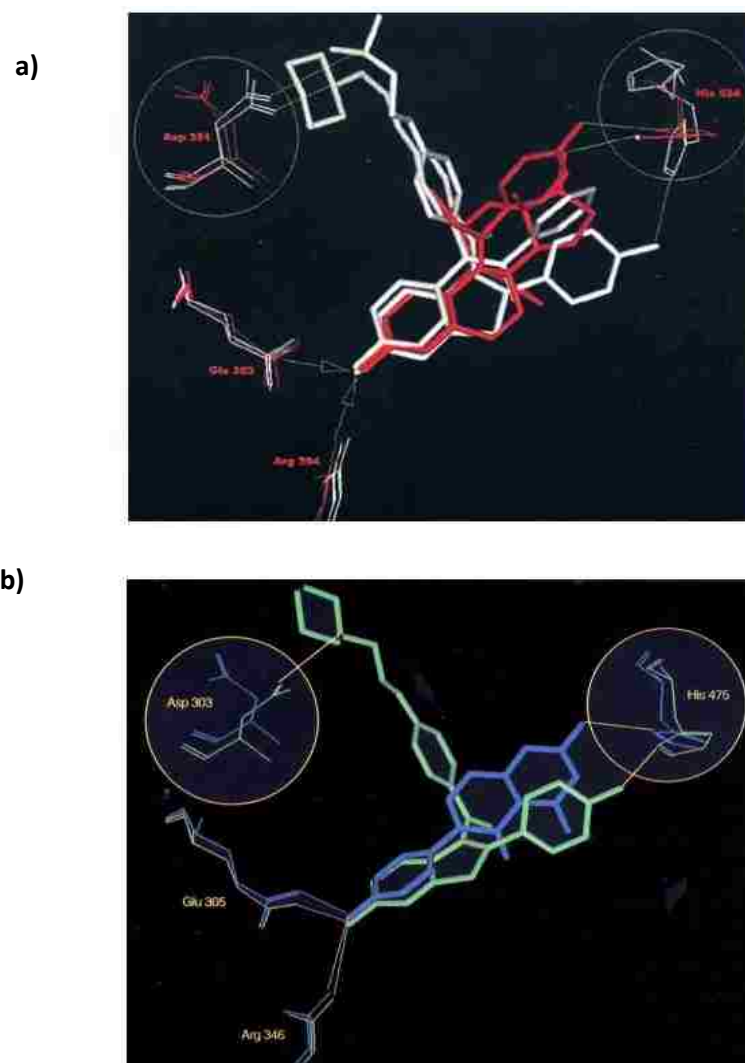


Figure 1.10: a) The binding interactions in the ER α for agonists (red) and antagonists (white). b) binding interactions in ER β for agonist (blue) and antagonist (green)²

Table 1.1: “Classification of SERMs” (Adapted from Selective Estrogen Receptor Modulators, Cano, *et. al*, Springer, 2006, pg 51)⁵¹

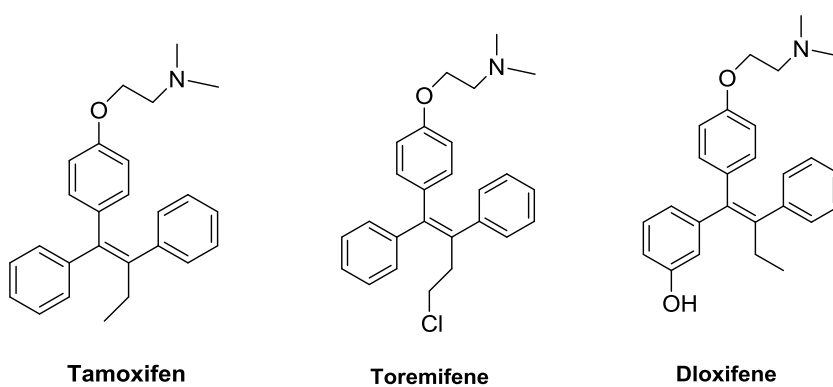
Chemical Class	SERM	
Triphenylethylenes	Tamoxifen*	AstraZeneca
	Toremifene*	Orion
	Droloxifene [#]	Pfizer
	Idoxifene [#]	Smithkline Beecham
Benzothiophenes	Raloxifene*·†	Eli Lilly & Co
	Arzoxifene†	Eli Lilly & Co
Naphthylenes	Lasofoxifene†	Pfizer
	Trioxifene [#]	
Indoles	Bazedoxifene†	Wyeth
	Pipendoxifene†	Wyeth
Benzopyrans	EM-800†	Schering Plough
	Acolbifene†	Schering Plough
	Levormeloxifene*	Novo-Nordisk

* Commercialized for different indications: breast cancer treatment, contraception, Ovulation induction, prevention and treatment of postmenopausal osteoporosis.

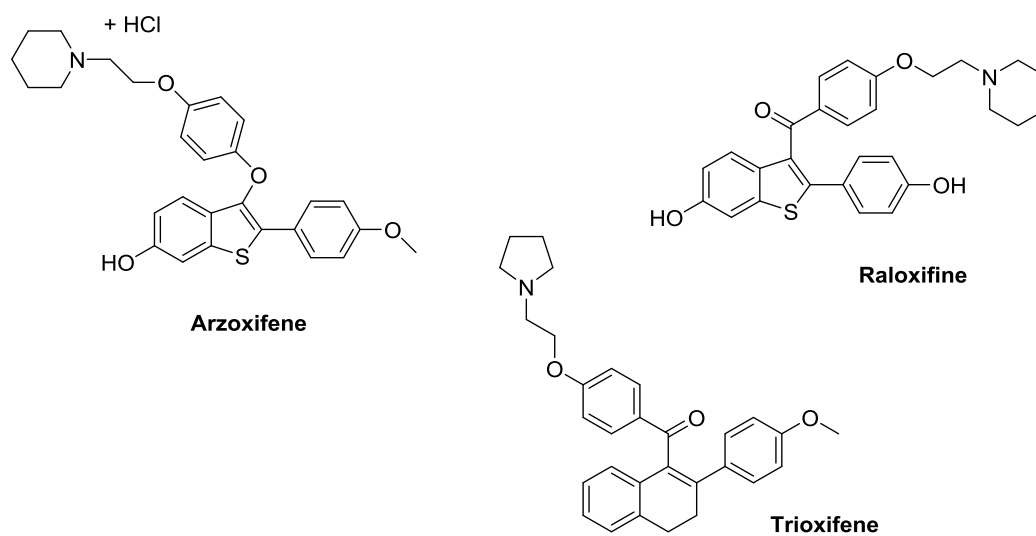
† Phase III clinical research

Clinical development cancelled

a) Triphenylethylene derivatives



b) Benzothiophenes and Naphthalene derivatives



c) Indoles and Benzopyran derivatives

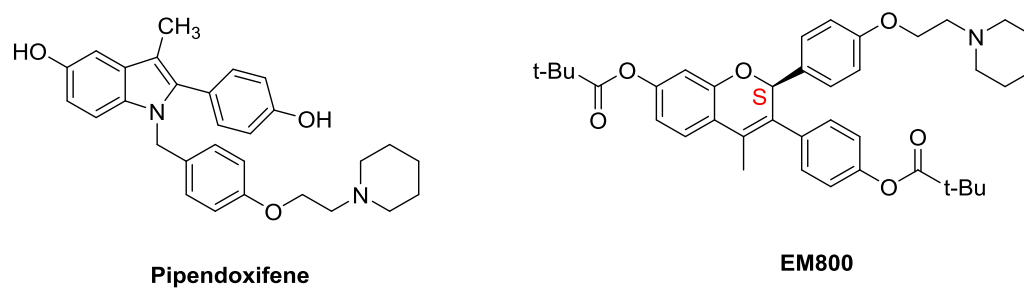


Figure 1.11: Selected chemical structures of SERMs ⁵¹

1.6 Review of ER β Subtype Selective Ligands

Estradiol has nearly equivalent binding affinity for ER β and ER α . While there are a considerable amount of compounds known which have greater selectivity for ER α , only a limited number molecules with greater selectivity for ER β have been reported.⁶⁰ Among natural products, coumestrol, genistein, liquiritigenin, naringenin and apigenin are some examples of ER β -selective agonists (Figure 1.12). They are found in many plants (phytoestrogen) and foods, especially in soybeans. The isoflavone genistein shows nearly 20 to 30-fold selectivity for ER β over ER α and it was the first ER β selective natural product characterized from X-ray crystallography (Figure 1.13).⁶⁴ Coumestrol, liquiritigenin, naringenin, and apigenin also show considerable selectivities for ER β in binding affinity assays (β/α 7, 11, 20, and 30 respectively).^{7, 10, 60, 65-67}

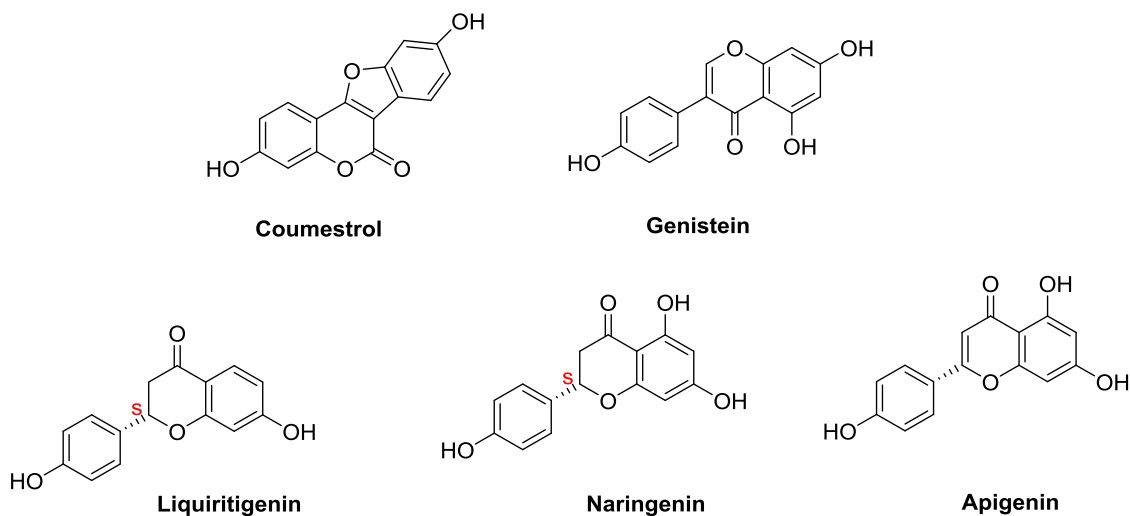


Figure 1.12: Examples of natural ER β -selective agonists⁶⁰



Figure 1.13: a) “Schematic representations of hER β –GEN complex. Helices are depicted as rods and H12 is colored in green.” b) “Comparison of ligand-binding mode of GEN (protein-light blue; ligand, green) in hER β -LBD and E2 (protein-red; ligand-purple) in hER α -LBD (PDB code: 1ERE) within the cavity. The ligands are viewed looking down from the β -face of the cavity and only those side chains that interact with the bound ligand or exhibit different orientations are shown. Hydrogen bonds are depicted as broken lines”⁶⁴

1.6.1 Design of Non-Steroidal ER β Selective Agonists

The design and development of non-steroidal ER β selective agonists has piqued much interest due to their potential lower carcinogenic properties compared to steroidal molecules.⁶⁰ To date, several non-steroidal selective ER β agonists have been synthesized and a few selected examples are discussed here.

In 2001, Katzenellenbogen and co-workers at the University of Illinois; discovered 2,3-bis(4-hydroxyphenyl)propionitrile (DPN), a chiral molecule, as one of the most potent and selective ER β agonists (Figure 1.14).^{60, 68} The racemic molecule has 70-fold higher relative binding affinity for ER β compared to ER α and 170-fold higher relative potency in transcription assays (ER β vs ER α).⁶⁸ Due to its present commercial availability, several researchers have used (\pm)-DPN as a pharmacological probe to evaluate the unique biology

of ER β in both *in vivo* and *in vitro* biological studies.^{60, 69-70} Subsequently; in 2009 Handa, *et.al*, separated the enantiomers by chiral HPLC. They reported that (S)-DPN demonstrated a higher affinity for ER β compared to (R)-DPN, and that (S)-DPN showed nearly 80-fold selectivity for ER β .⁷¹ In 2012, the Katzenellenbogen group prepared the (S)-and (R)- DPN by enantioselective synthesis. They confirmed the high affinity and potency preference of both enantiomers toward the ER β (80-300), however, in this study, authors reported that (R)-DPN as the preferred agonist for ER β activity.⁷² Computational docking of the (S)-stereoisomer with either ER α or ER β shows that the hydroxyl group of the β - ring (see structures for aromatic ring designation) exerts a favorable H-bonding network with Glu353 and Arg394 in ER α (or Glu305 and Arg346 in ER β) while the hydroxyl group of the α -ring interacts with His524 in ER α (or His475 in ER β). In this orientation, the CN group of DPN interacts with the sulfur atom of Met336 in ER β in a more favorable manner than with the similarly positioned Leu384 residue of ER α . In contrast, computational docking of (R)-DPN shows that the CN group projects in the opposite direction in comparison to the S-enantiomer and thus exerts a weaker interaction with the surrounding amino acid residues (Figure 1.14). These docking studies suggest that the selectivity of DPN racemate towards ER β mainly stems from the strongly interacting geometry of S-DPN and not from R-DPN at the ligand binding pocket.^{60, 68, 73}

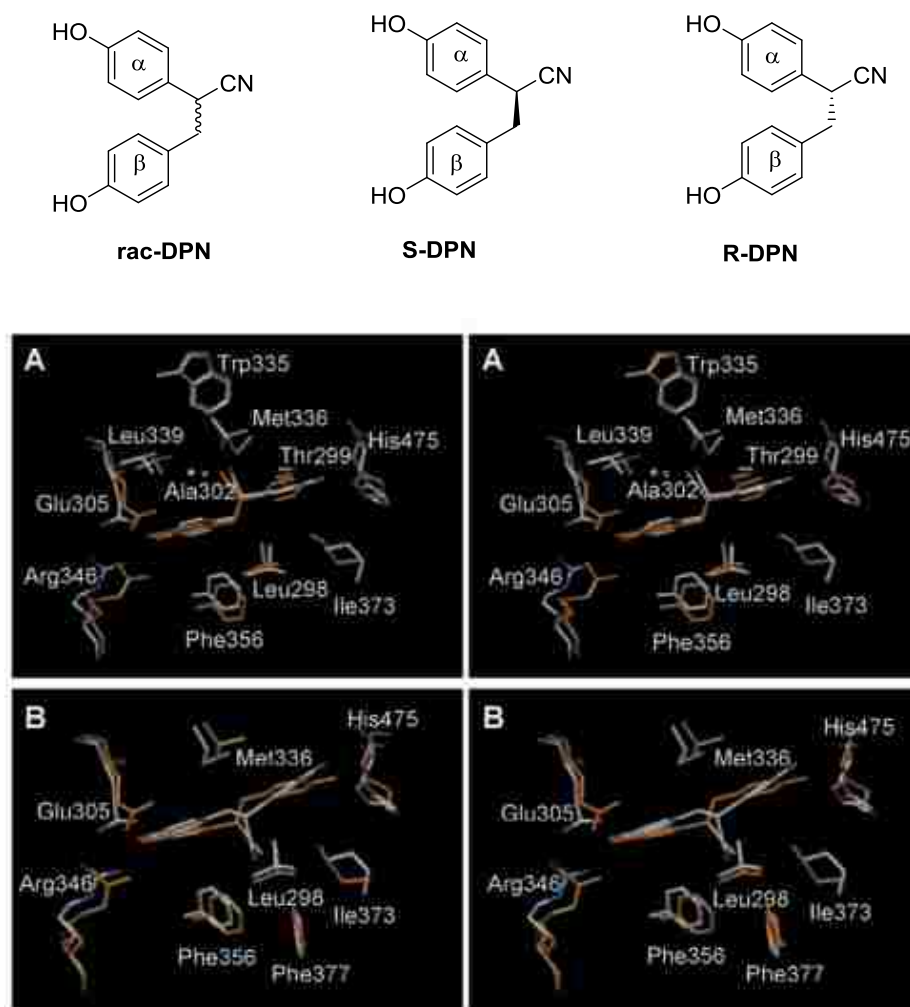


Figure 1.14: “Crossed stereo view of S-DPN (Panel A) and R-DPN (Panel B) docked and minimized in the ER and ER LBD Pockets, respectively. DPN and the ER β pocket residues are shown with standard atom colors, whereas in the ER α complex, DPN and the pocket residues are shown in orange.”⁷³

In 2004, the Wyeth research group reported a series of ER β selective agonists belonging to the benzoxazoles family.⁶⁰ The ERB-041, WAY-292, WAY-659, WAY-818, and WAY-200070 are some examples from the Wyeth compound library (Figure 1.15).^{9,}
^{60,74} Among these, ERB-041 showed a 250-fold highest selectivity for ER β having binding affinities (IC_{50}) of 1200 nM and 5.4 nM for ER α and ER β respectively. Both docking and X-ray crystallographic studies reveal that the hydroxyl group of the 3-fluoro-4-

hydroxyphenyl moiety forms H-bonds with nearby Glu305 and Arg346 of ER β residues while the benzoxazole hydroxyl group hydrogen bonds to His475. These interactions are common to both estrogen receptors (Figure 1.16). Notably, the benzoxazole vinyl substituent is positioned in close proximity to Ile373 of ER β while in ER α the vinyl group interacts with the Met421 residue (Figure 1.17). It was suggested that the increased steric interaction of the vinyl group with the larger Met residue, as compared to the more compact Ile373 was responsible for the higher selectivity of ERB-041 with ER β compared to ER α .⁹

60, 74-75

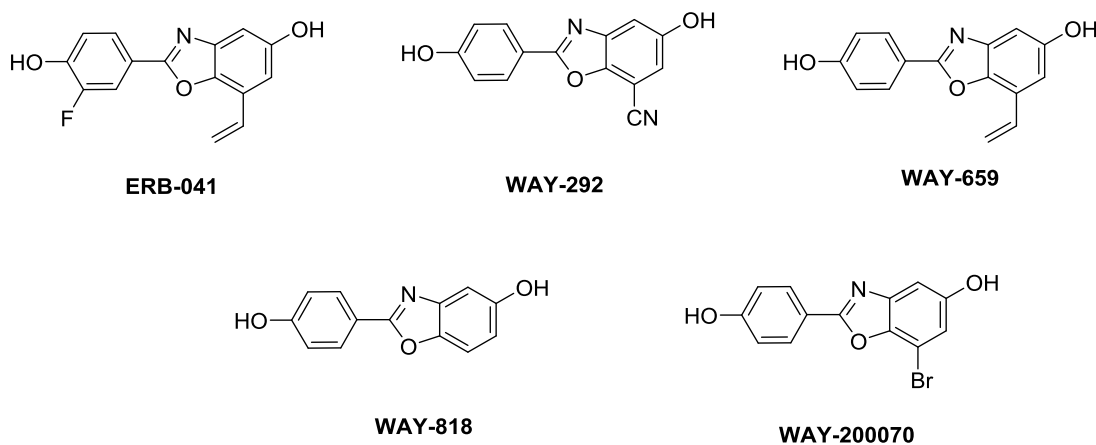


Figure 1.15: Examples of ER β -selective agonists from Wyeth library⁶⁰

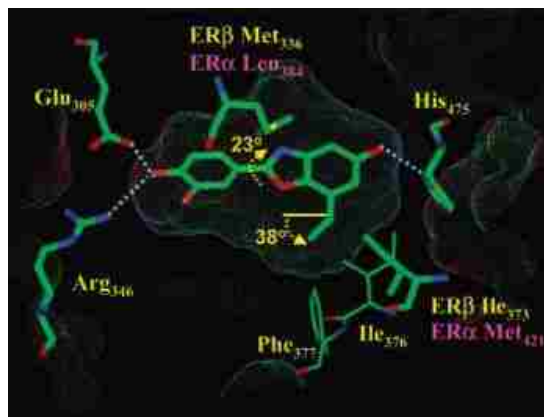


Figure 1.16: Schematic representation of ERB-041 complexed with ER α and ER β , showing key interactions within the ligand binding domain⁹

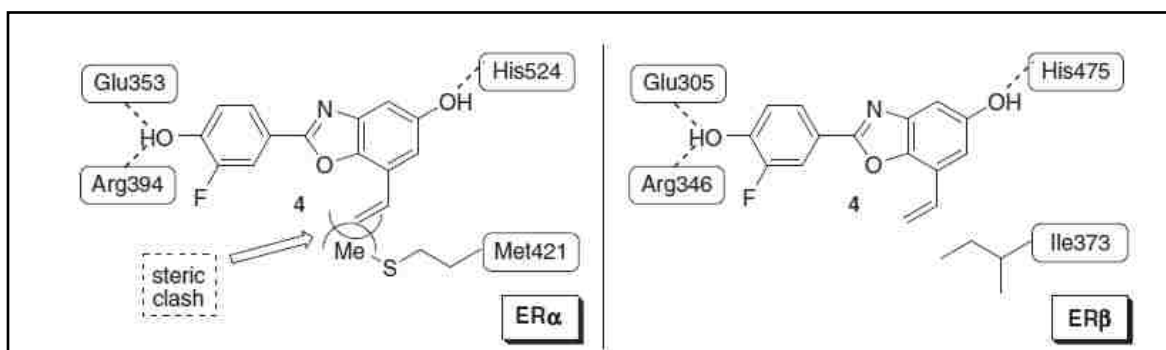


Figure 1.17: ERB-041 binding interactions with ER α and ER β ⁶⁰

In 2006, Eli Lilly group developed a series of polycyclic benzopyran (PBP) derivatives as selective ER β agonists (Figure 1.18).

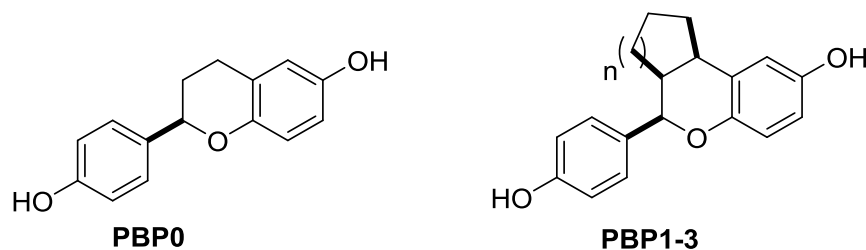


Figure 1.18: Racemic unadorned and racemic all-*cis* 3,4-cyclofused- ($n=1-3$) benzopyrans^{60, 76}

The racemic cyclopentyl annulated benzopyran ($n = 1$) exhibited good activity (0.47nM for ER β and 4.34nM for ER α) and modest selectivity ($\beta/\alpha = 9$). The enantiomers were separated by chiral chromatography and named as SERBA1 and SERBA-2. SERBA-1 demonstrated the higher affinity for both ER β and ER α (ER β , $K_i = 0.19$ nM; ER α $K_i = 2.68$ nM) compared to the enantiomer SERBA-2 (ER β , $K_i = 1.54$ nM; ER α $K_i = 14.5$ nM). Moreover, the ER β /ER α selectivity was greater for SERBA-1 (14.1) compared to SERBA-2 (9.4). This selectivity is mainly attributed to the two different binding orientations of SERBA-1 in both receptors. According to the X-ray crystal structures (Figure 1.19), the most efficient interactions arise with ER β , where the hydroxy of the phenol group is hydrogen bonded to Arg346/Glu305 while the benzopyran hydroxyl forms a H-bond with His475. The fused cyclopentane ring lodges a small hydrophobic pocket, near to Ile373 residue in ER β complex. In ER α , the presence of Met421 makes the pocket too small to accommodate the cyclopentane ring. Thus, binding of SERBA-1 in ER α forces a rotation of 180° along its central axis. This orientation preserves the Arg/Glu H-bonding network, but the OH-His524 H-bonding interaction is weakened due to the greater distance between these groups (Figure 1.20).^{60, 76-77}

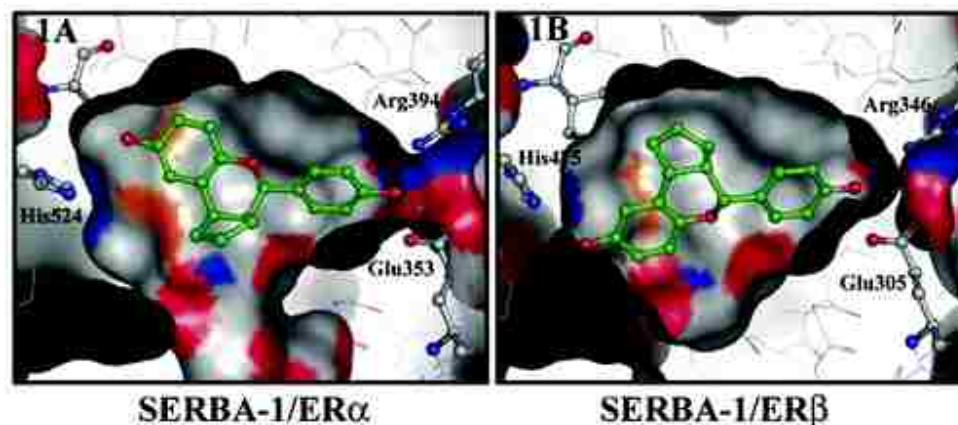


Figure 1.19: “Surface diagram of the X-ray structure of SERBA-1 complexed to ER α (1A) and ER β (1B)”⁷⁷

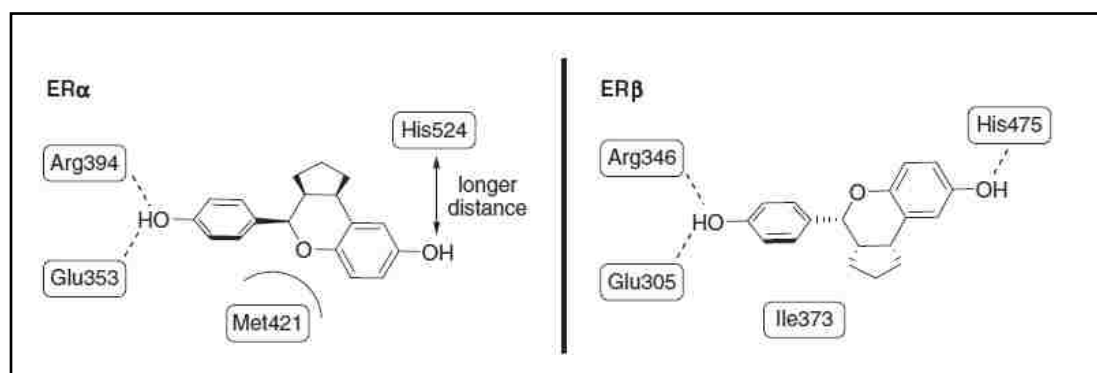


Figure 1.20: SERBA-1 binding interactions with ER α and ER β ⁶⁰

In 2011, the Katzenellenbogen group prepared estrogen analogs lacking the B ring (i.e. ACD- pseudosteroids), as ER β selective agonists (Figure 1.21).⁴⁷ While these authors initially reported⁷⁸ the preparation of a *trans*-hydrindane skeleton, this was later corrected⁷⁹ to a *cis*-hydrindane (ACD-1, Figure 1.21) on the basis of X-ray crystallography. The *trans*-hydrindane structure was eventually prepared⁸⁰ and binding assays were performed on these compounds as well as on selected A-ring substituted variants. From their ACD library, all compounds showed lower overall affinity but more importantly greater selectivity towards ER β .

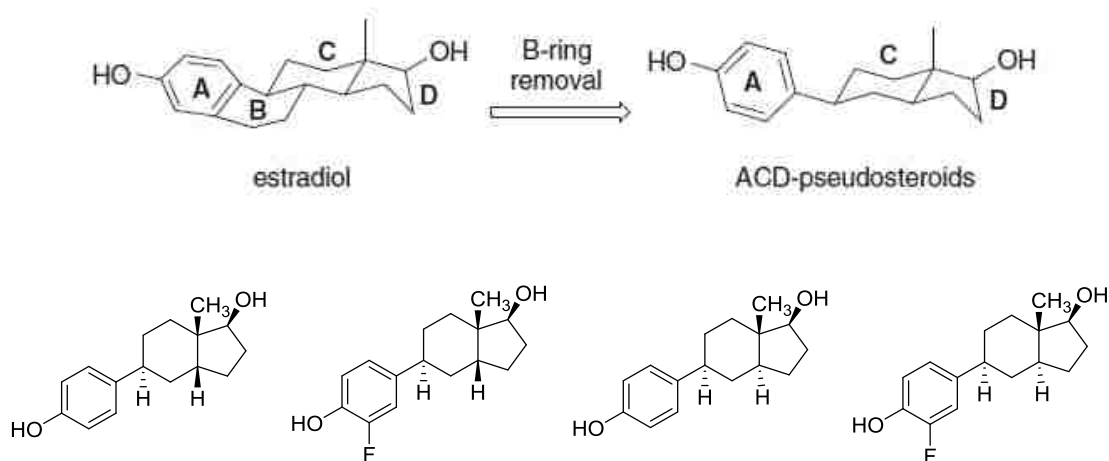


Figure 1.21: Design of ACD-pseudosteroids as ER β selective agonists

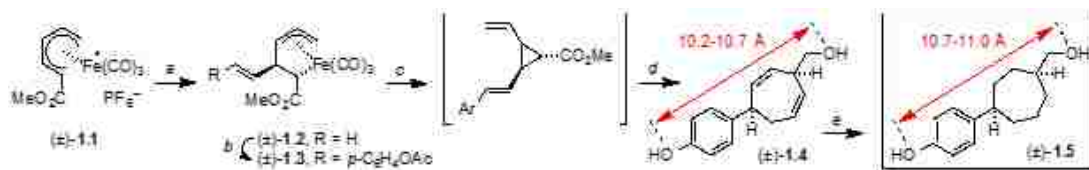
In addition to the aforementioned compounds, several other ER β agonists with varied structural scaffolds (naphthalenes, quinolines, aromatic aldoximes, sulfonamides, salicylaldoximes, and carboranes etc.) have been developed by several research groups.⁵⁸⁻⁶⁰ However, only limited number of compounds display comparable selectivity and potency simultaneously with the acceptable pharmacological profile. Therefore, the challenge faced by ER β targeted drug design process is to develop novel molecules with improved ER β selectivity, potency, as well as reduced side effects.

1.7 Design of 4-Cyclohexyl or Cycloheptyl Phenolic Derivatives as Selective ER β Agonists

The basic requirements for any pharmacophore depends on size, shape and specific interactions with the surrounding residues of the target receptor. While there is a variety of structural classes of molecules that possess greater affinity for the ER β , there are some

significant prerequisites in guiding the development of ER β selective pharmacophores. A phenolic OH is essential to establish the hydrogen bond network involving Arg346, Glu305 and water triad in the ER β binding cavity. A second hydroxyl group, should be positioned nearly $11.0 \pm 0.5 \text{ \AA}$ relative to the phenolic OH in order to exert hydrogen bonding interaction with His475 as well as Thr 299 in ER β . This Thr299-OH interaction is specific to ER β and might contribute to the ER β subtype selectivity. Further, the presence of Met336 and Ile373 residues seems significant since they determine the size of a substituents that can be accommodated within the cavity and thereby ER β selectivity.⁶⁰

Based on these prerequisites, our research group focused on the design of non-steroidal ER β selective agonists for hippocampal memory consolidation in post-menopausal women. In this regards, the Donaldson laboratory developed a unique structural class of compound, *cis*-4-(4-hydroxyphenyl)cycloheptane methanol from organoiron methodology (Scheme 1.3). The compound is comprised of a phenolic and cycloheptane-hydroxymethyl core; the 1st generation synthesis is outlined in Scheme 1.3.⁸¹



Scheme 1.3: 1st generation synthesis of *cis*-4-(4hydroxyphenyl)cycloheptane methanol [reagents: **a**, vinylmagnesium chloride/THF/CH₂Cl₂ (57%); **b**, 4-acetoxystyrene (2 eq), 5% Grubbs' 1st generation catalyst (64%); **c**, H₂O₂/HO⁻, **d**, LiAlH₄, then 140°C. (32%); **e**, H₂, 10% Pd/C (50%)]

The *cis*-4-(4-hydroxyphenyl)cycloheptane methanol proved to be a potent agonist in cell-based ER β agonist assays with an IC₅₀ of $5.4 \pm 0.3 \text{ nM}$ and nearly 1000-fold selectivity for ER β over ER α , making (±)-**1.5** the most selective ER β agonist reported.⁸¹

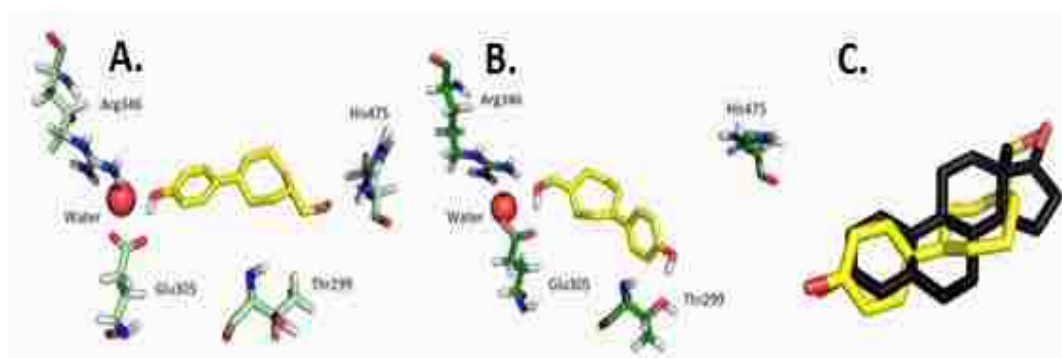


Figure 1.22: Predicted binding orientation of the lead compound **A)** in ER β agonist conformation **B)** in antagonist conformation **C)** Overlay of estradiol (black) and lead compound (yellow)⁸¹

In Figure 1.22 is shown the lowest energy docking representation into human ER α and ER β in agonist and antagonist conformations of our lead compound. Initial docking studies were conducted with estradiol crystal structure to confirm the method validity and obtained results were as expected. Docking pose predictions indicate a higher ER β affinity in agonist conformation where it forms two hydrogen bonds, one with tightly bound water and the other with His 475. On the contrary, a different binding mode is shown in the ER β antagonist conformation where hydrogen bonding of the phenolic hydroxyl is to Thr299 rather than His 475. Moreover, molecular overlay of estradiol and our lead compound reveals the well-aligned nature of both oxygen atoms of the two molecules in the ER β pocket.⁸¹

Using 4-(1-hydroxyphenyl)-1-hydroxymethylcycloheptane as a starting point, the research described in this dissertation seeks to expand on these results. A second scaffold has been developed which exhibits high ER β vs ER α selectivity, as evidenced by cell-based functional assays. Compounds from these two scaffolds were taken forward into

animal model studies for the consolidation of memory acquisition, and information on interactions with hERG, cytochromes and other nuclear receptors was obtained.

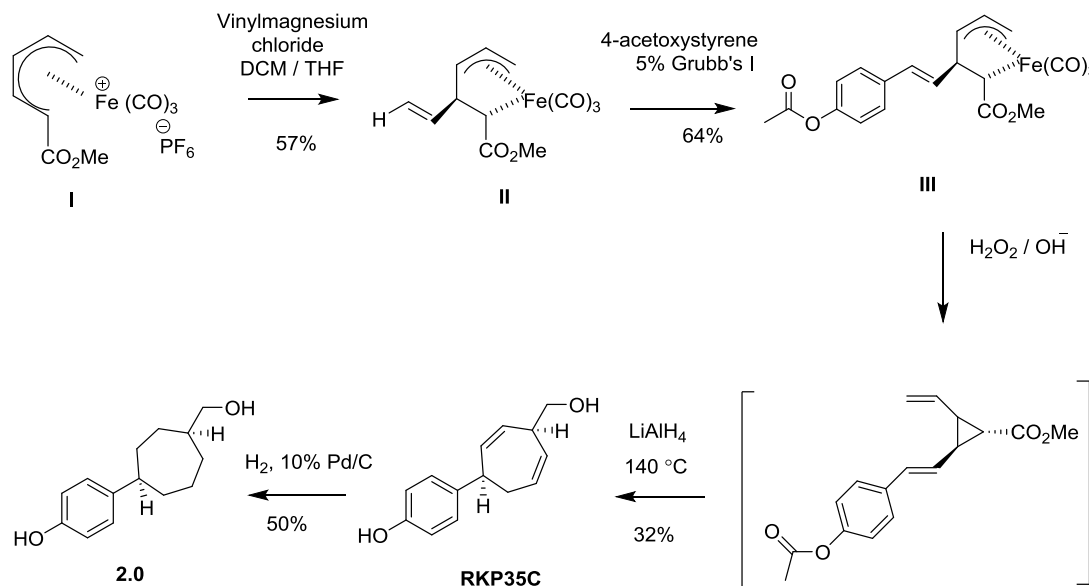
CHAPTER 2

DEVELOPMENT OF 4-(4-HYDROXYPHENYL)CYCLOHEPTANEMETHANOL AND ANALOGUES

2.1 Background and 1st Generation Synthesis of 4-(4-(hydroxyphenyl)cycloheptanemethanol

As part of initial efforts in the Donaldson laboratory to prepare estradiol analogs, an iron-mediated synthesis of 2,6-cycloheptadiene-1-methanols was adapted with olefin cross-metathesis.⁸²⁻⁸³ The first generation synthesis of 4-(4-(hydroxyphenyl)cycloheptanemethanol, as carried out by Dr. Rajesh Pandey, is presented in Scheme 2.1. The precursor, 1-methoxycarbonylpentadienyl) Fe(CO)₃⁺ cation **I**, was prepared from furan in 5 steps (32.8% yield) according to the previously published procedure.⁸⁴ Addition of vinyl magnesium chloride to cation **I**, in CH₂Cl₂ as reaction medium, gave the 2-vinyl-3-pentene-1,5-diyl complex **II** in moderate yield (57%, Scheme 2.1). The cross-metathesis reaction of **II** with 4-acetoxystyrene (2 equivalents) gave complex **III**, along with the self-metathesis products, in 64% yield. Oxidatively induced-reductive elimination of **III**, followed by ester reduction and thermal Cope [3,3] rearrangement afforded (±)-(4-(hydroxymethyl)cyclohepta-2,5-dien-1-yl)phenol **RKP35C** in 32% yield over two steps. Finally exhaustive hydrogenation of **RKP35C** yielded desired (±)-4-(4-(hydroxyphenyl)cycloheptanemethanol in 50% unoptimized yield.⁸¹ Thus the 1st generation synthesis gave **2.0** in 10 steps, 1.9% yield from commercially available furan. While this approach gave initial access to **2.0** for ER binding assays, it has several limitations. These include low overall chemical yield (ca.

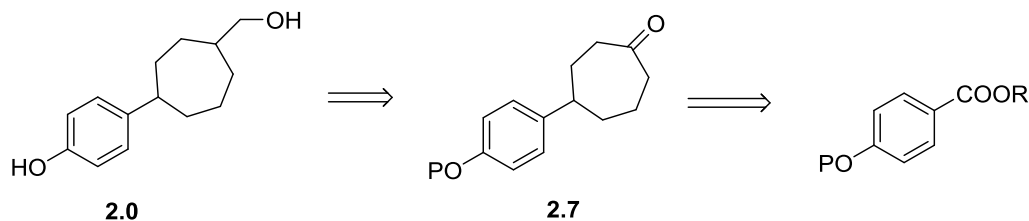
2%), preparation of racemic material, use of stoichiometric iron, access to only the *cis*-stereoisomer and difficulties in translation to other analogs. In addition, attempts to prepare additional samples of **2.0** by this pathway were problematic as the cross-metathesis reaction did not prove robust in a subsequent student's hands. Therefore, a second-generation route to **2.0** was pursued.



Scheme 2.1: 1st Generation synthesis of 4-(4-hydroxyphenyl)cycloheptanemethanol from organoiron methodology

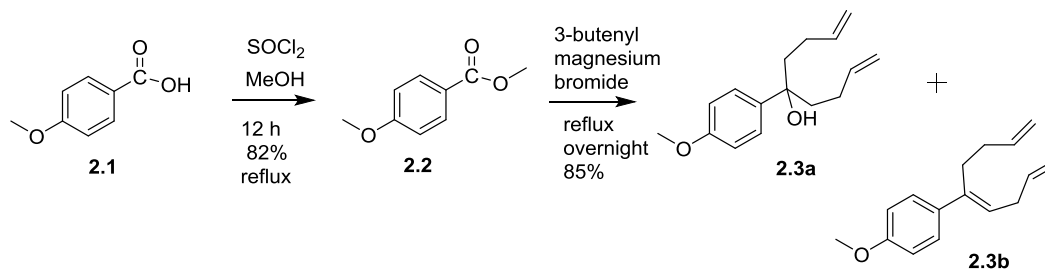
2.2 2nd Generation Synthesis of 4-(4-hydroxyphenyl)cycloheptanemethanol

In order to circumvent a number of the low yielding steps, it was decided to pursue the preparation of **2.0** from a non-organoiron approach. This strategy involved preparation of a protected analog of 4-(4-hydroxyphenyl)cycloheptanone (**2.7**), followed by introduction of the hydroxymethyl substituent (Scheme 2.2).

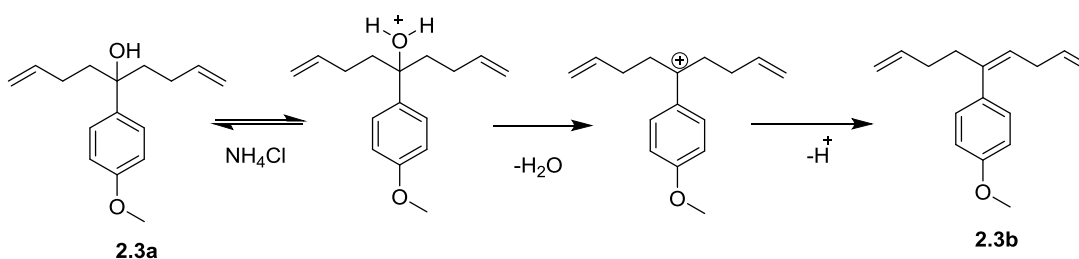


Scheme 2.2: Retrosynthetic analysis for preparation of 4-(4-hydroxyphenyl)-1-hydroxymethylcycloheptane

To this end, esterification of commercially available para-anisic acid **2.1** with thionyl chloride in the presence of methanol led to the formation of methyl 4-methoxybenzoate (**2.2**, Scheme 2.3), which was identified by comparison of its ^1H and ^{13}C NMR spectral data with the literature values.⁸⁵ The Grignard reaction of **2.2** with *in situ* generated 3-butenyl magnesium bromide in 1:4 ratio under dry conditions gave the 3° alcohol **2.3a** as a major product (85%). Obtaining these yields was dependent on a number of crucial experimental conditions. Use of 4-equivalents of Grignard reagent was necessary; use of only 2 equivalents of 3-butenyl magnesium bromide gave a lower yield (13%). In addition, the length of time for exposure of the crude reaction mixture to the NH_4Cl workup conditions must be kept short, since longer exposure led to the formation of triene **2.3b** (Scheme 2.3) as a by-product. The formation of compound **2.3b** can be rationalized by slow dehydration of **2.3a** in the presence of acidic ammonium chloride ($\text{pK}_a = 9.24$) (Scheme 2.4).



Scheme 2.3: Preparation of tertiary alcohol intermediate **2.3a**

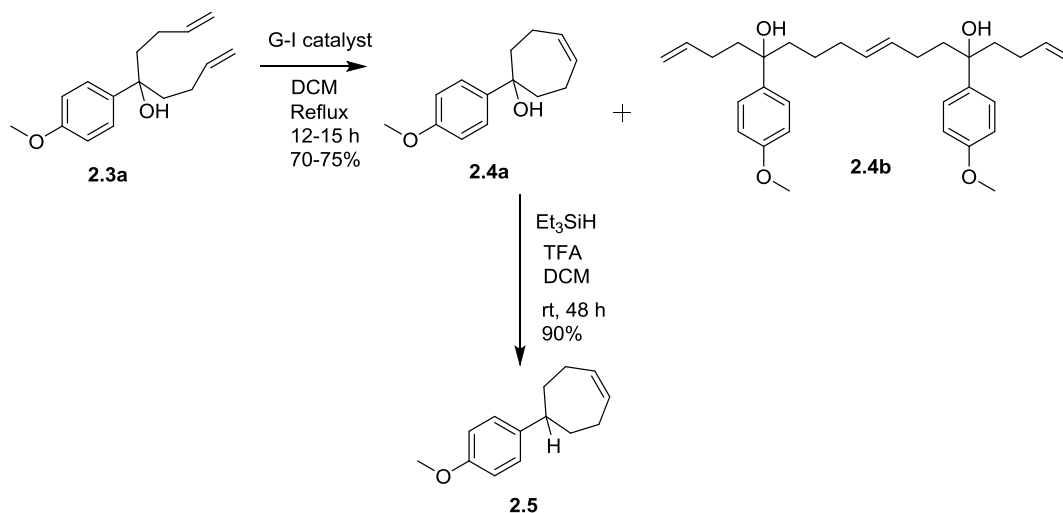


Scheme 2.4: Mechanism of formation of compound **2.3b**

The structures of **2.3a** and **2.3b** were assigned on the basis of their NMR spectral data. In particular, the signals at δ 4.88 – 4.98 (m, 4 H) and 5.73 - 5.84 (m, 2 H) ppm in the ^1H NMR spectra of each are characteristic for the vinyl protons while two doublets of doublets at δ 6.88 and 7.28 ppm are typical for a 1,4-disubstituted phenyl substituents. The peak at δ 76.9 ppm in the ^{13}C NMR spectrum of **2.3a** was assigned to the tertiary alcohol carbon. A triplet signal at δ 5.8 ppm in the ^1H NMR spectrum of **2.3b** was assigned to the proton of the trisubstituted olefin.

Reaction of **2.3a** with Grubbs' 1st generation catalyst (G-I) under optimum experimental conditions (0.01 M concentration, slow addition of 4% of G-I over 8 h via syringe pump, 45 °C, and G-I quench with 50 equiv. DMSO) led to **2.4a** as a major product

in 70- 75% yield (Scheme 2.5). However, in certain instances the formation of self- or cross metathesis (CM) product **2.4b** from **2.3a** was observed (Scheme 2.5).



Scheme 2.5: Ring closing metathesis and ionic reduction

The structural assignment for **2.4a** was based on its NMR spectral data. In particular, signals at δ 5.83-5.86 (m, 2 H) and at δ 1.82-1.90 (m, 2 H), 1.97-2.10 (m, 4 H), 2.44-2.55 (m, 2 H) in the ^1H NMR spectrum of **2.4a** correspond to the hydrogens within the cycloheptenol ring, while signals at δ 113.5 and 76.5 ppm in the ^{13}C NMR spectrum correspond to the cycloheptenol olefinic and alcohol carbons respectively.

Ionic reduction⁸⁶ **2.4a** with 5 equivalents of triethylsilane and 10 equivalents of trifluoroacetic acid, in dry CH_2Cl_2 , gave **2.5** (90%). The removal of the OH group was confirmed by the presence of a signal at δ 49.4 ppm in the ^{13}C NMR spectrum and a triplet of triplets at δ 2.69 ppm in ^1H NMR spectrum which correspond to the benzylic carbon and its attached proton.

Our first strategy for olefin-to-ketone conversion relied on epoxidation of **2.4a** with meta-chloroperoxybenzoic acid to provide a mixture of *cis*- and *trans*-epoxides **2.5a** (I and

II, Figure 2.1) in good yield (74%). The structure of **2.5a** was assigned based on its ^1H NMR spectral data; no olefinic proton signals were observed and instead two new triplets of triplets and three multiplets were observed in δ 2.14-3.19 ppm region. The same behavior was observed in the ^{13}C NMR spectrum where the eighteen signals appear as a doublet set of nine for each stereoisomer.

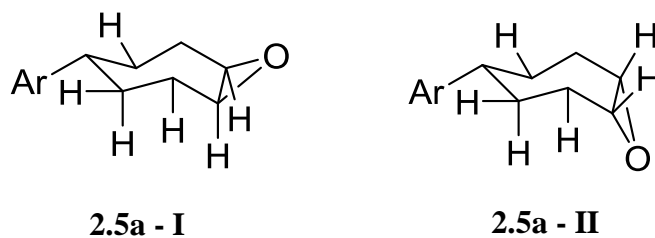
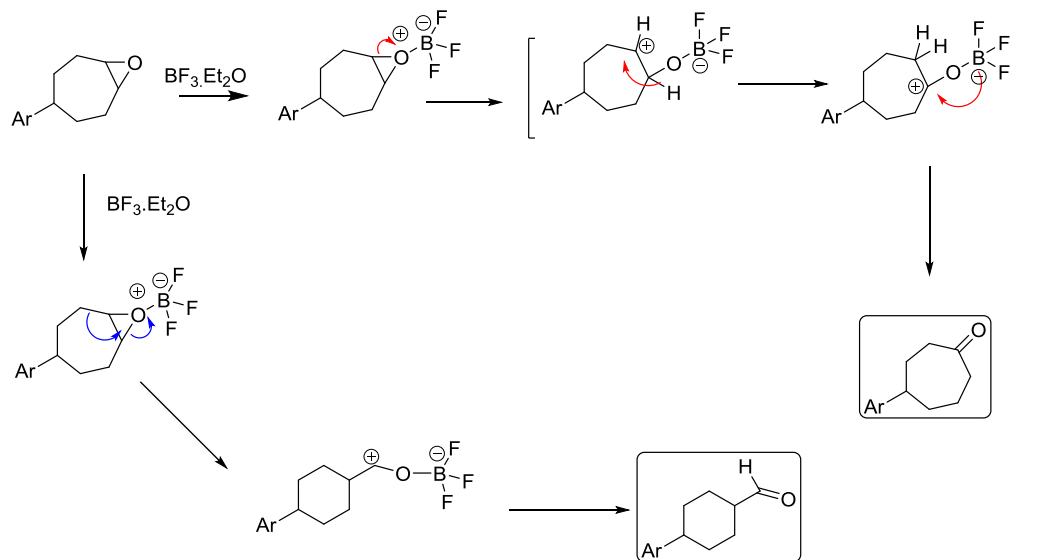


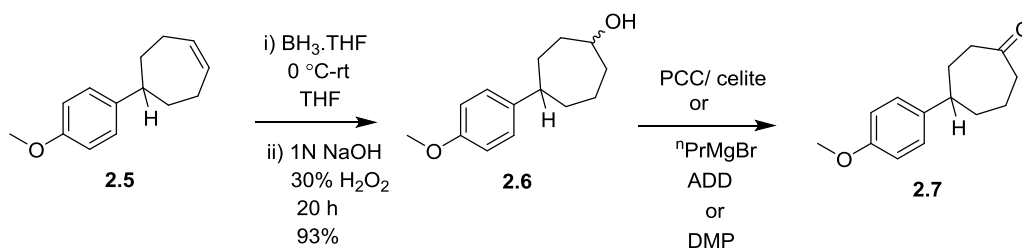
Figure 2.1: Diastereomers of compound **2.5a** (I and II)

Lewis acid-mediated ring opening of epoxide **2.5a** was carried out with boron trifluoride etherate in anhydrous benzene to give the known⁸⁷ cycloheptanone **2.7**, albeit in low yield (26%). Moreover, an aldehydic by-product was observed which can be rationalized by the following mechanism (Scheme 2.6).



Scheme 2.6: Possible mechanism for generation of **2.7** and aldehydic by-product

Alternatively, hydroboration of compound **2.5** with $\text{BH}_3\cdot\text{THF}$ followed by oxidation from 30% H_2O_2 and 1N NaOH gave alcohol **2.6** in 93% yield (Scheme 2.7). Notably, attempted oxidative workup with sodium borate gave **2.6** in lower yields (20-30%). The absence of the olefinic signals and the presence of two multiplets at δ 3.90-4.06 ppm (1H) in ^1H NMR spectrum of **2.6** and the presence of two new peaks at δ 72.7, 71.5 ppm in its ^{13}C NMR spectrum support the presence of this product as a mixture of diastereomers.



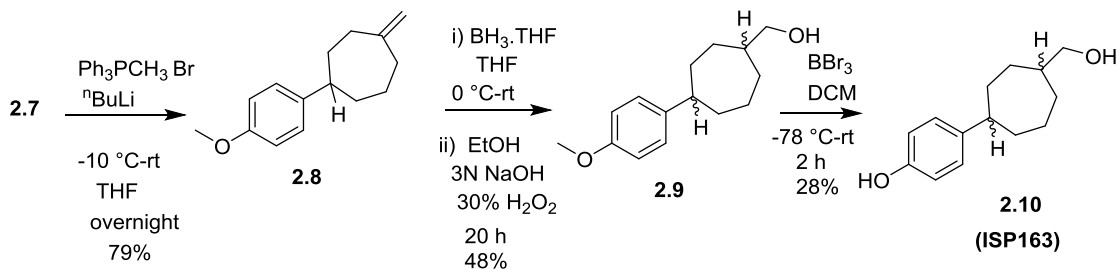
Scheme 2.7: Transformation of olefin **2.5** into cycloheptanone **2.7**

Oxidation of the secondary alcohol **2.6** to the corresponding ketone **2.7** was effected using either pyridinium chlorochromate and silica or celite as an adsorbent (55% yield), or n-propylmagnesium bromide and 1,1'-(azodicarbonyl)dipiperidine (20% yield),⁸⁸ or Dess-Martin periodinane with addition of 2-5 drops of water (50% yield, Scheme 2.7). The product was identified by comparison of its spectral data with the literature values.⁸⁷

Wittig reaction of **2.7** with two equivalents of the ylide generated from reaction of methyltriphenylphosphonium bromide with $^n\text{butyllithium}$ provided the exocyclic olefin **2.8** (79%, Scheme 2.8). The structural assignment of **2.8** was supported by the presence of characteristic peaks for the exocyclic alkene at δ 4.77 (2H) ppm in the ^1H NMR spectrum and δ 113.8 and 110.9 ppm in the ^{13}C NMR spectrum.

Hydroboration of **2.8** with $\text{BH}_3 \cdot \text{THF}$, followed by oxidation with 30% H_2O_2 and 3N NaOH afforded alcohol **2.9** (48-60%) as a mixture of *cis*- and *trans*- diastereomers (Scheme 2.8). The doublet at δ 3.46 ppm (2H) in the ^1H NMR spectrum of **2.9** and peaks at δ 68.6 and 68.4 in ^{13}C NMR spectrum were evidence of this mixture.

Finally, deprotection of the methyl ether was achieved under BBr_3 conditions to give the desired 4-(4-(hydroxyphenyl)cycloheptanemethanol **2.10 (ISP163)** (28%) as a mixture of *cis*- and *trans*-isomers (Scheme 2.8). The *cis*-stereoisomer was identified by comparison of its NMR spectral data with the literature values,⁸¹ while the doubling of many of the peaks was taken as evidence of the *trans*-stereoisomer. This assignment of the ^{13}C NMR signals for the *trans*-stereoisomer was eventually corroborated by HPLC separation of the stereoisomers as well as X-ray crystallography (*vide infra*)

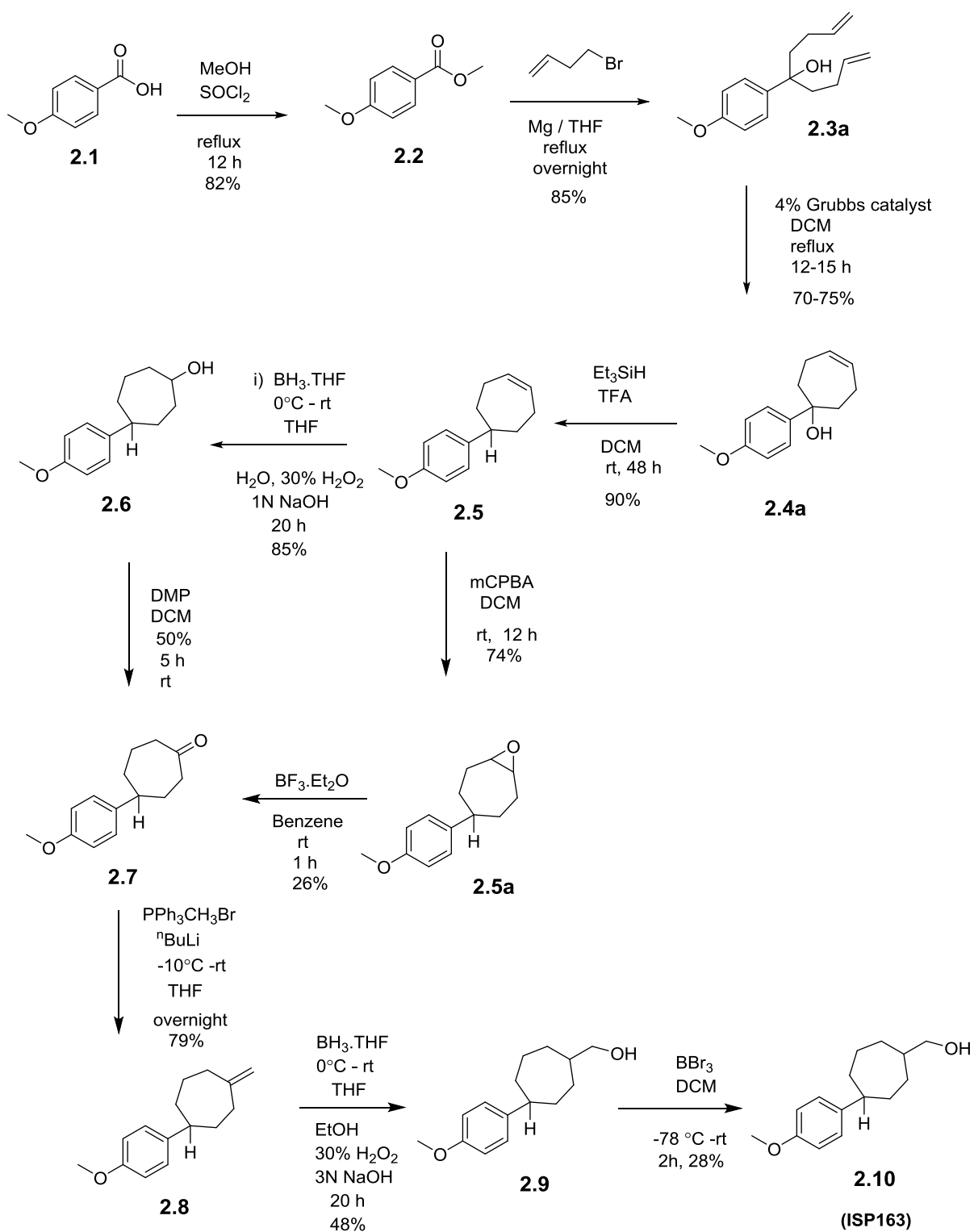


Scheme 2.8: Conversion of **2.7** into 4-(4-(hydroxyphenyl)cycloheptanemethanol

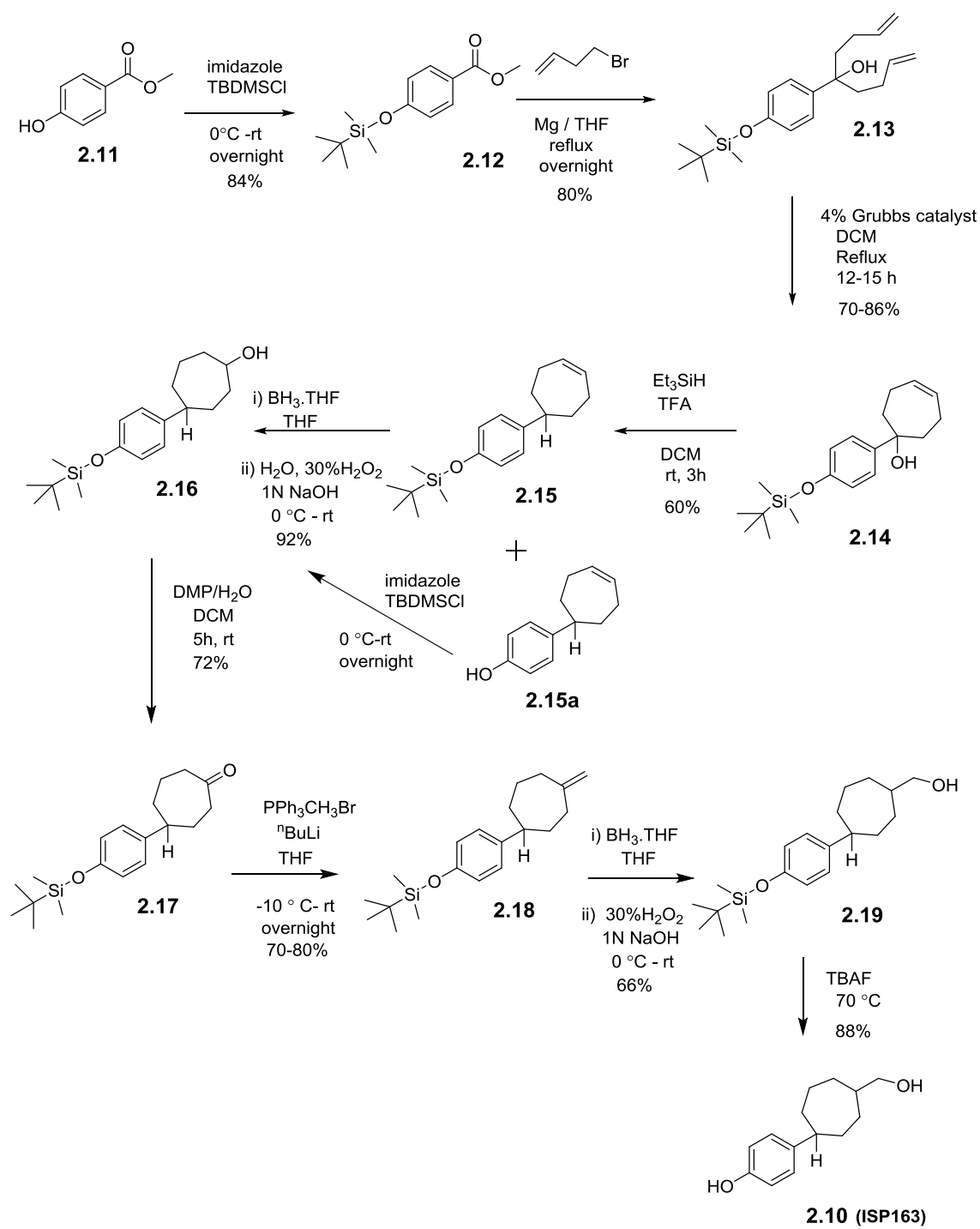
The overall route (summarized in Scheme 2.9) requires 9 steps from commercially available material, and while it proceeded in a slightly improved overall yield (2.1%), compared to the original synthesis, the harsh conditions of the final step dictated the need for a different phenolic protecting group.

2.3 3rd Generation Synthesis of 4-(4-hydroxyphenyl)cycloheptanemethanol

Our next focus was to introduce a readily cleavable protecting group. Protection of commercially available methyl 4-hydroxybenzoate **2.11** as the t-butyldimethylsilyl ether provided **2.12** (84%, Scheme 2.10). Characteristic signals for the t-butyl and two methyl groups appear at δ 0.99 (9H) and 0.22 (6H) ppm in the ^1H NMR spectrum and at δ 18.1/25.7 and -4.3 ppm respectively in the ^{13}C NMR spectrum of **2.12**. The same 7 step synthetic sequence (Grignard addition, RCM, ionic reduction, hydroboration/oxidation, Wittig olefination, hydroboration/oxidation) eventually led to **2.19** under optimized conditions. However, the ionic reduction of **2.14** under acidic conditions, proceeded in a lower 60% yield due to silyl ether cleavage to give the degraded by-product **2.15a**. The by-product **2.15a** could be recycled by further TBDMS protection. Use of 3N NaOH in the oxidative workup for hydroboration/oxidation of **2.18** also resulted in cleavage of the TBDMS group and afforded lower yields (40%). Alternatively, use of 1N NaOH for the workup gave the product **2.19** without silyl ether cleavage (66%). Deprotection of **2.19** was carried out under TBAF conditions to give **2.10 (ISP163)** in 88% yield as a clean product. Following this procedure, the mixture of stereoisomers was obtained in 9 steps from commercially available methyl 4-hydroxybenzoate, and in 10.7% overall yield.



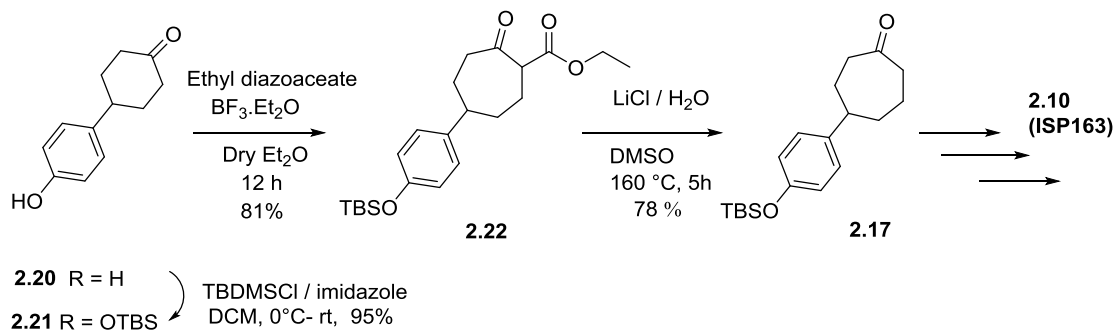
Scheme 2.9: 9-Step, 2nd generation synthesis of 4-(4-(hydroxyphenyl)cycloheptane methanol (2.1% yield)



Scheme 2.10: 3rd Generation synthesis of 4-(4-(hydroxyphenyl)cycloheptanemethanol (10.7% yield)

2.4 4th Generation Synthesis of 4-(4-hydroxyphenyl)cycloheptanemethanol

While the 3rd generation synthesis (Scheme 2.10) proceeded in 4.4% yield, the length of this route (9 steps) and the use of expensive precursors (4-bromo-1-butene, \$ 248/mol) and reagents (Grubbs' 1st generation catalyst, Dess-Martin periodinane) necessitated the development of a shorter synthesis of intermediate **2.17**. This synthesis commenced from commercially available 4-(4-hydroxyphenyl)cyclohexanone **2.20** that was protected with TBDMSCl to give the silyl ether **2.21** (95%, Scheme 2.11). The presence of peaks at δ 0.98 (9H) and 0.19 (6H) ppm in ¹H NMR verifies the product formation. Ring expansion of cyclohexanone ring to cycloheptanone ring (**2.22**) was achieved under Büchner–Curtius–Schlotterbeck conditions⁸⁹ with the use of ethyl diazoacetate and boron trifluoride etherate in dry ether (81%). Krapcho-decarboethoxylation of keto-ester **2.22** with LiCl/ H₂O in DMSO at 160 °C furnished the key intermediate **2.17** in 78% yield. Subsequent transformation of **2.17** to **2.10**, by the route previously developed in Scheme 2.10, resulted in an 6-step, 20% overall yield route to a mixture of *cis*- and *trans* isomers of 4-(4-(hydroxyphenyl)cycloheptanemethanol. Utilizing this route, a sample of 2 g of **2.10** was eventually prepared. This mixture of stereoisomers was subjected to ER binding assays; the results of these assays are described in Chapter 4.



Scheme 2.11: Preparation of 4-(4-(hydroxyphenyl)cycloheptanone) intermediate by ring expansion

2.5 Separation of Stereoisomers of 4-(4-(hydroxyphenyl)cycloheptanemethanol

Since the 2nd, 3rd, and 4th generation syntheses furnished the target compound as a mixture of four stereoisomers, the next aim was to separate these isomers in order to identify the most potent candidate. Figure 2.2 depicts the analytical HPLC chromatogram of **ISP163** using a chiral cellulose 2(OZH) column with isopropanol : hexanes (1:4) as eluent and UV detection at 254 nm. This clearly reveals the presence of 4 stereoisomers at different retention times.

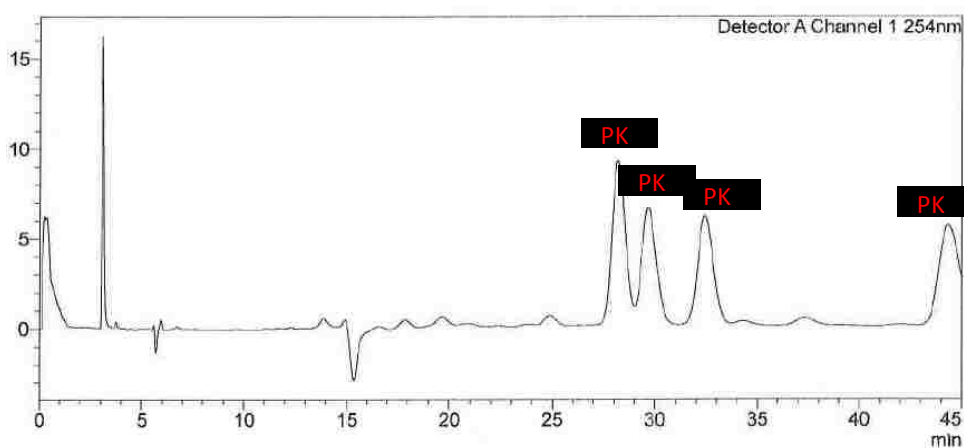


Figure 2.2: Identification of presence of four isomers of **ISP163**

Due to the prohibitive cost of a preparative HPLC column, it was decided to contract a preparative separation of the mixture, to access the individual isomers. This would provide sufficient quantities of the stereoisomers for ER binding assay as well as absolute configuration determination. The company Phenomenex (Torrence, CA) was contracted for these chromatographic services.

Initial analytical method development by Phenomenex revealed that a Lux Cellulose-35 μm column and isocratic mobile phase of ethanol: 2-propanol: hexanes (4.33:8.66:87) was optimal, with detection at 280 nm. The isolation process utilized a 250 x 30 mm preparative column and the aforementioned solvent system. This method produced a 12 min HPLC run with the first desired peak eluting just before 8 minutes (Figure 2.3). The blue color zones were collected as pure isomeric products.

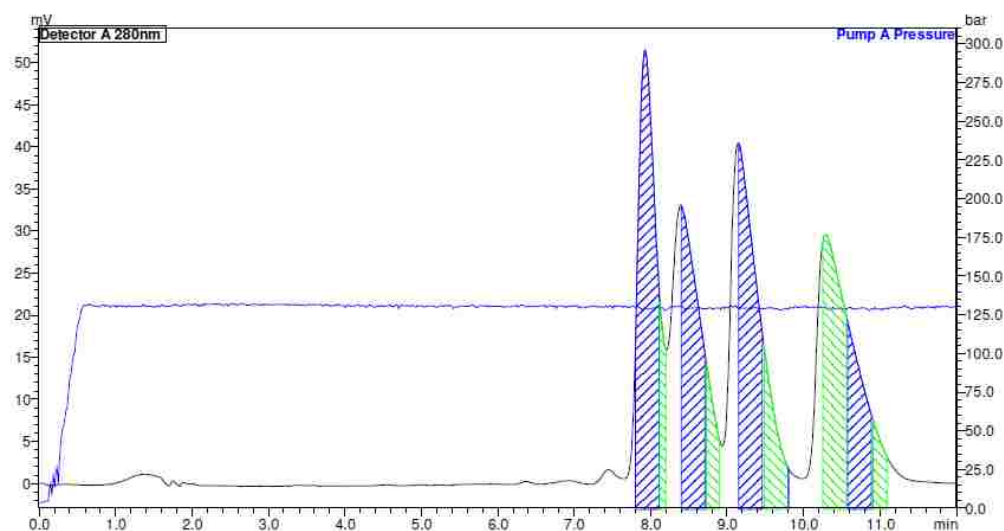


Figure 2.3: Prep Chromatogram of **ISP163** for a single injection (courtesy of Phenomenex)

Since these conditions were isocratic, stacked injections were implemented to accelerate the process. In this regards, subsequent injections were made 6 min after the

previous injection with the products from the first injection collected shortly after the second injection was made (Figure 2.4).

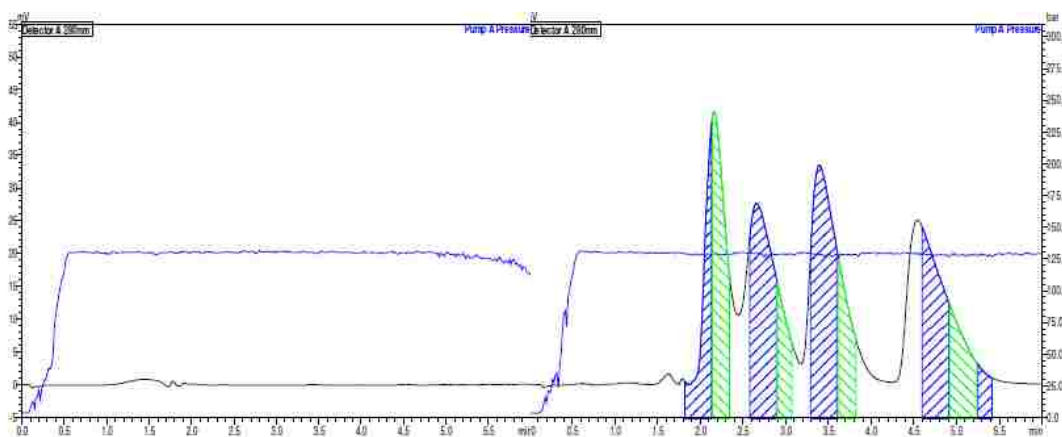


Figure 2.4: Implemented Stacked Injections for **ISP163** (courtesy of Phenomenex)

Analytical QC was developed to assess the separation. Two Lux Cellulose-35 μm 150 x 4.6 mm columns were used in series with ethanol : 2-propanol : hexanes (2 : 7 : 91) as an isocratic solvent system (Figure 2.5). The analytical QC chromatograms confirmed separation of the stereoisomers and indicated that each fraction was of > 94% enantiomeric excess.

However, these chromatograms also indicated “system” impurity peaks at ca. 7.5 and 9.5 min. Furthermore, ^1H NMR analysis of the fractions returned by Phenomenex indicated signals due to an unidentifiable contaminant. Fortunately, this contaminant was considerably more soluble in CDCl_3 than the desired compound, and thus extracting the solids with this solvent gave a solid product which was essentially contaminant free by ^1H NMR spectroscopy (Figure 2.6).

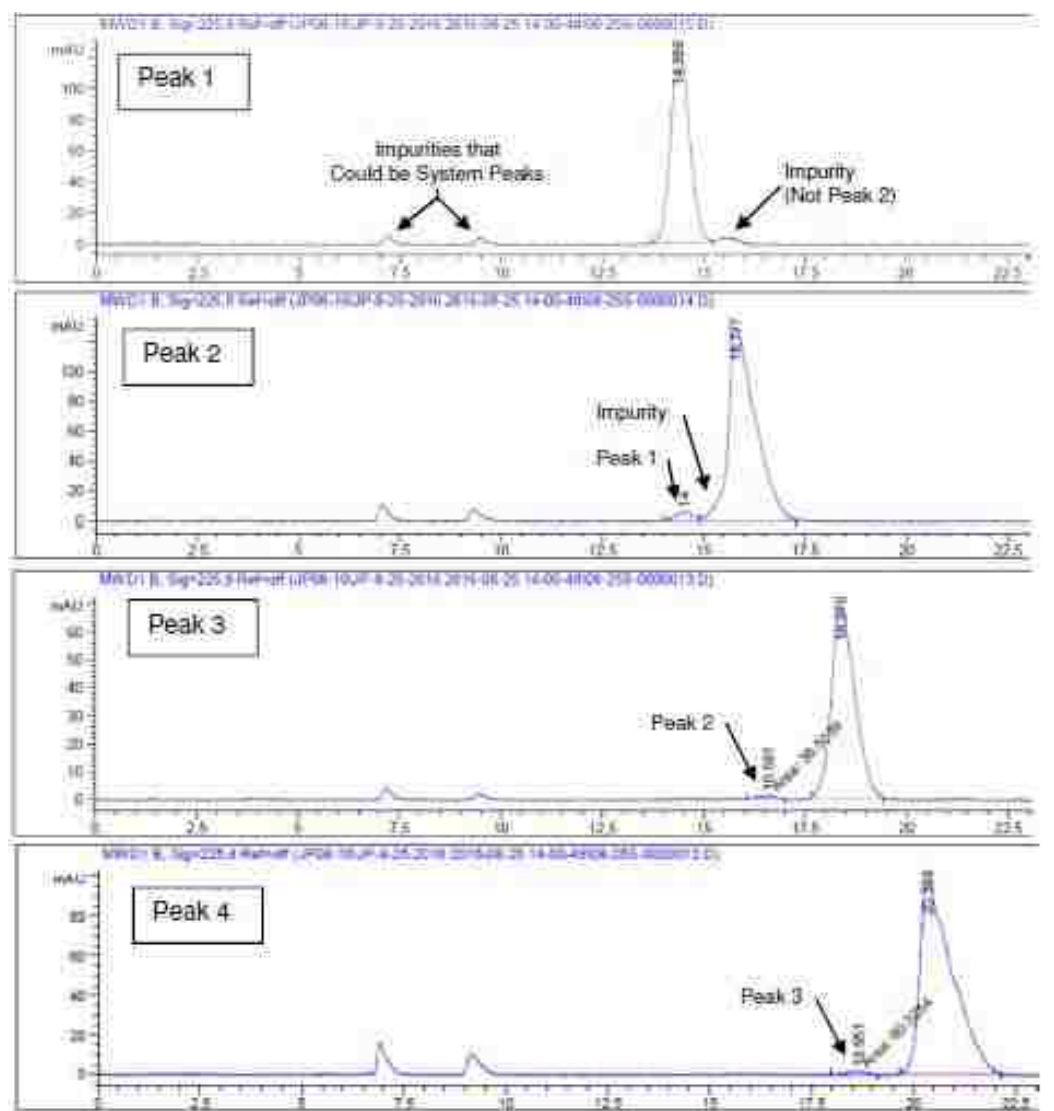


Figure 2.5: Analytical QC chromatograms of all four isomers of **ISP163** (courtesy of Phenomenex)

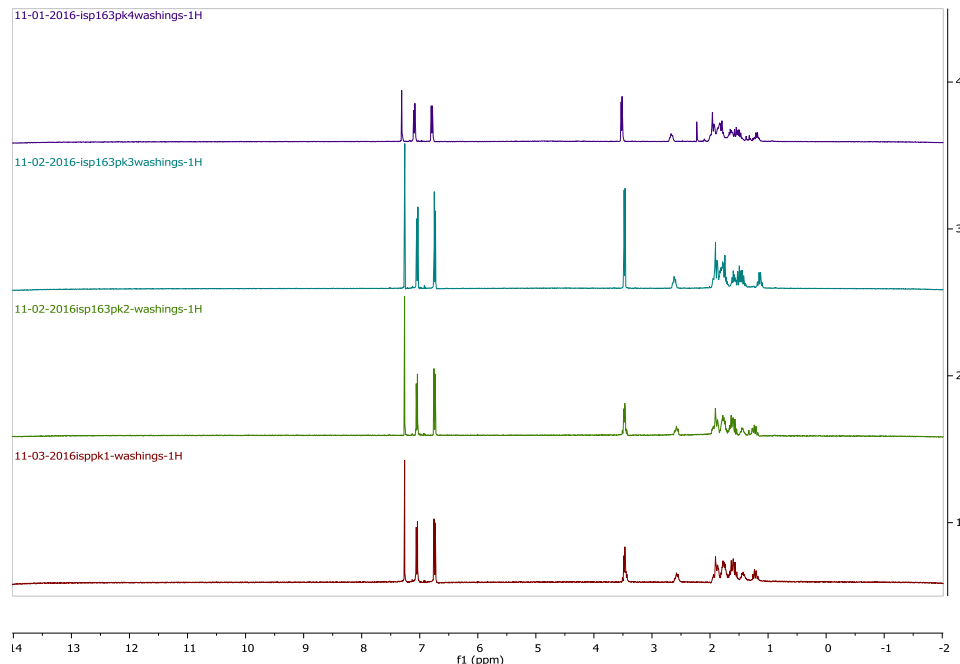


Figure 2.6: ^1H NMR analysis of all four isomers of **ISP163**

Comparison of the ^{13}C NMR spectra of peaks 3 and 4 with that previously obtained for *cis*-4-(4-(hydroxyphenyl)cycloheptanemethanol (obtained from the 1st generation synthesis), indicated that these fractions corresponded to the *cis*-isomer, and by deduction the lack of correspondence of the ^{13}C NMR spectra for peaks 1 and 2 with the previously obtained material indicated that they had the *trans*-stereochemistry. These spectroscopic assignments were eventually corroborated by single crystal X-ray diffraction of three of the fractions. Figure 2.7 contains the ORTEP projections of peak 3 and peak 4 isomers, including not only relative configuration (*cis*) but also absolute stereochemistry (7R, 10S for peak 3; 7S, 10R for peak 4, crystallographic numbering). The 7-membered ring in each structure has a somewhat twisted long chair confirmation.

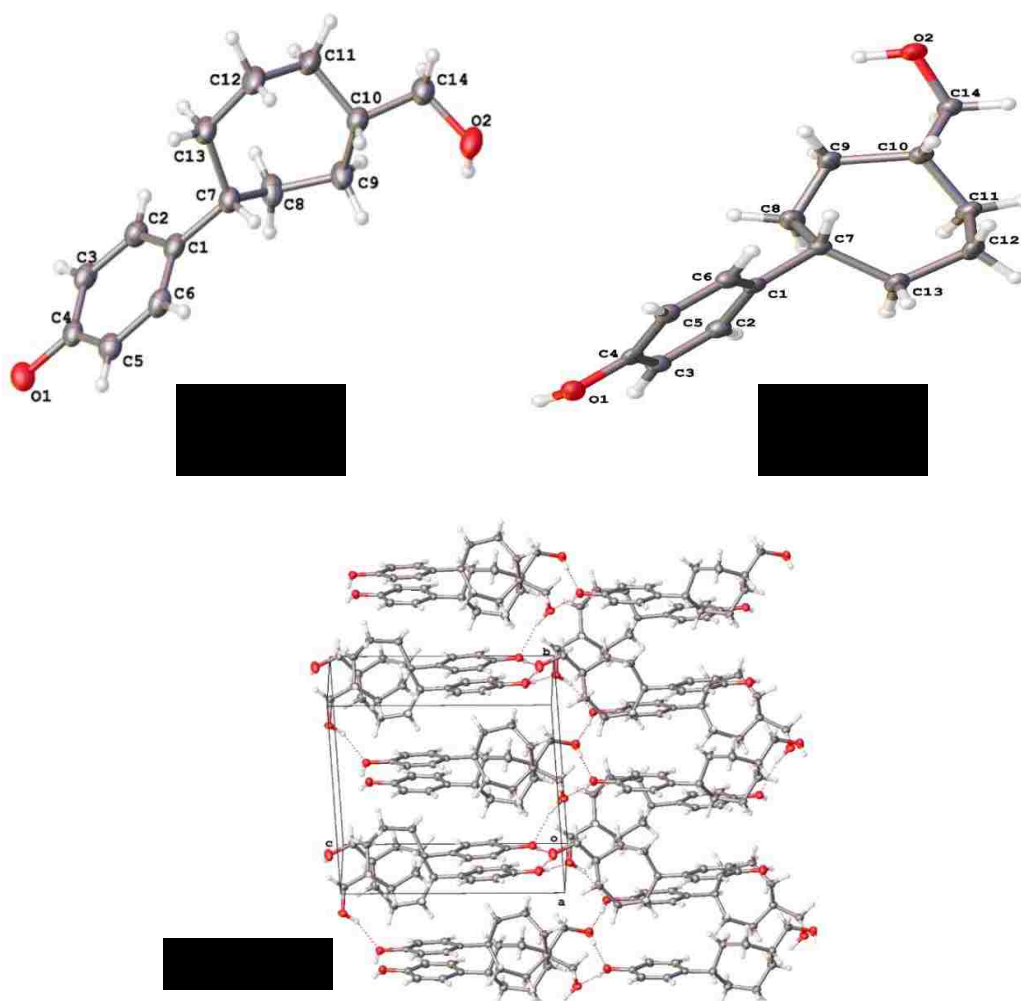


Figure 2.7: a) ORTEP projections of the stereoisomers of trans- 4-(4-(hydroxyphenyl)cycloheptanemethanol; a) peak 3 (7R, 10S); b) peak 4 (7S, 10R); c) 3D-crystal packing of peaks 3 and 4 (identical) in solvent

The X-ray crystal structure of the peak 1 isomer contains two symmetrically independent molecules of the same chirality (Figure 2.8). The ordered 7-membered ring in structure **a** has a long chair conformation with both substituents in an equatorial orientation. However, the situation with structure **b** is more complex since it has a disordered 7-membered ring structure with an overlap of 7/10,11-chair over 10/7,13-chair. Thus, the absolute configuration of this isomer was indeterminate.

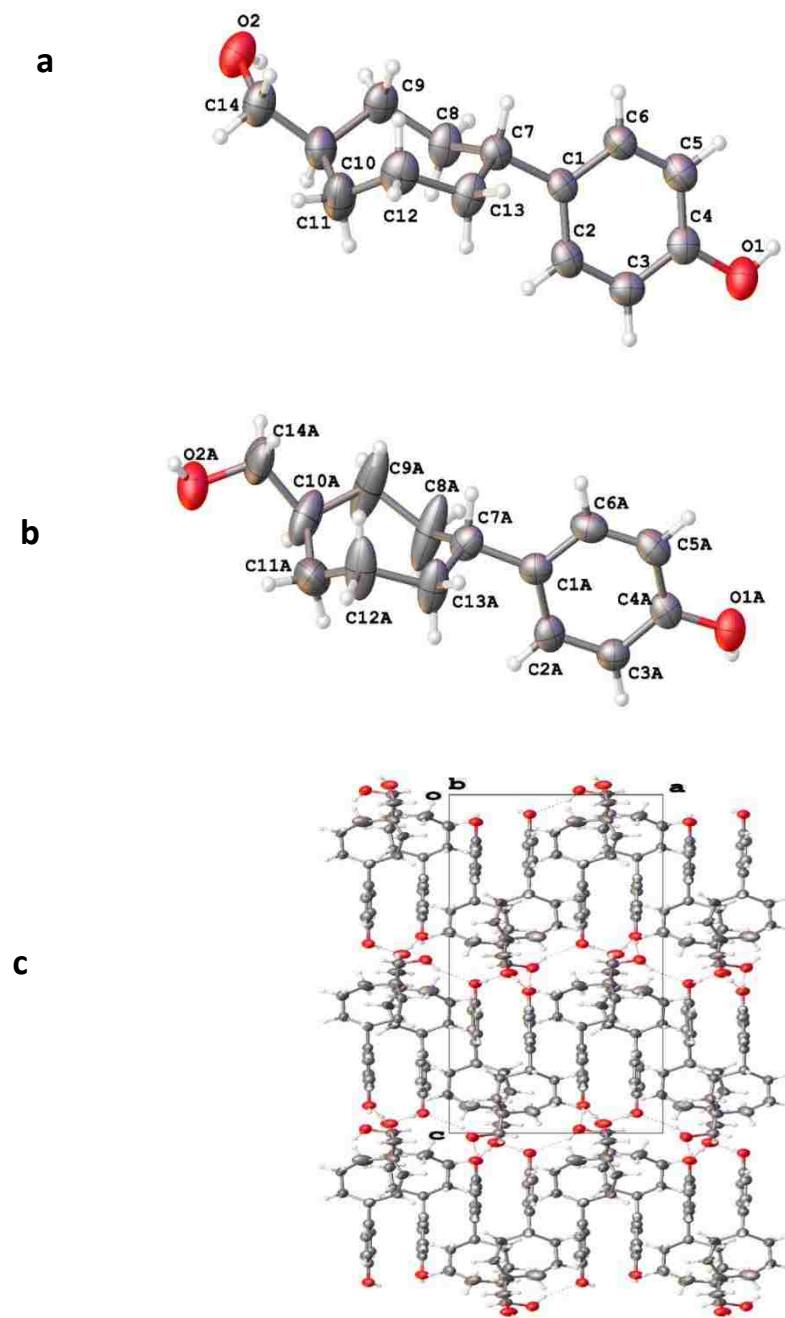
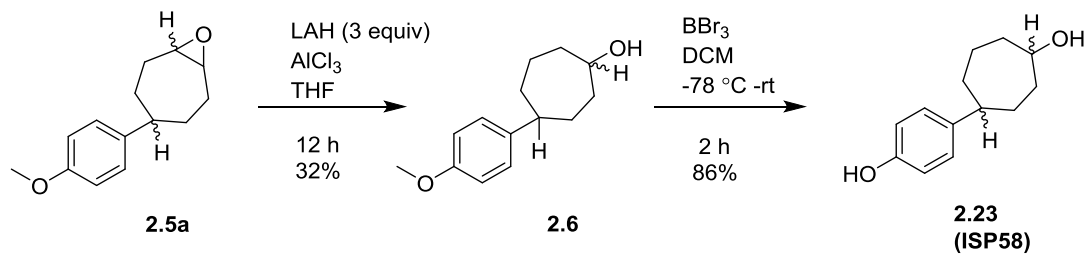


Figure 2.8: a) and b) Two possible X-ray crystal structure of pk1 isomer c) 3D-crystal packing in solvent

2.6 Synthesis of Other 4-Cycloheptylphenol Analogues for SAR Studies

Having established **ISP163** (compound **2.10**) as a lead compound, our next approach was to design a series of 4-cycloheptylphenol based analogs with various functional moieties in order to test the SAR studies.

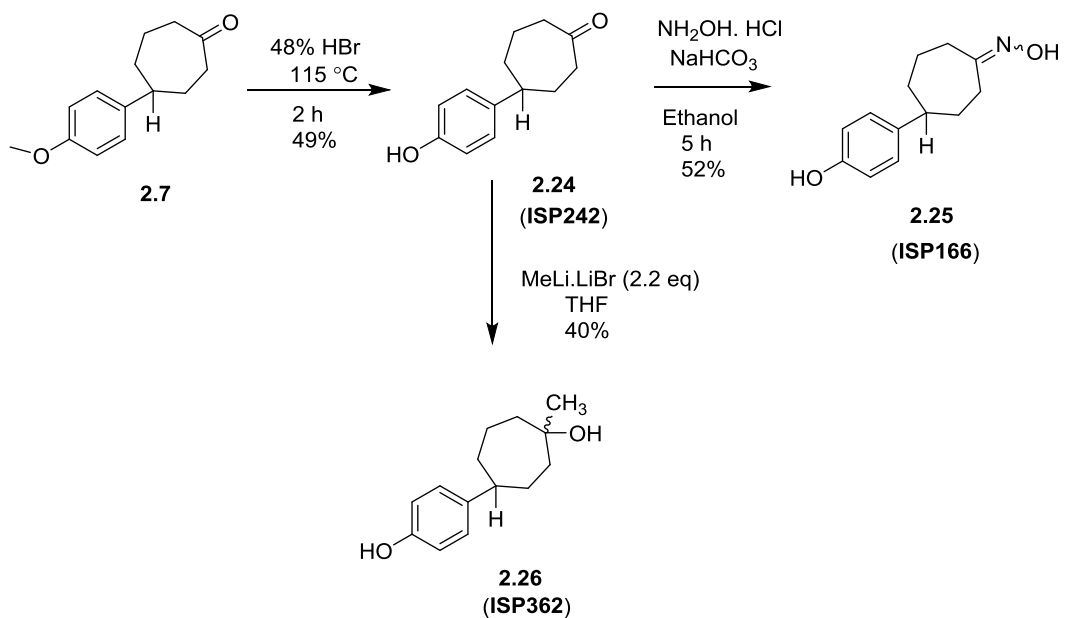


Scheme 2.12: Synthesis of analog **2.23**

Treatment of the mixture of diastereomeric epoxides **2.5a** with three equivalents of lithium aluminum hydride in dry THF, gave a mixture of two diastereomeric alcohols **2.6** in low yield (35%) which were identified by comparison of their NMR spectra with that previously prepared. (Scheme 2.12). Since the two diastereomers did not show clear separation by TLC, the mixture was carried forward in the next reaction step. The mixture of diastereomers **2.6** was subjected to the ether cleavage using excess BBr_3 in anhydrous CH_2Cl_2 to afford compound **2.23** (86%, **ISP58**). The product was a mixture of diastereomers (1:1 ratio) and the presence of the phenol group was confirmed by a singlet at 4.84 ppm assigned to the phenolic hydrogen in its ^1H NMR spectrum.

Cycloheptanone **2.7** was demethylated with 48% HBr under refluxing conditions to afford phenol **2.24** (49%, **ISP242**, Scheme 2.13). The use of BBr_3 conditions was problematic, as the ^1H NMR spectrum of the crude product did not show any peaks belonging to a ketone functionality. The removal of the methyl ether in **2.24** was evidenced

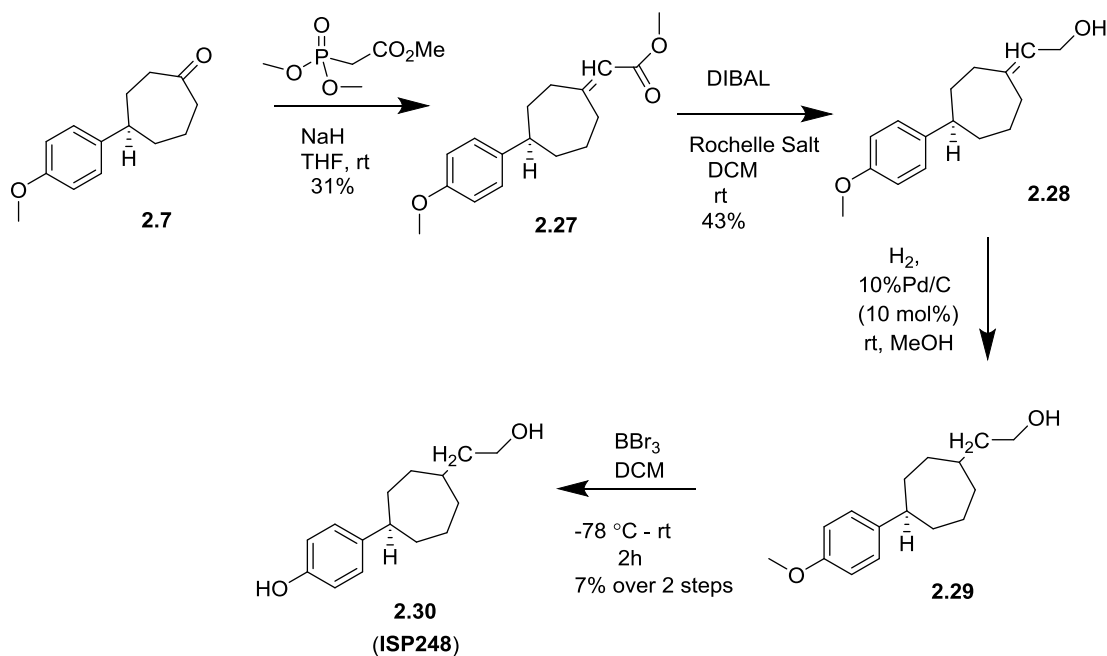
by an absence of the signals for the OMe group. Reaction of **2.24** with hydroxylamine hydrochloride in the presence of NaHCO₃ gave oxime **2.25** (52%, **ISP166**) as a mixture of *E*- and *Z*- stereoisomers. The occurrence of characteristic signals at δ 140.4 and 141.3 ppm in the ¹³C NMR spectrum of **2.25** corresponded to the C=N carbons of the diastereomers. Alternatively, treatment of phenolic cycloheptanone **2.24** with 2.2 equivalents of MeLi. LiBr complex provided the diastereomeric tertiary alcohol **2.26** (40%, **ISP362**). The two singlets at δ 1.23 and 1.21 ppm in ¹H NMR spectrum, integrating to three protons in total, correspond to the methyl group of the diastereomeric product.



Scheme 2.13: Synthesis of analogs **2.24**, **2.25** and **2.26**

Horner–Wadsworth–Emmons olefination of **2.7** with the anion generated from the reaction of trimethyl phosphonoacetate with NaH gave **2.27** as a mixture of *E*- and *Z*- stereoisomers (31%, Scheme 2.14). Formation of the 3,3-disubstituted enoate was evidenced by the presence of a singlet at δ 5.74 ppm and two singlets at δ 3.69 ppm in the

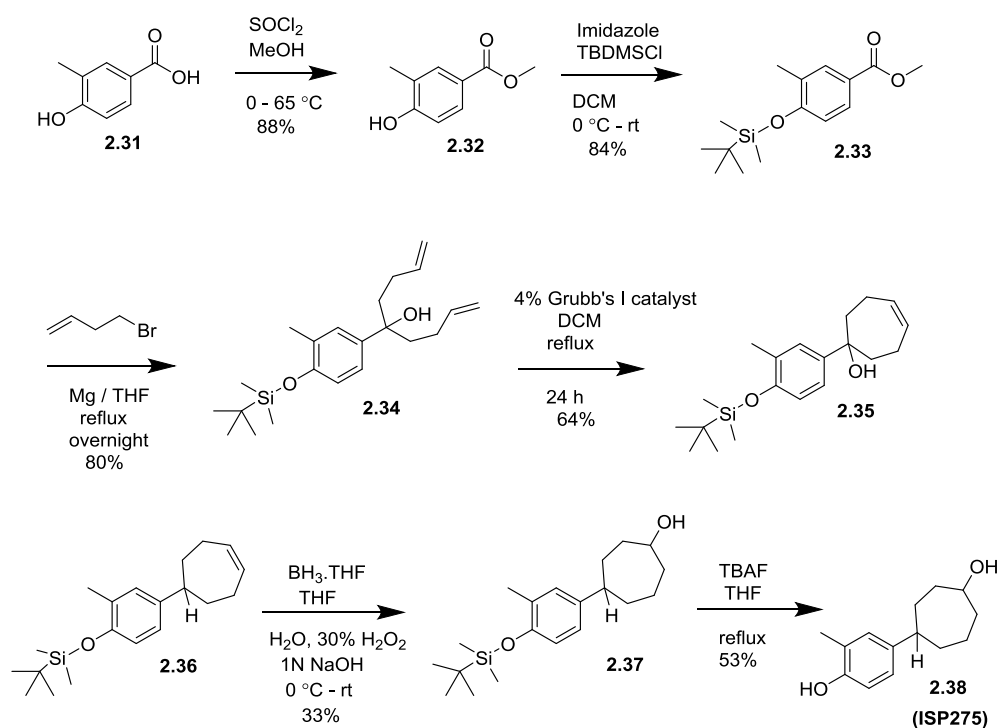
^1H NMR spectrum of this product, which correspond to the olefinic CH and the OMe protons of the two stereoisomers. Reduction of the methyl ester with DIBAL furnished the primary allylic alcohols **2.28** (43%), again as a mixture of *E*- and *Z*- stereoisomers. The multiplet at δ 5.42-5.50 ppm and the doublet at δ 4.19 ppm in ^1H NMR spectrum of this product correspond to the olefinic C-H and alcohol methylene protons respectively. Subsequent hydrogenation of **2.28** followed by demethylation with BBr_3 provided the 4-(2-hydroxyethyl)cycloheptylphenol **2.30** (**ISP248**) in low yield over 2 steps (7%). This low yield was primarily attributed to the harsh methyl ether cleavage conditions.



Scheme 2.14: Synthesis of 4-(2-hydroxyethyl)cycloheptylphenol

3-Methyl-4-hydroxybenzoic acid **2.31** was converted into its methyl ester **2.32** by reaction with thionyl chloride in methanol under refluxing conditions (88%, Scheme 2.15). Formation of the methyl ester was confirmed by the presence of two singlets at δ 2.27 (3H) and 3.89 (3H) ppm in the ^1H NMR spectrum of **2.32**, corresponding to the OMe and Ar-

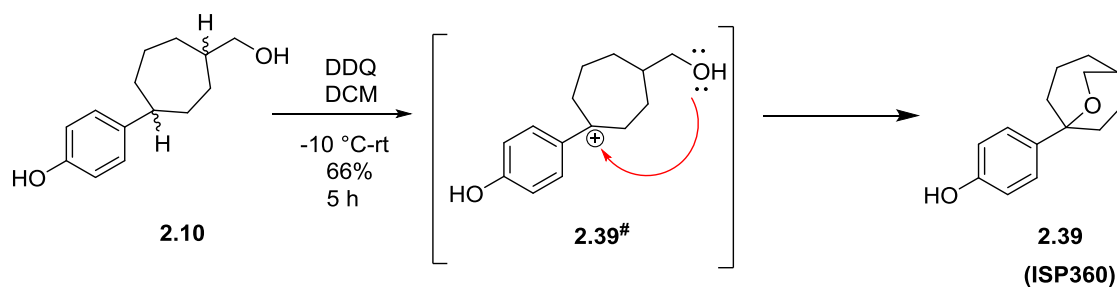
CH₃ protons. Protection of **2.32** with tert-butyldimethyl silyl chloride gave the silyl ether **2.33** (84%). Transformation of **2.33** to the cycloheptanol **2.37** utilized the sequence of steps developed in the 2nd and 3rd generation syntheses of **2.10** (i.e. Grignard addition, RCM, ionic reduction, and hydroboration/oxidation). Deprotection of **2.37** was carried out using TBAF/THF at reflux to obtain the 4-(4-hydroxy-3-methylphenyl)cycloheptan-1-ol **2.38** (53%, **ISP275**) as a mixture of diastereomers. The six-step sequence gave 6.62 % overall yield over 6 steps. The structures of **2.34-2.38** were assigned by comparison of their ¹H NMR spectral data with that obtained for the parent compounds **2.13-2.16** and **2.23** (see Schemes 2.10 and 2.13).



Scheme 2.15: Synthesis of 4-(4-hydroxy-3-methylphenyl)cycloheptan-1-ol

The primary differences appeared in the aromatic region (signals due to 1,2,4-trisubstituted benzene vs 1,4-disubstituted benzene) and the appearance of a singlet at ca. δ 2.2 ppm due to the aryl methyl group.

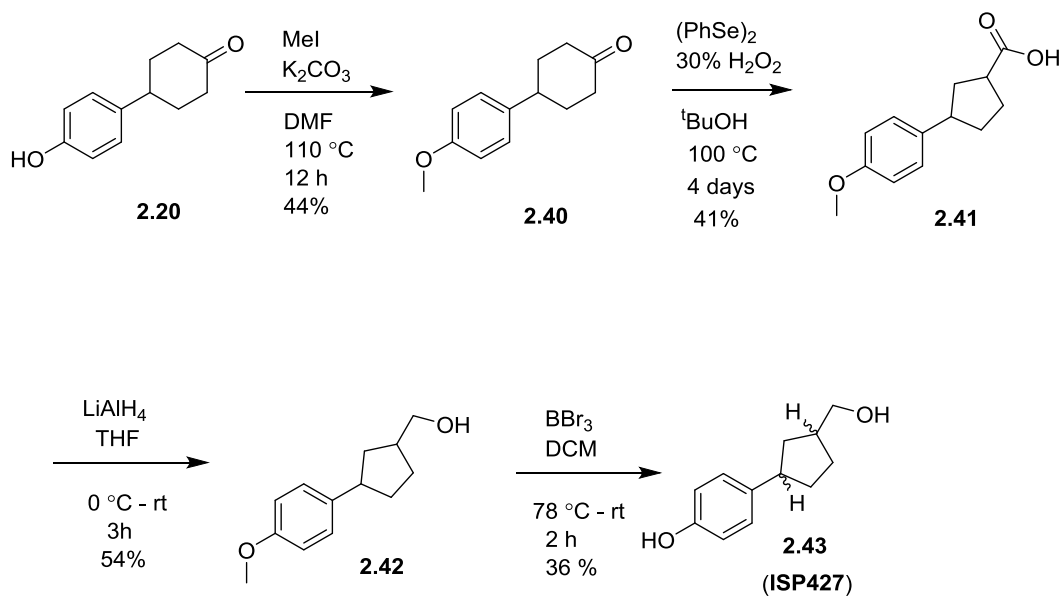
Oxidation of the mixture of *cis*- and *trans*- 4-(4-(hydroxyphenyl)cycloheptanemethanol (**2.10**) with DDQ in CH_2Cl_2 gave the tricyclic ether **2.39** (66%, **ISP360**, Scheme 2.16). The structural assignment for **2.39** was supported by its NMR data. In particular, the presence of two multiplets at δ 3.84-3.90 and 3.96-4.07 ppm in ^1H NMR spectrum integrating to one proton each correspond to the diastereotopic ether protons, while signals at δ 69.9 and 76.5 ppm in the ^{13}C NMR spectrum correspond to the secondary and quaternary aliphatic ether carbons respectively. This cyclization is rationalized by oxidation of **2.10** to the benzyl carbocation intermediate **2.39**[#] (Scheme 2.16) which is trapped by intramolecular attack of the hydroxymethyl group, followed by deprotonation.



Scheme 2.16: Oxidative cyclization of **2.10** to generate tricyclic ether **2.39**

In order to explore the effects of the aliphatic ring size on ER binding affinity and selectivity, six- and five-membered analogs of **2.10** were prepared. The synthesis of 4-(4-(hydroxyphenyl)cyclohexanemethanol and other derivatives are discussed in Chapter 3. For the cyclopentyl analog, commercially available 4-(4-(hydroxyphenyl)cyclohexan-1-one

2.20 was converted into the known⁹⁰ methyl ether **2.40** (44% unoptimized, Scheme 2.17) using iodomethane and K_2CO_3 in DMF. The key ring contraction of **2.40** was effected with diphenyldiselenide and 30% H_2O_2 in $tBuOH$ ⁹¹ to afford the carboxylic acid **2.41** in low yield (40%). The product was identified by comparison of its NMR spectral data with the literature values.⁹² Finally, reduction of **2.41** with lithium aluminium hydride, followed by demethylation under BBr_3 conditions afforded the 3-(4-(hydroxyphenyl)cyclopentanemethanol **2.43** (36%, **ISP427**) as a mixture of diastereomers.



Scheme 2.17: Synthesis of 3-(4-(hydroxyphenyl)cyclopentanemethanol

CHAPTER 3

DEVELOPMENT OF 4-[4-(HYDROXYMETHYL)CYCLOHEXYL]PHENOL AND ANALOGUES

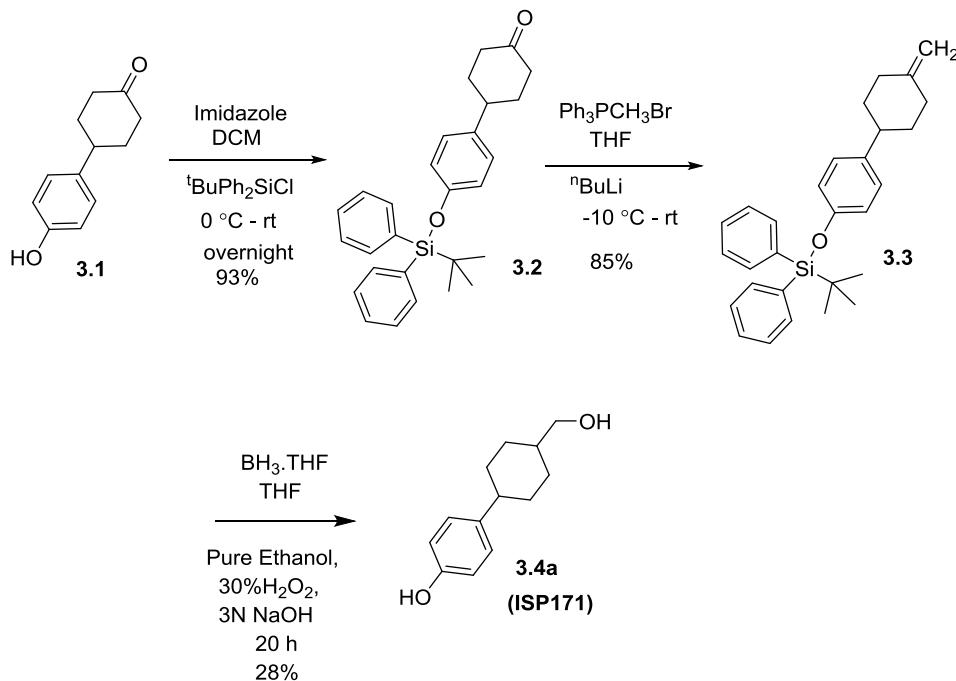
3.1 Synthesis of 4-[4-(Hydroxymethyl)cyclohexyl]phenol

Based on estrogen receptor literature,⁴⁷ the binding site cavity for ER β is smaller in volume (279 Å³) than that for ER α (379 Å³). Thus, in addition to the lead compound 4-(4-(hydroxyphenyl)cycloheptanemethanol, described in the previous chapter, it was desirable to prepare analogs with varying cycloalkane ring(s). In particular, the differences in molecular flexibilities between a “rigid” cyclohexane ring and a “floppy” cycloheptane ring, as well as the O-O interatomic distance, upon ligand binding and functional activation would shed light on important pharmacophore parameters. Molecular mechanics calculations of the O-O interatomic distances in *cis*-4-(4-(hydroxyphenyl)cycloheptanemethanol varied between 10.7-11.0 Å. This range of distances is due to (i) the flexible nature of the seven-membered ring, and (ii), rotation about the ring-to-CH₂OH bond. The calculated distances are similar to those observed in the crystal structures (10.63-11.15 Å, see Figure 2.7 and 2.8). In comparison, the O-O interatomic distance calculated for *trans*-4-[4-(hydroxymethyl)cyclohexyl]phenol (10.7 Å) is within the range for known ligands of the estrogen receptor. In this regards, syntheses of 4-[4-(hydroxymethyl)cyclohexyl]phenol and its analogs were designed from commercially available 4-(4-hydroxyphenyl)cyclohexan-1-one (**3.1**, Scheme 3.1).

Protection of the phenol hydroxyl moiety of **3.1** with tert-butyldiphenylsilyl chloride (TBDPSCl) in CH₂Cl₂ gave **3.2** (93%). The formation of the silyl ether was

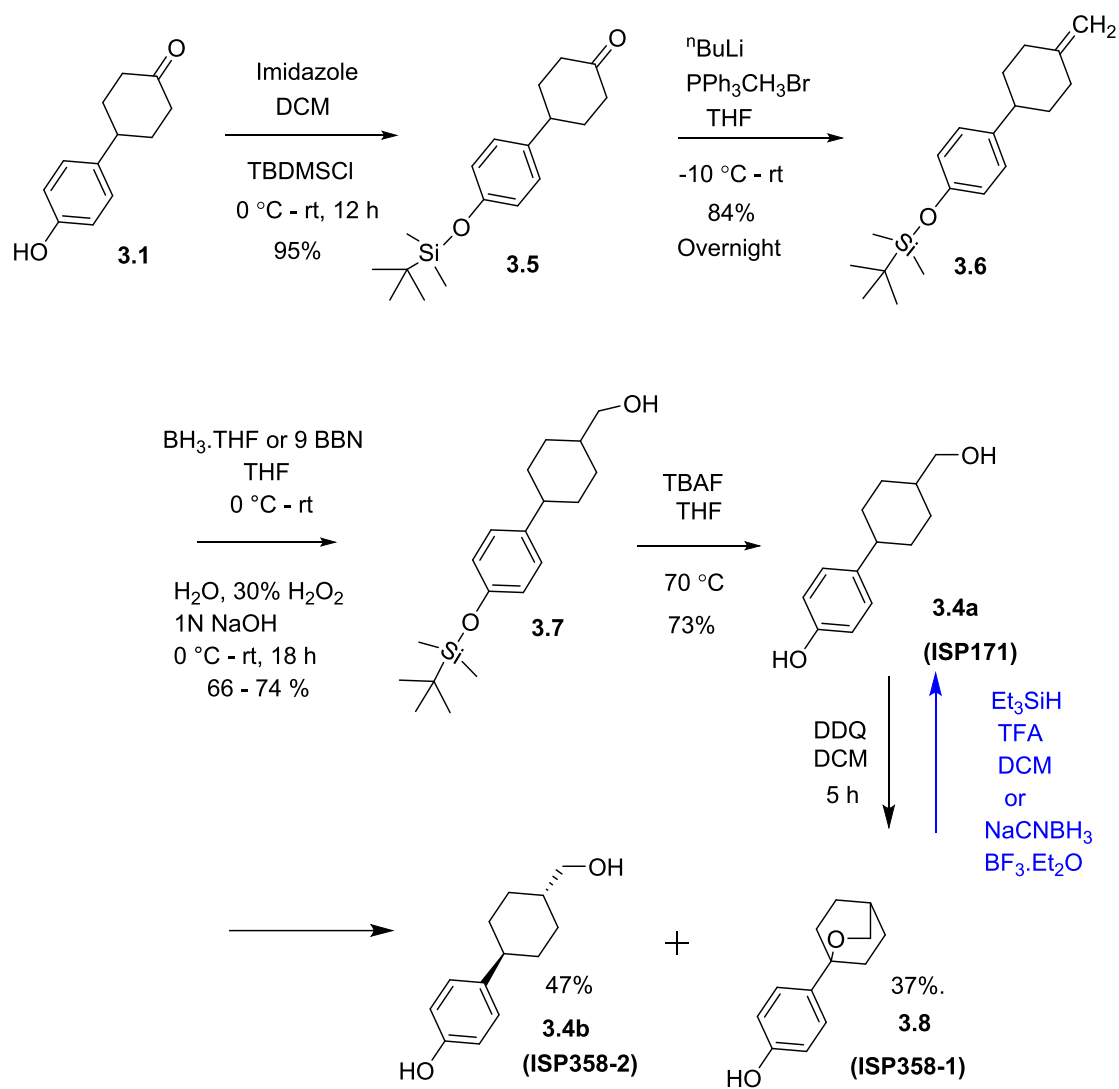
confirmed by the presence of peaks at δ 7.74-7.70 (m, 4H), 7.45-7.34 (m, 6H), and 1.09 (s, 9H) ppm in ^1H NMR spectrum of the product. Attempted Wittig olefination of **3.2** with the ylide generated from methoxymethyl triphenylphosphonium chloride and *n*-butyllithium or *t*-BuOK as the base, was ineffective (Scheme 3.1). In contrast, reaction of **3.2** with the ylide generated from methyltriphenylphosphonium bromide with *n*-butyllithium afforded the product **3.3** (85%). The presence of a peak at δ 107.4 ppm in the ^{13}C NMR spectrum and a peak at δ 4.65 (narrow t, 2H) ppm in the ^1H NMR spectrum of **3.3** is characteristic of the exocyclic olefinic carbon and its attached protons. Subsequent hydroboration of **3.3** with $\text{BH}_3\cdot\text{THF}$ followed by oxidation with 30% H_2O_2 and 3*N* NaOH in ethanol gave 4-[4-(hydroxymethyl)cyclohexyl]phenol **3.4a** (**ISP171**) (28%). Notably, the use of 3*N* NaOH led to cleavage of the TBDPS protecting group. This product was determined to be a mixture of *cis*- and *trans*-stereoisomers (ca. 3 : 1 ratio) by integration of the alcoholic methylene protons at δ 3.60 (1.5H) and 3.39 (0.5H) in the ^1H NMR spectrum. These relative chemical shifts are characteristic of *cis*- and *trans*-4-substituted cyclohexanemethanols.⁹³⁻⁹⁵

The lower yield of the last step led us to explore an alternative protecting group strategy. Protection of **3.1** with *tert*-butyldimethylsilyl chloride (TBDMSCl) provided compound **3.5** (95%, Scheme 3.2). Signals at δ 0.99 (9H) and 0.20 (6H) ppm in the ^1H NMR spectrum and δ -4.2, 18.4 and 25.9 ppm in ^{13}C NMR spectrum of **3.5** are characteristic of the *t*-butyldimethylsilyl ether. In a fashion similar to that in Scheme 3.1, Wittig methenylation of **3.5** gave **3.6** (84%). Hydroboration of **3.6** with $\text{BH}_3\cdot\text{THF}$, followed by oxidation with 30% H_2O_2 , and 3*N* NaOH proceeded with concomitant cleavage of the TBDMS group afforded **3.4a** (40%).



Scheme 3.1: 1st Generation synthesis of 4-(4-(hydroxymethyl)cyclohexyl)phenol

Alternatively, the TBDMS protecting group was stable under workup conditions of 1N NaOH to afford **3.7** (66%). Under the $\text{BH}_3 \cdot \text{THF}$ conditions, the product was found to be a 3:2 mixture of *cis:trans* stereoisomers by ^1H NMR integration and LC/MS data. Alternatively, use of 9-BBN instead of $\text{BH}_3 \cdot \text{THF}$, followed by 30% H_2O_2 /1N NaOH produced **3.7** (74%) as a 2:3 mixture of *cis:trans* stereoisomers. The use of these two borane reagents have been previously demonstrated as a method to tune the *cis:trans* outcome for 4-substituted methylenecyclohexanes.⁹⁶ Finally, removal of the TBDMS group was achieved under TBAF conditions to give **3.4a (ISP171)** as a mixture of *cis*- and *trans*-stereoisomers (Figure 3.1). The synthesis of this mixture was achieved in 43% overall yield over a four-step sequence.



Scheme 3.2: 2nd Generation synthesis of 4-(4-(hydroxymethyl)cyclohexyl)phenol

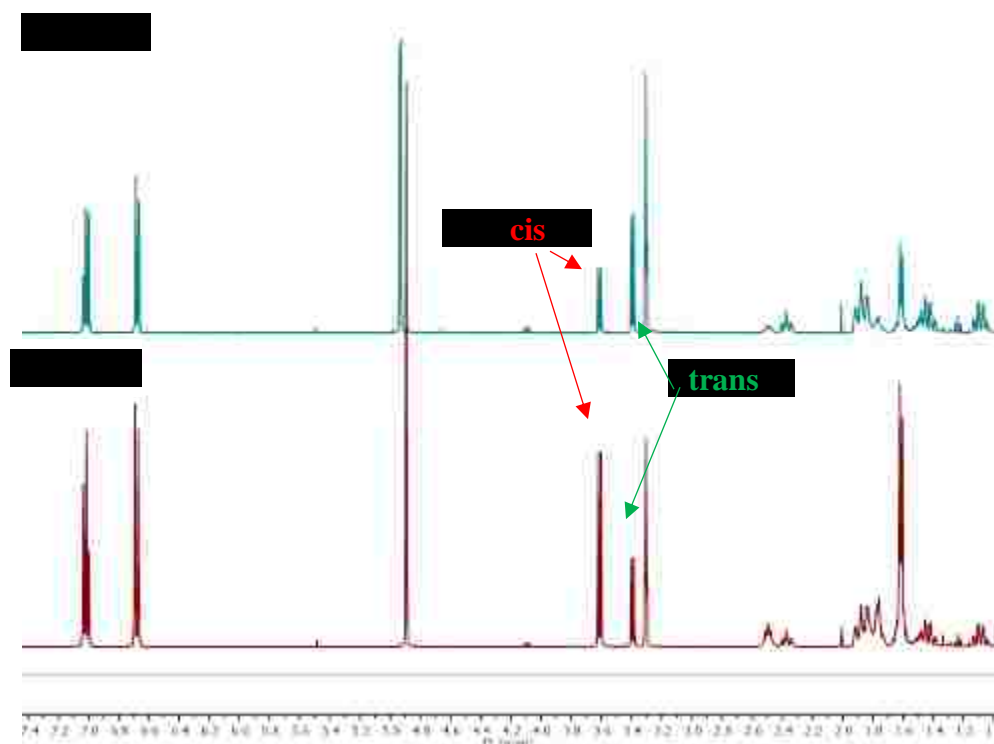


Figure 3.1: ^1H NMR spectra of 4-[4-(hydroxymethyl)cyclohexyl]phenol from **a**) produced using 9-BBN **b**) produced using $\text{BH}_3\cdot\text{THF}$ as hydroboration reagent (solvent = CD_3OD)

Treatment of the mixture of *cis*- and *trans*-4-[4-(hydroxymethyl)cyclohexyl]phenol (**ISP171**) with 1.1 equivalent of DDQ in dichloromethane gave a separable mixture of the bicyclic ether **3.8** (**ISP358-1**, 40%, Scheme 3.2), and unreacted *trans*-**3.4b** (**ISP358-2**, 20% borsm). The oxidative conditions were optimized using the 2:3 mixture of *cis:trans* stereoisomers produced from 9-BBN hydroboration, 0.5 equivalent of DDQ and 5 h reaction time resulting in 47% maximum recovery of **3.4b** along with 37% of cyclic ether **3.8**. The structure of **3.4b** (**ISP358-2**), tentatively assigned on the basis of its ^1H NMR spectral data, was eventually corroborated by single crystal X-Ray diffraction analysis (Figure 3.2). The cyclohexane ring has a chair conformation with both substituents in an

equatorial orientation. The O-O distance found in this X-ray crystal structure (10.658 Å) is quite similar to that calculated on the basis of molecular mechanics (10.7 Å).

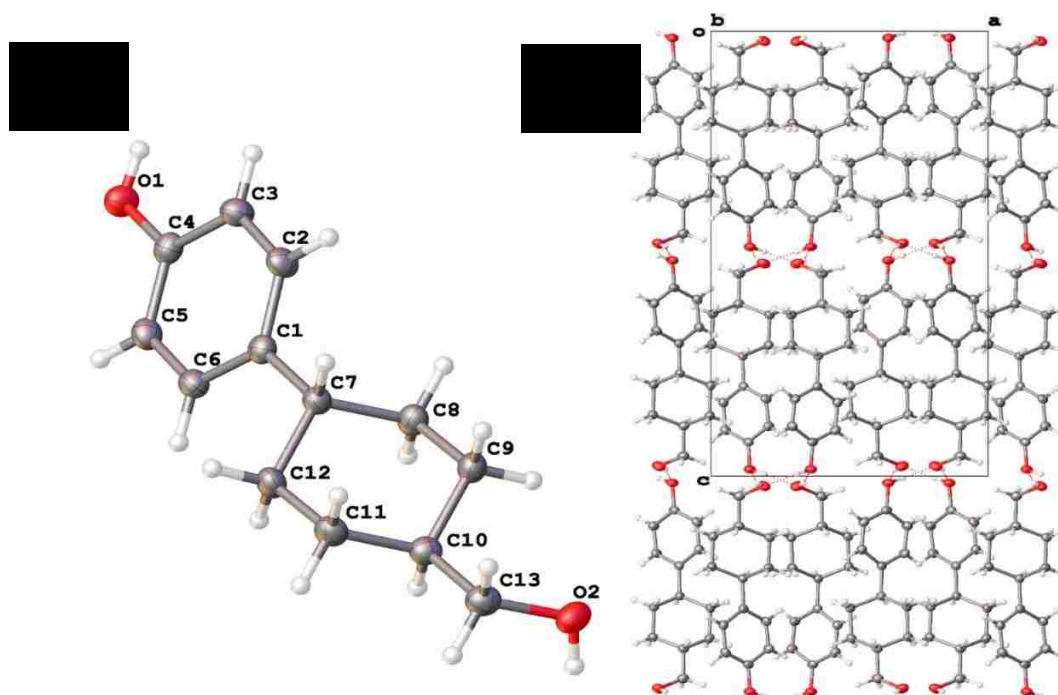
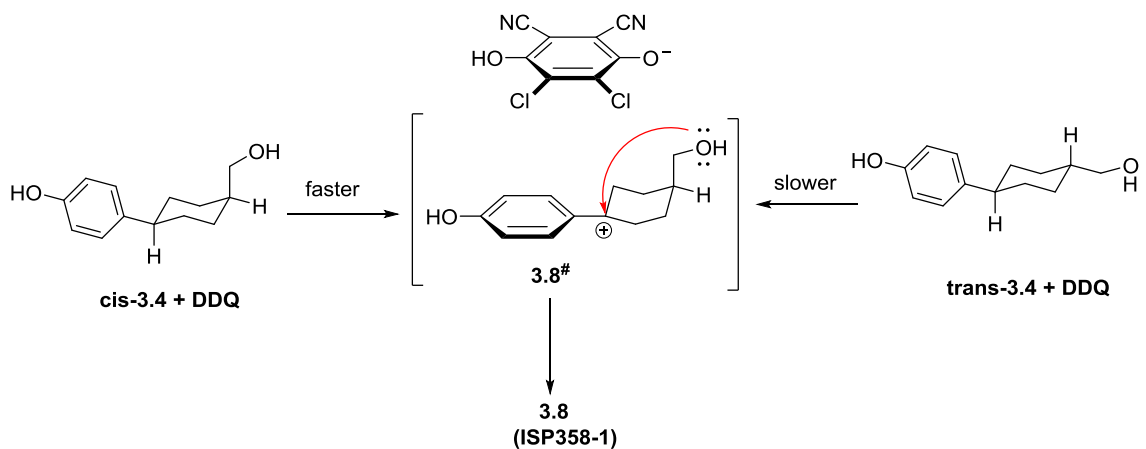


Figure 3.2: a) X-ray crystal structure of compound **3.4b** (ISP358-2) b) Crystal packing nature of compound **3.4b** in solution

Oxidation of either the *cis*- or *trans*-stereoisomer of 4-[4-(hydroxymethyl)cyclohexyl]phenol would result in the same benzylic carbocation intermediate **3.8[#]** (Scheme 3.3). Thus, the formation of the separable mixture of **3.8** (ISP358-1) and the *trans*-isomer **3.4b** (ISP358-2) is due to the faster rate of generation of intermediate **3.8[#]** from the *cis*-isomer. Since the *cis*-isomer is less stable, and therefore higher in energy, compared to the *trans*-isomer, the barrier to oxidation of *cis*-**3.4a** to **3.8[#]** (plus the DDQ reduction anion) should be lower, and thus the rate of oxidation is faster, than for *trans*-**3.4b** (plus the DDQ reduction anion).

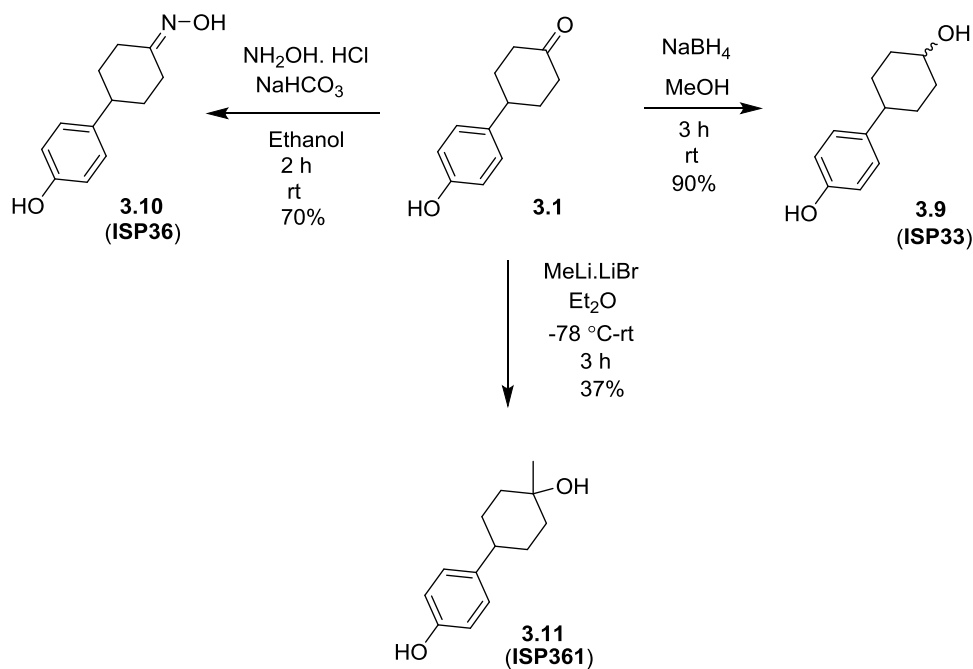


Scheme 3.3: Mechanistic rationale for bicyclic ether formation of *cis*-isomer over *trans* isomer

With a route to the *trans*-isomer **3.4b** secured, the ring opening of bicyclic ether **3.8** was examined as a selective means for preparation of the *cis*-isomer. Ionic reduction of **3.8** with either sodium cyanoborohydride/ $\text{BF}_3 \cdot \text{Et}_2\text{O}$ or triethylsilane/ CF_3COOH gave a mixture of *cis*- and *trans*- 4-[4-(hydroxymethyl)cyclohexyl]phenol in 1:4 and 2:3 ratios respectively.

3.2 Synthesis of 4-Cyclohexylphenol Analogs

To explore structure activity relationship (SAR) further, and search for compounds with improved potencies, physicochemical and biological properties several other 4-cyclohexylphenol analogs were synthesized.

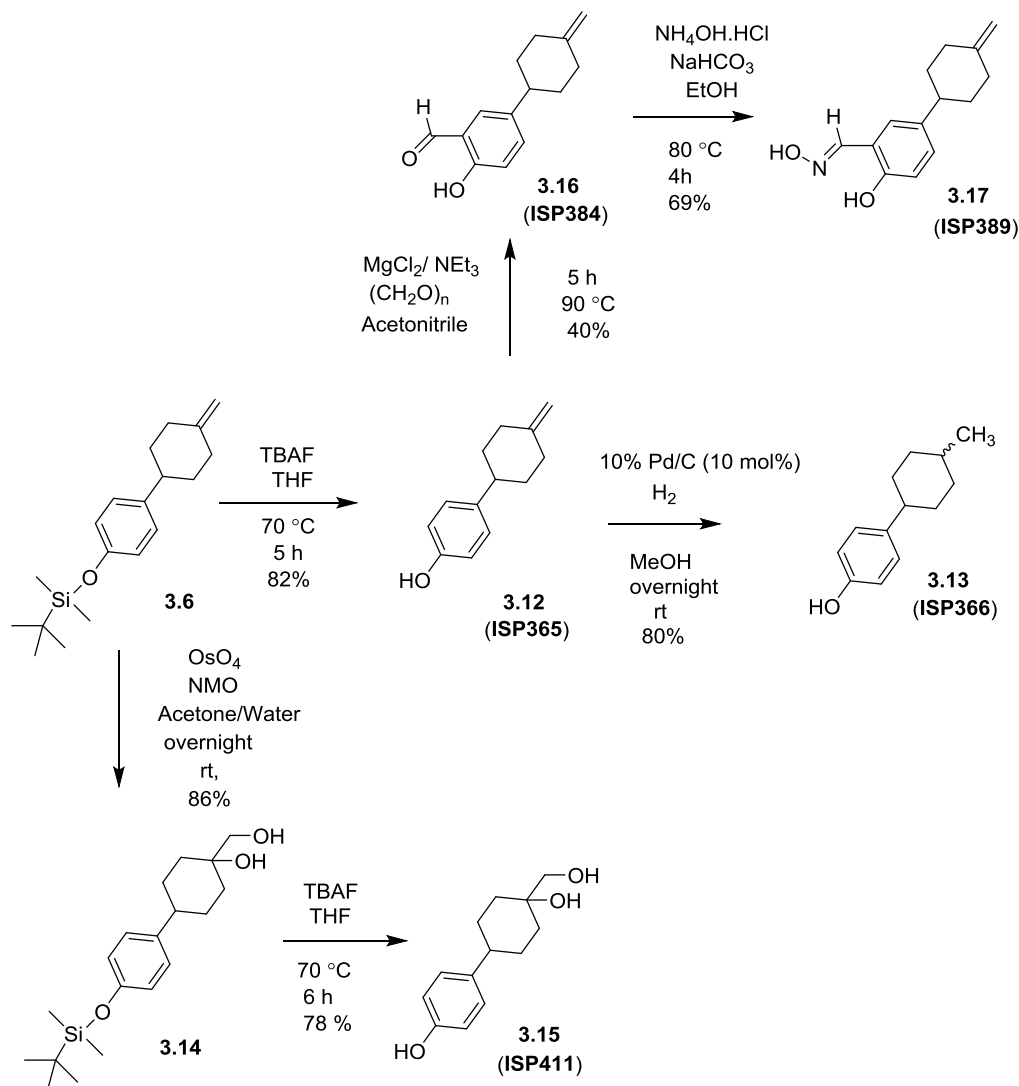


Scheme 3.4: Synthesis of analogs **3.9**, **3.10**, and **3.11**

Reduction of **3.1** with sodium borohydride afforded the secondary alcohol **3.9** (ISP33, 90%, Scheme 3.4). Similarly, reaction of **3.1** with $\text{NH}_2\text{OH} \cdot \text{HCl}$ in the presence of NaHCO_3 gave oxime **3.10** (ISP36, 70%). Finally, nucleophilic addition of MeLi to **3.1** gave the tertiary alcohol **3.11** (ISP361, 37%) in moderate yield under unoptimized conditions. The alcohol **3.9** was determined to be a mixture of isomers whereas alcohol **3.11** was a single isomer from their ^1H and ^{13}C NMR spectral data.

Removal of the protecting group from **3.6** with TBAF gave 4-(4-methylenecyclohexyl)phenol **3.12** (ISP365, 83%) and subsequent hydrogenation over Pd/C furnished the 4-(4-methylcyclohexyl)phenol **3.13** (ISP366, 80%, Scheme 3.5). Dihydroxylation of **3.6** with OsO_4 in the presence of N-methylmorpholine-N-oxide (NMO)

gave diol **3.14** in 86% yield. The presence of peaks at δ 66.2 and 72.4 ppm in ^{13}C NMR spectrum of **3.14** were assigned to the primary and tertiary alcohol carbons respectively.



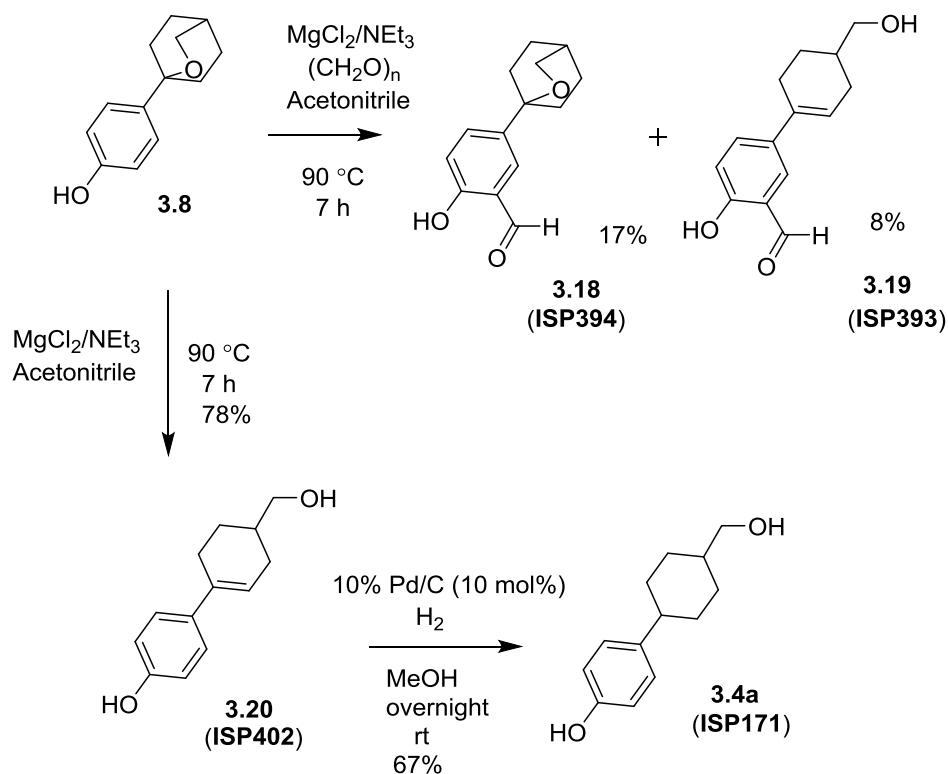
Scheme 3.5: Synthesis of analogs **3.12**, **3.13**, **3.15**, **3.16** and **3.17**

Removal of TBDMS group gave 4-[4-hydroxy-4-(hydroxymethyl)cyclohexyl]phenol **3.15** (**ISP411**, 78%). Reaction of **3.12** with paraformaldehyde, MgCl₂ and NEt₃⁹⁷ effected carbonylation ortho to the phenol group to

give **3.16** (**ISP384**, 44%). Reaction of **3.16** with $\text{NH}_4\text{OH}\cdot\text{HCl}$ in the presence of NaHCO_3 gave oxime **3.17** (**ISP389**, 69%) as an inseparable mixture of *E*- and *Z*- stereoisomers. Katzenellenbogen, *et. al.*, have previously reported on similar salicylketoximes as potent ER β agonists that display antiproliferative activities in a glioma model.⁹⁸

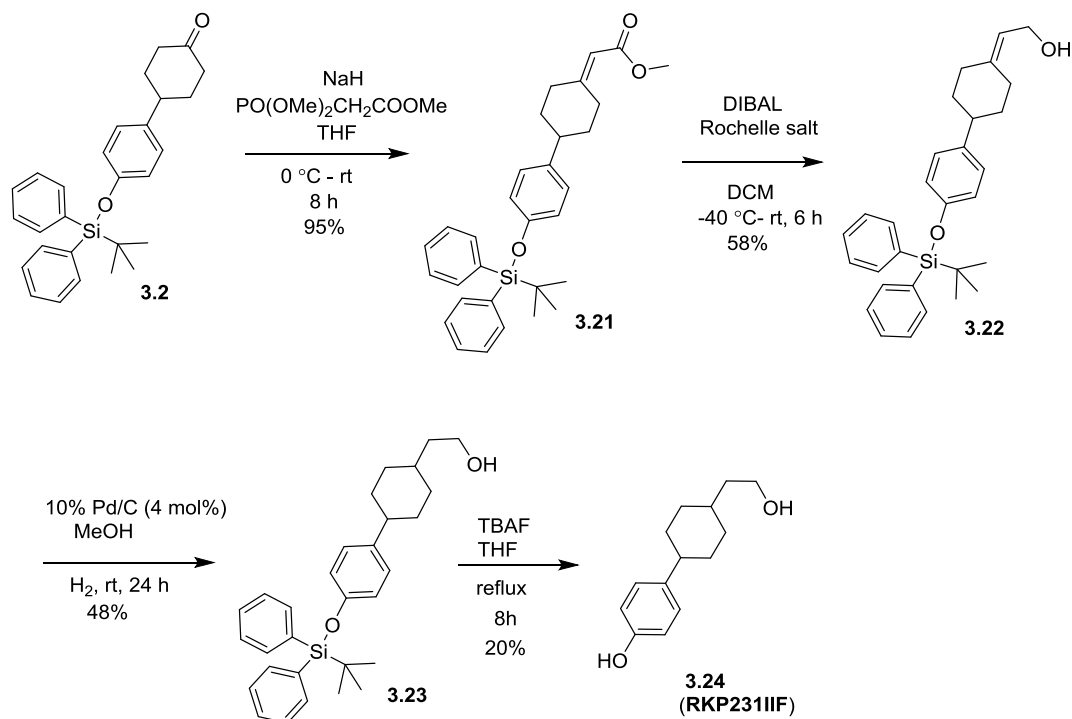
Ortho carbonylation of bicyclic ether **3.8** was attempted using the same protocol as mentioned previously (Scheme 3.6). The anticipated product **3.18** (**ISP394**) was obtained in very low yield (17%) along with the unsaturated alcohol **3.19** (**ISP393**, 8%). The structures of **3.18** and **3.19** were assigned on the basis of their ^1H NMR spectral data. For **3.18**, signals in its ^1H NMR spectrum at δ 9.99 (s, 1H) and 4.06 (s, 2H) ppm correspond to the aldehyde and ether methylene protons respectively, while for **3.19** signals at δ 10.01 (s, 1H), 6.10 (s, 2H) and 3.49 (d, 2H) ppm correspond to the aldehyde, olefinic and hydroxymethylene protons respectively.

The unsaturated aldehyde **3.19** presumably arises via eliminative opening of the 7-oxabicyclo[2.2.2] octane ring of **3.8** under the $\text{MgCl}_2/\text{NEt}_3$ reaction conditions. To test this hypothesis, treatment of bicyclic ether **3.8** with MgCl_2 and NEt_3 *in the absence of formaldehyde* gave unsaturated product **3.20** (**ISP402**, 78%). Peaks at δ 5.97-5.92 (m, 1H) and 3.48 (dd, 2H) ppm in the ^1H NMR spectrum correspond to the vinylic and methylene protons respectively. Hydrogenation of **3.20** over Pd/C gave a mixture of the *cis*- and *trans*-stereoisomers **3.4a** (**ISP171**, 67%) in 3:2 *cis* : *trans* ratio.



Scheme 3.6: Synthesis of analogs **3.18**, **3.19** and **3.20**

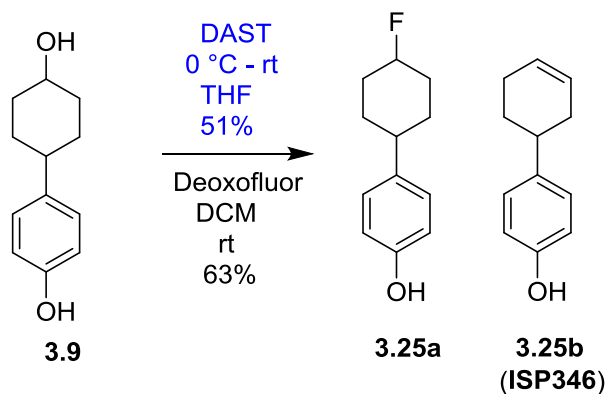
Horner–Wadsworth–Emmons olefination of **3.2** with trimethyl phosphonoacetate and NaH, afforded enoate **3.21** (95%, Scheme 3.7). Peaks at δ 5.65 (s, 1H) and 3.69 (s, 3H) ppm in the ^1H NMR spectrum of **3.21** correspond to the olefinic and methyl ester protons respectively, while a signal in its ^{13}C NMR spectrum at δ 51.1 ppm is characteristic of the methyl ester carbon. Selective ester reduction of **3.21** was accomplished using excess DIBAL to give the allylic alcohol **3.22** (58%). The triplet at δ 5.42 and doublet at δ 4.17 ppm in the ^1H NMR spectrum of **3.22** correspond to the olefinic C-H and the hydroxymethylene protons. Hydrogenation of **3.22** followed by removal of the TBDPS protecting group under TBAF conditions gave 4-[4-(2-hydroxyethyl)cyclohexyl]phenol **3.24** (RKP231IIF, 20%). The overall yield of the synthesis is 5% over 5 steps.



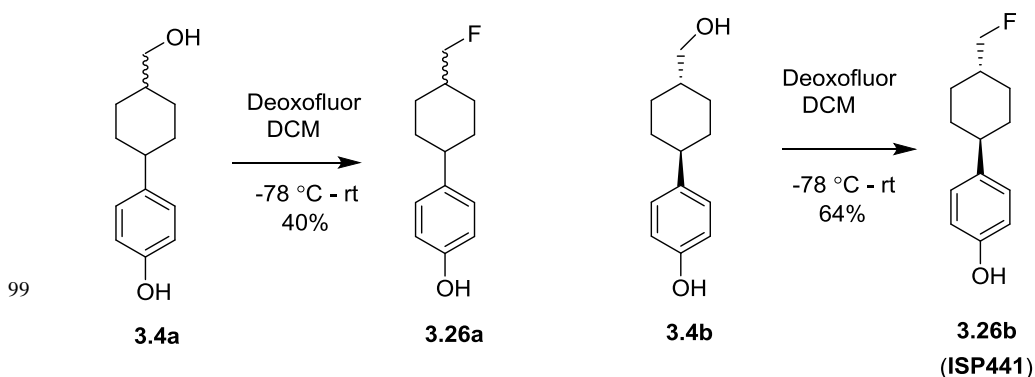
Scheme 3.7: Synthesis of 4-[4-(2-hydroxyethyl)cyclohexyl]phenol

3.3 Synthesis of Fluorine Containing 4-Cyclohexylphenol Analogs

The introduction of fluorine into drug-like molecules is promising since it generates new pharmaceutical candidates with potentially improved pharmacological profiles. While fluorine mimics hydrogen with respect to steric requirements (van der Waals radius: H, 1.20 Å; F, 1.35 Å), the presence of F alters electronic properties of the molecule due to its higher electronegativity. Incorporation of fluorine into drug candidates also enhance their *in vivo* metabolic stability, lipophilicity and blood-brain barrier penetration.⁹⁹⁻¹⁰⁰



Scheme 3.8: Synthesis of analog **3.25b**

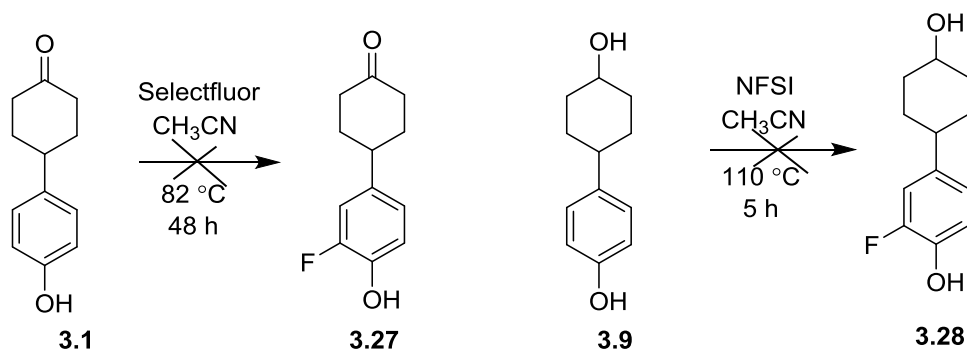


Scheme 3.9: Synthesis of analogs **3.26a** and **3.26b**

Attempts to generate **3.25a** from **3.9** by substitution using diethylaminosulfur trifluoride [DAST] or bis(2-methoxyethyl)aminosulfur trifluoride [DeoxofluorTM] at room temperature was ineffective and instead afforded the elimination product 1',2',3',6'-tetrahydro-[1,1'-biphenyl]-4-ol **3.25b** (ISP346, 51-63%, Scheme 3.8). Since secondary alcohols favor the elimination product, deoxyfluorination of primary alcohols was examined.¹⁰¹⁻¹⁰² Reaction of the mixture of *cis*- and *trans*-stereoisomers **3.4a** with deoxofluor gave **3.26a** as a mixture of diastereomers (40%, Scheme 3.9). Encouraged by these results, the pure *trans*-stereoisomer, **3.4b** was then subjected to the same conditions and afforded the desired fluoro product **3.26b** (ISP441, 64%). The structure of **3.26b** was

based on its NMR spectral data. In particular, doublets at δ 89.4 ppm ($^1J_{C-F} = 166$ Hz) in the ^{13}C NMR spectrum and at δ 4.23 ppm ($^2J_{H-F} = 47.8$ Hz) in the ^1H NMR spectrum correspond to the fluoromethylene substituent.

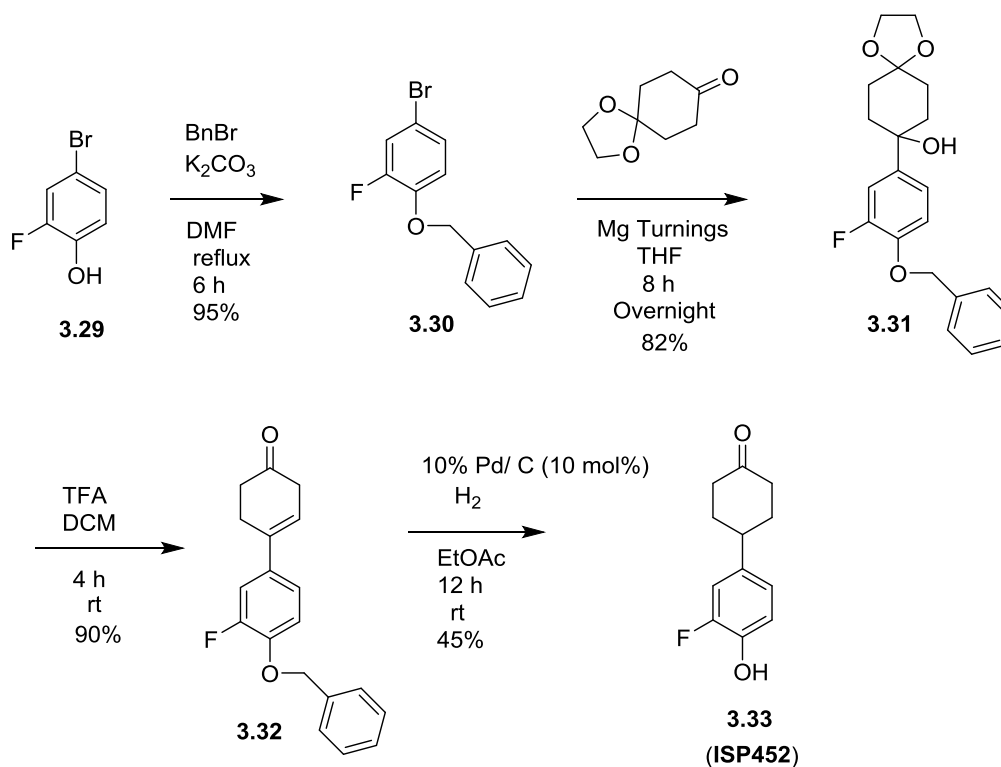
Ortho-fluorination of compound **3.1** or **3.9** was attempted with 1-chloromethyl-4-fluoro-1,4-diazoniabicyclo[2.2.2]octane bis(tetrafluoroborate) [SelectfluorTM] or N-fluorobenzenebenzenesulfonamide (NFSI) as fluorinating reagents¹⁰³⁻¹⁰⁵ (Scheme 3.10). Unfortunately, in each case only starting material was recovered.



Scheme 3.10: Attempted synthesis towards analogs **3.27** and **3.28**

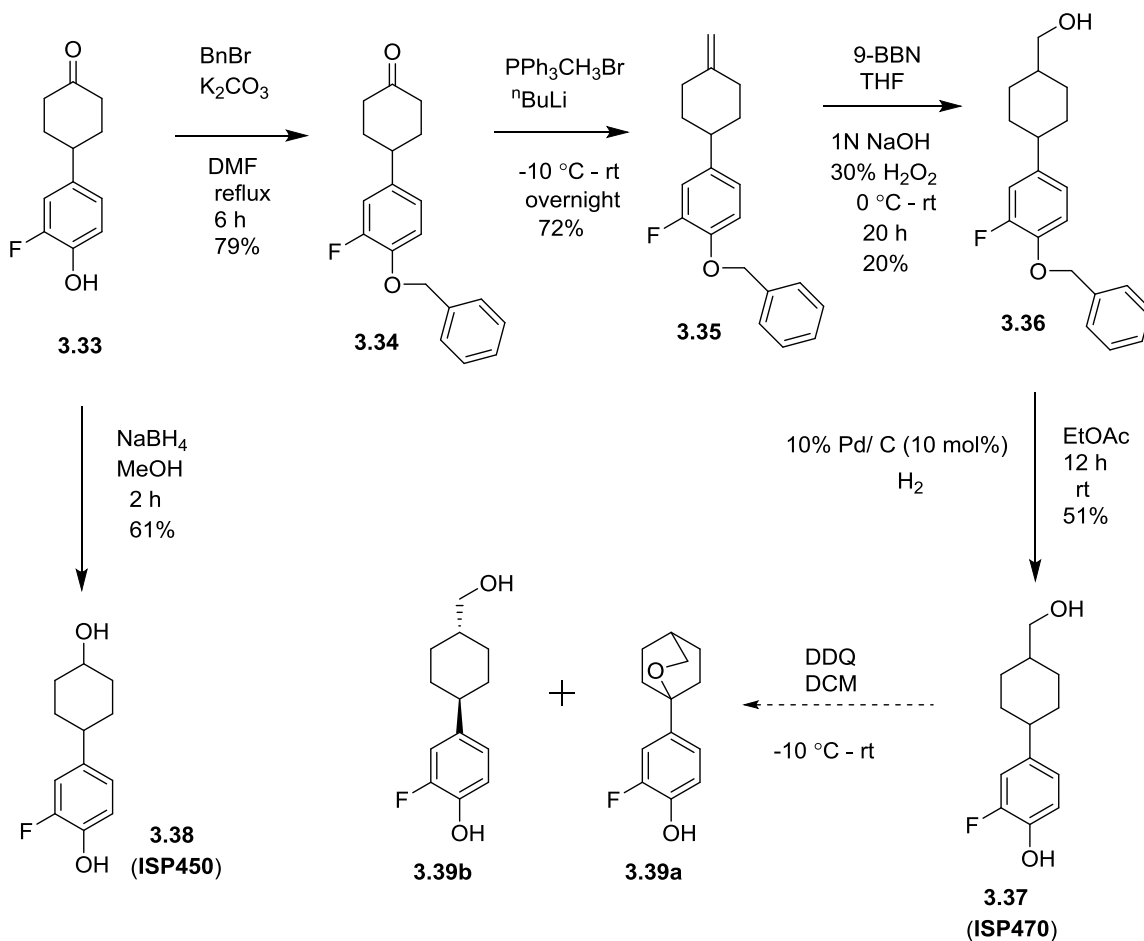
Consequently, an alternative approach was conceived. Protection of phenol **3.29** with benzyl bromide produced **3.30** (95%, Scheme 3.11). The multiplet at δ 7.47-7.32 (5H) ppm and a singlet at δ 5.13 (2H) ppm in the ^1H NMR spectrum of **3.30** corresponds to the benzyl group. Addition of the Grignard reagent generated from **3.30** with 1,4-dioxaspiro[4.5]decan-8-one afforded the tertiary alcohol **3.31** (82%). Treatment of **3.31** with 2-3 drops of concentrated H₂SO₄ acid in THF/water to effect hydrolysis of the cyclic ketal proceeded with concomitant dehydration to give **3.32** in moderate yield (52%). However, large scale synthesis was unreliable from this protocol. Alternatively, use of trifluoroacetic acid, instead of sulfuric acid, in CH₂Cl₂ furnished the product **3.32** in

excellent yield (90%). Reduction of **3.32** with H₂ in the presence of 10% Pd/C proceeded with both hydrogenation of the alkene and hydrogenolysis of the benzyl ether to deliver the desired **3.33** (ISP452, 45%).



Scheme 3.11: Synthesis of intermediate **3.33**

The triplet of triplets at δ 3.00 (1H) ppm in ¹H NMR spectrum of **3.33** corresponds to the benzylic hydrogen of the cyclohexanone ring while the peak at δ 214.1 ppm in ¹³C NMR spectrum corresponds to the carbonyl carbon. Cyclohexanone **3.33** is the ortho-fluoro analog of 4-(4-hydroxyphenyl)cyclohexan-1-one and as such can serve as a starting material for synthesis of fluorinated analogs using previously established routes.



Scheme 3.12: Synthesis of **3.38** and proposed routes to **3.39a** and **3.39b**

Attempted reaction of **3.33** with either TBDMSCl or TBDMSTf as previously demonstrated for **3.1** (see Scheme 3.2), was sluggish even at optimal conditions. The lack of reactivity of **3.33** under these reaction conditions is most probably a consequence of the electron withdrawing nature of the ortho fluorine atom on the nucleophilicity of the phenolic hydroxyl group.

Alternatively, benzyl protection of **3.33** proceeded in a fashion similar to **3.29** gave **3.34** (79%, Scheme 3.12). Subsequent Wittig methenylation of **3.34** followed by hydroboration/oxidation using 9-BBN led to **3.36** in 16% yield over 2 steps. Finally,

cleavage of the benzyl protection was accomplished under hydrogenation conditions to give 2-fluoro-4-[4-(hydroxymethyl)cyclohexyl]phenol **3.37 (ISP470)** as a mixture of *cis*- and *trans*-stereoisomers. The overall yield of the synthesis is 1.8% over 8 steps. Reduction of **3.33** with NaBH₄ gave the corresponding cyclohexanol **3.38 (ISP450)** as a mixture of *cis*- and *trans*-stereoisomers (61%). Conversion of **3.37** to its corresponding bicyclic ether **3.39a**, thereby chemical separation of *trans* isomer **3.39b** will be conducted in future.

CHAPTER 4

BIOLOGICAL EVALUATION OF ER β SELECTIVE COMPOUNDS

4.1 *In vitro* and *In vivo* Biological Evaluation – Assay Summary

Compounds prepared in the previous chapters were evaluated for *in vitro* ER activity, interaction with selected CYP enzymes, hERG activity, and nuclear receptor screening, and *in vivo* efficacy for memory consolidation. The *in vitro* biological studies with respect to ER α and ER β activity, conducted by Alicia Schultz and Lucky Lu from the Sem lab at Concordia University-Wisconsin, include:

- TR-FRET (Time Resolved Fluorescence Resonance Energy Transfer) ER β binding assay, which measures the displacement of a fluorescently labelled estradiol from the ligand binding domain protein;
- Selected compounds were carried forward to a cell-based functional assay, which depends upon cell membrane penetration, the ability of ligand binding to ER and to effect dimerization and subsequent protein transcription. These were conducted for both ER β and ER α , in both agonism as well as antagonism mode;
- CYP inhibition/binding activity, which measures the inhibition of selected CYP liver enzymes toward the metabolism of luciferin releasing substrates

No-stress/no-reward *in vivo* memory consolidation studies, conducted by Jaekyoon Kim from the Frick lab at University of Wisconsin Milwaukee, include:

- Object placement (answers the “where” memory question) by direct hippocampal and intraperitoneal injections
- Object recognition (answers the “what” memory question) by direct hippocampal and intraperitoneal injections

4.2 Description of *In vitro* Assays and Results

4.2.1 TR-FRET ER β Binding Assay

A Lanthascreen TR-FRET ER β binding assay was conducted to assess the binding affinity of synthesized ligands. Assays were conducted using a commercially available ER β assay kit from ThermoFisher and verified to work with the Spectramax M5 (white plates) plate reader. The screen consists of ER β ligand-binding domain (LBD) tagged with glutathione-S-transferase and a terbium-labeled anti-GST antibody. A proprietary fluorescein-labeled ligand, Fluormone ES2 Green, is bound in the LBD. Excitation of the terbium label causes fluorescence at 488 nm, which is transferred to the tagged ligand which fluoresces at 518 nm (Figure 4.1). When the ligand is bound, the ratio of 518nm/488nm is high; displacement of the fluorescent ligand by a competitor results in diminished fluorescence at 518 nm, and thus a lower 518 nm/488 nm ratio. Eight different concentrations were examined to obtain a K_i value. Typical data, as represented for the stereoisomers of **ISP163**, are shown in Figure 4.2.

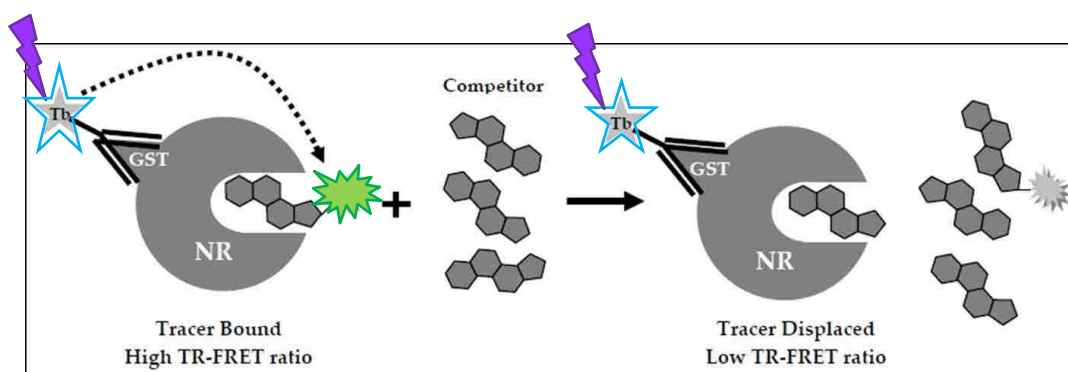


Figure 4.1: Simplified schematic for TR-FRET ER β binding assay (<http://slideplayer.com/slide/8532001/26/images/32/Receptor+binding+assay.jpg>)

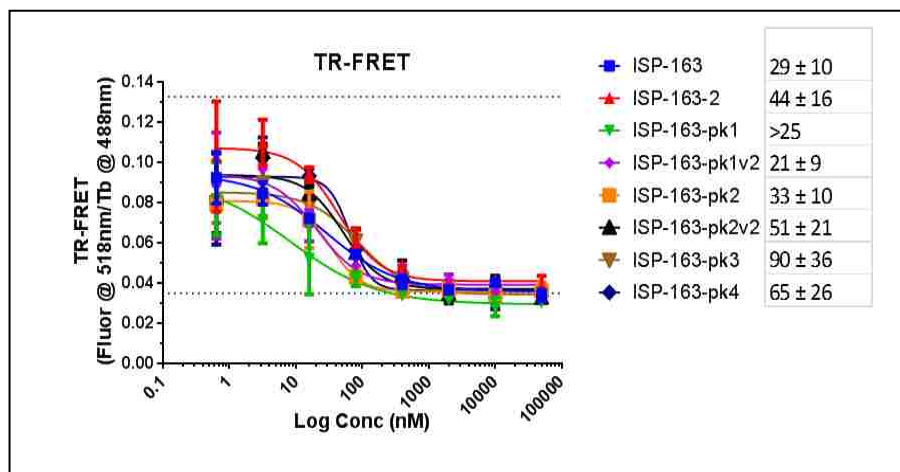


Figure 4.2: TR-FRET ER β binding profile of **ISP163** isomers

4.2.2 ER α and ER β Cell-Based Assay

Cell based assays were carried out to investigate the agonist and antagonist activity of synthesized ligands. Assays were conducted using a commercially available ER β assay kits from Indigo Biosciences. The assay involves non-human mammalian cells engineered to express human estrogen beta (NR3A2) incorporating both the N-terminal DNA binding domain and the C-terminal ligand binding domain. Cells incorporate the cDNA encoding beetle luciferase. Upon binding, the encoded protein forms homo- and heterodimers that interact with specific DNA sequences to activate transcription, including the production of luciferase (Figure 4.3). Quantifying changes in luciferase expression (via relative luminescence) provides a surrogate measure of the changes in ER β activity. As compared to the TR-FRET assay, an increase in fluorescence indicates the increased agonism. The assay can be used to detect either agonist activity or antagonist activity. In the antagonist mode, where the addition of estradiol ($EC_{75} = 3.2$ nM) serves as an agonist and thus effects transcription and production of luciferase, a decrease in fluorescence signifies that the test

compound serves as an antagonist against the action of E2. Similar kits are available to assess functional ER α activity. The agonist assay was conducted under optimized biological conditions delineated in the kit manual, verified to work with the Spectramax M5 (white plates) plate reader, and performed in duplicate. Seven different concentrations were examined to obtain an IC₅₀ value. Typical data for ER β activity, as represented for the four isomers of **ISP163**, are shown in Figure 4.4.

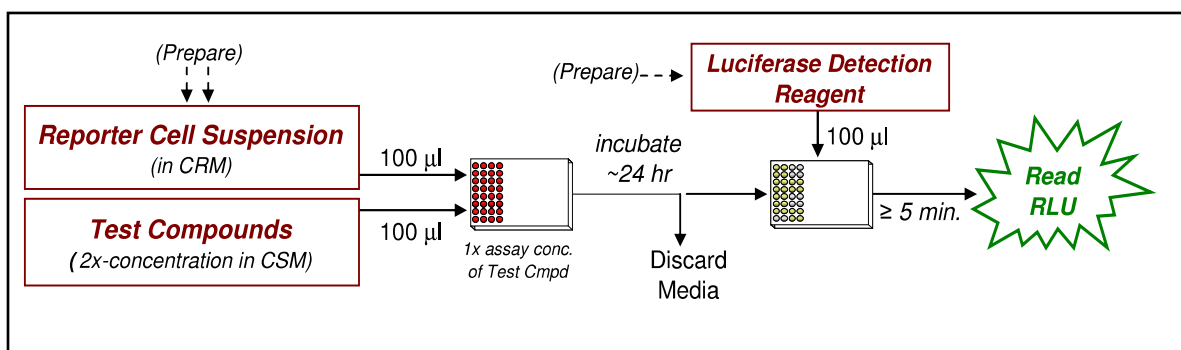


Figure 4.3: Schematic representation of ER α and ER β cell-based assay (<https://www.caymanchem.com/pdfs/15739.pdf>)

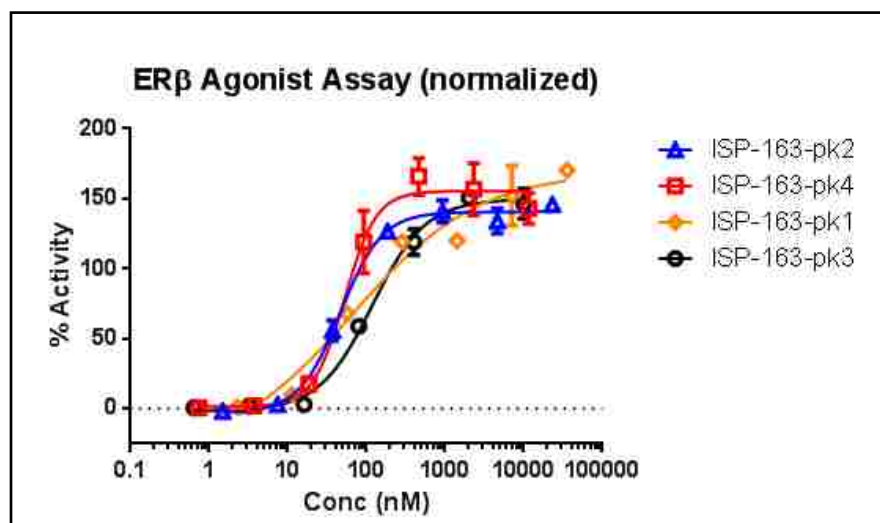


Figure 4.4: ER β cell-based agonist assay profile of **IS163** isomers

4.2.3 TR-FRET Results for 4-(4-(hydroxymethyl)cyclohexyl)phenol and its Analogs

The binding affinity (K_i) values of lead 4-(4-(hydroxymethyl)cyclohexyl)phenol (**ISP 171**) and its analogs were first studied in Lanthascreen TR-FRET ER β binding assay (Table 4.1). In particular; compounds bearing a hydroxymethyl functionality attached to the cyclohexyl core showed higher affinities in the range 80-240 nM. Of the two components in the mixture of *cis*- and *trans*-stereoisomers (**ISP 171**, $IC_{50} = 240$ nM), it was found that the *trans*-isomer was more potent (**ISP 358-2**, $IC_{50} = 80$ nM) than the mixture. Introduction of unsaturation within the six-membered ring (**ISP 402**, $IC_{50} = 89$ nM) did not greatly change the binding affinity compared to **ISP358-2**. Attachment of the OH group directly to the cyclohexyl core (**ISP33**, **ISP361**) did reduce the affinity by approximately one to two orders of magnitude. This is presumably due to the less than optimal distance between phenolic OH and hydroxyl group for proper binding to the receptor. The combination of both a hydroxyl and hydroxymethyl group attached to the six-membered ring (**ISP 411**, 2,500 nM) exhibited a 30-fold reduction in affinity compared to **ISP358-2**. This result might be attributed to the interaction of the second OH with neighboring water molecule inside the cavity thereby creating a disruption of the optimal conformation within the ligand binding pocket. On the other hand, extension of the chain length to a hydroxyethyl group (**RKP231IIF**, 7 nM) increased the affinity, but this trend was reversed with the insertion of an exocyclic alkene moiety (**RKP228**, 521 nM). This decrease in affinity may be due to the reduced flexibility of the side arm.

Replacing the hydroxymethyl group with different polar groups such as ketone (**SM01**, 4500 nM), oxime (**ISP36**, 215 nM) or ethyl acrylate functionality (**RKP230**, 681 nM) resulted in some decrease in ER β binding. The presence of the aliphatic hydroxyl

group was not crucial for binding affinity. In fact, ligands with hydrophobic groups attached to the cyclohexyl ring revealed pronounced affinity (**ISP366**, 11 nM; **RKP231IF**, 15 nM) or similar affinity (**ISP365**, 85 nM). The ability of simple 4-alkyl phenols to bind to ER β and ER α has previously been reported.¹⁰⁶ For example, 4-adamantyl phenol (AdP, Figure 4.5) was found to have ER β IC₅₀ = 200 \pm 1 nM and ER α IC₅₀ = 1000 \pm 1000 nM respectively.¹⁰⁶ While these binding affinities are considerably less than for E2, they highlight the relative importance of the hydrogen bonding between the phenol OH and Glu/Arg residues, along with the hydrophobic interactions of the alkyl portion, in comparison to hydrogen bonding interactions between His and an aliphatic OH group.

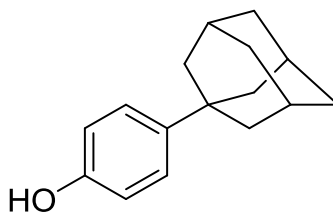
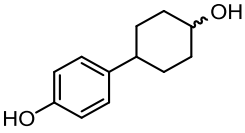
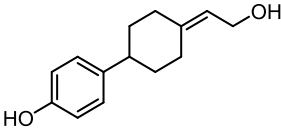
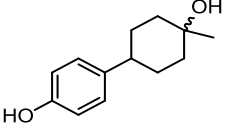
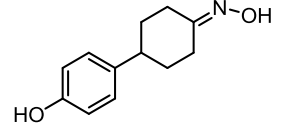
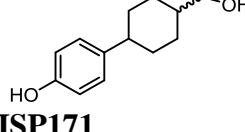
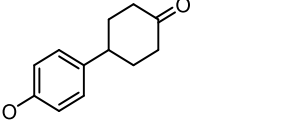
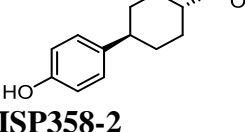
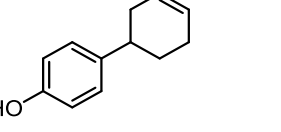
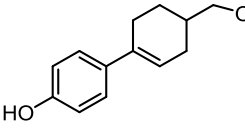
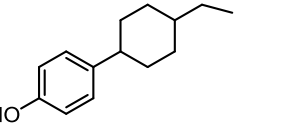
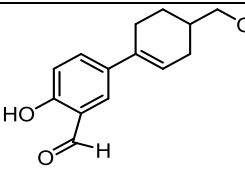
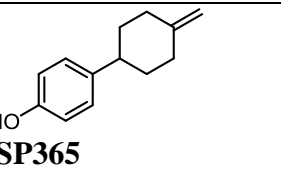
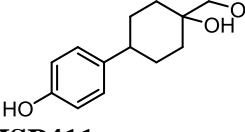
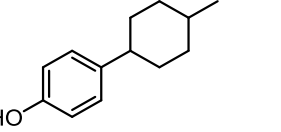
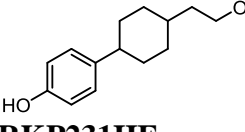
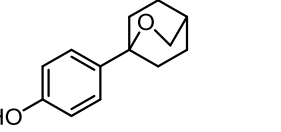


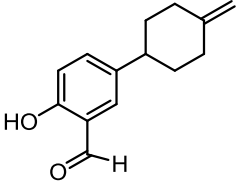
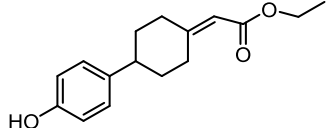
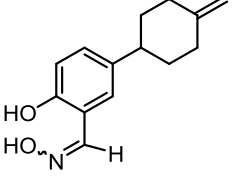
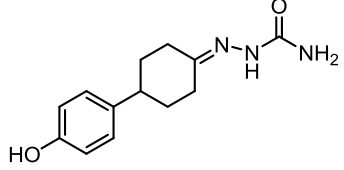
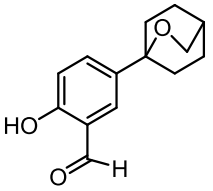
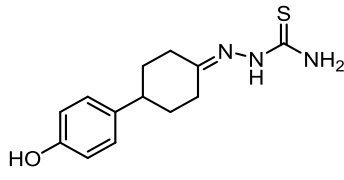
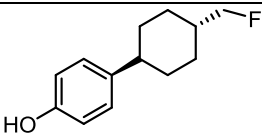
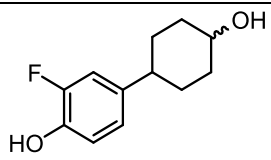
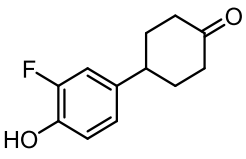
Figure 4.5: Reported ER β agonist 4-adamantyl phenol (AdP)

The cyclic ether had diminished affinity (**ISP358-1**, 250 nM). Introduction of a 2-methylenehydrazine-1-carboxamide (**ML431**, 16,000 nM) or 2-methylenehydrazine-1-carbothioamide (**ML432**, 5,000 nM) to the cyclohexyl ring greatly reduced binding affinity due to rigid and longer chain lengths.

Meanwhile, compound **ISP389**, bearing an oxime functionality ortho to the phenolic oxygen showed modest affinity whereas those bearing an aldehyde ortho to phenolic oxygen such as **ISP384**, **ISP393**, and **ISP394** reflected significantly lower binding affinities ranging from 900 -2100 nM. Furthermore, an introduction of fluorine

Table 4.1: TR-FRET ER β binding data for six-membered analog

Compound	TR-FRET Data (nM)	Compound	TR-FRET Data (nM)
 ISP33	960 \pm 700	 RKP228	521 \pm 87
 ISP361	6,000 \pm 1600	 ISP36	215 \pm 129
 ISP171	240 \pm 14	 SM01	4500 \pm 2800
 ISP358-2	80 \pm 21	 ISP346	570 \pm 130
 ISP402	89 \pm 22	 RKP231IF	15 \pm 2
 ISP393	900 \pm 300	 ISP365	85 \pm 16
 ISP411	2,500 \pm 500	 ISP366	11 \pm 2.7
 RKP231IIF	7 \pm 1	 ISP358-I	250 \pm 56

Compound	TR-FRET Data (nM)	Compound	TR-FRET Data (nM)
 ISP384	1,100±430	 RKP230	681±240
 ISP389	270±66	 ML431	16,000±8,000
 ISP394	21,000±5000	 ML432	5,000±2400
 ISP441	49.5±18.3	 ISP450	4,281±2,516
 ISP452	880±464		

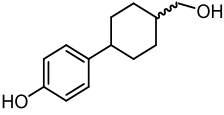
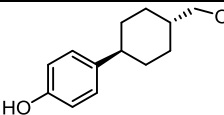
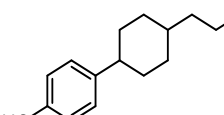
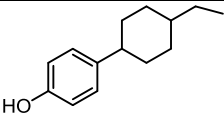
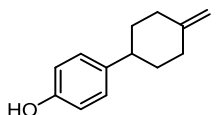
ortho to the phenolic oxygen such as **ISP450** and **ISP452** decreased the affinity dramatically (4281 nM and 880 nM respectively) compared to their non-fluorinated analogs. However, replacing the hydroxyl group in the side chain with fluorine as in

ISP441 showed slightly higher affinity (49.5 nM) compared to the parent molecule (**ISP358-2**, 80 nM).

4.2.4 Cell-based Functional Assay Results for Selected 4-[(hydroxymethyl)cyclohexyl]phenol Analogs

4-[4-(Hydroxymethyl)cyclohexyl]phenol and analogs having lower IC₅₀ values ranging from 7 to 240 nM were further tested in cell based assays to evaluate both their binding affinity as well as ER β selectivity (Table 4.2). The mixture of *cis*- and *trans*-stereoisomers (**ISP171**) and the *trans*-only isomer (**ISP358-2**) showed identical ER β agonist potencies (IC₅₀ 31 nM) and these results indicated the compounds to be more potent in the functional based assay than the TR-FRET ligand displacement assay. In contrast, compounds **RKP231IIF**, **RKP230** and **ISP365** resulted in poorer ER β potencies (IC₅₀ 72, 89, 101 nM respectively) compared to their TR-FRET assay results. These differences may be due to the nature of the assays; the TR-FRET assay measures only displacement of a labelled estradiol from the ligand binding domain, while the cell-based assay depends upon effecting conformational changes in the ER such that homo-dimerization and DNA binding/transcription must occur. Additional interactions between the aliphatic hydroxyl group and the His475 may play a role in these latter conformational changes. All compounds showed no ER β antagonist activity (> 10,000 nM), or ER α agonist or antagonist activity thus demonstrating their pronounced selectivity towards the ER β . Of those, **ISP358-2** gave > 3000-fold selectivity for ER β over ER α in the cell-based functional assay, making it the most selective agonist thus reported.

Table 4.2: Cell-based assay data for selected six-membered analogs and comparison to TR-FRET assay

Compound	TR-FRET ER β Agonist (nM)	ER β Agonist (nM)	ER β Antagon. (nM)	ER α Agonist (nM)	ER α Antagon. (nM)
 ISP171	240 \pm 14	30 \pm 15	>10,000	700,000 \pm 80,000	>10,000
 ISP358-2	80 \pm 21	31 \pm 7	>10,000	100,000 \pm 17,000	>10,000
 RKP231IIF	7 \pm 1	72 \pm 16	>10,000	72,000 \pm 22,000	>10,000
 RKP231IF	15 \pm 2	89 \pm 6	>10,000	25,000 \pm 13 00	>10,000
 ISP365	85 \pm 16	101 \pm 10	>10,000	In progress	In progress

4.2.5 TR-FRET and Cell-based Assay Results for 4-[4-(hydroxymethyl)cycloheptyl]phenol and Analogs

The ER β binding affinity (K_i) of lead 4-[4-(hydroxymethyl)cycloheptyl]phenol (**ISP163**) and its analogs were determined in the TR-FRET assay as previously described (Table 4.3). The lead molecule **ISP163** showed higher affinity as $IC_{50} = 44$ nM. Extension or shortening of the distance between the phenolic and aliphatic hydroxyl groups (**ISP248** or **ISP58**, $IC_{50} = 37$ and 31 nM respectively) has similar binding affinity (within the error limits); this change in potency was not as significant as shown in the six membered analogs (see Table 4.1) from TR-FRET assay.

Introduction of a methyl group ortho to the phenolic oxygen (**ISP275**) decreased the affinity by > 100-fold, compared to **ISP58**, indicating adverse steric interactions in the ligand binding pocket. Introduction of two alkenes to the cycloheptyl ring (**RKP35C**, IC_{50} 378 nM) or the bicyclic ether functionality (**ISP365**, IC_{50} 400 nM) diminished the binding affinities by 9-fold compared to **ISP163**, thus emphasizing the need for flexibility in the ring system. A change in oxidation state of the hydroxyl group, to the cycloheptanone ring (**ISP242**) decreased the binding affinity by 6-fold in comparison to **ISP58**. Compounds having lower IC_{50} values were further evaluated in cell-based functional assays (Table 4.4).

Table 4.3: TR-FRET ER β binding data for seven-membered analogs

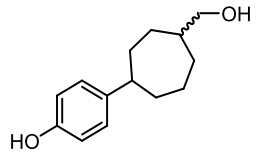
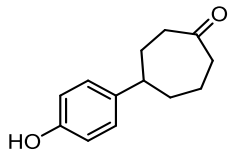
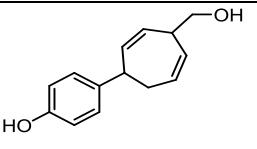
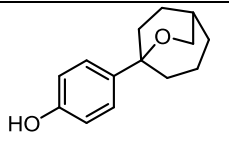
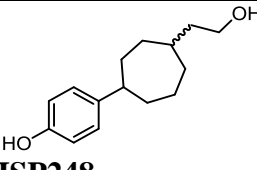
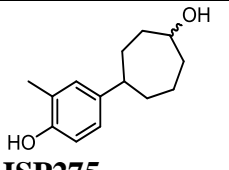
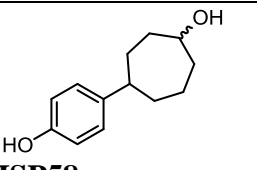
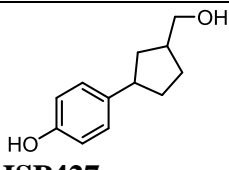
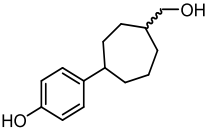
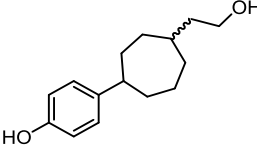
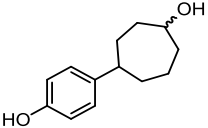
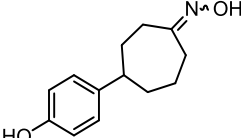
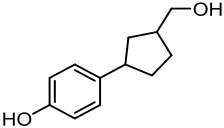
Compound	TR-FRET DATA (nM)	Compound	TR-FRET DATA (nM)
 ISP163	44 \pm 16	 ISP 242	182 \pm 63
 RKP35C	378 \pm 97	 ISP360	400 \pm 100
 ISP248	37 \pm 9	 ISP275	3400 \pm 1500
 ISP58	31 \pm 7	 ISP427	3,370 \pm 3,560

Table 4.4: TR-FRET and cell-based assay data for selected seven- and five-membered analogs

Compound	TR-FRET DATA (nM)	ER β Agonist (nM)	ER β Antagon. (nM)	ER α Agonist (nM)	ER α Antagon. (nM)
 ISP163	44 \pm 16	30 \pm 9	>100,000	10,500 \pm 200	>10,000
 ISP248	37 \pm 9	104 \pm 27	>10,000	45,000 \pm 17000	>10,000
 ISP58	31 \pm 7	401 \pm 29	>10,000	1,400 \pm 400	>10,000
 ISP166	Not done	1,460 \pm 305	>10,000	350,000 \pm 250 000	>10,000
 ISP427	3,370 \pm 3,560	2,100 \pm 250	>10 000	>10,000	>10,000

The lead molecule, **ISP163**, displayed similar potency for ER β agonist activity as found in the TR-FRET assay. The seven-membered analogs varying in distance between the hydroxyl groups (**ISP248**, and **ISP58**) resulted in lower potencies ($IC_{50} > 100$ nM) as ER β agonists, while the oxime analog (**ISP166**) was nearly 50-fold less potent. Similar to the cyclohexyl compounds, these analogs did not show any ER β antagonist activity ($> 10,000$ nM), or ER α agonist or antagonist activity, indicating their greater selectivity towards the ER β agonist activity. From those, **ISP163** gave > 350 -fold selectivity for ER β agonist activity over ER α making it as the most selective agonist among the seven-membered series. The five-membered ring analog 4-[3-(hydroxymethyl)cyclopentyl]phenol (**ISP427**) showed very poor potency in both the TR-FRET ligand displacement and cell-based functional assays. This may be due to the inability of this smaller ring to occlude water molecules from the binding site.

4.2.6 TR-FRET and Cell-based Assay of the Stereoisomers of 4-[4-(hydroxymethyl)-cycloheptyl]phenol

Since **ISP163** is a mixture of four stereoisomers it was crucial to evaluate the potency and selectivity of the individual isomers. Toward this end, binding affinity from TR-FRET assay and agonist activity from cell based assay were evaluated (Table 4.5 and Figure 4.6). The two *trans*-stereoisomers (**PK1** and **PK2**) reflected greater affinity than the mixture (**ISP163**) whereas the *cis*-stereoisomers **PK3** (1*R*,4*S* absolute configuration) and **PK4** (1*S*,4*R* absolute configuration) reflected lower affinity in the TR-FRET assay. In contrast, all four isomers revealed lower potency in the cell-based ER β agonist assay (IC_{50} 47-119 nM) in comparison to the mixture of stereoisomers. Of those, **PK2** and **PK4** showed higher ER β agonist activity than for **PK1** or **PK3**. All of the stereoisomers

exhibited no ER β antagonist activity ($> 10\mu\text{M}$), and no agonist or antagonist activity ($> 10\mu\text{M}$) toward ER α . However, in search for the better ER β agonist selectivity between isomers, percent ER α agonist activity at highest concentration was assessed. In this study, **PK4** (1S,4R absolute configuration) manifested 47% activity at $12\mu\text{M}$ compared to the **PK2** (34% activity at $10\mu\text{M}$).

Table 4.5: TR-FRET and cell-based assay data for **ISP163** stereoisomers

ISP 163 Isomers	TR-FRET ER β (nM)	ER β Agonist (nM)	ER β Antagon. (μM)	ER α Agonist (μM)	% Agonist Activity @ Highest Concentration (μM)	ER α Antagon. (μM)
Mixture	44 \pm 16	30 \pm 9	>100	10.5 \pm 0.2		>10
PK1	>25	68 \pm 48	>36	5 \pm 3	150% @ 36	>36
PK2	33 \pm 10	47 \pm 4	>23	>10	34% @ 10	>10
PK3	90 \pm 36	119 \pm 13	>10	>10	10% @ 10	>10
PK4	65 \pm 26	53 \pm 10	>12	>12	47% @ 12	>12

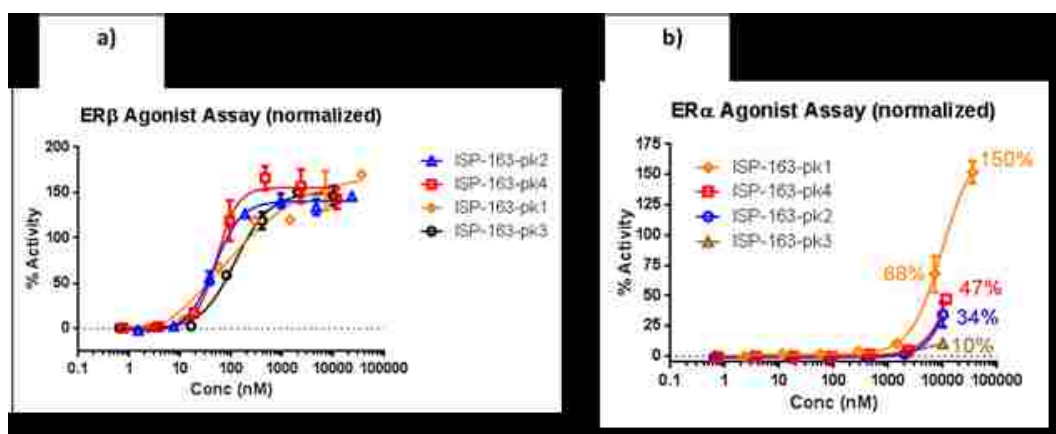


Figure 4.6: ER β cell-based assay profiles for individual **ISP163** stereoisomers

4.2.7 CYP450 Assay and Results for ISP358-2 and ISP163

The four-main drug metabolizing cytochrome P450 isoforms are CYP1A2, CYP2D6, CYP2C9, and CYP3A4.¹⁰⁷ The interaction of ligands with these CYP450 isoforms may be evaluated using P450-Glo™ inhibition assay kits available from Thermo Fisher. Isoform-specific substrates (Luciferin-ME, Luciferin-MEEGE, Luciferin-H, Luciferin-PPXE for CYP1A2, CYP2D6, CYP2C9, and CYP3A4 respectively) are incubated with the appropriate CYP enzyme, NADPH regeneration system and the test compound. Each CYP enzyme acts on a specific luminogenic P450-Glo™ substrate (Reaction A) to produce a luciferin product that generates light (chemiluminescence) upon interaction with the luciferin detection reagent (Reaction B), which is added after the CYP reaction has been completed (Figure 4.7). Light is used to monitor CYP activity since the amount of light produced is proportional to the amount of luciferin product formed after the CYP reaction.

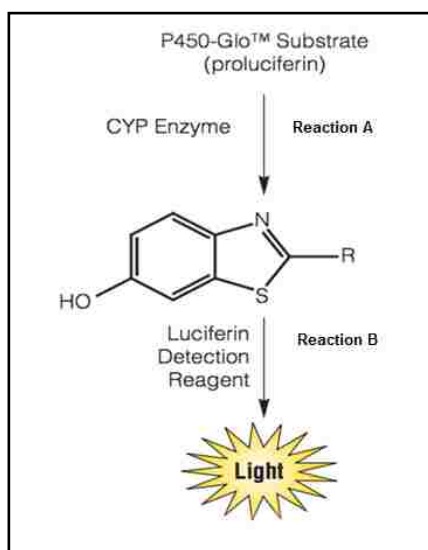


Figure 4.7: Schematic diagram for basis of CYP450 assay (http://www.lumflu.com/A_Info.asp?id=36)

Interaction of the ligand with the CYP, either by metabolism or by inhibition of the CYP, causes a decrease in the luminescence. Typical data for inhibition of CYP2C9 by **ISP358-2** are shown in Figure 4.8.

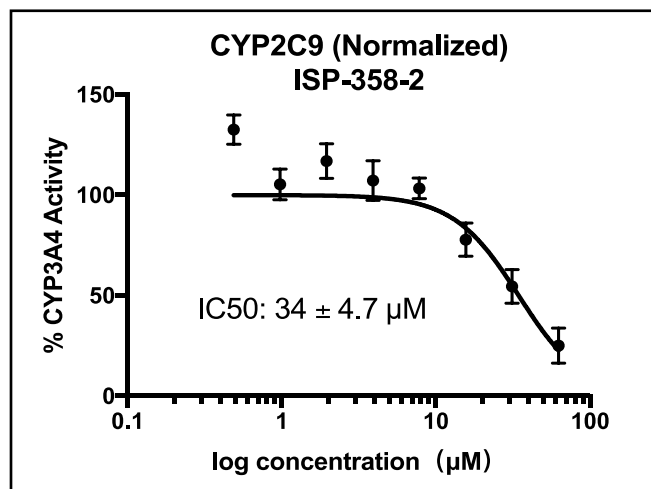


Figure 4.8: CYP2C9 assay profile for **ISP358-2**

The results for the best six-membered ring lead (**ISP358-2**) and the mixture of seven-membered ring stereoisomers (**ISP163**) are detailed in Table 4.6. The concentrations at which the two lead substances either inhibit these CYP450s and/or are metabolized by these CYP450s are significantly greater than their effective ER β binding concentrations, thus confirming their suitability as drug candidates for further development.

Table 4.6: CYP450 assay data for **ISP358-2** and **ISP163**

CYP Enzyme	ISP358-2 IC₅₀ (μM)	ISP163 IC₅₀ (μM)
CYP 2D6	Did not converge	>62.5
CYP 3A4	>62.5	31±2.7
CYP 1A2	>62.5	>62.5
CYP 2C9	34±4.7	1.8±0.3

4.2.8 hERG Assay results for **ISP358-2**

hERG (the human Ether-à-go-go-Related Gene) assay evaluates a compound's inhibition activity towards the K_v11.1, the alpha subunit of a voltage-gated potassium ion channel. This channel is involved in cardiac action potential repolarization (electrical activity) of the heart that regulates the heart's beating, inhibition of which is linked with the fatal disorder known as ventricular arrhythmias.¹⁰⁸ Compound **ISP358-2** was submitted to Thermo Fisher to evaluate (on a per-fee basis) the inhibition hERG ion channel (Figure 4.9). The results indicate 13% inhibition at 100 μM, representing an IC₅₀ of > 100 μM. This results again indicates safety of this lead compound against irregular heartbeat at the effective ERβ agonist concentration.

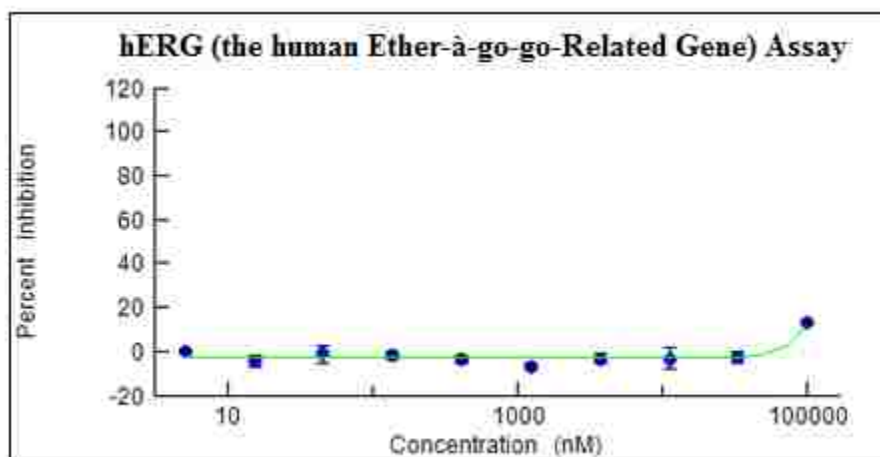


Figure 4.9: hERG profile of **ISP358-2**

4.2.9 Nuclear Receptor Panel Screening

Since ER is a nuclear receptor it is important to establish if potential agonists of ER β are agonists towards other nuclear receptors. A selected panel of receptors consisted of androgen receptor (AR, essential for normal female fertility and male skeletal integrity), glucocorticoid receptor (GR, a major component of the endocrine influence, specifically stress response), mineralocorticoid receptor (MR, important for expressing proteins which regulate ion and water transport), peroxisome proliferator-activator receptor delta (PPAR- Δ , involved in development of diabetes, obesity, atherosclerosis and cancer), progesterone receptor (PR, involved in cell proliferation), thyroid hormone receptor beta (TR- β , mediates functions of thyroid hormone), and the vitamin D receptor (VDR, involved in mineral metabolism) were considered. The panel screenings for **ISP358-2** and **ISP163-PK4** were conducted by Thermo/Life (on a per-fee basis) from GeneBlazer Cell based assay and results are summarized in Tables 4.7 and 4.8. Both compounds showed no

activity at 0.25, 2.5 and 25 μM concentrations thus confirming no cross-reactivity towards the aforementioned receptors at the effective ER β agonist concentration.

Table 4.7: Nuclear receptor panel screen data for **ISP358-2**

Nuclear receptor	ISP 358-2 @ 25 μM	ISP 358-2 @ 2.5 μM	ISP 358-2 @ 0.25 μM
AR	-6	-5	-6
GR	-1	0	2
MR	0	0	-1
PPAR- δ	2	3	2
PR	-2	0	-1
TR- β	-1	-1	-1
VDR	-1	-1	-1

Table 4.8: Nuclear receptor panel screen data for **ISP163-PK4**

Nuclear receptor	ISP 163-PK4 @ 25 μM	ISP 163-PK4 @ 2.5 μM	ISP 163-PK4 @ 0.25 μM
AR	-4	-6	-5
GR	1	-1	-1
MR	0	0	1
PPAR- δ	2	2	3
PR	-1	-2	-1
TR- β	-2	-1	0
VDR	0	0	-1

4.3 Description of *In vivo* Assays and Results

4.3.1 Assessment of Memory Consolidation in Ovariectomized Mice

The effects of lead compounds on memory consolidation were assessed. In particular, two types of behavioral tasks were utilized and which diverge in terms of the protocol for testing. The object recognition (OR) task tests the knowledge of object identity (“what”) and object placement task (OP) tests the knowledge of object location or spatial

memory (“where”). These tasks are sensitive to E2, exert low stress on subjects and a single training trial is ideal for mediating rapid biochemical activations to memory formation.^{33, 69, 109} Prior to testing, female mice (C57BL/6) used in this study were ovariectomized. For assay of administration directly to the brain, these mice were also implanted with a bilateral guide cannula aimed at the dorsal hippocampus. After one week of recovery, mice were trained in a square arena and were allowed to accumulate 30 s exploring two identical objects placed near the adjacent corners. Immediately after this training, mice were administered, either by dorsal hippocampal infusion (DH) or intraperitoneal injection (IP), with either vehicle (negative control); DPN, a known agonist (positive control), or the lead compound (**ISP358-2**) in different concentrations. For OP retention, animals were retested after 24 h with one of the objects in a different position; for OR retention animals were tested after 48 h with one new/novel object in place of a familiar object (Figure 4.10).

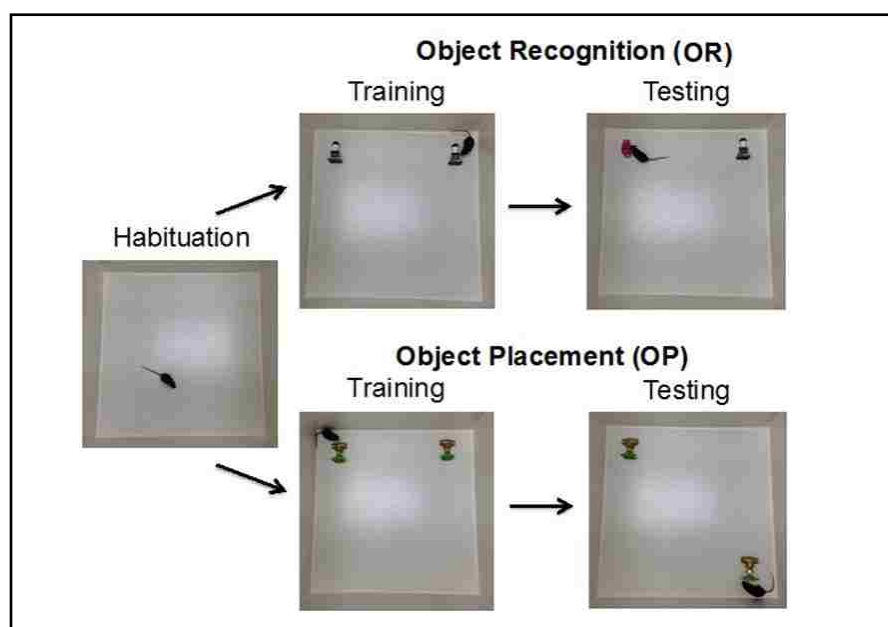


Figure 4.10: Illustration of object placement (OP) and object recognition (OR) protocols

Since mice are inherently drawn to novelty¹¹⁰ under unthreatened environment, mice who remember the training objects spend more time than chance (15 s) with either the new placement (OP assay) or novel object (OR assay) and less time than chance exploring the familiar object in these assays.

4.3.2 Assessment of Memory Consolidation by Dorsal Hippocampal Infusion

Due to its potency and high ER β selectivity, as well as its ease of preparation, *trans*-4-[4-(hydroxymethyl)cyclohexyl]phenol (**ISP358-2**) was selected for initial screening by single DH infusion. Five groups of mice (10 mice per group) were tested with each group receiving either vehicle (1% DMSO in saline), or DPN (10 pg/hemisphere), or **ISP358-2** (10 pg/hemisphere, 100 pg/hemisphere, 1 ng/hemisphere). For the object recognition task, mice receiving vehicle or the 10 pg dose of **ISP358-2** did not spend more than chance time with the novel object, while mice receiving the known ER β agonist DPN, or **ISP358-2** at the 100 pg or 1 ng/hemisphere dose spent statistically significant more time than chance with the novel object (Figure 4.11a). Similar results were obtained for the object placement task; neither administration of the vehicle nor the 10 pg dose of **ISP358-2** exhibited differences in exploring the familiar vs. the moved object, while treatment with DPN, 100 pg and 1 ng/hemisphere of **ISP358-2** did result in statistically significant more time spent with the moved object vs. the familiar object (Figure 4.11b). These data were confirmed by one-sample t-test, one-way ANOVA, and Fisher's LSD posthoc tests^{70, 109} and suggest that 100 pg and 1 ng of **ISP358-2**, administered by dorsal hippocampal infusion, enhances object recognition and object placement memory consolidation in the ovariectomized mouse model.

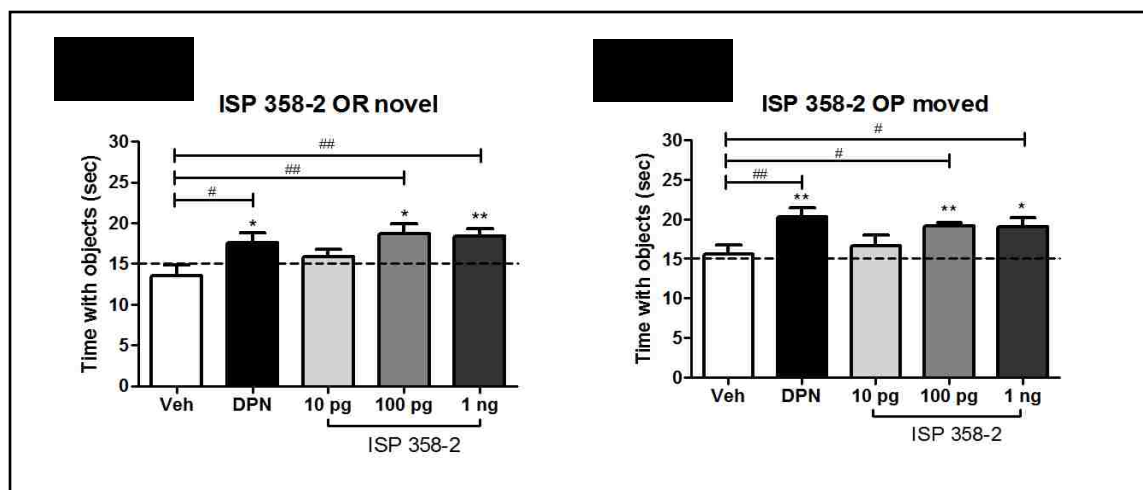


Figure 4.11: a) Amount of time (of 30 sec total) spent with the novel object in OR assay; b) Amount of time (of 30 sec total) spent with the novel in OP assay [DH infusion]

4.3.3 Assessment of Memory Consolidation by Intraperitoneal Administration

While the above results demonstrate the effectiveness of ER β agonist **ISP358-2** for memory consolidation in this animal model, dorsal hippocampal infusion is a less than ideal means of therapeutic administration. Studies of CNS drugs indicate that optimal characteristics for crossing the blood-brain barrier correspond to molecular weight ≤ 400 , $\log P = 1.5-2.7$, polar surface areas (PSA) = 60-70 \AA^3 , number of (nitrogen + oxygen atoms) ≤ 5 , and low molecular flexibility.¹¹¹⁻¹¹² **ISP358-2** fits the majority of these criteria except that it has PSA $\sim 40 \text{\AA}^3$. In order to determine if this compound is capable of passing the blood-brain barrier and arriving at the hippocampus, object recognition and object placement tasks were conducted after a single intraperitoneal administration (IP) of **ISP358-2** (Figure 4.12 a and b). Four groups (10 mice per group) of mice were tested: vehicle (1% DMSO in saline), positive control DPN (0.05 mg/kg) and two doses of **ISP-358-2** (0.5 mg/kg and 5 mg/kg). These doses of **ISP358-2** were based in relationship to

the known effective dose of DPN previously established by the Frick group. For the object recognition task, mice receiving vehicle did not spend time more than chance with the novel object while mice receiving the 0.5 mg/kg or 5 mg/kg dose of **ISP358-2** by IP injection spent more time with the novel object. The same trend was observed in the object placement task, and both OR and OP data were confirmed by one-sample t-test, one-way ANOVA, and Fisher's LSD posthoc tests.^{70, 109} These results suggest that 0.5 mg and 5 mg of **ISP358-2** enhanced the object recognition and object placement memory consolidation after intraperitoneal administration. Gratifyingly, these results confirmed both effectivity and blood-brain barrier (BBB) permeability of **ISP358-2** which is an essential requirement of central nervous system (CNS) drugs.

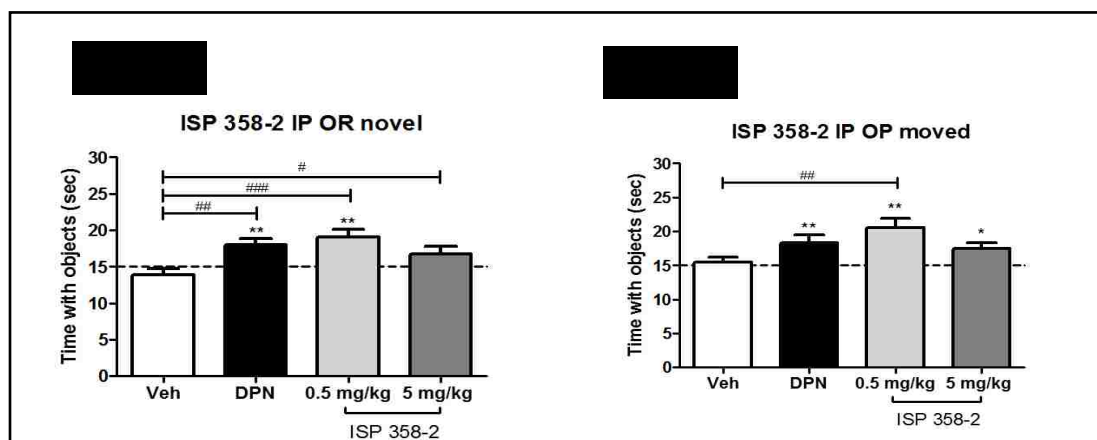


Figure 4.12: a) Amount of time (of 30 sec total) spent with the novel object in OR assay;
 b) Amount of time (of 30 sec total) spent with the novel in OP assay [IP injection]

CHAPTER 5

CONCLUSIONS AND OUTLOOK

5.1 Summary

The overall goal of this research was the design, synthesis and biological evaluation of ER β selective agonists for hippocampal memory consolidation in postmenopausal women. Two major types of non-steroidal compounds were synthesized and evaluated for *in vitro* ER β vs. ER α agonism, and *in vivo* effect on memory consolidation in an ovariectomized mouse model.

After identifying important prerequisites from the literature and from docking studies, research was focused towards the design of (4-hydroxyphenyl)cyclohexyl or cycloheptyl derivatives as selective ER β agonists. Toward this end, *cis*-4-(4-(hydroxymethyl)cycloheptyl)phenol was first prepared from organoiron methodology and found to be an ER β agonist in the 50 nM range with >1000- fold selectivity for ER β over ER α in cell-based assays.⁸¹ While these biological results were promising, the organoiron synthetic route was problematic and difficult to replicate. Three alternative syntheses were established using cheaper starting materials and more robust synthetic protocols; the most efficient route proceeded in fewer steps and with greater yields (20% in six steps). These new protocols gave a racemic mixture of diastereomers of 4-(4-(hydroxymethyl)cycloheptyl)phenol (**ISP163**); the individual stereoisomers were obtained by preparative chiral HPLC. The relative stereochemistry of the diastereomers was established by NMR spectroscopy, while the absolute configuration of the individual *cis*-isomers were determined by single crystal X-ray diffraction analysis. A second lead

molecule, 4-(4-(hydroxymethyl)cyclohexyl)phenol (**ISP171**) was synthesized by sharing common synthetic pathways as in **ISP163**. The product was a mixture of *cis*- and *trans*-stereoisomers and a chemical separation of the mixture, via faster oxidative cyclization of the *cis*-isomer, afforded the *trans*- isomer **ISP358-2** in 47% yield under optimal conditions. Several other 4-cyclohexyl and cycloheptyl phenolic analogs were prepared with varying functional groups, chain lengths, and molecular rigidity in order to establish structure activity relationships (SARs).

A TR-FRET ER β binding assay was conducted as an initial screen for the binding affinity of the synthesized ligands. The incorporation of an aliphatic hydroxyl functionality at the end of the side chain, but not directly to the ring core appeared to have a stronger effect on the binding affinity of both six- and seven-membered ring scaffolds (**ISP163**, **ISP171**, **ISP358-2**, **ISP402**, **ISP248** and **RKP231IIF**). In contrast, introduction of an alkene functionality, and thereby rigidity within the ring structure decreased the binding affinity of ligands (**ISP346** and **RKP35c**). To supplement the TR-FRET findings, cell-based assays were conducted for selected compounds having higher binding affinity to investigate their potential for binding and ability to effect transcription. Among the six-membered series the *trans* isomer **ISP358-2** revealed the highest potency as ER β agonists (~ 30 nM). The same trend was observed in the seven-membered series where **ISP163** exhibited the highest ER β agonist activity (~ 30 nM). In general, all compounds which were tested in cell based assay did not have any observable effect on ER β antagonist, ER α agonist or ER α antagonist activity. Of particular note is that **ISP358-2** and **ISP163** exhibit > 3000-fold and > 300-fold selectivity for ER β over ER α , thus making these compounds the most selective ER β agonists yet reported. Finally, the cell based assay for the individual

ISP163 stereoisomers (PK1-PK4) revealed that **ISP163-PK4** [4(*S*)-(4-hydroxyphenyl)-1-(*R*)-hydroxymethylenecycloheptane] possessed the best combination of potency (~ 53 nM) and ER β :ER α selectivity (226-fold).

Having recognized **ISP163** and **ISP358-2** as best ER β agonist from each series, their metabolic stability was evaluated. Both compounds exhibited poor inhibitory activity (> 30 μ M) against four known drug metabolizing CYP450s, thus confirming their stability inside the liver. The exception was **ISP163** which exhibited IC₅₀ = 1.8 μ M for CYP2C9. This value is still considerably poorer than the ER β IC₅₀ (30 nM). Neither **ISP163-PK4** nor **ISP358-2** exhibited cross reactivity with other common nuclear receptors (<2% activation at 25 μ M). Additionally, **ISP358-2** did not show any observable effect on hERG inhibition indicating its non-cardiotoxicity.

Memory consolidation in ovariectomized mice (C57BL/6) was assessed for **ISP358-2** via DH infusion and IP administration. A statistically significant effect was observed for memory consolidation in both object placement and object recognition tests at the 100 pg/hemisphere (DH) and 0.5 mg/Kg (IP) dose level. These are both approximately one order of magnitude less potent in comparison to the DPN; 10 pg/hemisphere (DH) and 0.05mg/Kg (IP). These relative efficacies are consistent with the relative ER β agonist activity of **ISP358-2** compared to DPN. The IP data also provides strong evidence for the blood-brain-barrier (BBB) permeability of **ISP358-2**.

5.2 Conclusion

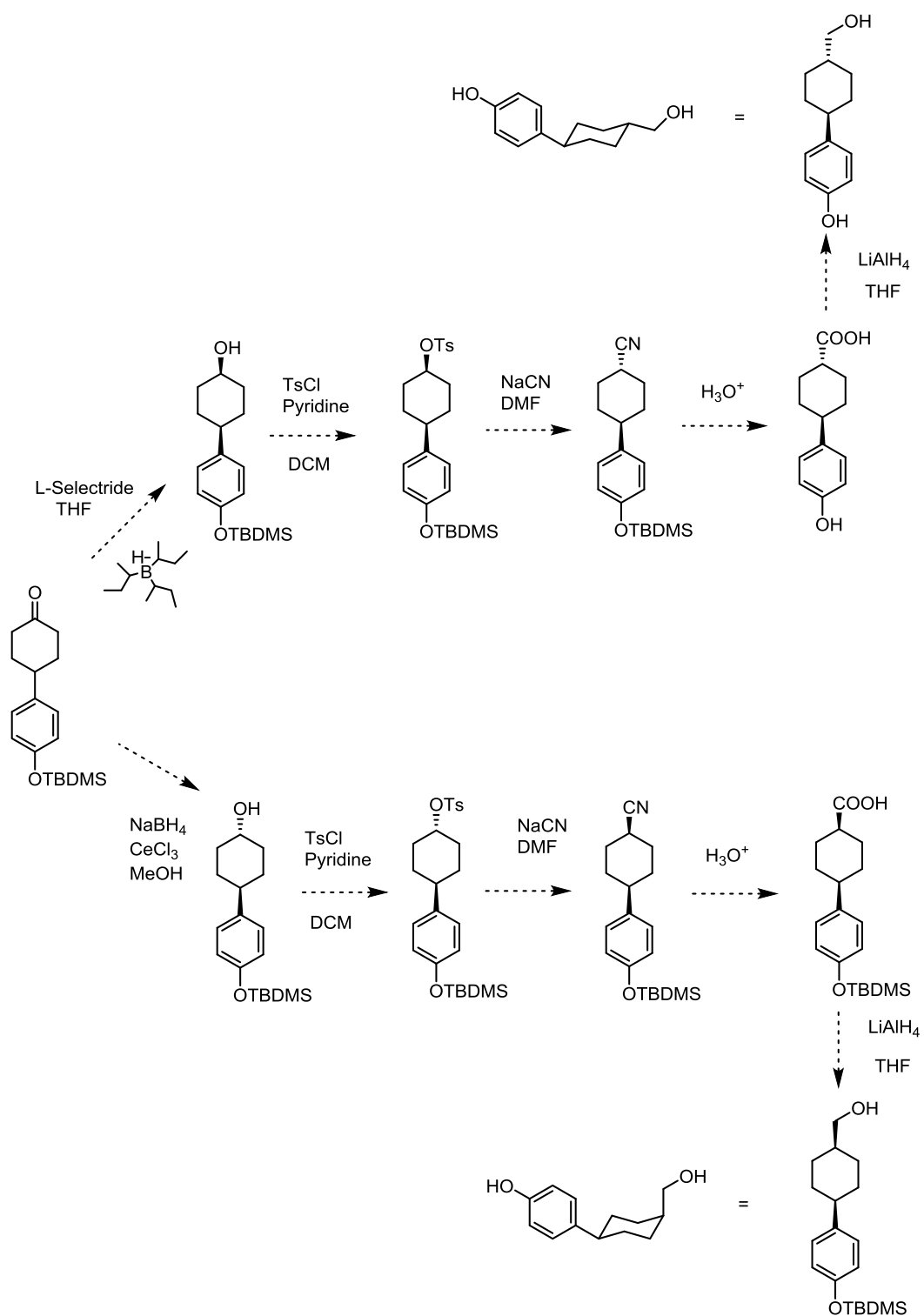
The results presented in this dissertation demonstrate the development of two types of non-steroidal selective ER β agonists. Among those, [4(*S*)-(4-hydroxyphenyl)-1-(*R*)-hydroxymethylenecycloheptane] (**ISP163-PK4**) and *trans*-4-(4-(hydroxymethyl)cyclohexyl)phenol (**ISP358-2**) display > 225-fold and > 3000-fold selectivity for ER β over ER α respectively. **ISP358-2** was shown to have a statistically significant effect on memory consolidation in ovariectomized mice by either DH and IP administration. The lack of off-target nuclear receptor activity, as well as lack of hERG activity, and the high metabolic stability (compared to effective dose) highlight the potential for this compound as a potential therapeutic for hippocampal memory consolidation.

5.3 Outlook

It is evident that great deal of research over the past two decades has focused on the design of estrogen receptor beta selective ligands as drug candidates. There is extensive literature on relationships between ER β agonists and hippocampal physiology for the development of new CNS drugs.

The (4-hydroxyphenyl)cyclohexyl or cycloheptyl based ER β agonists, specifically **ISP163** and **ISP358-2**, described herein serve as a foundation for the development of small non-steroidal molecules as ER β agonists. Nevertheless, scalable stereo-specific synthesis of those is essential for further biological studies. Moreover, it is important to synthesize the *cis*-**ISP171** to compare its potency with respect to *trans*-stereoisomer (**ISP358-2**). One potential route to this compound is outlined in Scheme 5.1.

The crystal structures of **ISP358-2** with ER β and ER α should provide valuable information into the origin of its selectivity. It will be necessary to establish collaborations for these studies. Additionally, while **ISP358-2** interacts with the panel of four CYP enzymes at concentrations 1,000-fold greater than the ER β IC₅₀ value, it will be important to assess the metabolic products produced from this compound with human liver microsomes. Furthermore, while the memory consolidation efficacy of **ISP358-2** via intraperitoneal administration demonstrates the ability of this compound to pass the blood-brain barrier, the ability of this compound to be transported across intestinal mucosa is, yet, unknown. This will require assessment of this lead molecule to be transported across a Caco-2 cell monolayer. A correlation between the Caco-2 monolayer permeability and *in vivo* absorption is well recognized.¹¹³⁻¹¹⁴ Additionally, OP and OR testing via oral (gavage) administration could provide evidence for intestinal adsorption.



Scheme 5.1: Proposed synthetic protocol for *cis*- and *trans*-ISP171

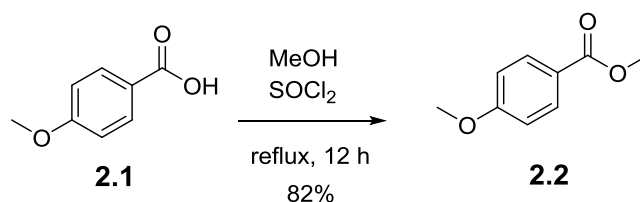
CHAPTER 6

SYNTHESIS AND CHARACTERIZATION

6.1 Chemicals and General Methods

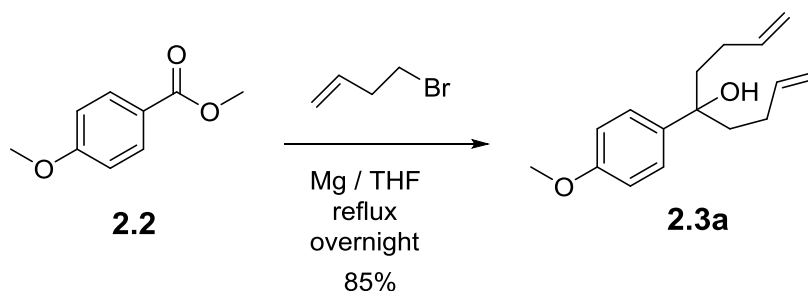
All the chemicals were purchased from Sigma-Aldrich, Matrix scientific, or Alfa Aesar and used as received. Reactions with moisture- or air-sensitive reagents were conducted under an inert atmosphere of nitrogen in oven-dried glassware with anhydrous solvents. Reactions were followed by TLC on precoated silica plates (60 Å, F₂₅₄, EMD Chemicals Inc) and were visualized by UV lamp (UVGL-25, 254/365 nm). Flash column chromatography was performed by using flash silica gel (32–63 μ). NMR spectra were recorded on Varian UnityInova 400 MHz instrument. CDCl₃, [D₆] dimethylsulfoxide and [D₆] acetone were purchased from Cambridge Isotope Laboratories. ¹H NMR spectra were calibrated to δ = 7.26 ppm for residual CHCl₃, δ = 2.50 ppm for d₅-DMSO and δ = 3.30 ppm for residual d₃-CD₃OD. ¹³C NMR spectra were calibrated from the central peak at δ = 77.23 ppm for CDCl₃, δ = 39.52 ppm for d₆-DMSO and δ = 49.00 ppm for CD₃OD.

6.2 Experimental Details



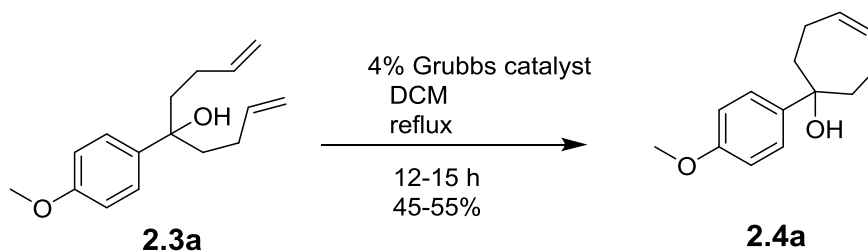
Methyl 4-methoxybenzoate (2.2). Para anisic acid **2.1** (8.010 g, 52.56 mmol) was dissolved in methanol (200 mL) and SOCl₂ (10 mL, 6.8 mmol) was added dropwise with stirring at 0 °C over 30 min. The system was heated at 65 °C for 12 h under N₂. The

resulting mixture was cooled to room temperature and diluted with water (50 mL). Methanol was evaporated and the pH was adjusted to pH = 7 with saturated sodium bicarbonate solution (5 mL). The resulting solution was extracted with ethyl acetate (3 × 30 mL). The combined organic extracts were washed with brine (20 mL), dried (MgSO₄), and concentrated to give **2.2** as a colorless solid (7.16 g, 82%). ¹H NMR (400 MHz, d₆-DMSO) δ 7.04 and 6.17 (AA'BB', J_{AB} = 8.7 Hz, 4H), 2.95 (s, 3H), 2.93 (s, 3H) ppm. ¹³C NMR (100 MHz, d₆-DMSO) δ 165.9, 163.2, 131.2, 121.8, 114.0, 55.5, 52.0 ppm. The NMR spectral data for **2.2** are consistent with the literature values.¹¹⁵



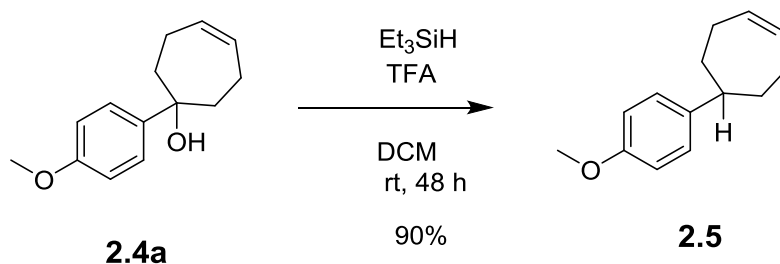
5-(4-Methoxyphenyl)-1,8-nonadien-5-ol (2.3a). Dry magnesium turnings (3.654 g, 152.1 mmol) were placed in a flame dried three-necked flask followed by THF (30 mL). The system was connected to the N₂ environment while stirring and fitted with a condenser and an addition funnel. The addition funnel was loaded with a solution of 4-bromo-1-butene (7.72 mL, 76.1 mmol) in THF (20 mL). A little amount of the bromobutene solution (2 mL) was added slowly to the magnesium turnings, and the contents were heated to reflux. Once the Grignard formation had started, the remaining bromide solution was added dropwise maintaining a gentle reflux. The reaction was stirred until most of the magnesium had reacted. A solution of methyl 4-methoxybenzoate **2.2** (2.528 g, 15.20 mmol) in THF (30 mL) was loaded into the addition funnel and added dropwise over 30 min. After stirring

overnight at ambient temperature, a saturated solution of NH_4Cl (30 mL) was added to quench the reaction. The resultant emulsion was stirred for 2 h and the solution was extracted with ether (3 x 40 mL). The combined organic layers were washed with water (30 mL), then brine (2 x 20 mL) and dried (MgSO_4). The solvent was evaporated to give alcohol **2.3a** as a yellow oil (3.182 g, 85%). ^1H NMR (400 MHz, CDCl_3) δ 7.29 and 6.88 (AA'BB', $J_{\text{AB}} = 8.9$ Hz, 4H), 5.84-5.73 (m, 2H), 4.98-4.88 (m, 4H), 3.81 (s, 3H), 1.96-1.84 (m, 8H) ppm. ^{13}C NMR (100 MHz, CDCl_3) δ 158.2, 139.0, 137.9, 126.6, 114.8, 113.7, 77.1, 55.3, 42.4, 28.1 ppm.

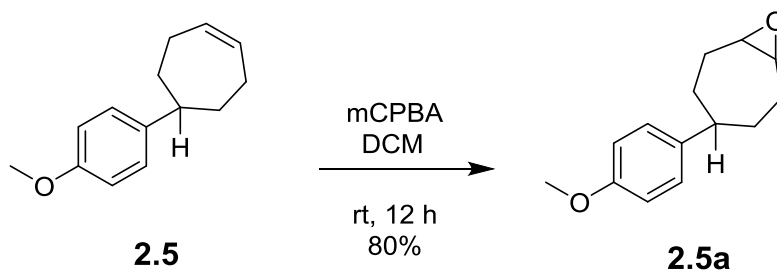


1-(4-Methoxyphenyl)-4-cyclohepten-1-ol (2.4a). Alcohol **2.3a** (1.015 g, 4.126 mmol) was dissolved in dry CH_2Cl_2 (415 mL, 0.01 M) to give a colorless solution. A solution of Grubbs I catalyst (0.136 g, 0.165 mmol, 4%) in CH_2Cl_2 (15 mL) was added slowly through the syringe pump over 10 h and the mixture was heated at 40 °C with stirring for 12-18 h. The reaction mixture was cooled to room temperature, quenched with DMSO (50 eq, 0.600 mL) and continued to stir for 12 h. The mixture was concentrated to dryness and the crude material was purified by column chromatography (SiO_2 , hexanes-diethyl ether = 80:20) to give **2.4a** (0.675 g, 75%) as a green oil. ^1H NMR (400 MHz, CDCl_3) δ 7.43 and 6.87 (AA'BB', $J_{\text{AB}} = 9.0$ Hz, 4H), 5.86-5.83 (m, 2H), 3.80 (s, 3H), 2.55-2.44 (m, 2H), 2.10-1.97

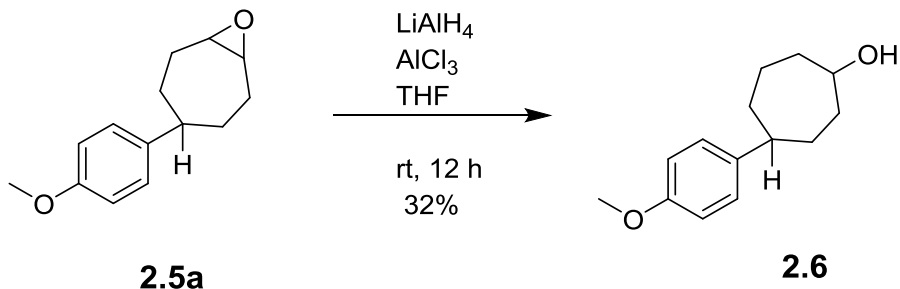
(m, 4H), 1.90-1.82 (m, 2H), ppm. ^{13}C NMR (100 MHz, CDCl_3) δ 158.3, 142.3, 132.1, 125.8, 113.5, 76.5, 55.2, 40.1, 23.0 ppm.



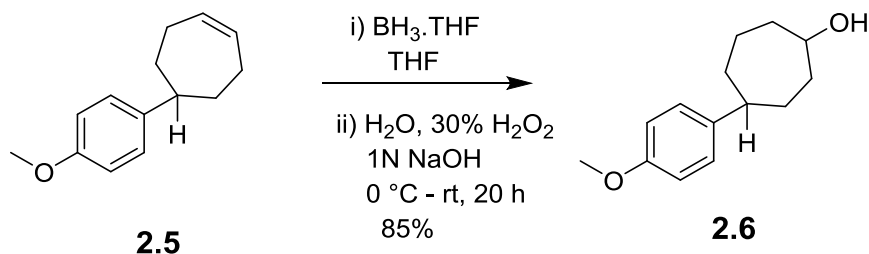
5-(4-Methoxyphenyl)-1-cycloheptene (2.5). Alcohol **2.4a** (1.720 g, 7.880 mmol) was dissolved in dry CH_2Cl_2 (50 mL) to give a light green solution. Triethylsilane (1.4 mL, 8.8 mmol) was added followed by TFA (6.2 mL, 79 mmol). The mixture was stirred at room temperature for 48 h while monitoring the reaction by TLC. After complete disappearance of starting material, the solution was concentrated to a bilayer oil and purified by column chromatography (SiO_2 , hexanes-ethyl acetate = 50:50) to give **2.5** as a brown oil (1.433 g, 90%). ^1H NMR (400 MHz, CDCl_3) δ 7.11 and 6.84 (AA'BB', $J_{\text{AB}} = 8.6$ Hz, 4H), 5.91-5.87 (m, 2H), 3.79 (s, 3H), 2.69 (tt, $J = 11.3, 3.2$ Hz, 1H), 2.35-2.25 (m, 2H), 2.23-2.13 (m, 2H), 1.91-1.83 (m, 2H), 1.54-1.43 (m, 2H) ppm. ^{13}C NMR (100 MHz, CDCl_3) δ 157.9, 141.8, 132.5, 127.7, 113.9, 55.5, 49.6, 35.2, 28.2 ppm.



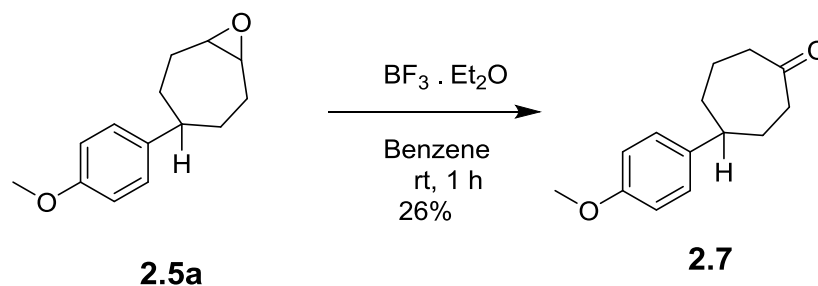
1,2-Epoxy-5-(4-methoxyphenyl)cycloheptane (2.5a). A solution of cycloheptene **2.5** (0.551g, 2.73 mmol) in freshly distilled CH_2Cl_2 (20 mL) was stirred for 10 min. To this solution was added dropwise a solution of m-chloroperoxybenzoic acid (mCPBA) (1.008 g, 70% wt, 4.090 mmol) in freshly distilled CH_2Cl_2 (10 mL). The solution was stirred under nitrogen and the reaction was followed by TLC. The solvent was evaporated and residue was treated with saturated sodium bicarbonate solution (20 mL) with stirring for 30 min. The mixture was extracted with CH_2Cl_2 (3 x 20 mL), concentrated and purified by column chromatography (SiO_2 , hexanes-ethyl acetate = 50:50) to give **7** (0.441 g, 74%) as a yellow oil. This was determined to be a mixture of *cis*- and *trans*-stereoisomers by ^1H and ^{13}C NMR spectroscopy. ^1H NMR (400 MHz, CDCl_3) δ 7.12-7.05 (m, 4H), 6.86-6.79 (m, 4H), 3.78 (s, 3H), 3.77 (s, 3H), 3.20-3.16 (m, 2H), 3.13-3.07 (m, 2H), 2.55 (tt, $J = 11.1$, 3.3 Hz, 1H), 2.41-2.28 (m, 4H), 2.13 (tt, $J = 11.1$, 2.2 Hz, 1H), 1.93-1.84 (m, 2H), 1.83-1.77 (m, 2H), 1.75-1.67 (m, 2H), 1.66-1.57 (m, 4H), 1.51-1.39 (m, 2H) ppm. ^{13}C NMR (100 MHz, CDCl_3) δ 157.8/157.6, 141.2, 139.9, 127.6/127.3, 113.8/113.7, 56.1, 55.1, 49.2, 48.0, 32.6, 32.0, 28.8, 27.5 ppm.



4-(4-Methoxyphenyl)cycloheptanol (2.6). Epoxide **2.5a** (0.100 g, 0.460 mmol) was dissolved in dry THF under N₂. To this solution was added LiAlH₄ (0.048 g, 1.4 mmol) and AlCl₃ (0.056 g, 0.46 mmol). The resulting mixture was stirred for 12 h, then treated with water (15 drops) and diluted with saturated aqueous KOH (3 mL) and water (10 mL). The mixture was filtered through celite and extracted with ether (3 × 20 mL). The combined organic extracts were dried (MgSO₄), and solvent was evaporated. The residue was purified by column chromatography (SiO₂, hexanes-ethyl acetate = 20:80) to give **2.6** (0.032 g, 32%) as a light-yellow oil. This product was determined to be a mixture of *cis*- and *trans*-stereoisomers on the basis of ¹H and ¹³C NMR spectroscopy. ¹H NMR (400 MHz, CDCl₃) δ 7.11 and 7.09 (2 × d, J = 8.3 Hz, 2H total), 6.83 (d, J = 8.2 Hz, 2H), 4.06-4.00 and 3.99-3.90 (2 × m, 1H total), 3.78 (s, 3H), 2.72–2.56 (m, 1H), 2.15-2.05 (m, 1H), 2.02–1.50 (m, 10H) ppm. ¹³C NMR (100 MHz, CDCl₃) δ 157.6, 141.4, 127.5, 113.7, 72.7, 71.6, 55.2, 46.2, 38.2, 37.6, 36.9, 35.7, 31.7, 29.6, 23.3, 21.3 ppm.

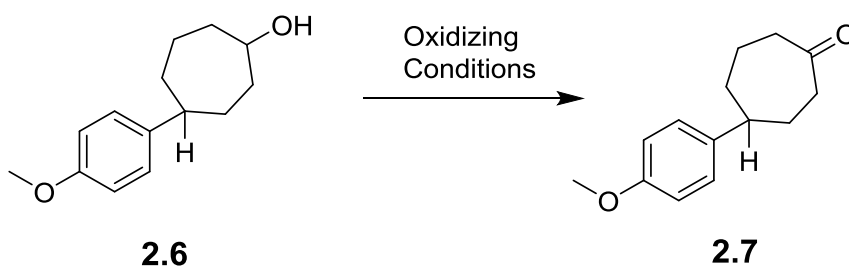


4-(4-Methoxyphenyl)cycloheptanol (2.6). To a solution of cycloheptene **2.5** (1.24 g, 6.14 mmol) in freshly distilled THF (25 mL) at 0°C , was added dropwise a solution of borane-tetrahydrofuran complex (1M in THF, 11.3 mL, 11.3 mmol). The solution was gradually warmed to room temperature and stirred for 20 h under N_2 . The reaction mixture was cooled to 0°C , and water (440 mL) was added slowly followed by 30% hydrogen peroxide (8.50 mL) and 1N sodium hydroxide (14.5 mL). The resulting solution was stirred at room temperature for 30 min and extracted with ethyl acetate (2 x 20 mL), concentrated and purified by column chromatography (SiO_2 , hexanes-ethyl acetate = 60:40) to give **2.6** (1.150 g, 85%) as a yellow oil. This was determined to be a mixture of diastereoisomers by ^1H and ^{13}C NMR spectroscopy by comparison to a sample previously prepared.



4-(4-Methoxyphenyl)cycloheptanone (2.7). A solution of epoxide **2.5a** (0.038 g, 0.17 mmol) in benzene (20 mL) was treated with borontrifluoride etherate (0.15 mL, 0.87 mmol) under N_2 . The light yellow solution became darker in color and was stirred for 1 h. The

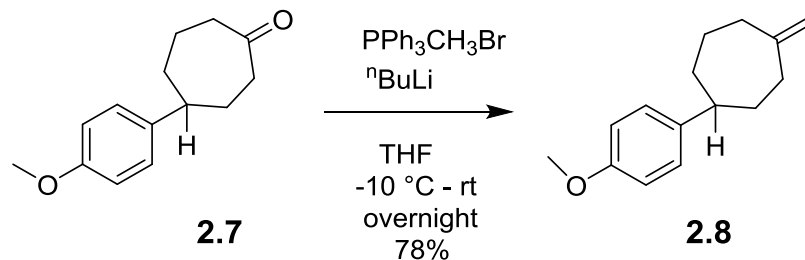
mixture was treated with saturated aqueous sodium carbonate (25 mL), and the organic layer was separated and dried (MgSO_4). The solvent was evaporated under reduced pressure to give a yellow crude oil. The residue was purified by column chromatography (SiO_2 , hexanes-ethyl acetate = 80:20) to afford **2.7** (0.010 g, 26%) as a colorless oil. ^1H NMR (400 MHz, CDCl_3) δ 7.10 and 6.84 (AA'BB', $J_{\text{AB}} = 8.7$ Hz, 4H), 3.79 (s, 3H), 2.77–2.53 (m, 4H), 2.16–1.52 (m, 7H) ppm. ^{13}C NMR (100 MHz, CDCl_3) δ 215.0, 157.9, 139.9, 127.4, 113.9, 55.3, 47.9, 43.8, 42.9, 38.6, 32.2, 23.8 ppm. The spectral data obtained for **9** was consistent with the literature values.⁸⁷



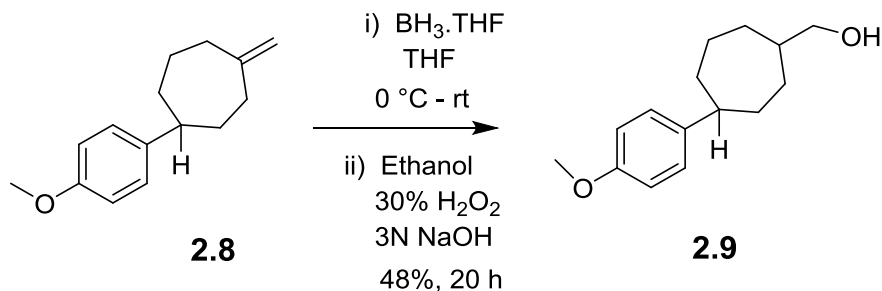
4-(4-Methoxyphenyl)cycloheptanone (2.7). Method A: To a solution of cycloheptanecol alcohol **2.6** (0.701g, 3.19 mmol) in CH_2Cl_2 (30 mL) at room temperature, were added pyridinium chlorochromate (1.39 g, 6.44 mmol) and silica (or celite) (1.52 g), and the resulting mixture was stirred at room temperature for 4 h. The solution was filtered through a small pad of silica gel eluting with CH_2Cl_2 . The filtrate was concentrated in vacuo, and the residue was purified by column chromatography (SiO_2 , hexanes-ethyl acetate = 80:20) to afford **2.7** (0.389 g, 55%) as a colorless oil. The ^1H NMR spectrum of the product was identical to that previously obtained.

Method B: Dry magnesium turnings (0.152 g, 6.33 mmol) were placed in a flame dried three-necked flask followed by THF (10 mL). A solution of propylbromide (0.200 mL, 1.27 mmol) in THF (2 mL) was added dropwise while refluxing under nitrogen environment. Once the Grignard formation was completed, the mixture was cooled to room temperature and a solution of 1,1'-(azodicarbonyl)dipiperidine (0.319g, 2.53 mmol) in THF (4 mL) was added dropwise over 15 min. Then alcohol **2.6** (0.132 g, 0.600 mmol) was slowly added while stirring overnight at ambient temperature. A saturated solution of NH₄Cl (30 mL) was added to quench the reaction. The resultant emulsion was stirred for 30 min and the solution was extracted with ether (2 x 20 mL). The combined organic layers were washed with water (30 mL), then brine (20 mL) and dried (MgSO₄). The solvent was evaporated and purified by column chromatography (SiO₂, hexanes-ethyl acetate = 80:20) to afford **2.7** (0.027 g, 20%) as a colorless oil. The ¹H NMR spectrum of the product was identical to that previously obtained.

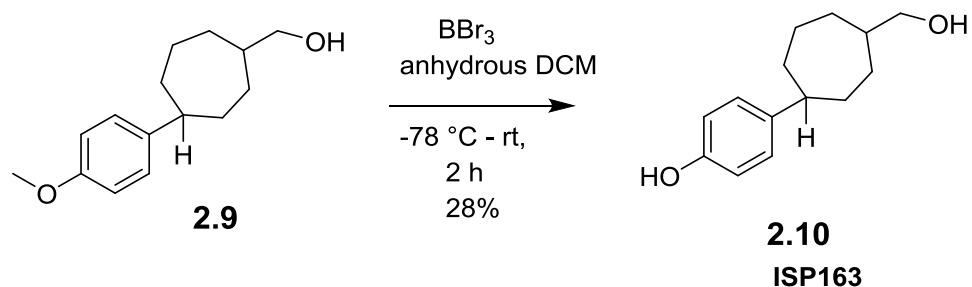
Method C: To a solution of cycloheptane-alcohol **2.6** (0.787 g, 3.58 mmol) in CH₂Cl₂ (38 mL) at room temperature, were added Dess–Martin periodinane (4.55 g, 10.7 mmol) and water (0.2 mL) and mixture was stirred at room temperature for 6 h. The mixture was quenched with 1:1 mixture of saturated Na₂S₂O₃ and NaHCO₃ solution and continued to stir for 30 min. The resulting solution was stirred at room temperature for 30 min and extracted with ethyl acetate (2 x 20 mL), dried (MgSO₄) concentrated and purified by column chromatography (SiO₂, hexanes ethylacetate = 80:20) to afford **2.7** (0.389 g, 50%) as a colorless oil. The ¹H NMR spectrum of the product was identical to that previously obtained.



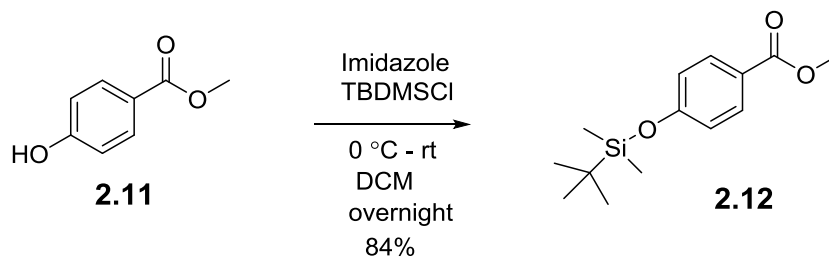
1-(4-Methoxyphenyl)-4-methylenecycloheptane (2.8). To a stirred solution of $\text{PPh}_3\text{CH}_3\text{Br}$ (1.25 g, 3.50 mmol) in anhydrous THF (30 mL) at -10°C under N_2 , was added a solution of n-butyl lithium (1.6 M in hexanes, 2.3 mL, 3.7 mmol) dropwise. After complete addition, the deep yellow mixture was stirred for another 45 min at -10°C before slowly adding a solution of **2.7** (0.380 g, 1.74 mmol) in THF (6 mL). The solution changed from a deep to light yellow in color, and the mixture was gradually warmed to room temperature and stirred overnight. The solution was diluted with water (20 mL) and aqueous layer was extracted with ethyl acetate (2×20 mL). The combined organic extracts were washed with brine and dried (MgSO_4). The residue was purified by column chromatography (SiO_2 , hexanes-ethyl acetate = 80:20) to give **2.8** (0.296 g, 79%) as a light-yellow oil. ^1H NMR (400 MHz, CDCl_3) δ 7.10 and 6.83 (AA'BB', $J_{\text{AB}} = 8.4$ Hz, 4H), 4.77 (s, 2H), 3.79 (s, 3H), 2.61–2.45 (m, 2H), 2.32 (broad t, $J = 12.2$ Hz, 2H), 2.00–1.84 (m, 3H), 1.71–1.48 (m, 4H) ppm. ^{13}C NMR (100 MHz, CDCl_3) δ 157.6, 151.9, 141.6, 127.7, 113.8, 110.9, 55.5, 47.5, 37.9, 37.2, 36.1, 35.3, 27.4 ppm.



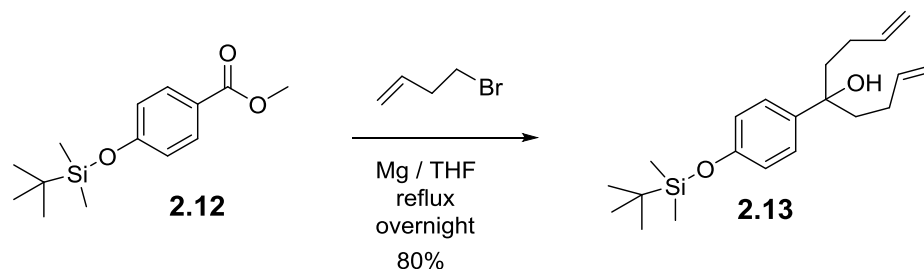
(4-(4-Methoxyphenyl)cycloheptyl)methanol (2.9). To a solution of **2.8** (0.296 g, 1.37 mmol) in freshly distilled THF (10 mL) at $0\text{ }^\circ\text{C}$, was added dropwise a solution of borane-tetrahydrofuran complex (1M in THF, 2.75 mL, 2.7 mmol). The resulting mixture was warmed to room temperature and stirred for 20 h. The reaction mixture was cooled to $0\text{ }^\circ\text{C}$, and pure ethanol (115 mL) was added slowly followed by 30% hydrogen peroxide (2 mL) and 3N sodium hydroxide (10 mL). The mixture was heated at reflux for 1 h, extracted with ethyl acetate ($2 \times 20\text{ mL}$), dried (MgSO_4), and the solvent evaporated. The crude material was purified by column chromatography (SiO_2 , hexanes-ethyl acetate = 60:40) to give **2.9** (0.155 g, 48%) as a colorless gum. This was determined to be a mixture of diastereoisomers by ^1H and ^{13}C NMR spectroscopy. ^1H NMR (400 MHz, CDCl_3) δ 7.11 and 6.83 (AA'BB', $J_{\text{AB}} = 8.8\text{ Hz}$, 4H), 3.77 (s, 3H), 3.46 (d, $J = 6.4\text{ Hz}$, 2H), 2.69–2.55 (m, 1H), 2.00–1.72 (m, 8H), 1.68–1.39 (m, 4H) ppm. ^{13}C NMR (100 MHz, CDCl_3) δ 157.6, 142.1, 141.8, 127.7, 113.8, 68.6, 68.4, 55.4, 47.2, 46.0, 42.2, 41.0, 38.8, 36.8, 36.5, 33.0, 31.5, 30.6, 29.9, 28.5 ppm.



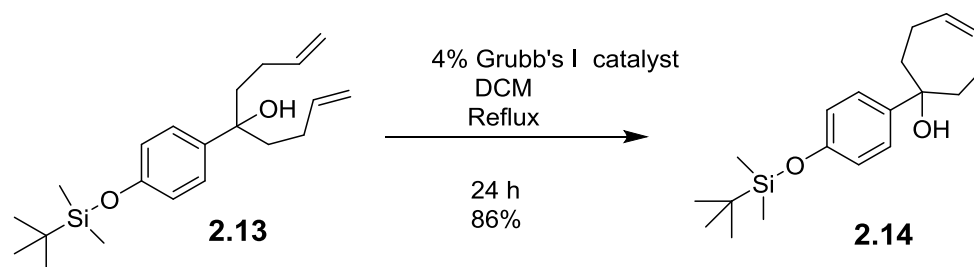
4-(4-(Hydroxymethyl)cycloheptyl)phenol (2.10). To a stirred solution of **2.9** (0.180 g, 0.769 mmol) in anhydrous CH_2Cl_2 (10 mL) at $-78\text{ }^\circ\text{C}$, was added dropwise a solution of boron tribromide (1M in CH_2Cl_2 , 2.31 mL, 2.31 mmol). After complete addition, the reaction mixture was stirred for 30 min at $-78\text{ }^\circ\text{C}$ and gradually warmed to room temperature over a 2 h period. The mixture was quenched with water (10 mL) and the aqueous layer was extracted with CH_2Cl_2 ($3 \times 20\text{ mL}$). The combined organic extracts were washed with brine and dried (MgSO_4). Evaporation of the solvent and purification from column chromatography (SiO_2 , hexanes-ethyl acetate = 50:50) gave **2.10** (0.048 g, 28%) as a colorless solid. This product was determined to be a mixture of *cis*- and *trans*-stereoisomers on the basis of ^1H and ^{13}C NMR spectroscopy. mp $60\text{--}63\text{ }^\circ\text{C}$. ^1H NMR (400 MHz, CDCl_3) δ 7.03 and 6.74 (AA'BB', $J_{\text{AB}} = 8.5\text{ Hz}$, 4H), 5.10 (s, 1H), 3.48 (d, $J = 6.6\text{ Hz}$, 2H), 2.67–2.49 (m, 1H), 1.97–1.32 (m, 11 H) ppm. ^{13}C NMR (400 MHz, CDCl_3) δ 153.8, 142.0, 141.8, 127.9, 127.8, 115.4, 68.6, 68.5, 47.2, 46.1, 42.2, 41.3, 38.9, 36.7, 36.5, 33.0, 31.5, 30.6, 29.9, 28.5, 27.4, 24.3 ppm.



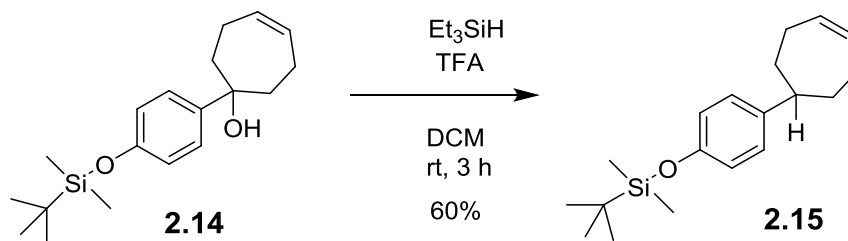
Methyl 4-((tert-butyldimethylsilyl)oxy)benzoate (2.12). To a stirred solution of methyl-4-hydroxybenzoate **2.11** (8.000 g, 52.5 mmol) in anhydrous CH₂Cl₂ (80 mL) under N₂ was added imidazole (10.7 g, 157 mmol) while stirring at 0 °C. After 45 min, tert-butyldimethylsilyl chloride (11.9 g, 78.9 mmol) was added and stirred at 0 °C for 2 h, and at room temperature overnight. The resulting mixture was diluted with brine (70 mL) and partitioned with CH₂Cl₂ (3 x 30 mL). The combined organic extracts were dried (MgSO₄), concentrated and purified by column chromatography (SiO₂, hexanes -ethyl acetate = 90:10) to give **2.12** as a colorless gum. (11.73 g, 84%). ¹H NMR (400 MHz, CDCl₃) δ 7.93 and 6.84 (AA'BB', J_{AB} = 8.9 Hz, 4H), 3.86 (s, 3H), 0.97 (s, 9H), 0.21 (s, 6H) ppm. ¹³C NMR (100 MHz, CDCl₃) δ 170.0, 160.2, 131.5, 123.2, 119.9, 51.9, 25.7, 18.1, -4.3 ppm. The spectral data for this compound were consistent with the literature values.¹¹⁶



5-(4-((tert-Butyldimethylsilyl)oxy)phenyl)nona-1,8-dien-5-ol (2.13). Dry magnesium turnings (6.75 g, 0.281 mmol) were placed in a flame dried three-necked flask followed by THF (25 mL). The system was under N₂ while stirring and fitted with a condenser and an addition funnel. The addition funnel was loaded with a solution of 4-bromo-bute-1-ene (11.5 mL, 0.113 mol) in THF (20 mL). A slight amount of bromobutene solution (3 mL) was added slowly to the magnesium turnings, and the contents were heated at 65 °C to reflux. Once the Grignard formation was started, the remaining bromide solution was added dropwise. The reaction was stirred until most of the magnesium had reacted and a solution of **2.12** (5.000 g, 18.8 mmol) in THF (25 mL) was loaded into the addition funnel and added dropwise over 45 min. The mixture was stirred overnight at ambient temperature and a saturated solution of NH₄Cl (30 mL) was added to quench the reaction. The resultant emulsion was stirred for 1 h and the solution was extracted with ether (3 x 30 mL). The combined organic extracts were washed with water (30 mL), followed by brine (2 x 20 mL) and dried (MgSO₄). The solvent was evaporated to give pure alcohol **2.13** as a colorless oil (5.208 g, 80%). ¹H NMR (400 MHz, CDCl₃) δ 7.23 and 6.82 (AA'BB', J_{AB} = 8.6 Hz, 4H), 5.85-5.73 (m, 2H), 5.01-4.86 (m, 4H), 2.13-1.80, (m, 9H), 1.01 (s, 9H), 0.22 (s, 6H) ppm. ¹³C NMR (100 MHz, CDCl₃) δ 154.2, 140.0, 138.4, 126.4, 119.6, 114.6, 76.8, 42.2, 28.2, 25.8, 18.3, -4.3 ppm.

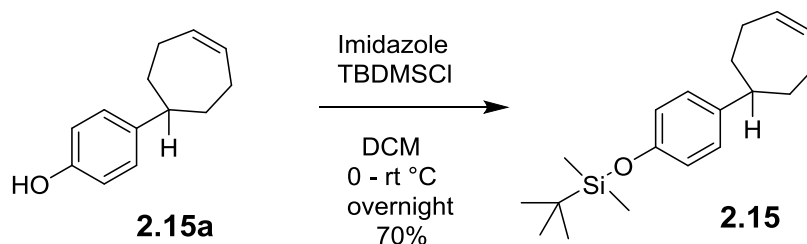


1-(4-((tert-Butyldimethylsilyloxy)phenyl)cyclohept-4-en-1-ol (2.14). To a solution of **2.13** (0.313 g, 0.903 mmol) in dry CH_2Cl_2 (100 mL, 0.01 M) was added a solution of Grubbs I catalyst (0.029 g, 0.032 mmol, 4%) in CH_2Cl_2 (10 mL) via syringe pump over 10 h and the mixture was stirred at 40 °C for 24 h. Reaction mixture was cooled to room temperature, quenched with DMSO (50 eq, 0.15 mL) and continued to stir for another 12 h. The mixture was concentrated to a dark brown crude material and directly subjected to the column chromatography (SiO_2 , hexanes- diethyl ether = 80:20) to give **2.14** (0.247 g, 86%) as a colorless oil. ^1H NMR (400 MHz, CDCl_3) δ 7.35 and 6.79 (AA'BB', $J_{\text{AB}} = 8.7$ Hz, 4H), 5.86-5.79 (m, 2H), 2.54-2.43 (m, 2H), 2.10–1.94 (m, 4H), 1.90-1.82 (m, 2H), 1.73 (s, 1H), 0.99 (s, 9H), 0.20 (s, 6H) ppm. ^{13}C NMR (100 MHz, CDCl_3) δ 154.5, 142.9, 132.3, 125.9, 119.8, 76.7, 40.3, 25.7, 23.2, 18.3, -4.2 ppm.

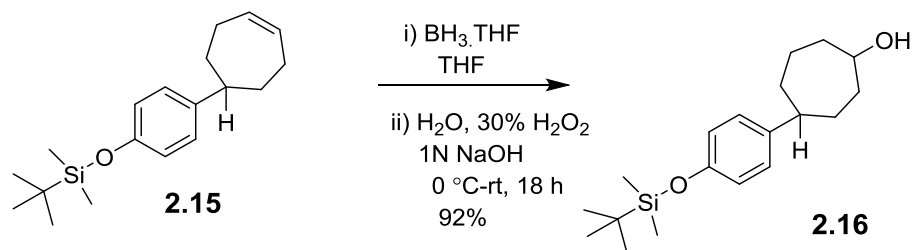


tert-Butyl(4-(cyclohept-4-en-1-yl)phenoxy)dimethylsilane (2.15). To a solution of **2.14** (1.601 g, 5.034 mmol) in anhydrous CH_2Cl_2 (20 mL) was added triethylsilane (0.8 mL, 5.0

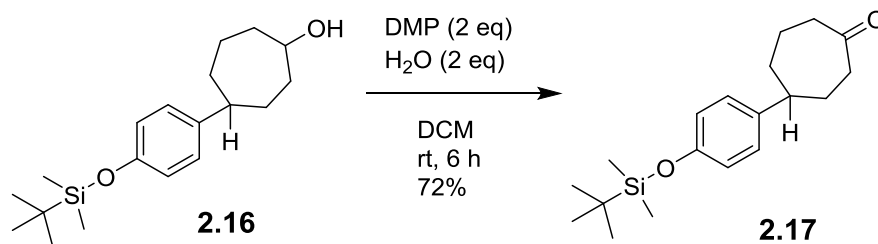
mmol) followed by TFA (4.0 mL, 20 mmol). The mixture was stirred at room temperature for 3 h while monitoring the reaction by TLC. After detecting the decomposition of both starting material and product, the solution was concentrated to a dark brown oil and directly subjected to the column chromatography (SiO₂, hexanes = 100%) to give **2.15** as a light-yellow oil (0.906 g, 60%). ¹H NMR (400 MHz, CDCl₃) δ 7.05 and 6.78 (AA'BB', J_{AB} = 8.7 Hz, 4H), 5.92-5.89 (m, 2H), 2.69 (tt, J = 11.2, 3.2 Hz, 1H), 2.36-2.27 (m, 2H), 2.24-2.14 (m, 2H), 1.93-1.85 (m, 2H), 1.55-1.44 (m, 2H), 1.01 (s, 9H), 0.22 (s, 6H) ppm. ¹³C NMR (100 MHz, CDCl₃) δ 153.6, 142.1, 132.7, 127.7, 120.0, 49.8, 35.2, 28.1, 25.9, 18.3, -4.2 ppm.



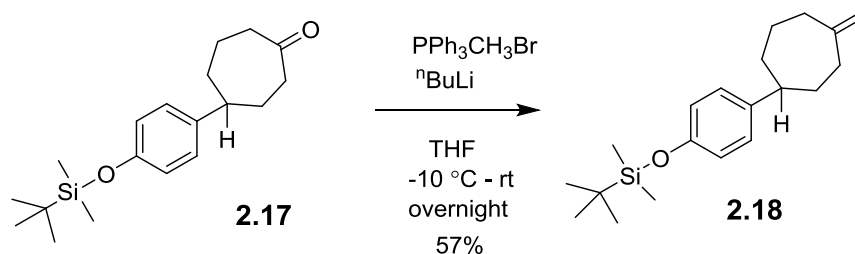
tert-Butyl(4-(cyclohept-4-en-1-yl)phenoxy)dimethylsilane (2.15). To a solution of phenol **2.15a** (0.212 g, 1.13 mmol) in anhydrous CH₂Cl₂ (20 mL) was added imidazole (0.230 g, 3.38 mmol) while stirring at 0 °C under N₂. After 30 min tert-butyldimethyl silyl chloride (0.254 g, 1.69 mmol) was added at 0 °C and mixture was gradually warmed to room temperature overnight. The resulting mixture was diluted with brine (20 mL) and extracted with CH₂Cl₂ (2 x 20 mL). The combined organic extracts were dried (Na₂SO₄), concentrated and purified by column chromatography (SiO₂, hexanes-ethyl acetate = 90:10) to give **2.15** as a light-yellow oil (0.240, 70%). The ¹H NMR spectral data was identical to that previously obtained.



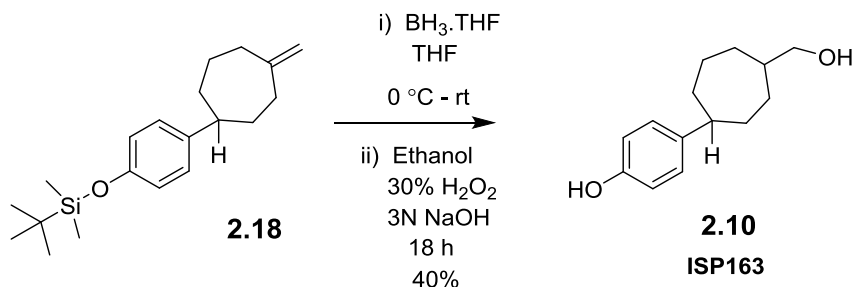
4-(4-((tert-Butyldimethylsilyl)oxy)phenyl)cycloheptan-1-ol (2.16). To a solution of **2.15** (0.906 g, 2.99 mmol) in freshly distilled THF (20 mL) at 0 °C under N_2 was added dropwise a solution of borane-tetrahydrofuran complex (1M in THF, 6.0 mL, 6.0 mmol). The solution was gradually warmed to room temperature and stirred for 18 h. The reaction mixture was cooled to 0 °C, and water (250 mL) was added slowly followed by 30% hydrogen peroxide (4.5 mL) and 1N sodium hydroxide (7.5 mL). The resulting solution was stirred at room temperature for another 30 min and extracted with ethyl acetate (2 x 25 mL), concentrated and purified by column chromatography (SiO_2 , hexanes-ethyl acetate = 80:20) to give **2.16** (0.880 g, 92%) as a yellow oil. This was determined to be a mixture of diastereoisomers by ^1H and ^{13}C NMR spectroscopy. ^1H NMR (400 MHz, CDCl_3) δ 7.01 (m, 2H), 6.74 (m, 2H), 4.06-3.99 and 3.98-3.90 (2 x m, 1H total), 2.69-2.53 (m, 1H), 2.14-1.49 (m, 11H), 0.97 (s, 9H), 0.18 (s, 6H) ppm. ^{13}C NMR (100 MHz, CDCl_3) δ 153.6, 142.1, 127.5, 120.0, 73.0, 71.9, 46.4, 46.1, 38.3, 37.8, 37.3, 37.1, 37.0, 35.9, 31.8, 29.8, 25.9, 23.5, 21.5, 18.4, - 4.2 ppm.



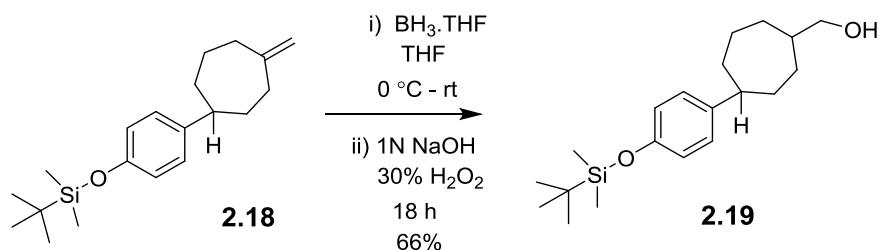
4-(4-((tert-Butyldimethylsilyloxy)phenyl)cycloheptan-1-one (2.17). To a solution of **2.16** (0.050 g, 0.16 mmol) in CH_2Cl_2 (10 mL) at room temperature, was added Dess–Martin periodinane (0.132 g, 0.312 mmol) and water (0.1 mL) and mixture was stirred at room temperature for 6 h. The mixture was quenched with 1:1 mixture of saturated $\text{Na}_2\text{S}_2\text{O}_3$ and NaHCO_3 solution and continued to stir for another 30 min. The resulting solution was extracted with CH_2Cl_2 (2 x 20 mL), dried (Na_2SO_4), concentrated and purified by column chromatography (SiO_2 , hexanes-ethyl acetate = 80:20) to afford **2.17** (0.036 g, 72%) as a colorless oil. ^1H NMR (400 MHz, CDCl_3) δ 7.01 and 6.75 (AA'BB', $J_{\text{AB}} = 8.6$ Hz, 4H), 2.72–2.51 (m, 5H), 2.13–2.06 (m, 1H), 2.04–1.95 (m, 2H), 1.86–1.68 (m, 2H), 1.62–1.52 (m, 1H), 0.97 (s, 9H), 0.18 (s, 6H) ppm. ^{13}C NMR (100 MHz, CDCl_3) δ 215.3, 153.9, 140.6, 127.5, 120.1, 48.1, 44.0, 43.1, 38.7, 32.2, 25.9, 24.1, 18.3, -4.2 ppm.



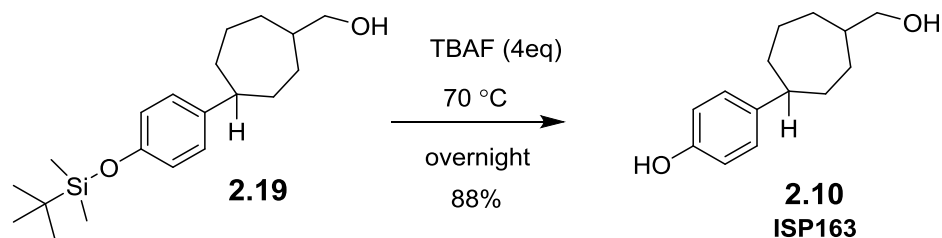
tert-Butyldimethyl(4-(4-methylenecycloheptyl)phenoxy)silane (2.18). To a stirred solution of $\text{PPh}_3\text{CH}_3\text{Br}$ (0.476 g, 1.33 mmol) in anhydrous THF (20 mL) at -10°C under N_2 , was added a solution of n-butyl lithium (1.6 M in hexanes, 0.83 mL, 1.3 mmol) dropwise. After complete addition, the deep yellow mixture was stirred for another 45 min at -10°C before slowly adding a solution of **2.17** (0.212 g, 0.667 mmol) in THF. The solution changed from a deep to light yellow in color, and the mixture was gradually warmed to room temperature and stirred overnight. The solution was diluted with water (20 mL) and aqueous layer was extracted with ethyl acetate (2×25 mL). The combined organic extracts were washed with brine and dried (Na_2SO_4). Removal of the solvent and purification from column chromatography (SiO_2 , hexanes–ethyl acetate = 90:10) gave **2.18** (0.120 g, 57%) as a light-yellow oil. ^1H NMR (400 MHz, CDCl_3) δ 7.03 and 6.75 (AA'BB', $J_{\text{AB}} = 8.7$ Hz, 4H), 4.76 (s, 2H), 2.59–2.45 (m, 2H), 2.37–2.26 (m, 2H), 2.01–1.85 (m, 3H), 1.70–1.48 (m, 4H), 1.00 (s, 9H), 0.20 (s, 6H) ppm. ^{13}C NMR (100 MHz, CDCl_3) δ 153.4, 151.9, 142.3, 127.7, 120.0, 110.7, 47.6, 40.0, 37.2, 36.3, 35.4, 27.6, 25.9, 18.4, -4.2 ppm.



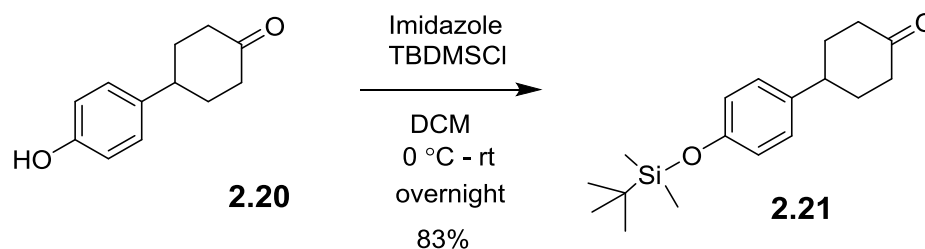
4-(4-(Hydroxymethyl)cycloheptyl)phenol (2.10). To a solution of **2.18** (0.320 g, 1.01 mmol) in freshly distilled THF (10 mL) at $0\text{ }^\circ\text{C}$, was added dropwise a solution of borane-tetrahydrofuran complex (1M in THF, 2.1 mL, 2.1 mmol). The resulting mixture was warmed to room temperature and stirred for 18 h. The reaction mixture was cooled to $0\text{ }^\circ\text{C}$, and pure ethanol (85 mL) was added slowly followed by 30% hydrogen peroxide (2.0 mL) and 3N sodium hydroxide (2.5 mL). The mixture was stirred for 1 h at room temperature, extracted with ethyl acetate ($2 \times 20\text{ mL}$), dried (Na_2SO_4), and the solvent evaporated. The crude material was purified by column chromatography (SiO_2 , hexanes-ethyl acetate = 60:40) to give **2.10** (0.088 g, 40%) as a colorless solid. This was determined to be a mixture of diastereoisomers by ^1H and ^{13}C NMR spectroscopy. mp $60\text{--}63\text{ }^\circ\text{C}$. ^1H NMR (400 MHz, CDCl_3) δ 7.03 and 6.74 (AA'BB', $J_{\text{AB}} = 8.7\text{ Hz}$, 4H), 5.53 (s, OH), 3.48 (d, $J = 6.4\text{ Hz}$, 2H), 2.65–2.49 (m, 1H), 1.97–1.30 (m, 12H). ^{13}C NMR (100 MHz, CDCl_3) δ 153.8, 142.0, 141.8, 127.7, 115.4, 68.8, 68.5, 47.2, 46.1, 42.2, 41.3, 38.9, 36.7, 36.5, 33.0, 31.5, 30.6, 29.9, 28.5, 27.5, 24.3 ppm. The NMR spectral data is consistent with previously observed values.



(4-(4-((tert-Butyldimethylsilyloxy)phenyl)cycloheptyl)methanol (2.19) To a solution of **2.18** (0.821 g, 2.60 mmol) in freshly distilled THF (10 mL) at 0 °C, was added dropwise a solution of borane-tetrahydrofuran complex (1M in THF, 5.4 mL, 5.4 mmol). The resulting mixture was warmed to room temperature and stirred for 18 h. The reaction mixture was cooled to 0 °C, and 1N sodium hydroxide (3.2 mL) was added slowly followed by 30% hydrogen peroxide (1.5 mL). The mixture was stirred for 1 h at room temperature, extracted with ethyl acetate (2 × 25 mL), dried (Na₂SO₄), and the solvent evaporated. The crude material was purified by column chromatography (SiO₂, hexanes-ethyl acetate = 80:20) to give **2.19** (0.572 g, 66%) as a colorless oil. This was determined to be a mixture of diastereoisomers by ¹H and ¹³C NMR spectroscopy. ¹H NMR (400 MHz, CDCl₃) δ 7.02 and 6.74 (AA'BB', J_{AB} = 8.3 Hz, 4H), 3.45 (d, J = 6.5 Hz, 2H), 2.67–2.53 (m, 1H), 1.98–1.38 (m, 11H), 1.29–1.09 (m, 1H), 0.98 (s, 9H), 0.19 (s, 6H) ppm. ¹³C NMR (100 MHz, CDCl₃) δ 153.5, 142.6, 142.4, 127.6, 127.5, 119.9, 68.7, 68.5, 47.3, 46.1, 42.2, 41.2, 38.9, 36.8, 36.4, 33.1, 31.5, 30.7, 30.0, 28.5, 27.6, 26.1, 24.2, 18.3, -4.2 ppm.

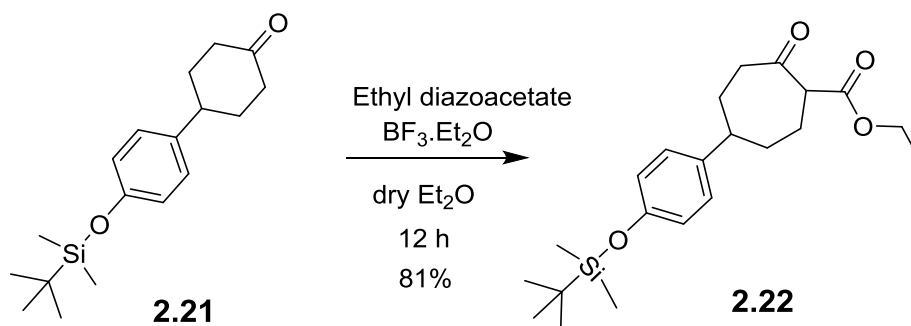


4-(4-(Hydroxymethyl)cycloheptyl)phenol (2.10). To a solution of **2.19** (0.873 g, 2.61 mmol) in anhydrous THF (20 mL) was added a solution of TBAF (1M in THF, 10.0 mL, 0.010 mol) while stirring. The mixture was heated to reflux at 70 °C overnight and cooled to room temperature. The solution was partitioned between ethyl acetate and water. The organic layer was washed with brine, dried (Na₂SO₄) and concentrated. Purification by column chromatography (SiO₂, hexanes-ethyl acetate = 60:40) gave **2.10** (0.508 g, 88%) as a colorless solid. mp 60-63 °C. The ¹H NMR spectral data is consistent with that previously obtained.



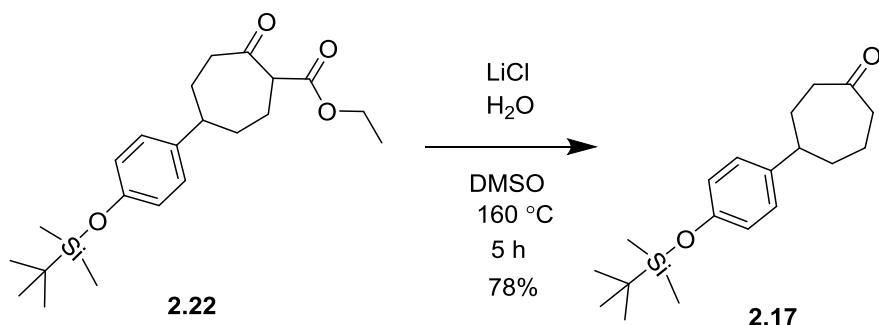
4-(4-((tert-Butyldimethylsilyloxy)oxy)phenyl)cyclohexan-1-one (2.21). To a stirred solution of 4-(4-hydroxyphenyl)cyclohexanone **2.20** (4.0 g, 0.021 mol) in anhydrous CH₂Cl₂ (40 mL) at 0 °C was added imidazole (4.3 g, 0.063 mol) under N₂. After 30 min tert-butyldimethyl silyl chloride (4.6 g, 0.032 mol) was added at 0 °C and mixture was gradually warmed to room temperature overnight. The resulting mixture was diluted with

brine (25 mL) and partitioned with CH₂Cl₂ (2 x 30 mL). The combined organic extracts were dried (Na₂SO₄), concentrated and purified by column chromatography (SiO₂, hexanes-ethyl acetate = 90:10) to give **2.21** (6.081 g, 95%) as a colorless solid. mp 39-42 °C. ¹H NMR (400 MHz, CDCl₃) δ 7.08 and 6.78 (AA'BB', J_{AB} = 8.4 Hz, 4H), 2.96 (br t, J = 12.3 Hz, 1H), 2.56–2.40 (m, 4H), 2.25–2.14, (m, 2H), 1.97–1.82 (m, 2H), 0.98 (s, 9H), 0.19 (s, 6H) ppm. ¹³C NMR (400 MHz, CDCl₃) δ 211.6, 154.3, 137.7, 127.7, 120.1, 42.2, 41.6, 34.6, 25.9, 18.4, -4.2 ppm.

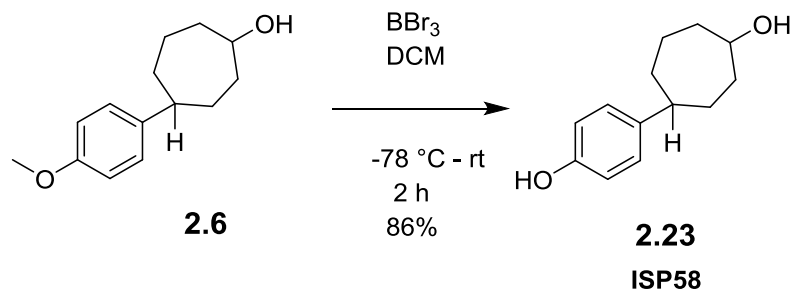


Ethyl 5-(4-((tert-butyldimethylsilyloxy)phenyl)-2-oxocycloheptane-1-carboxylate (2.22). To a solution of ketone **2.21** (1.14 g, 3.74 mmol) in anhydrous diethyl ether (15 mL) at 0 °C under N₂ was added an aliquot of BF₃·Et₂O (0.92 mL, 7.5 mmol). A solution of ethyl diazoacetate (0.77 mL, 7.47 mmol) in anhydrous ether (5 mL) was added dropwise over a period of 20 min and the resulting solution was stirred at room temperature for 12 h. The reaction mixture was cooled to 0 °C and neutralized with saturated sodium bicarbonate solution (20 mL). The resulting mixture was extracted with CH₂Cl₂ (3 x 15 mL), the combined organic extracts washed with brine (20 mL), dried (Na₂SO₄) and concentrated. The dark yellow crude oil was purified by column chromatography (SiO₂, hexanes-diethyl ether = 70:30) to give keto ester **2.22** (1.182 g, 81%) as a colorless oil.

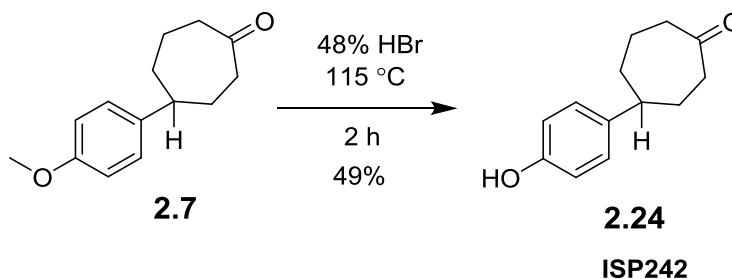
The product is in equilibrium with its keto-enol tautomer. ^1H NMR (400 MHz, CDCl_3) δ 12.74 (s, 0.4H), 7.02-6.97 (m, 2H), 6.77-6.72 (m, 2H), 4.27-4.16 (m, 2H), 3.64-3.56 (m, 0.3H), 2.94-2.78 (m, 1H), 2.72-2.58 (m, 2H), 2.48-2.24 (m, 1H), 2.16-1.76 (m, 4H), 1.65-1.54 (m, 1H), 1.32 and 1.29 (2 x t, $J = 7.2$ Hz, 3H total), 0.97 (s, 9H), 0.18 (s, 6H) ppm. ^{13}C NMR (100 MHz, CDCl_3) δ 209.0, 208.8, 178.9, 173.0, 170.6, 154.0, 140.9, 139.9, 127.7, 127.5, 120.2, 120.0, 101.5, 61.4, 60.7, 59.6, 58.5, 49.6, 47.9, 47.2, 42.2, 36.8, 35.4, 34.6, 32.8, 32.2, 27.8, 25.9, 23.9, 22.6, 18.4, 14.5, -4.2 ppm.



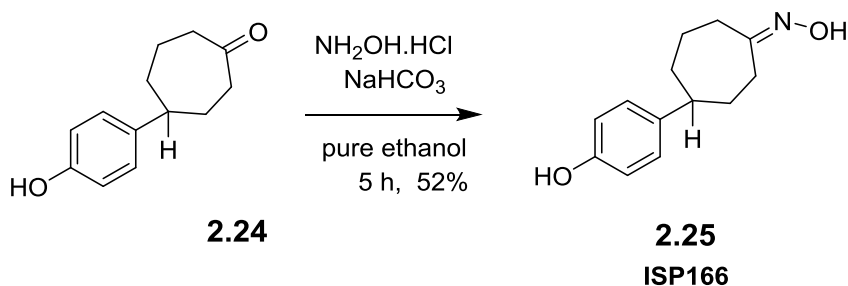
4-(4-((tert-Butyldimethylsilyloxy)phenyl)cycloheptan-1-one (2.17). To a stirred solution of **2.22** (1.74 g, 4.46 mmol) in DMSO (20 mL) at room temperature was added sequentially lithium chloride (1.3 g, 0.031 mol) and water (2.8 mL) at room temperature. The mixture was heated to reflux at $160\text{ }^\circ\text{C}$ for 5 h, cooled to room temperature and poured into water. The resulting solution was extracted with ether and ethyl acetate (3 x 20 mL), washed with brine, dried (Na_2SO_4) and evaporated in vacuo to provide desired product **2.17** (1.114 g, 78%) as a colorless oil. The NMR spectral data for the product is consistent with that previously obtained.



4-(4-Hydroxycycloheptyl)phenol (2.23). To a stirred solution of **2.6** (0.028 g, 0.13 mmol) in anhydrous CH_2Cl_2 (30 mL) at -78°C , was added dropwise a solution of boron tribromide in CH_2Cl_2 (1M, 0.3 mL, 0.03 mmol). After complete addition, the reaction mixture was stirred for 30 min at -78°C and gradually warmed to room temperature over a 2 h period. The mixture was quenched with water (10 mL) and aqueous layer was extracted with CH_2Cl_2 (3×20 mL). The combined organic extracts were washed with brine and dried (MgSO_4). Evaporation of the solvent gave **2.23** (0.024 g, 86%) as a yellow crystalline solid. This product was determined to be a mixture of *cis*- and *trans*-stereoisomers on the basis of ^1H and ^{13}C NMR. ^1H NMR (400 MHz, CDCl_3) δ 7.11-6.99 (m, 2H), 6.80-6.70 (m, 2 H), 4.85 (s, OH), 4.56-4.48 and 4.42-4.34 ($2 \times$ m, 1H total), 2.78–2.59 (m, 1H), 2.53–1.38 (m, 11H) ppm. ^{13}C NMR (100 MHz, CDCl_3) δ 153.5, 141.0, 127.7, 115.9, 56.1, 55.7, 45.9, 45.3, 40.0, 39.4, 39.2, 37.7, 37.6, 36.3, 34.2, 31.3, 25.2, 23.5 ppm.

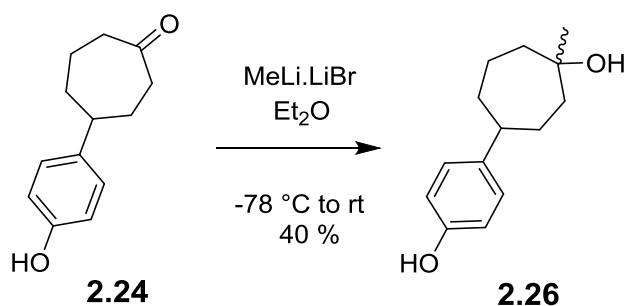


4-(4-Hydroxyphenyl)cycloheptanone (2.24). A sample of **2.7** (0.074 g, 0.339 mmol) was dissolved in 48 % HBr (8 mL) and the mixture heated to reflux at 115 °C for 2 h. Then the mixture was cooled to room temperature and portioned between ethyl acetate and water. The organic layer was washed with sodium bicarbonate solution, followed by brine, dried (Na_2SO_4) and concentrated. The residue was purified by column chromatography (SiO_2 , hexanes-ethyl acetate = 20:80) to give **2.24** (0.057 g, 82%) as a brown syrup. ^1H NMR (400 MHz, CD_3OD) δ 6.98 and 6.70 (AA'BB', $J_{\text{AB}} = 8.5$ Hz, 4H), 4.98 (s, 1H), 2.77–2.39 (m, 4H), 2.02–1.47 (m, 7H) ppm. ^{13}C NMR (100 MHz, CD_3OD) δ 218.1, 156.4, 140.3, 128.5, 116.1, 49.0, 44.6, 43.7, 39.6, 33.1, 24.3 ppm.

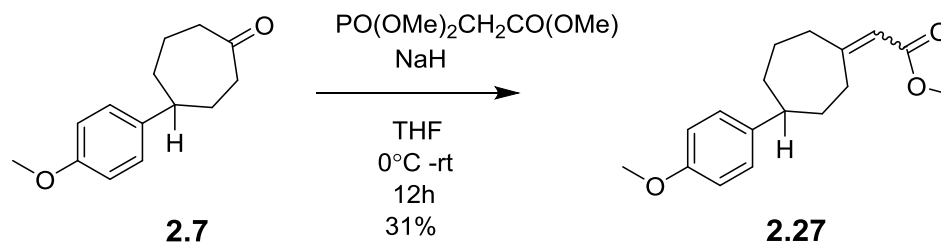


4-(4-Hydroxyphenyl)cycloheptanone oxime (2.25). To a solution of **2.24** (0.048 g, 0.23 mmol) in ethanol (10 mL), was added sodium bicarbonate (0.024 g) and hydroxylamine hydrochloride (0.023 g, 0.32 mmol). The mixture was stirred at room temperature for 5 h and extracted with ethyl acetate (2×10 mL). The combined organic extracts were dried

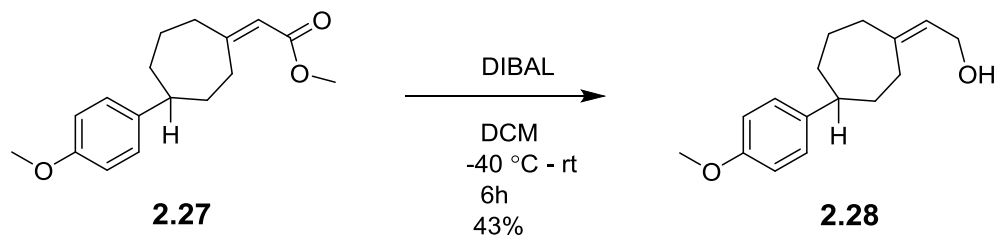
(MgSO₄) and concentrated. Purification of the residue by column chromatography (SiO₂, hexanes-ethyl acetate = 65:35) gave **2.25** as a light brown gum (0.026 g, 52%). ¹H NMR (400 MHz, CD₃OD) δ 6.98 and 6.67 (AA'BB', J_{AB} = 8.5 Hz, 4H), 2.86-2.30 (m, 4H), 2.09-1.20 (m, 8H) ppm. ¹³C NMR (100 MHz, CD₃OD) δ 165.0, 164.8, 156.4, 156.3, 141.3, 140.4, 128.5, 128.3, 116.1, 40.0, 39.7, 37.1, 34.1, 33.7, 33.3, 29.6, 28.4, 27.9, 24.8 ppm.



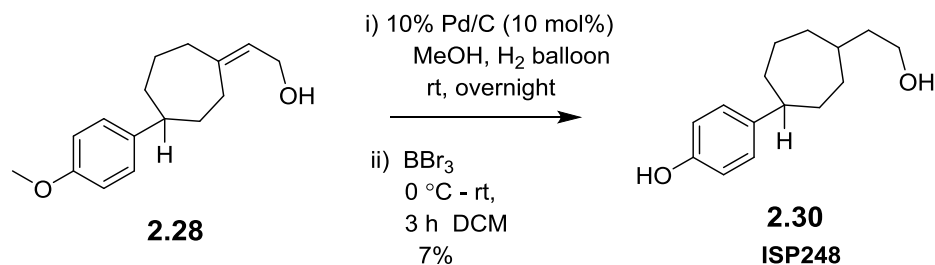
4-(4-hydroxyphenyl)-1-methylcycloheptan-1-ol (2.26). To a solution of **2.24** (0.158 g, 0.773 mmol) in dry Et₂O (15 mL) at -78 °C under N₂, was added slowly a solution of methyllithium-lithium bromide complex (1.5 M in ether, 1.1 mL, 1.7 mmol). The mixture was stirred for another 30 min at -78 °C, warmed to room temperature and stirred for another 1 h. The mixture was cooled to 0 °C and quenched with water. The mixture was extracted with diethyl ether (2 × 30 mL), dried (Na₂SO₄) and concentrated. The residue was purified from column chromatography (SiO₂, hexanes-ethyl acetate = 80:20) to give **2.26** (0.068 g, 40%) as a colorless solid. ¹H NMR (400 MHz, MeOD) δ 6.97 and 6.67 (AA'BB', J_{AB} = 8.5 Hz, 4H), 2.63–2.44 (m, 1H), 1.97–1.30 (m, 10H), 1.23 (s, 1H) 1.21 (s, 2H) ppm. ¹³C NMR (100 MHz, MeOD) δ 156.3, 141.7, 128.6, 128.4, 116.0, 74.6, 74.5, 64.4, 44.2, 43.4, 42.8, 40.8, 40.4, 39.0, 38.5, 31.5, 31.2, 23.7, 23.6 ppm.



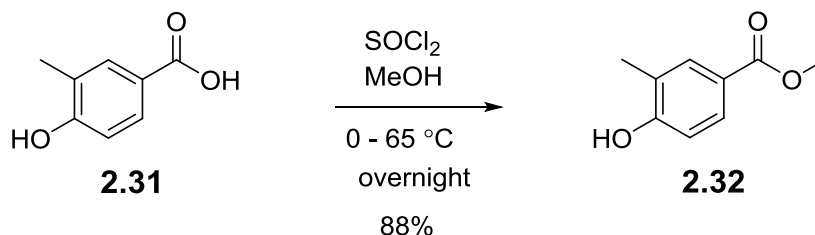
Methyl-2-(4-(4-methoxyphenyl)cycloheptylidene)acetate (2.27). Sodium hydride (32 mg, 55% in mineral oil, 0.80 mmol) was added to a stirring solution of trimethyl phosphonoacetate (0.130 mL, 0.80 mmol) in dry THF (3 mL) at 0 °C. After 45 min, a solution 4-(4-methoxyphenyl)cycloheptanone **2.27** (0.147 g, 0.673 mmol) in dry THF (5 mL) was added and the reaction mixture was stirred at room temperature for 12 h. The mixture was diluted with water (15 mL) and the resulting mixture was extracted with ether (2 × 20 mL), dried (MgSO₄) and concentrated. The residue was purified by column chromatography (SiO₂, hexanes–ethyl acetate = 90:10) to give **2.27** (0.057 g, 31%) as a colorless oil. The product was determined to be a mixture of *E* and *Z* stereoisomers from ¹H and ¹³C NMR spectroscopy. ¹H NMR (400 MHz, CDCl₃) δ 7.08 and 6.82 (AA'BB', J_{AB} = 8.1 Hz, 4H), 5.74 (s, 1H), 3.78 (s, 3H), 3.69 (d, J = 3.6 Hz, 3H), 2.86 (broad t, J = 14.9 Hz, 1H), 2.72-2.36 (m, 3H), 2.10-1.86 (m, 3H), 1.80-1.44 (m, 6H) ppm. (Solvent peaks are overlapped in 1.30-2.20 ppm region). ¹³C NMR (100 MHz, CDCl₃) δ 167.2, 167.1, 166.8, 166.6, 157.9, 157.8, 141.1, 140.7, 127.6, 115.5, 113.9, 77.6, 55.4, 51.0, 47.7, 47.1, 38.9, 38.2, 38.0, 37.4, 36.7, 35.3, 32.6, 31.3, 27.2, 25.9, 22.9, 14.3 ppm.



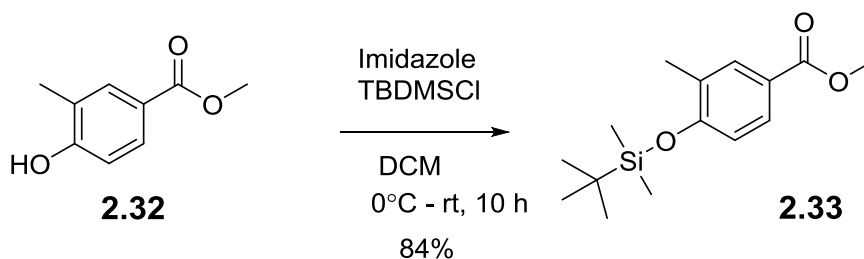
(Z)-2-(4-(4-Methoxyphenyl)cycloheptylidene)ethan-1-ol (2.28). To a solution of **2.27** (0.200 g, 0.730 mmol) in dry CH_2Cl_2 (5 mL) under nitrogen at $-40\text{ }^\circ\text{C}$ was added a solution of diisobutylaluminum hydride in CH_2Cl_2 (1.58 mL, 1.2 M, 1.9 mmol). After 90 min, saturated aqueous potassium sodium tartrate was added and reaction mixture was gradually warmed to room temperature. After 4 h the mixture was filtered through a pad of celite and extracted several times with water ($2 \times 15\text{ mL}$). The combined organic layers were dried (MgSO_4), and concentrated to give **2.28** (0.078 g, 43%) as a colorless gum. The crude product was used in the next step without any further purification. ^1H NMR (400 MHz, CDCl_3) δ 7.09 and 6.83 (AA'BB', $J_{\text{AB}} = 8.7\text{ Hz}$, 4H), 5.50-5.42 (m, 1H), 4.19 (d, $J = 7.2\text{ Hz}$, 2H), 3.79 (s, 3H), 2.67-2.19 (m, 4H), 2.14-1.85 (m, 4H), 1.69-1.44 (m, 3H) ppm. ^{13}C NMR (100 MHz, CDCl_3) δ 157.7, 145.1, 141.5, 141.3, 129.4, 127.6, 127.6, 124.2, 124.1, 113.8, 59.2, 55.4, 47.6, 47.0, 38.3, 37.6, 37.4, 36.8, 36.1, 30.2, 29.2, 27.8, 26.5 ppm.



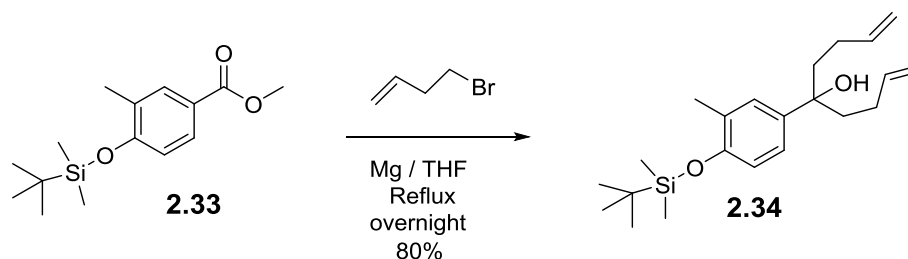
4-(4-(2-Hydroxyethyl)cycloheptyl)phenol (2.30). To a solution of compound **2.28** (0.078 g, 0.32 mmol) in methanol (10 mL) was added 10% Pd/C (0.040 g, 10 mol %). The mixture was stirred under H₂ balloon at room temperature for 12 h. The reaction mixture was filtered through a pad of celite, concentrated and dried (MgSO₄) to give the crude hydrogenated product (0.080 g, 0.323 mmol). The crude product was dissolved in anhydrous CH₂Cl₂ (8 mL), cooled to -78 °C, and a solution of boron tribromide (1M in CH₂Cl₂, 0.97 mL, 0.97 mmol) was added dropwise. After complete addition, the reaction mixture was stirred for 30 min at -78 °C and gradually warmed to room temperature over a 2 h period. The mixture was quenched with water (5 mL) and the aqueous layer was extracted with CH₂Cl₂ (3 × 10 mL). The combined organic extracts were washed with brine and dried (MgSO₄). Evaporation of the solvent and purification by column chromatography (SiO₂, hexanes-ethyl acetate = 65:35) gave **2.30** (0.005 g, 7%) as a light brown solid. This was determined to be a mixture of diastereoisomers by ¹H and ¹³C NMR spectroscopy. ¹H NMR (400 MHz, CDCl₃) δ 7.04 and 6.74 (AA'BB', J_{AB} = 8.7 Hz, 4H), 3.71 (td, J = 6.9, 1.4 Hz, 2H), 2.66-2.48 (m, 1H), 1.96-1.13 (m, 13H) ppm. ¹³C NMR (100 MHz, CDCl₃) δ 153.6, 142.2, 127.8, 115.3, 61.5, 47.1, 45.9, 41.1, 40.9, 38.8, 36.8, 36.3, 35.9, 35.4, 34.8, 34.5, 33.9, 33.0, 32.1, 27.3, 24.4 ppm.



Methyl 4-hydroxy-3-methylbenzoate (2.32). To a solution of 4-hydroxy-3-methylbenzoic acid **2.31** (5.000 g, 0.033 mol) in anhydrous methanol (80 mL) was added dropwise through an addition funnel SOCl_2 (5 mL, 0.066 mol) over 1 h while stirring at 0 °C. After 30 min the system was heated at reflux overnight under N_2 . The resulting mixture was cooled to the room temperature and diluted with water (50 mL). Methanol was evaporated and the pH was adjusted to pH = 7 with saturated sodium bicarbonate solution (15 mL). The resulting solution was extracted with ethyl acetate (3×40 mL). The combined organic extracts were washed with brine (20 mL), dried (Na_2SO_4), and concentrated to give methyl ester **2.32** (4.80 g, 88%) as a light orange solid. mp 124-125 °C. ^1H NMR (400 MHz, CDCl_3) δ 7.84 (s, 1H), 7.78 (d, $J = 8.3$ Hz, 1H), 6.83 (d, $J = 8.4$ Hz, 1H), 6.48 (s, OH), 3.89 (s, 3H), 2.27 (s, 3H) ppm. ^{13}C NMR (100 MHz, CDCl_3) δ 168.0, 158.9, 133.1, 129.6, 124.4, 122.0, 115.4, 52.4, 16.0 ppm. The ^1H and ^{13}C NMR spectral data are consistent with the literature values.¹¹⁷⁻¹¹⁸

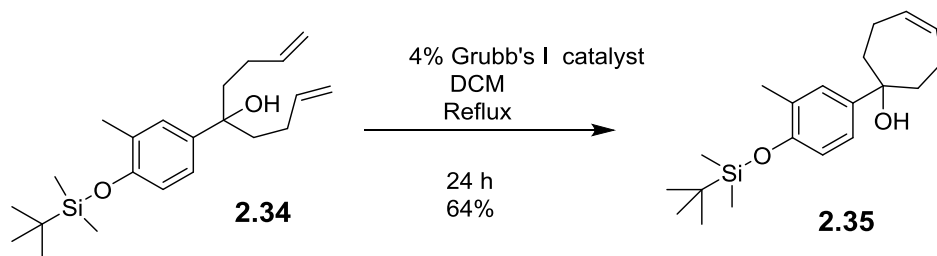


Methyl 4-((tert-butyldimethylsilyl)oxy)-3-methylbenzoate (2.33). To a stirred solution of **2.32** (0.500 g, 3.01 mmol) in anhydrous CH₂Cl₂ (25 mL) at 0 °C under N₂, was added imidazole (0.410 g, 6.02 mmol). After 30 min tert-butyldimethyl silyl chloride (0.680 g, 4.52 mmol) was added at 0 °C and mixture was gradually warmed to room temperature overnight. The resulting mixture was diluted with brine (25 mL) and partitioned with CH₂Cl₂ (2 x 20 mL). The combined organic extracts were dried (Na₂SO₄), concentrated in vacuo and purified by column chromatography (SiO₂, hexanes-ethyl acetate = 10:90) to give **2.33** (0.712 g, 84%) as a colorless gum. ¹H NMR (400 MHz, CDCl₃) δ 7.84 (d, J = 2.3 Hz, 1H), 7.77 (dd, J = 2.3, 8.4 Hz, 1H), 6.77 (d, J = 8.4 Hz, 1H), 3.86 (s, 3H), 2.22 (s, 3H), 1.01 (s, 9H), 0.23 (s, 6H) ppm. ¹³C NMR (100 MHz, CDCl₃) δ 167.2, 158.4, 132.7, 129.1, 128.8, 123.1, 118.1, 51.9, 25.9, 18.3, 16.9, -3.8 ppm.



5-(4-((tert-Butyldimethylsilyl)oxy)-3-methylphenyl)nona-1,8-dien-5-ol (2.34). Dry magnesium turnings (2.65 g, 0.110 mol) were placed in a flame dried three-necked flask

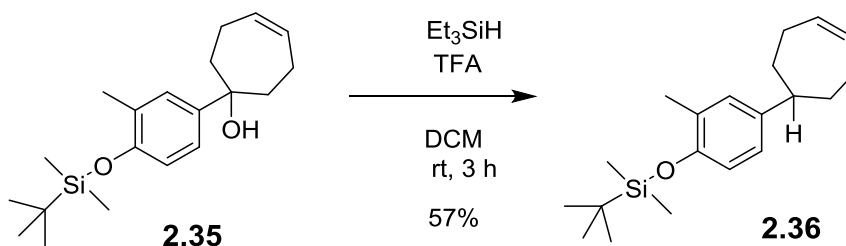
under N₂ followed by THF (25 mL). A solution of 4-bromo-1-butene (6.70 mL, 0.066 mol) in THF (20 mL) was loaded to the addition funnel and a small amount of bromobutene solution (2 mL) was added slowly to the magnesium turnings. The solution was heated at 65 °C to reflux. Once the Grignard formation was started, the remaining bromide solution was added dropwise over 45 min. The reaction was stirred until most of the magnesium had reacted and solution of **2.33** (3.086 g, 0.011 mol) in THF (15 mL) was filled into the addition funnel and added dropwise over 30 min. The mixture was gradually cooled and stirred at ambient temperature overnight. A solution of saturated NH₄Cl (30 mL) was slowly added in order to quench the reaction and resultant emulsion was stirred for 1 h. The mixture was extracted with ether (3 x 30 mL) and the combined organic extracts were washed with brine (2 x 20 mL) and dried (Na₂SO₄). The solvent was removed to give alcohol **2.34** (2.217 g, 56%) as a colorless oil. ¹H NMR (400 MHz, CDCl₃) δ 7.13 (d, J = 2.4 Hz, 1H), 7.03 (dd, J = 2.6, 8.4 Hz, 1H), 6.74 (d, J = 8.4 Hz, 1H), 5.85-5.74 (m, 2H), 4.99-4.88 (m, 4H), 2.22 (s, 3H), 2.11-1.97 (m, 2H), 1.93-1.81 (m, 7H), 1.02 (s, 9H), 0.22 (s, 6H) ppm. ¹³C NMR (100 MHz, CDCl₃) δ 152.5, 139.2, 138.1, 128.5, 128.1, 123.6, 118.1, 114.6, 77.1, 42.2, 28.3, 25.9, 18.4, 17.4, -4.0 ppm.



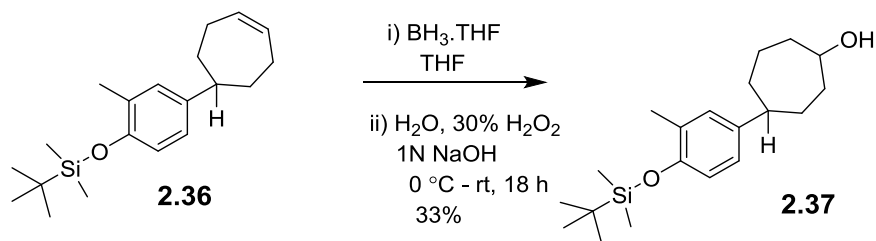
1-(4-((tert-Butyldimethylsilyloxy)-3-methylphenyl)cyclohept-4-en-1-ol (2.35).

Alcohol **2.34** (0.974 g, 2.70 mmol) was cyclized using Grubbs' catalyst **I** (0.090 g, 0.108

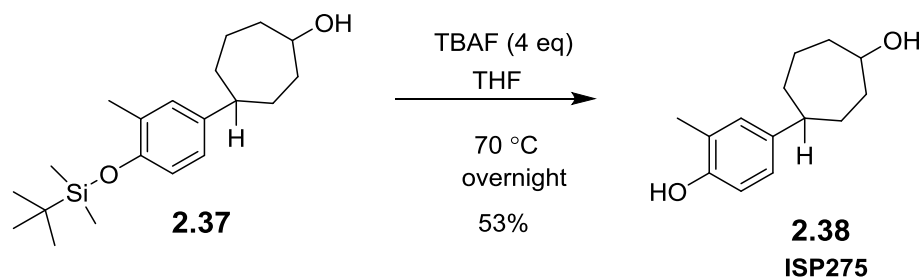
mmol, 4%) in a fashion similar to the preparation of **2.14**. Purification of the crude product by column chromatography (SiO₂, hexanes-diethyl ether = 80:20) gave **2.35** (0.573 g, 64%) as a light green oil. ¹H NMR (400 MHz, CDCl₃) δ 7.28 (br d, J = 2.3 Hz, 1H), 7.18 (dd, J = 2.5, 8.4 Hz, 1H), 6.72 (d, J = 8.5 Hz, 1H), 5.87-5.82 (m, 2H), 2.50 (br t, J = 13.3 Hz, 2H), 2.22 (s, 3H), 2.11–1.97 (m, 4H), 1.91-1.83 (m, 2H), 1.68 (s, 1H), 1.02 (s, 9H), 0.22 (s, 6H) ppm. ¹³C NMR (100 MHz, CDCl₃) δ 152.6, 142.7, 132.3, 128.4, 127.7, 122.9, 117.9, 77.1, 40.3, 25.9, 23.3, 18.5, 17.2, -4.0 ppm.



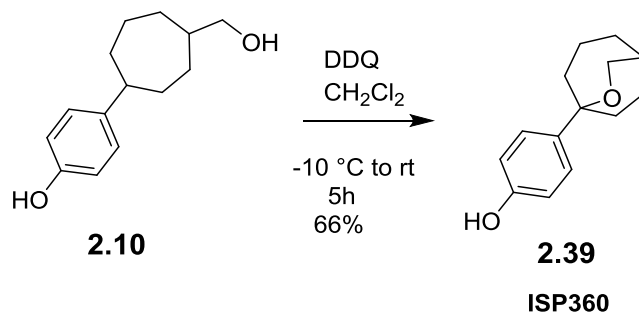
tert-Butyl(4-(cyclohept-4-en-1-yl)-2-methylphenoxy)dimethylsilane (2.36). Ionic reduction of tertiary alcohol **2.35** (0.209 g, 0.623 mmol) in anhydrous CH₂Cl₂ (15 mL) with triethylsilane (0.1 mL, 0.626 mmol) and TFA (0.5 mL, 6.23 mmol) was carried out in a fashion similar to the preparation of **2.15**. Purification of the crude product by column chromatography (SiO₂, hexanes = 100%) gave **2.36** (0.113 g, 57%) as a colorless oil. ¹H NMR (400 MHz, CDCl₃) δ 7.00 (d, J = 2.2 Hz, 1H), 6.91 (dd, J = 8.1, 2.2 Hz, 1H), 6.72 (d, J = 8.4 Hz, 1H), 5.94-5.90 (m, 2H), 2.68 (tt, J = 11.5, 3.4 Hz, 1H), 2.38-2.28 (m, 2H), 2.27-2.16 (m, 5H), 1.95-1.87 (m, 2H), 1.58-1.44 (m, 2H), 1.06 (s, 9H), 0.26 (s, 6H) ppm. ¹³C NMR (100 MHz, CDCl₃) δ 151.9, 142.1, 132.7, 129.5, 128.8, 125.1, 118.4, 49.7, 35.1, 28.1, 25.9, 18.3, 17.2, -4.0 ppm.



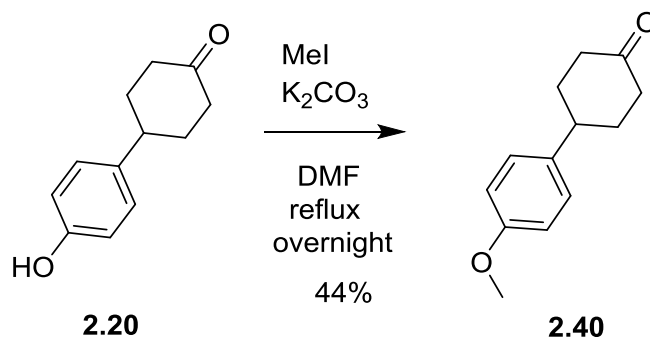
4-(4-((tert-Butyldimethylsilyl)oxy)-3-methylphenyl)cycloheptan-1-ol (2.37). The hydroboration-oxidation of cycloheptene **2.36** (0.334 g, 1.06 mmol) was carried out in a fashion similar to the preparation of **2.16**. Purification of the crude product by column chromatography (SiO_2 , hexanes-ethyl acetate = 80:20) gave **2.37** (0.116 g, 33%) as a colorless oil. This was determined to be a mixture of diastereoisomers by ^1H and ^{13}C NMR spectroscopy. ^1H NMR (400 MHz, CDCl_3) δ 6.94 (d, $J = 7.9$ Hz, 1H), 6.84 (br t, $J = 7.4$ Hz, 1H), 6.66 (d, $J = 8.3$ Hz, 1H), 4.06-3.99 and 3.98-3.89 (2 \times m, 1H total), 2.66-2.49 (m, 1H), 2.18 (s, 3H), 2.13-2.05 (m, 1H), 2.02-1.48 (m, 10H), 1.00 (s, 9H), 0.20 (s, 6H) ppm. ^{13}C NMR (100 MHz, CDCl_3) δ 151.9, 141.9, 141.8, 129.4, 128.7, 124.6, 118.3, 73.1, 71.9, 46.4, 46.1, 38.3, 37.9, 37.3, 37.2, 37.0, 35.9, 31.9, 29.8, 26.0, 21.5, 18.4, 17.2, -4.0 ppm.



4-(4-Hydroxy-3-methylphenyl)cycloheptan-1-ol (2.38). To a solution of **2.37** (0.100 g, 0.299 mmol) in anhydrous THF (15 mL) was added a solution of tetrabutylammonium fluoride (1M in THF, 1.2 mL, 1.2 mmol). The mixture was heated at 70 °C overnight and cooled to room temperature. The solution was partitioned between ethyl acetate (2 x 15 mL) and water (2 x 10 mL). The organic layer was washed with brine, dried (Na_2SO_4) and concentrated. Purification by column chromatography (SiO_2 , hexanes-ethyl acetate = 50:50) gave **2.38** (0.035g, 53%) as a colorless solid. ^1H NMR (400 MHz, CDCl_3) δ 6.92 (d, $J = 8.2$ Hz, 1H), 6.86 (br t, $J = 7.3$ Hz, 1H), 6.69 (d, $J = 8.2$ Hz, 1H), 5.84 (s, OH) 4.08-4.01 and 4.00-3.90 (2 x m, 1H total), 2.66-2.44 (m, 1H), 2.22 (s, 3H), 2.16-1.48 (m, 11H) ppm. ^{13}C NMR (100 MHz, CDCl_3) δ 152.4, 141.4, 129.4, 124.9, 124.0, 114.9, 73.2, 72.1, 46.4, 46.1, 38.4, 37.9, 37.1, 37.0, 36.9, 35.7, 31.9, 29.8, 23.5, 21.5, 16.2 ppm.

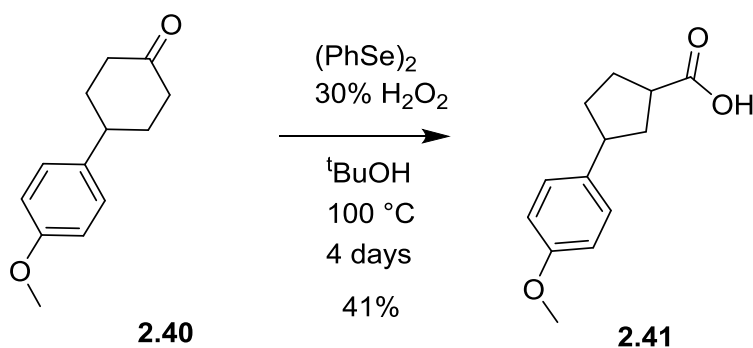


4-(6-Oxabicyclo[3.2.2]nonan-5-yl)phenol (2.42). Cyclic ether formation of 4-(4-(hydroxymethyl)cycloheptyl)phenol **2.10** (0.075 g, 0.34 mmol) was carried out in a fashion similar to the preparation of **3.8**. Purification by column chromatography (SiO₂, hexanes-ethyl acetate = 60: 40) gave **2.42** (0.049 g, 66%) as a light yellow viscous oil. ¹H NMR (400 MHz, CDCl₃) δ 7.15 and 6.58 (AA'BB', J_{AB} = 7.8 Hz, 4H), 6.30 (s, 1H), 4.07–3.96 (m, 1H), 3.90–3.84 (m, 1H), 2.25–1.60 (m, 11H) ppm. ¹³C NMR (100 MHz, CDCl₃) δ 154.3, 142.5, 125.6, 114.9, 76.5, 69.9, 42.9, 33.8, 32.5, 30.3, 22.6, 21.5 ppm.



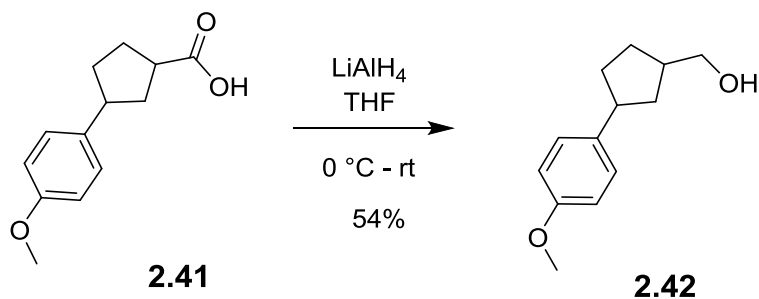
4-(4-methoxyphenyl) Cyclohexanone (2.40). To a solution of 4-(4-hydroxyphenyl)cyclohexanone (0.500 g, 2.63 mmol) in DMF (10 mL) was added K₂CO₃ (0.545 g, 3.94 mmol) and iodomethane (0.21 mL, 0.485 g, 3.42 mmol). The reaction was heated at reflux overnight. The reaction was cooled, diluted with H₂O and extracted with ethyl acetate. The organic extracts were combined and washed with brine, dried (Na₂SO₄),

and concentrated. The residue was purified by column chromatography (hexanes-ethyl acetate = 80:20) to give **2.40** (0.238 g, 44%) as a colorless solid. mp 70-74 °C. [lit. mp 74 °C].⁹⁰ ¹H NMR (CDCl₃) δ 7.17 and 6.87 (AA'BB', J_{AB} = 8.6 Hz, 4H), 3.79 (s, 3H), 2.98 (tt, J = 11.9, 3.8 Hz, 1H), 2.56-2.44 (m, 4H), 2.24-2.15 (m, 2H) and 1.97-1.84 (m, 2H) ppm. The NMR data was consistent with the literature values.⁹⁰

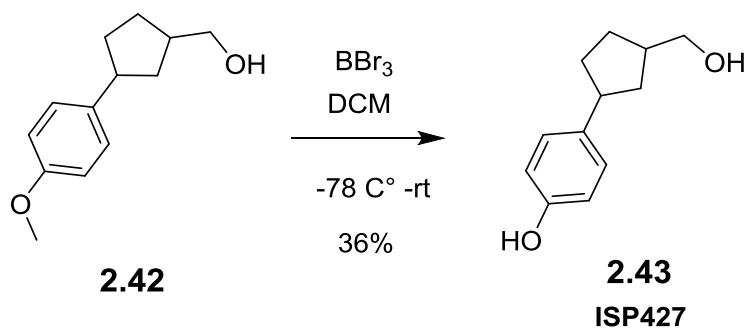


3-(4-Methoxyphenyl)cyclopentane-1-carboxylic acid (2.41). To a solution of cyclohexanone **2.40** (0.100 g, 0.490 mmol) in a heavy-walled reaction vessel was added diphenyldiselenide (0.002 g, 0.005 mmol), *t*-BuOH (4 mL) and 30% H₂O₂ (0.4 mL). The reaction vessel was sealed and heated at 100 °C for 4 d. After cooling the reaction vessel was opened and 10% Pd/C (20 mg) was added and solvent was distilled off. The residue was treated with 10% aqueous Na₂CO₃ (40 mL) and extracted with CH₂Cl₂ (3 × 20 mL). The aqueous phase was adjusted to pH 1 with HCl and extracted with CH₂Cl₂ (3 × 25 mL). The combined extracts were dried (Na₂SO₄) and concentrated. The residue was purified by column chromatography (SiO₂, hexanes-ethyl acetate = 60:40) to give **2.41** (0.044 g, 41%) as a colorless oil. This product was determined to be a mixture of *cis*- and *trans*-stereoisomers on the basis of ¹H and ¹³C NMR spectroscopy. ¹H NMR (400 MHz, CDCl₃) δ 7.18, 7.06 and 6.84 (AA'BB', J_{AB} = 8.7 Hz, 4H total), 3.79 (s, 3H), 3.24–3.16 (m, 0.4H), 3.15–2.92 (m, 1.6H), 2.72–2.63 (m, 0.3H), 2.42–2.33 (m, 0.7H), 2.21–1.69 (m, 5H) ppm.

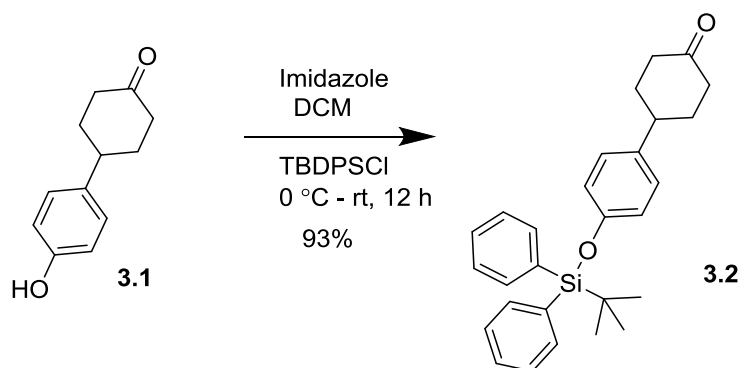
^{13}C NMR (100 MHz, CDCl_3) δ 182.7, 179.9, 158.2, 136.5, 135.9, 128.9, 128.2, 114.0, 113.9, 59.5, 55.5, 45.7, 43.6, 38.5, 37.6, 34.2, 29.3, 27.7 ppm. The ^1H NMR data for this compound were consistent with the literature values.⁹²



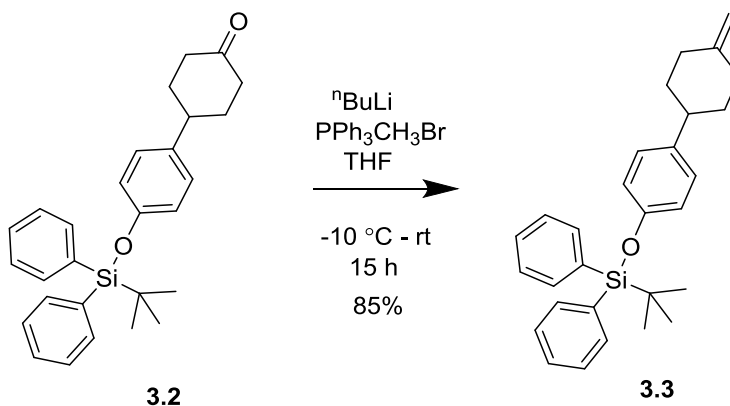
(3-(4-Methoxyphenyl)cyclopentyl)methanol (2.42). To a solution of **2.41** (0.083 g, 0.377 mmol) in anhydrous THF (5 mL) at 0 °C under N_2 was slowly added LiAlH_4 (0.043 g, 1.13 mmol). After addition was completed the reaction was gradually warmed to room temperature and continued to stir for 3 h. The mixture was cautiously quenched with water and extracted with ethyl acetate (3 \times 15 mL). The combined extracts were dried (Na_2SO_4) and concentrated. The residue was purified by column chromatography (SiO_2 , hexanes-ethyl acetate = 80:20) to give **2.42** (0.042 g, 54%) as a colorless oil. This product was determined to be a mixture of *cis*- and *trans*- stereoisomers on the basis of ^1H and ^{13}C NMR spectroscopy. ^1H NMR (400 MHz, CDCl_3) δ 7.17 and 6.84 (AA'BB', $J_{\text{AB}} = 8.7$ Hz, 4H), 3.79 (s, 3H), 3.61 (d, $J = 6.7$ Hz, 1.7H), 3.57 (d, $J = 7.1$ Hz, 0.3H), 3.08–2.97 (m, 1H), 2.40–2.15 (m, 2H), 2.13–1.98 (m, 1H), 1.94–1.81 (m, 1H), 1.68–1.52 (m, 2H), 1.34–1.23 (m, 1H) ppm. ^{13}C NMR (100 MHz, CDCl_3) δ 157.9, 137.7, 128.0, 113.8, 67.7, 67.6, 55.4, 45.3, 43.9, 42.0, 41.4, 38.5, 37.1, 35.1, 33.7, 29.4, 28.4 ppm.



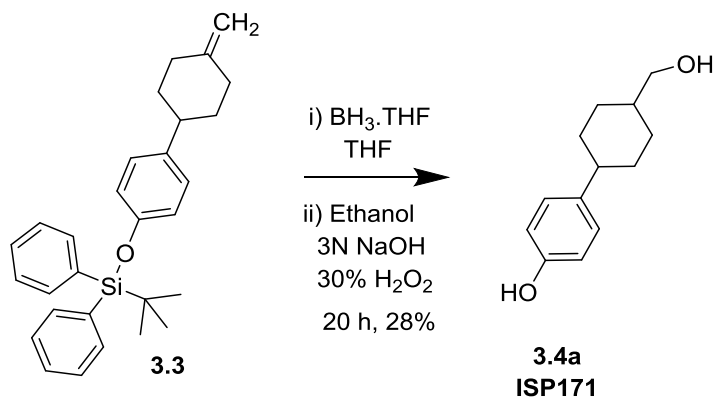
4-(3-(Hydroxymethyl)cyclopentyl)phenol (2.43). To a solution of **2.42** (0.030 g, 0.145 mmol) in anhydrous CH_2Cl_2 (8 mL) at $-78\text{ }^\circ\text{C}$, was added dropwise a solution of boron tribromide (1M in CH_2Cl_2 , 0.44 mL, 0.44 mmol). After complete addition, the reaction mixture was stirred for 30 min at $-78\text{ }^\circ\text{C}$ and gradually warmed to room temperature over a 2 h period. The mixture was quenched with water (10 mL) and the aqueous layer was extracted with CH_2Cl_2 (3×15 mL). The combined organic extracts were washed with brine, dried (MgSO_4) and concentrated. The residue was purified by column chromatography (SiO_2 , hexanes-ethyl acetate = 50:50) to give **2.43** (0.010 g, 36%) as a colorless solid. This product was determined to be a mixture of *cis*- and *trans*-stereoisomers on the basis of ^1H and ^{13}C NMR spectroscopy. ^1H NMR (400 MHz, CDCl_3) δ 7.10 and 6.76 (AA'BB', $J_{\text{AB}} = 8.2$ Hz, 4H), 3.62 (d, $J = 6.7$ Hz, 1.6H), 3.58 (d, $J = 7.2$ Hz, 0.4H), 3.06–2.93 (m, 1H), 2.40–2.14 (m, 2H), 2.11–1.94 (m, 1H), 1.93–1.71 (m, 1H), 1.67–1.49 (m, 2H), 1.33–1.20 (m, 1H) ppm. ^{13}C NMR (100 MHz, CDCl_3) δ 153.9, 137.7, 128.2, 115.3, 67.8, 67.7, 45.3, 44.0, 42.0, 41.4, 38.5, 37.2, 35.0, 33.7, 29.4, 28.4 ppm.



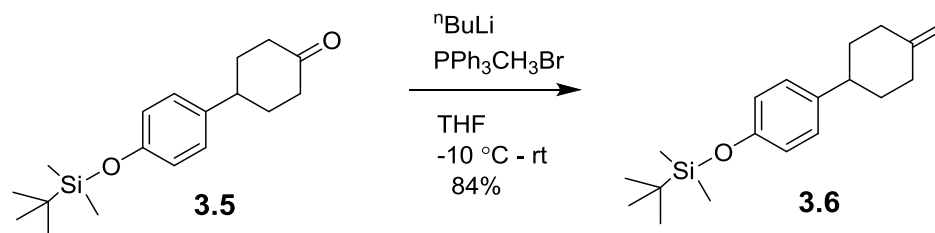
4-(4-((tert-Butyldiphenylsilyloxy)phenyl)cyclohexan-1-one (3.2). To a solution of 4-(4-hydroxyphenyl)cyclohexanone (0.815 g, 4.28 mmol) in dry CH₂Cl₂ (30 ml) at 0 °C, was added imidazole (0.583 g 8.57 mmol). After stirring for 30 min, a solution of t-butyldiphenylsilyl chloride (1.60 mL, 5.57 mmol) in CH₂Cl₂ (9 mL) was added dropwise while maintaining the temperature at 0 °C. The reaction mixture was slowly warmed to room temperature and stirred for 12 h. The mixture was diluted with water (20 mL) and partitioned with CH₂Cl₂ (40 mL). The organic portion was separated, washed with brine, dried (Na₂SO₄), and concentrated. The residue was purified by column chromatography (SiO₂, hexanes-ethyl acetate = 80: 20) to give **3.2** (1.70 g, 93%) as a colorless solid. mp 83-84 °C. ¹H NMR (400 MHz, CDCl₃) δ 7.74-7.70 (m, 4H), 7.45-7.34 (m, 6H), 6.96 and 6.71 (AA'BB', J_{AB} = 8.6 Hz, 4H), 2.90 (tt, J = 12.1, 3.3 Hz, 1H), 2.49-2.42 (m, 4H), 2.19-2.10 (m, 2H), 1.91-1.77 (m, 2H), 1.09 (s, 9H) ppm. ¹³C NMR (100 MHz, CDCl₃) δ 211.6, 154.3, 137.3, 135.7, 133.2, 130.1, 127.9, 127.5, 119.8, 42.1, 41.6, 34.3, 26.7, 19.7.



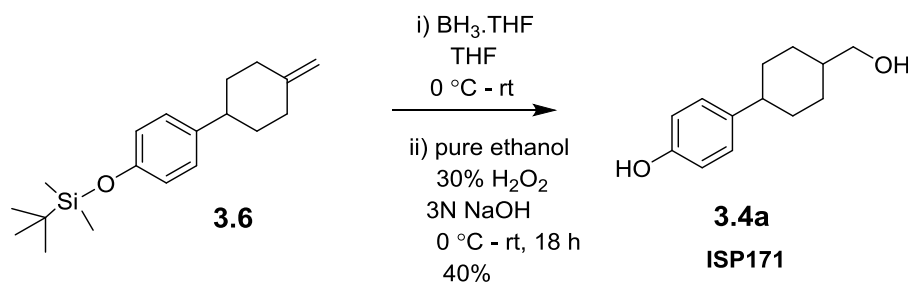
tert-Butyl(4-(4-methylenecyclohexyl)phenoxy)diphenylsilane (3.3). A solution of n butyllithium in hexane (1.6 M, 1.5 mL, 2.4 mmol) was added to a stirring solution of methyltriphenylphosphonium bromide (0.836 g, 2.34 mmol) in dry THF (20 mL) at $-10\text{ }^\circ\text{C}$. After 30 min, a solution of 4-(4-butyldiphenylsilyloxyphenyl)cyclohexanone **3.2** (0.502 g, 1.17 mmol) in dry THF (8 mL) was added dropwise. The reaction mixture was slowly warmed to room temperature and stirred overnight. After this time, the mixture was diluted with water (20 mL), extracted with ethyl acetate ($2 \times 25\text{ mL}$), dried (Na_2SO_4) and concentrated. The residue was purified by column chromatography (SiO_2 , hexanes-ethyl acetate = 80:20) to give **3.3** (0.423 g, 85%) as a colorless oil. $^1\text{H NMR}$ (400 MHz, CDCl_3) δ 7.75-7.71 (m, 4H), 7.46-7.34 (m, 6H), 6.93 and 6.69 (AA'BB', $J_{\text{AB}} = 8.6\text{ Hz}$, 4H), 4.65 (t, $J = 1.7\text{ Hz}$, 2H), 2.55 (tt, $J = 12.0, 3.3\text{ Hz}$, 1H), 2.42-2.34 (m, 2H), 2.20-2.09 (m, 2H), 1.95-1.87 (m, 2H), 1.50-1.38 (m, 2H), 1.10 (s, 9H) ppm. $^{13}\text{C NMR}$ (100 MHz, CDCl_3) δ 153.8, 149.2, 139.5, 135.7, 133.3, 130.0, 127.9, 127.6, 119.5, 107.4, 43.4, 35.9, 35.4, 26.7, 19.7 ppm.



4-(4-(Hydroxymethyl)cyclohexyl)phenol (3.4a). A solution of borane-THF complex in THF (1 M, 1.22 mL, 1.22 mmol) was added to a solution of **3.3** (0.261 g, 0.611 mmol) in THF (6 mL) at 0 °C. The reaction mixture was slowly warmed to room temperature and stirred for 20 h. The mixture was then cooled to 0 °C, followed by sequential addition of ethanol (50 mL), hydrogen peroxide solution (30% in water, 1.00 mL) and 3N NaOH solution (5.0 mL). The mixture was warmed to room temperature and stirred for 30 min. The reaction mixture was extracted with ethyl acetate (2 ×20 mL). The organic portion was washed with brine, dried (Na_2SO_4), and concentrated. The residue was recrystallized from chloroform to give **3.4a** (0.035 g, 28%) as a colorless solid. mp 118-122 °C. ^1H NMR (400 MHz, CD_3OD) δ 7.04-6.98 (m, 2H), 6.70-6.65 (m, 2H), 3.60 (d, $J = 7.6$ Hz, 1.5H), 3.39 (d, $J = 6.6$ Hz, 0.5H), 2.54–2.44 (m, 0.7H) and 2.37 (tt, $J = 12.1, 3.4$ Hz, 0.3H), 1.93–1.70 (m, 3H), 1.61 (d, $J = 6.3$ Hz, 4H), 1.46–1.37 (m, 1H), 1.14–1.02 (m, 1H) ppm. ^{13}C NMR (100 MHz, CD_3OD) δ 156.2, 139.6, 128.7, 116.0, 68.0, 64.4, 45.2, 44.0, 41.4, 37.0, 35.4, 31.2, 30.5, 28.0 ppm.

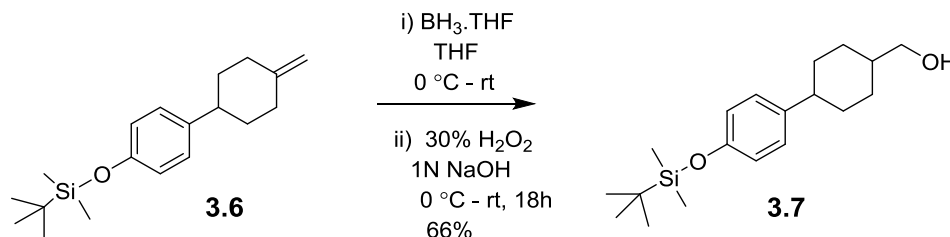


tert-Butyldimethyl(4-(4-methylenecyclohexyl)phenoxy)silane (3.6). Wittig methenylation of compound **3.5** (2.00 g, 6.57 mmol) was carried out in a fashion similar to the preparation of **3.3**. Purification of the crude residue by column chromatography (SiO_2 , hexanes-ethyl acetate = 90: 10) gave **3.6** (1.678 g, 84%) as a colorless oil. ^1H NMR (400 MHz, CDCl_3) δ 7.06 and 6.77 (AA'BB', $J_{\text{AB}} = 8.3$ Hz, 4H), 4.68 (s, 2H), 2.62 (tt, $J = 12.1$, 3.4 Hz, 1H), 2.42 (br d, $J = 13.5$ Hz, 2H), 2.18 (br t, $J = 13.2$ Hz, 2H), 2.00-1.93 (m, 2H), 1.57-1.45 (m, 2H), 0.99 (s, 9H), 0.20 (s, 6H) ppm. ^{13}C NMR (100 MHz, CDCl_3) δ 153.9, 149.2, 139.8, 127.8, 119.9, 107.4, 43.5, 36.0, 35.4, 25.9, 18.4, -4.2 ppm. Anal. calcd. for $\text{C}_{19}\text{H}_{30}\text{OSi}$: C, 75.43; H, 9.99. Found: C, 75.71; H, 10.02.

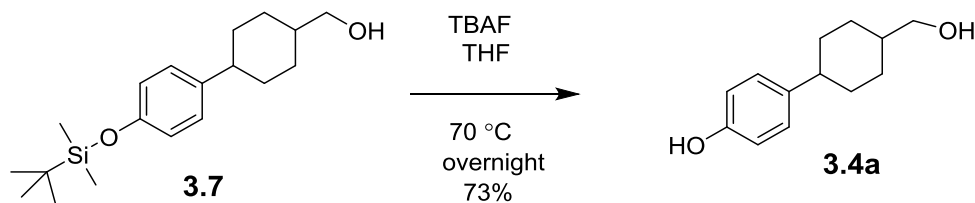


4-(4-(Hydroxymethyl)cyclohexyl)phenol (3.4a). Hydroboration-oxidation of **3.6** (0.350 g, 1.16 mmol) was carried out in a fashion similar to the hydroboration-oxidation of **3.3**. Purification of the residue by column chromatography (SiO_2 , hexanes-ethyl acetate =

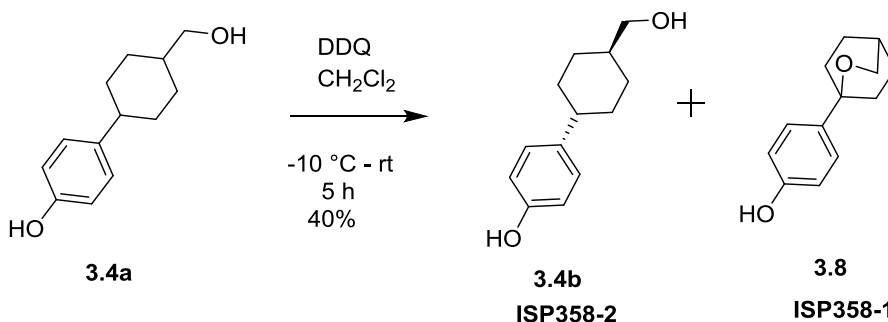
65:35) gave **3.4a** (0.095 g, 40%) as a colorless solid. The ^1H NMR spectral data were consistent with previously obtained values.



(4-(4-((tert-Butyldimethylsilyl)oxy)phenyl)cyclohexyl)methanol (3.7). The hydroboration of **3.6** (0.821 g, 2.71 mmol) was carried out in a fashion similar to the hydroboration of **3.3**. After stirring for 18 h, the reaction mixture was cooled to $0\text{ }^\circ\text{C}$, followed by sequential addition of 1 N sodium hydroxide solution (3.2 mL) and hydrogen peroxide solution (30% in water, 1.50 mL). The mixture was warmed to room temperature and stirred for 1.5 h. The reaction mixture was quenched with saturated sodium bicarbonate solution (10 mL), diluted with water (20 mL) and extracted with ethyl acetate ($2 \times 20\text{ mL}$). The combined organic extracts were washed with brine, dried (Na_2SO_4) and concentrated. The residue was purified by column chromatography (SiO_2 , hexanes-ethyl acetate = 70:30) to give **3.7** (0.572 g, 66%) as a colorless oil. ^1H NMR (400 MHz, CDCl_3) δ 7.06 and 6.76 (AA'BB', $J_{\text{AB}} = 8.5\text{ Hz}$, 4H), 3.69 (d, $J = 7.4\text{ Hz}$, 1.3H), 3.50 (d, $J = 6.5\text{ Hz}$, 0.7H), 2.59-2.51 (m, 0.5H), 2.42 (tt, $J = 12.1, 3.8\text{ Hz}$, 0.5H), 1.96-1.84 (m, 2H), 1.80-1.37 (m, 7H), 0.98 (s, 9H), 0.19 (s, 6H) ppm. ^{13}C NMR (100 MHz, CDCl_3) δ 153.7, 140.4, 140.0, 127.8, 119.9, 68.9, 64.6, 43.8, 42.6, 40.3, 36.2, 34.1, 30.0, 29.4, 27.0, 25.9, 18.4, -4.2 ppm.

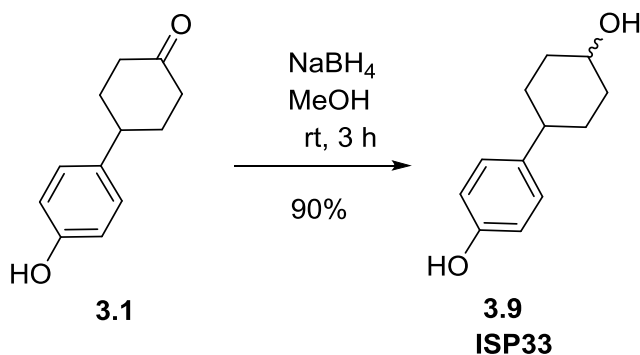


4-(4-(Hydroxymethyl)cyclohexyl)phenol (3.4a). To a solution of **3.7** (0.594 g, 1.85 mmol) in anhydrous THF (10 mL) was added a solution of TBAF (1M in THF, 7.5 mL, 7.5 mmol) while stirring. The mixture was heated to reflux at 70 °C overnight and cooled to room temperature. The solution was partitioned between ethyl acetate and water. The organic layer was washed with brine, dried (Na₂SO₄) and concentrated. Purification by column chromatography (SiO₂, hexanes-ethyl acetate = 60:40) gave **3.4a** (0.280 g, 73%) as a colorless solid. mp 118-122 °C. The ¹H NMR spectral data is consistent with that previously obtained.

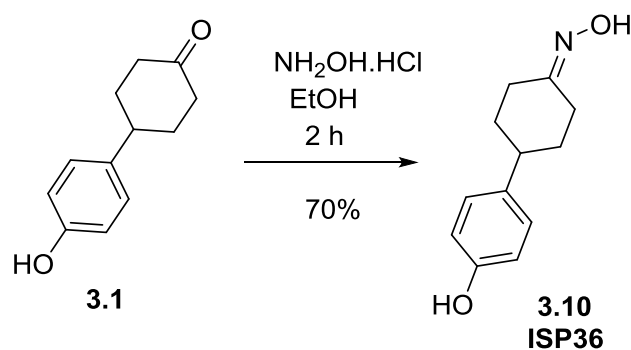


4-(2-Oxabicyclo[2.2.2]octan-1-yl)phenol (3.8) and **trans-4-(4-(Hydroxymethyl)cyclohexyl)phenol (3.4b).** To a solution of a mixture of *cis*- and *trans*-4-(4-(hydroxymethyl) cyclohexyl)phenol **3.4a** (0.050 g, 0.242 mmol) in anhydrous CH₂Cl₂ (15 mL) at -10 °C, was slowly added a suspension of 2,3-dichloro-5,6-dicyano-1,4-

benzoquinone (0.059 g, 0.262 mmol) in CH_2Cl_2 (5 mL) over a period of 30 min. The green solution continued to stir at 0 °C for 2 h and gradually warmed to room temperature and stirred for another 3 h. The mixture was quenched by slow addition of saturated sodium bicarbonate solution at 0 °C. After a few minutes, the layers were separated and the aqueous layer was extracted with CH_2Cl_2 (2 × 20 mL). The combined organic extracts were washed with brine, dried (Na_2SO_4), and concentrated. The residue was purified by column chromatography (SiO_2 , hexanes-ethyl acetate = 60: 40) to give **3.8** (0.020 g, 40%) followed by **3.4b** (0.010 g, 20%) both as colorless solids. **3.8**: mp 120-124 °C. ^1H NMR (400 MHz, CD_3OD) δ 7.18 and 6.64 (AA'BB', $J_{\text{AB}} = 7.9$ Hz, 4H), 4.04 (s, 2H), 2.01 (t, $J = 7.8$ Hz, 4H), 1.94–1.73 (m, 5H) ppm. ^{13}C NMR (100 MHz, CD_3OD) δ 157.2, 138.9, 127.1, 115.6, 73.0, 71.3, 34.5, 27.3, 25.9 ppm. Anal. calcd for $\text{C}_{13}\text{H}_{16}\text{O}_2$: C, 76.44; H, 7.89. Found: C, 76.39; H, 7.97. **3.4b**: mp 115-120 °C. ^1H NMR (400 MHz, CD_3OD) δ 7.00 and 6.68 (AA'BB', $J_{\text{AB}} = 8.7$ Hz, 4H), 3.39 (d, $J = 6.7$ Hz, 2H), 2.36 (tt, $J = 12.1, 3.0$ Hz, 1H), 1.87 (br t, $J = 15.4$, 4H), 1.55–1.36 (m, 3H), 1.14–1.02 (m, 2H) ppm. ^{13}C NMR (100 MHz, CD_3OD) δ 156.3, 139.8, 128.6, 116.0, 68.8, 45.1, 41.4, 35.3, 31.2 ppm. Anal. calcd for $\text{C}_{13}\text{H}_{18}\text{O}_2$: C, 75.69; H, 8.79. Found: C, 75.66; H, 9.09.

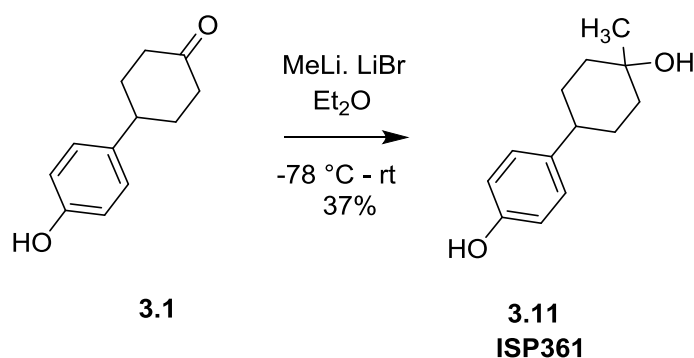


4-(4-Hydroxycyclohexyl)phenol (3.9). Cyclohexanone **3.1** (0.200 g, 1.05 mmol) was dissolved in anhydrous methanol (15 mL) and NaBH_4 (0.400 g, 10.6 mmol) was added while stirring at room temperature. Reaction was continued for 3 h and mixture was extracted with ethyl acetate (3× 20 mL). The combined extracts were concentrated to give product **3.9** (0.181 g, 90%) as a colorless solid. mp 196–208 °C. ^1H NMR (400 MHz, CD_3OD) δ 7.00 and 6.67 (AA'BB', $J_{\text{AB}} = 8.7$ Hz, 4H), 3.61–3.53 (m, 1H), 2.38 (tt, $J = 11.8, 3.4$ Hz, 1H), 2.05–1.98 (m, 2H), 1.87–1.78 (m, 2H), 1.56–1.30 (m, 4H) ppm. ^{13}C NMR (100 MHz, CD_3OD) δ 156.5, 139.1, 128.7, 116.0, 71.3, 49.3, 44.2, 36.8, 34.1 ppm. HRMS m/z 191.1077 [calcd for $\text{C}_{12}\text{H}_{15}\text{O}_2^-$ ($\text{M}-\text{H}^+$) 191.1078].



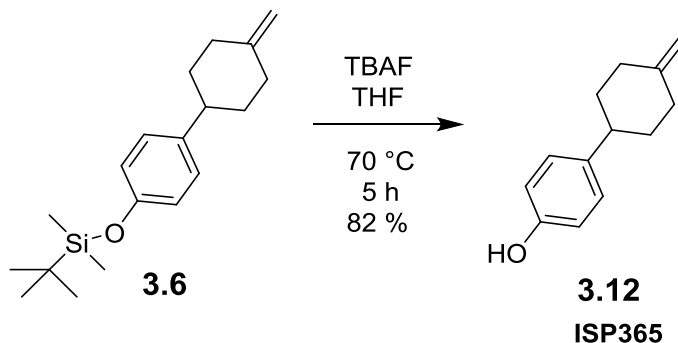
4-(4-Hydroxyphenyl)cyclohexanone oxime (3.10). To a solution of cyclohexanone **3.1** (0.050 g, 0.26 mmol) in ethanol (10 mL), were added Amberlyst (0.060 g) and

hydroxylamine hydrochloride (0.039 g, 0.560 mmol). The mixture was stirred at room temperature for 2 h and then filtered. The filtrate was concentrated and extracted with ethyl acetate (2 × 10 mL) and water (2 × 10 mL). The combined organic extracts were concentrated and dried (MgSO₄). Evaporation of the solvent gave **3.10** as a colorless solid (0.037 g, 70%). mp 171-174 °C. ¹H NMR (400 MHz, CD₃OD) δ 7.00 and 6.69 (AA'BB', J_{AB} = 8.2 Hz, 4H), 3.39 (br d, J = 13.5 Hz, 1H), 2.67 (t, J = 12.8 Hz, 1H), 2.41 (br d, J = 14.0 Hz, 1H), 2.20 (td, J = 14.6, 5.4 Hz, 1H), 1.93 (br t, J = 15.8 Hz, 2H), 1.81 (td, J = 14.0, 5.2 Hz, 1H), 1.61–1.42 (m, 2H) ppm. ¹³C NMR (100 MHz, CD₃OD) δ 160.8, 156.7, 138.3, 128.6, 116.2, 44.1, 35.8, 34.6, 32.8, 25.1 ppm.

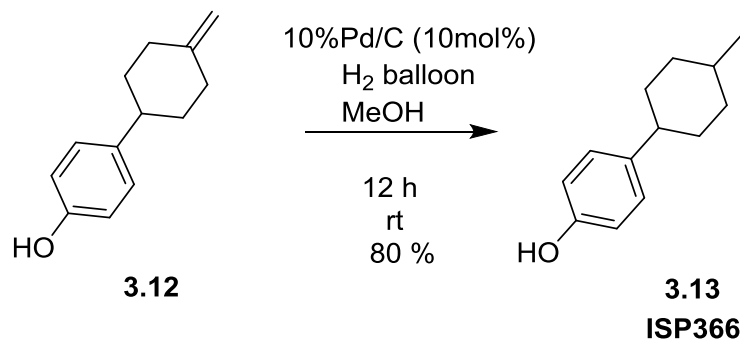


4-(4-Hydroxy-4-methylcyclohexyl)phenol (3.11). To a solution of **3.1** (0.100 g, 0.526 mmol) in dry Et₂O (20 mL) at -78 °C under N₂, was added slowly a solution of methyllithium-lithium bromide complex (1.5 M in ether, 0.78 mL, 1.2 mmol). The mixture was stirred for another 30 min at -78 °C, warmed to room temperature and stirred for another 1 h. The mixture was cooled to 0 °C and quenched with water. The mixture was extracted with diethyl ether (2 × 30 mL), dried (Na₂SO₄) and concentrated. The residue was purified from column chromatography (SiO₂, hexanes-ethyl acetate = 80:20) to give **3.11** (0.040 g, 37%) as a colorless solid. mp 126-131 °C. ¹H NMR (400 MHz, CD₃OD) δ

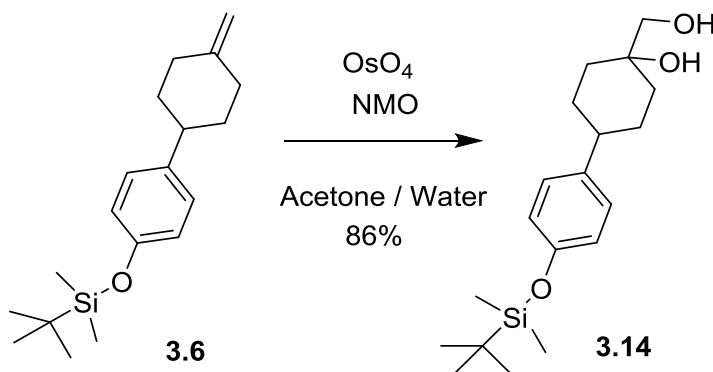
7.03 and 6.67 (AA'BB', $J_{AB} = 8.3$ Hz, 4H), 2.35 (tt, $J = 12.4, 3.6$ Hz, 1H), 1.87–1.69 (m, 4H), 1.61–1.44 (m, 4H), 1.21 (s, 3H) ppm. ^{13}C NMR (100 MHz, CD_3OD) δ 156.3, 139.9, 129.6, 116.0, 69.3, 44.3, 39.9, 31.8, 30.9 ppm. HRMS m/z 205.1234 [calcd for $\text{C}_{13}\text{H}_{17}\text{O}_2^-$ ($\text{M}-\text{H}^+$) 205.1234].



4-(4-Methylenecyclohexyl)phenol (3.12). To a solution of **3.6** (0.739 g, 2.44 mmol) in anhydrous THF (20 mL) was added a solution of TBAF (1M in THF, 9.8 mL, 9.8 mmol). The mixture was heated to reflux at 70 °C for 5 h and cooled to room temperature. The solution was partitioned between ethyl acetate (2 × 30 mL) and water (20 mL). The combined organic layers were washed with brine, dried (Na_2SO_4) and concentrated. Purification of the crude material by column chromatography (SiO_2 , hexanes-ethyl acetate = 80:20) gave **3.12** (0.379 g, 82%) as a colorless solid. mp 82–84 °C. ^1H NMR (400 MHz, CD_3OD) δ 6.99 and 6.67 (AA'BB', $J_{AB} = 8.5$ Hz, 4H), 4.63 (t, $J = 1.7$ Hz, 2H), 2.57 (tt, $J = 12.3, 4.3$ Hz, 1H), 2.41–2.33 (m, 2H), 2.22–2.11 (m, 2H), 1.94–1.85 (m, 2H), 1.45 (qd, $J = 12.3, 4.3$ Hz, 2H) ppm. ^{13}C NMR (100 MHz, CD_3OD) δ 156.5, 150.2, 139.1, 128.6, 116.0, 107.7, 44.7, 37.1, 36.2 ppm. HRMS m/z 187.1128 [calcd for $\text{C}_{13}\text{H}_{15}\text{O}^-$ ($\text{M}-\text{H}^+$) 187.1128].

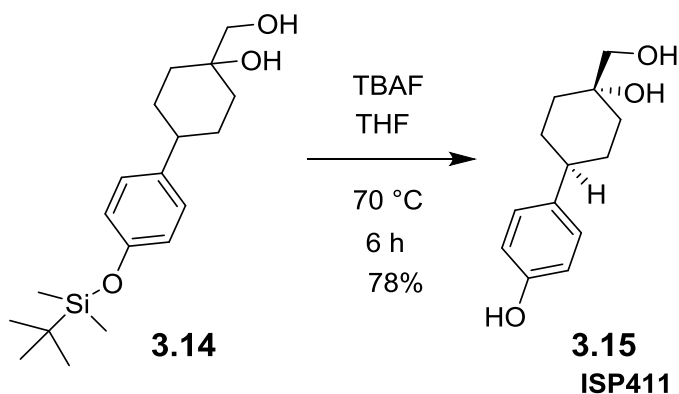


4-(4-Methylcyclohexyl)phenol (3.13). To a solution of **3.12** (0.150 g, 0.797 mmol) in methanol (10 mL) was added 10% Pd/C (0.085 g, 10 mol %) and the mixture was stirred under a balloon filled with H₂ at room temperature for 12 h. The reaction mixture was filtered through a pad of celite, dried (Na₂SO₄) and concentrated. The residue was purified by column chromatography (SiO₂, hexanes-ethyl acetate = 80:20) to give **3.13** (0.121 g, 80%) as a colorless solid. mp = 93-99 °C. [lit. mp 108°C].¹¹⁹ ¹H NMR (400 MHz, CD₃OD) δ 7.05–6.96 (m, 2H), 6.70–6.64 (m, 2H), 2.48–2.28 (m, 1H), 1.83–1.34 (m, 8H), 1.13–1.04 (m, 1H), 1.03 (d, J = 7.2 Hz, 1H), 0.92 (d, J = 6.6 Hz, 2H) ppm. ¹³C NMR (100 MHz, CD₃OD) δ 156.3, 140.0, 128.6, 116.0, 44.7, 36.9, 35.9, 33.7, 33.1, 30.0, 23.1 ppm. The NMR spectral data for this compound were consistent with the literature values.¹²⁰

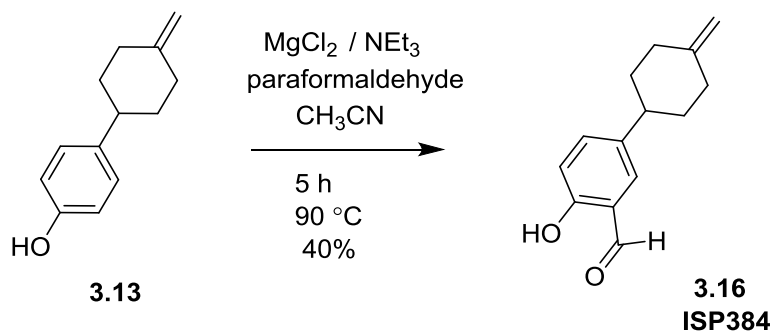


4-(4-((tert-Butyldimethylsilyloxy)phenyl)-1-(hydroxymethyl)cyclohexan-1-ol (3.14).

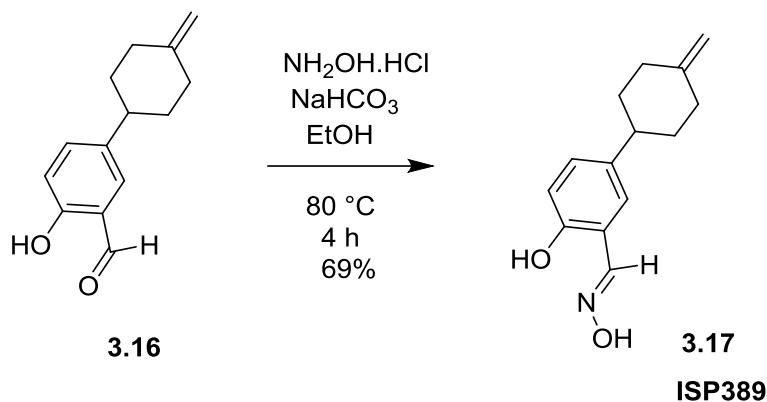
To a solution of **3.6** (0.280 g, 0.926 mmol) and N-methylmorpholine-N-oxide (0.15 g, 1.3 mmol) in acetone (6 mL) and distilled water (0.3 mL) was added a 2.5% solution of OsO_4 in tert-butanol (90 μL). The mixture was stirred overnight and a saturated solution of NaHSO_3 (10 mL) was added to quench the reaction. The mixture was diluted with ether (20 mL) and extracted with water (2×10 mL). The organic layer was dried (MgSO_4) and concentrated. Purification of the residue by column chromatography (SiO_2 , hexanes-ethyl acetate = 20:80) gave **3.14** (0.267 g, 86%) as a colorless solid. mp 80-86 $^\circ\text{C}$. ^1H NMR (400 MHz, CDCl_3) δ 7.04 and 6.76 (AA'BB', $J_{\text{AB}} = 8.5$ Hz, 4H), 3.69 (s, 1.7H), 3.47 (s, 0.3H), 2.58-2.39 (m, 1H), 2.04–1.72 (m, 4H, solvent peak overlapped), 1.61–1.37 (m, 4H), 0.97 (s, 9H), 0.18 (s, 6H) ppm. ^{13}C NMR (100 MHz, CDCl_3) δ 154.0, 138.9, 127.7, 120.0, 72.4, 66.2, 42.8, 35.4, 31.3, 25.9, 18.4, -4.2 ppm.



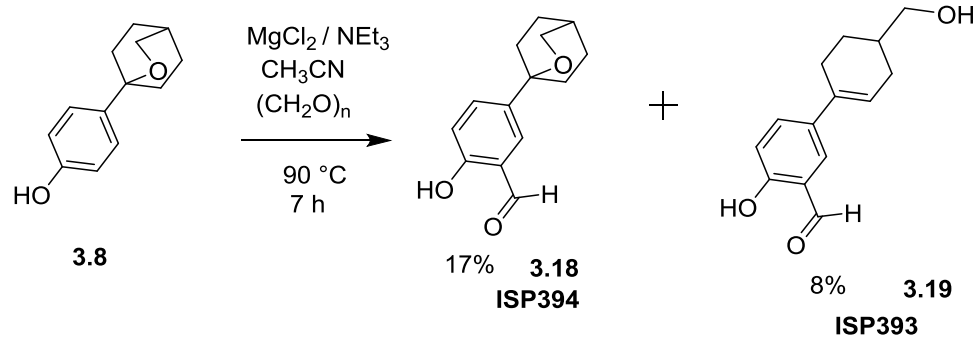
4-(4-Hydroxy-4-(hydroxymethyl)cyclohexyl)phenol (3.15). To a solution of **3.14** (0.230 g, 0.683 mmol) in anhydrous THF (10 mL) was added a solution of TBAF (1M in THF, 2.8 mL, 2.8 mmol). The mixture was heated to reflux at 70 °C for 6 h and cooled to room temperature. The solution was partitioned between ethyl acetate (2 × 20 mL) and water (20 mL). The combined organic layers were washed with brine, dried (Na₂SO₄) and concentrated. Purification of the crude material by column chromatography (SiO₂, ethyl acetate-methanol = 90:10) gave **3.15** (0.118 g, 78%) as a colorless solid. mp 182-188 °C. ¹H NMR (400 MHz, CD₃OD) δ 7.02 and 6.68 (AA'BB', J_{AB} = 8.5 Hz, 4H), 3.62 (s, 2H), 2.53–2.42 (m, 1H), 1.99–1.89 (m, 2H), 1.85–1.68 (m, 2H), 1.58–1.43 (m, 4H) ppm. ¹³C NMR (100 MHz, CD₃OD) δ 156.5, 138.7, 128.6, 116.0, 73.0, 66.5, 44.2, 35.8, 32.5 ppm. Anal. calcd. for C₁₃H₁₈O₃: C, 70.24; H, 8.16. Found: C, 70.18; H, 7.78.



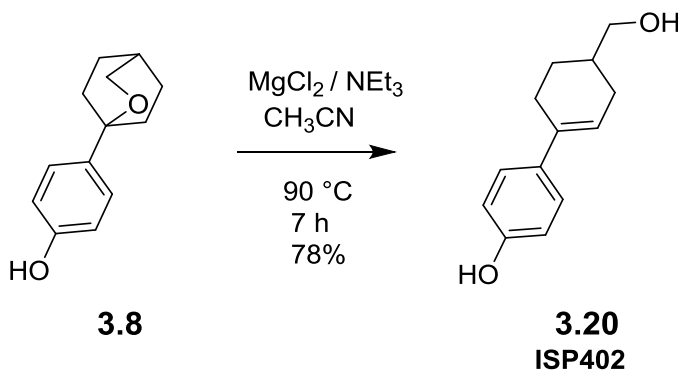
2-Hydroxy-5-(4-methylenecyclohexyl)benzaldehyde (3.16). To a solution of **3.13** (0.100 g, 0.532 mmol) in dry CH_3CN (20 mL) was added magnesium chloride (0.076 g, 0.797) and triethylamine (0.28 mL, 2.0 mmol), followed by paraformaldehyde (0.108 g, 3.59 mmol). The reaction mixture was heated at reflux for 6 h. The mixture was cooled to room temperature and quenched with 10% HCl (10 mL) and extracted with ethyl acetate (2×25 mL). The combined extracts were washed with brine, dried (Na_2SO_4) and concentrated. Purification of the residue by column chromatography (SiO_2 , hexanes-diethyl ether = 80:20) gave **3.16** (0.046 g, 40%) as a colorless oil. ^1H NMR (400 MHz, CD_3OD) δ 9.96 (s, 1H), 7.50 (s, 1H), 7.39 (d, $J = 8.5$ Hz, 1H), 6.85 (d, $J = 8.5$ Hz, 1H), 4.65 (t, $J = 1.7$ Hz, 2H), 2.68 (tt, $J = 12.0, 3.4$ Hz, 1H), 2.44–2.34 (m, 2H), 2.24–2.13 (m, 2H), 1.97–1.89 (m, 2H), 1.49 (qd, $J = 13.0, 4.0$ Hz, 2H) ppm. ^{13}C NMR (100 MHz, CD_3OD) δ 197.3, 160.9, 149.6, 139.8, 136.9, 131.5, 122.3, 118.0, 108.1, 44.1, 36.7, 36.0 ppm.



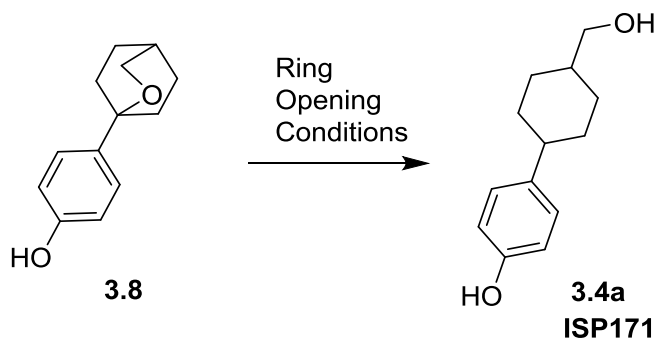
(E)-2-Hydroxy-5-(4-methylenecyclohexyl)benzaldehyde oxime (3.17). To a solution of **3.16** (0.050 g, 0.232 mmol) in pure ethanol (10 mL), were added sodium bicarbonate (0.024 g, 0.278 mmol) and hydroxylamine hydrochloride (0.025 g, 0.348 mmol). The reaction was heated at 80°C for 5 h, cooled and the mixture was extracted with ethyl acetate (2 × 20 mL). The combined organic extracts were dried (MgSO₄) and concentrated. Purification of the residue by column chromatography (SiO₂, hexanes-ethyl acetate = 65:35) gave **3.17** (0.037 g, 69%) as a colorless solid. This was determined to be a mixture of *E*- and *Z*-oxime stereoisomers by ¹H NMR spectroscopy. mp 120–125 °C. ¹H NMR (400 MHz, CD₃OD) δ 8.20 (s, 1H), 7.09–7.06 (m, 1H), 7.05 (d, J = 2.4 Hz, 1.8H), 6.99 (d, J = 7.9 Hz, 0.2H), 6.78 (d, J = 8.1 Hz, 0.8H), 6.68 (d, J = 8.6 Hz, 0.2H), 4.63 (t, J = 1.6 Hz, 2H), 2.60 (tt, J = 12.2, 3.3 Hz, 1H), 2.42–2.33 (m, 2H), 2.22–2.10 (m, 2H), 1.94–1.85 (m, 2H), 1.46 (qd, J = 12.5, 4.0 Hz, 2H) ppm. ¹³C NMR (100 MHz, MeOD) δ 156.4, 152.2, 150.0, 139.3, 130.1, 129.0, 128.6, 118.3, 117.0, 116.0, 107.8, 107.7, 44.6, 44.4, 37.1, 36.9, 36.2, 36.1 ppm. HRMS m/z 230.1187 [calcd for C₁₄H₁₆NO₂⁻ (M-H⁺) 230.1186].



5-(2-Oxabicyclo[2.2.2]octan-1-yl)-2-hydroxybenzaldehyde (3.18) and **4-Hydroxy-4'-(hydroxymethyl)-2',3',4',5'-tetrahydro-[1,1'-biphenyl]-3-carbaldehyde (3.19)**. To a solution of **3.8** (0.050 g, 0.25 mmol) in dry CH_3CN (15 mL) was added magnesium chloride (0.035 g, 0.367 mmol) and triethylamine (0.13 mL, 0.09 mmol) and the mixture was heated at reflux for 8 h. The mixture was cooled to room temperature and quenched with 10% HCl (10 mL) and extracted with ethyl acetate (2×25 mL). The combined organic extracts were washed with brine, dried (Na_2SO_4) and concentrated. Purification of the crude material by column chromatography (SiO_2 , hexanes-ethyl acetate = 65:35) gave **3.18** (0.010 g, 17%) followed by **3.19** (0.005 g, 8%) both as light-yellow oils. **3.18**: ^1H NMR (400 MHz, CD_3OD) δ 9.99 (s, 1H), 7.69 (br s, 1H), 7.57 (br d, $J = 8.7$ Hz, 1H), 6.87 (d, $J = 8.7$ Hz, 1H), 4.06 (s, 2H), 2.12–1.75 (m, 9H) ppm. ^{13}C NMR (100 MHz, CD_3OD) δ 197.3, 161.3, 140.0, 134.9, 130.1, 128.8, 117.7, 72.6, 71.3, 34.5, 27.3, 25.9 ppm. **3.19**: ^1H NMR (400 MHz, CD_3OD) δ 10.01 (s, 1H), 7.69 (s, 1H), 7.62 (d, $J = 8.5$ Hz, 1H), 6.89 (d, $J = 8.7$ Hz, 1H), 6.10 (s, 1H), 3.49 (d, $J = 6.1$ Hz, 2H), 2.54–2.28 (m, 3H), 2.05–1.73 (m, 3H), 1.47–1.35 (m, 1H) ppm. ^{13}C NMR (100 MHz, CD_3OD) δ 197.5, 161.4, 136.3, 135.6, 134.6, 129.8, 123.9, 122.2, 118.0, 67.7, 37.2, 29.9, 27.9, 26.9 ppm. HRMS m/z 231.1027 [calcd for $\text{C}_{14}\text{H}_{15}\text{O}_3^-$ ($\text{M}-\text{H}^+$) 231.1027].

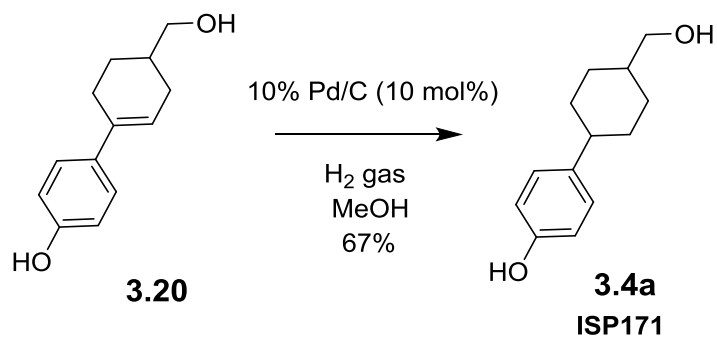


4'-(Hydroxymethyl)-2',3',4',5'-tetrahydro-[1,1'-biphenyl]-4-ol (3.20). To a solution of **3.8** (0.103 g, 0.505 mmol) in dry CH_3CN (25 mL) was added magnesium chloride (0.072 g, 0.756 mmol) and triethylamine (0.26 mL, 1.89 mmol). The mixture was heated at reflux for 8 h. The mixture was cooled to room temperature and quenched with 10% HCl (15 mL) and extracted with ethyl acetate (2×25 mL). The combined extracts were washed with brine, dried (Na_2SO_4) and concentrated. Purification of the crude material by column chromatography (SiO_2 , hexanes-ethylacetate = 65:35) gave **3.20** (0.080 g, 78%) as a colorless solid. mp 177–184°C. ^1H NMR (400 MHz, CDCl_3) δ 7.20 and 6.69 (AA'BB', $J_{\text{AB}} = 8.6$ Hz, 4H), 5.97–5.92 (m, 1H), 3.48 (dd, $J = 6.4, 2.6$ Hz, 2H), 2.49–2.23 (m, 3H), 2.01–1.71 (m, 4H), 1.43–1.31 (m, 1H) ppm. ^{13}C NMR (100 MHz, CDCl_3) δ 157.4, 137.5, 135.0, 127.1, 122.0, 115.8, 67.8, 37.3, 30.0, 28.1, 27.1 ppm. HRMS m/z 203.1078 [calcd for $\text{C}_{12}\text{H}_{15}\text{O}_2^-$ ($\text{M}-\text{H}^+$) 203.1077].

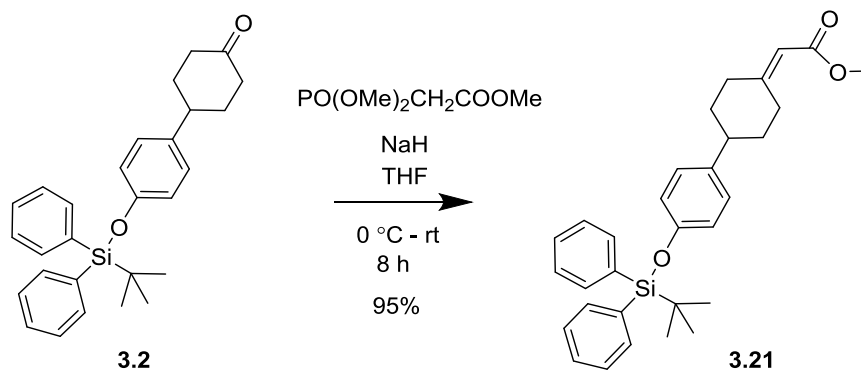


4-(4-(Hydroxymethyl)cyclohexyl)phenol (3.4a). Method A: To a solution of **3.8** (0.020 g, 0.098 mmol) dry CH_2Cl_2 (10 mL) was added triethylsilane (0.02 mL, 0.12 mmol) followed by trifluoroacetic acid (0.08 mL, 0.98 mmol). The reddish mixture was stirred at room temperature overnight and the solution was extracted with ethyl acetate (2×10 mL). The combined organic extracts were washed with H_2O (2×15 mL), dried (Na_2SO_4) and concentrated to give **3.4a** (0.012 g, 59%) as a colorless solid. The ^1H NMR spectrum showed the formation of a 2:3(cis: trans) mixture of isomers.

Method B: To a solution of **3.8** (0.050 g, 0.25 mmol) in dry THF (15 mL) cooled to -78 °C was added NaCNBH_3 (0.154 g, 2.48 mmol). The mixture was stirred at this temperature for 1 h and $\text{BF}_3 \cdot \text{Et}_2\text{O}$ (2.5 mL, 14 mmol) was added dropwise. The mixture was warmed to room temperature overnight, quenched with water (10 mL) and extracted with ether (2×20 mL). The combined organic extracts were washed with NaHCO_3 solution, brine, dried (Na_2SO_4) and concentrated to give **3.4a** (0.030, 60%) as a colorless solid. The ^1H NMR spectrum showed the formation of a 1:4 (cis: trans) mixture of isomers.

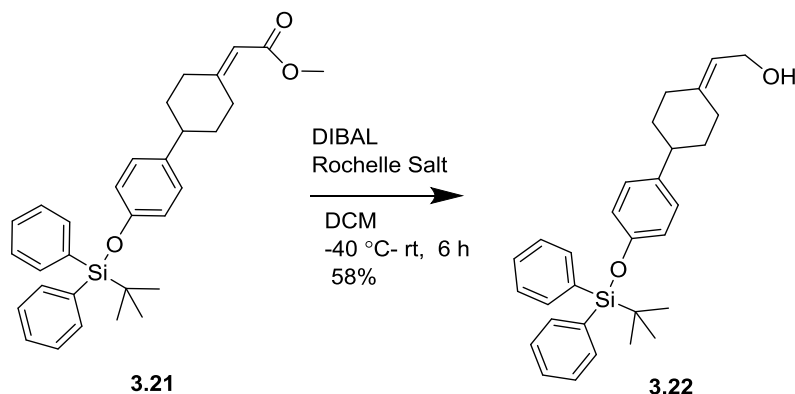


4-(4-(Hydroxymethyl)cyclohexyl)phenol (3.4a). To a solution of compound **3.20** (0.046 g, 0.23 mmol) in methanol (8 mL) was added 10% Pd/C (0.025 g, 10 mol %) and mixture was stirred under a balloon of H₂ at room temperature for 12 h. The reaction mixture was filtered through a pad of celite, and concentrated in vacuo to give **3.4a** (0.031g, 65%) as a colorless solid. The ¹H NMR spectrum showed the formation of a 3:2 (cis: trans) mixture of isomers.



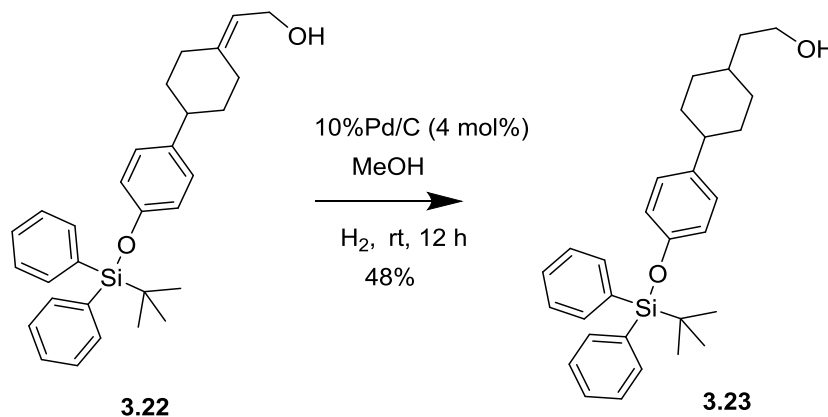
Methyl 2-(4-(4-((tert-butyl)diphenylsilyl)oxy)phenyl)cyclohexylidene)acetate (3.21). Sodium hydride (40 mg, 55% in mineral oil, 0.980 mmol) was added to a stirring solution of trimethyl phosphonoacetate (0.160 mL, 0.980 mmol) in dry THF (5 mL) at 0 °C. After 45 min, a solution of 4-(4'-t-butyl(diphenyl)silyloxyphenyl)cyclohexanone **3.2** (0.350 g,

0.818 mmol) in dry THF (5 mL) was added and the reaction mixture was stirred at room temperature for 8 h. The mixture was diluted with water (25 mL) and the resulting mixture was extracted with ether (2 × 30 mL), dried (MgSO₄) and concentrated. The residue was purified by column chromatography (SiO₂, hexanes–ethyl acetate = 90:10) to give compound **3.21** (0.376 g, 95%) as colorless gum. ¹H NMR (400 MHz, CDCl₃) δ 7.74–7.68 (m, 4H), 7.44–7.32 (m, 6H), 6.91 and 6.69 (AA'BB', J_{AB} = 8.6 Hz, 4H), 5.65 (s, 1H), 3.96–3.88 (m, 1H), 3.69 (s, 3H), 2.66 (tt, J = 12.1, 3.4 Hz, 1H), 2.38–2.24 (m, 2H), 2.04–1.93 (m, 3H), 1.59–1.46 (m, 2H), 1.08 (s, 9H) ppm. ¹³C NMR (100 MHz, CDCl₃) δ 167.4, 162.7, 154.0, 138.6, 135.7, 133.3, 130.0, 127.9, 127.5, 119.6, 113.3, 51.1, 43.3, 37.9, 35.9, 35.1, 29.7, 26.7, 19.7 ppm.

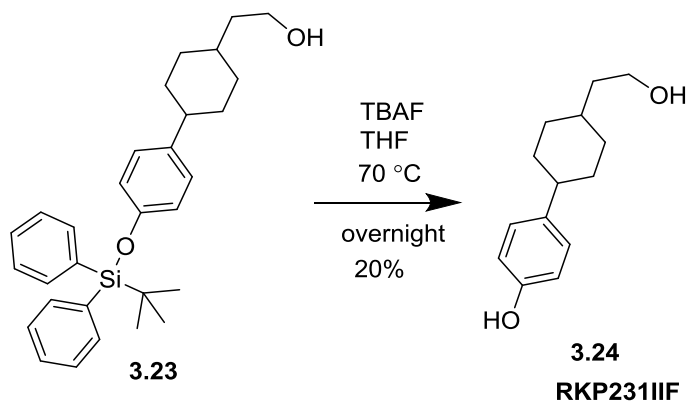


2-(4-(4-((tert-Butyldiphenylsilyl)oxy)phenyl)cyclohexylidene)ethan-1-ol (3.22). To a solution of **3.21** (0.109 g, 0.225 mmol) in dry CH₂Cl₂ (2 mL) under nitrogen at –40 °C was added a solution of diisobutylaluminum hydride (0.50 mL, 1.2 M in CH₂Cl₂, 0.60 mmol). After 90 min, saturated aqueous potassium sodium tartrate was added and reaction mixture was warmed to room temperature. After 4 h the mixture was filtered through a pad of celite and extracted several times with water (2 × 20 mL). The combined organic layers were

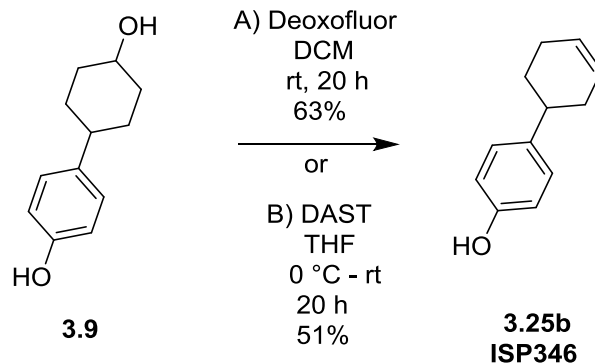
dried (MgSO_4), and concentrated to give **3.22** (0.059 g, 58%) as a colorless gum. This was used without further purification in the next step. ^1H NMR (400 MHz, CDCl_3) δ 7.72 (d, $J = 7.2$ Hz, 4H), 7.45-7.33 (m, 6H), 6.91 and 6.68 (AA'BB', $J_{\text{AB}} = 8.4$ Hz, 4H), 5.42 (t, $J = 7.2$ Hz, 1H), 4.17 (d, $J = 7.2$ Hz, 2H), 2.72 (br d, $J = 13.9$ Hz, 1H), 2.58 (tt, $J = 12.1, 3.2$ Hz, 1H), 2.37-2.26 (m, 1H), 2.23-2.13 (m, 1H), 1.97-1.85 (m, 3H), 1.51-1.34 (m, 2H), 1.08 (s, 9H) ppm. ^{13}C NMR (100 MHz, CDCl_3) δ 153.8, 143.4, 139.2, 135.7, 133.3, 130.0, 127.9, 127.5, 121.1, 119.6, 58.8, 43.8, 37.0, 35.9, 35.4, 28.7, 26.7, 19.6 ppm.



2-(4-(4-((tert-Butyldiphenylsilyloxy)phenyl)cyclohexyl)ethan-1-ol (3.23). To a solution of compound **45** (0.130 g, 0.285 mmol) in methanol (10 mL) was added, 10% Pd/C (0.012 g, 4 mol %). The reaction mixture was stirred under H_2 (30 psi) for 12 h. The reaction mixture was filtered through a pad of celite, and the solution was concentrated to give **3.23** (0.062 g, 48%) as a colorless oil. The product was used in the next step without further purification. ^1H NMR (400 MHz, CDCl_3) δ 7.79-7.72 (m, 4H), 7.47-7.35 (m, 6H), 6.99-6.92 (m, 2H), 6.76- 6.69 (m, 2H), 3.76-3.66 (m, 2H), 2.37 (t, $J = 12.5$ Hz, 1H), 2.27 (t, $J = 6.4$ Hz, 1H), 1.86 (d, $J = 11.2$ Hz, 3H), 1.73-1.56 (m, 3H), 1.56-1.49 (m, 1H), 1.48-1.27 (m, 3H), 1.13 (s, 9H) ppm. ^{13}C NMR (100 MHz, CDCl_3) δ 153.7, 140.2, 135.7, 133.3, 130.0, 127.9, 127.5, 119.4, 61.0, 43.7, 40.4, 34.5, 33.7, 30.3, 29.1, 26.7, 19.6 ppm.



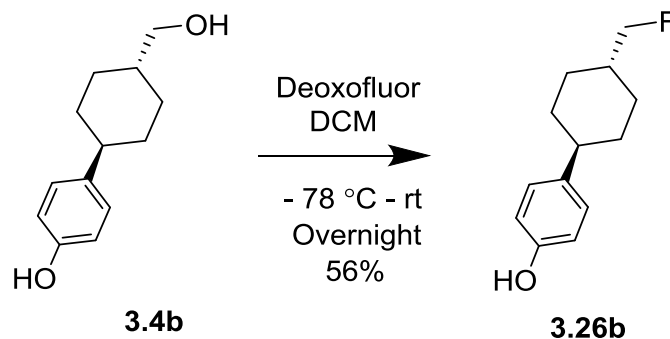
4-(4-(2-Hydroxyethyl)cyclohexyl)phenol (3.24). To a solution of **3.2** (0.063 g, 0.138 mmol) in anhydrous THF (8 mL) was added a solution of TBAF (1M in THF, 1.2 mL, 1.2 mmol) while stirring. The mixture was heated to reflux at 70 °C overnight and cooled to room temperature. The solution was partitioned between ethyl acetate and water. The organic layer was washed with brine, dried (Na₂SO₄) and concentrated. Purification by column chromatography (SiO₂, hexanes-ethyl acetate = 60:40) gave **3.24** (6 mg, 20%) as a colorless solid. mp 120-125 °C. ¹H NMR (300 MHz, (CD₃)₂CO) δ 8.02 (s, 1H), 7.08-7.01 (m, 2H), 6.77-6.71 (m, 2H), 3.65- 3.56 and 3.43-3.37 (m, 3H total), 2.52-2.33 (m, 1H), 1.91-1.00 (m, 11H) ppm.



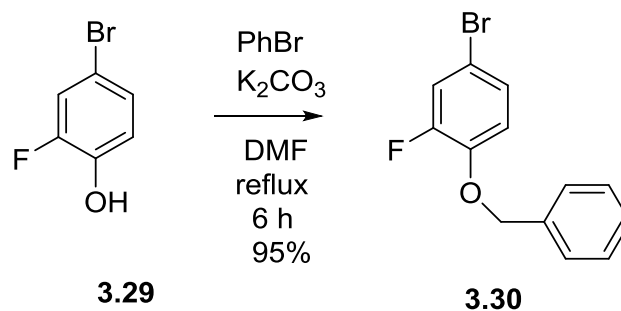
1',2',3',6'-tetrahydro-[1,1'-biphenyl]-4-ol (3.25b). Method A. To a solution of **3.9** (0.040 g, 0.21 mmol) in CH₂Cl₂ (10 mL) at room temperature under N₂ was added Deoxofluor (0.08 mL, 0.43 mmol) in CH₂Cl₂ (5 mL). The mixture was stirred for 20 h, after which saturated NaHCO₃ (10 mL) was poured into the mixture. After CO₂ evolution ceased the mixture was extracted into CH₂Cl₂ (2 × 20 mL). The combined extracts were dried (MgSO₄) and concentrated. The residue was purified by column chromatography (SiO₂, hexanes-ethyl acetate = 70:30) to give **3.25b** (0.023 g, 63%) as a colorless solid. mp 79-84 °C. ¹H NMR (400 MHz, CDCl₃) δ 7.12 and 6.80 (AA'BB', J_{AB} = 8.6 Hz, 4H), 5.79–5.76 (m, 2H), 4.92 (s, 1H), 2.81–2.71 (m, 1H), 2.32–2.07 (m, 4H), 1.95–1.88 (m, 1H), 1.78–1.66 (m, 1H) ppm. ¹³C NMR (100 MHz, CDCl₃) δ 153.8, 139.9, 128.1, 127.2, 127.0, 115.3, 39.4, 33.8, 30.2, 26.1 ppm.

Method B. To a solution of **3.9** (0.054 g, 0.28 mmol) in THF (20 mL) at room temperature under N₂ was added DAST (0.08 mL, 0.61 mmol) in THF (3 mL). The mixture was stirred for 20 h, then saturated NaHCO₃ (15 mL) was poured into the mixture. After CO₂ evolution ceased the mixture was extracted into ethyl acetate (2 × 10 mL). The combined extracts were dried (Na₂SO₄) and concentrated. The residue was purified by column chromatography (SiO₂, hexanes-ethyl acetate = 70:30) to give **3.25b** (0.025 g, 51%) as a

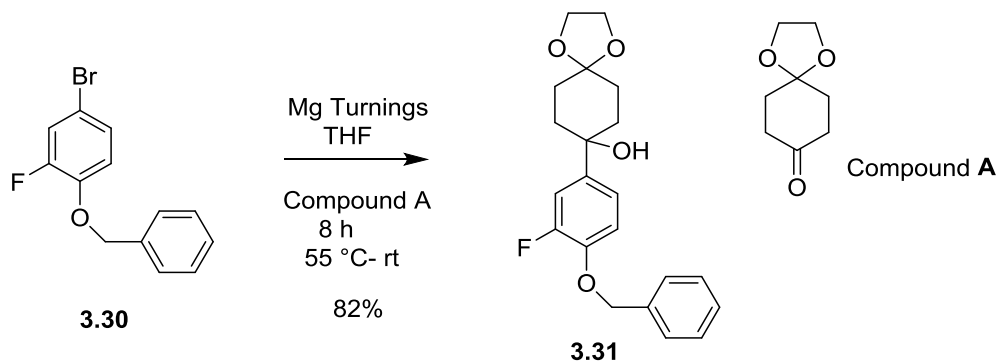
colorless solid. The NMR spectral data were consistent with the previously obtained values.



4-(4-(Fluoromethyl)cyclohexyl)phenol (3.26b). To a solution of **3.4b** (0.065 g, 0.315 mmol) in CH_2Cl_2 (12 mL) at $-78\text{ }^\circ\text{C}$ under N_2 was added a solution of Deoxofluor (0.09 mL, 0.473 mmol) in CH_2Cl_2 (3 mL). The mixture was gradually warmed to room temperature. On completion, saturated aqueous NaHCO_3 (10 mL) was poured in to the mixture and after CO_2 evolution ceased the mixture was extracted into CH_2Cl_2 (2×20 mL). The combined extracts were dried (Na_2SO_4) and concentrated. The residue was purified by column chromatography (SiO_2 , hexanes-ethyl acetate = 80:20) to give **3.26b** (0.037 g, 56%) as a colorless solid. mp $103\text{--}109\text{ }^\circ\text{C}$. ^1H NMR (400 MHz, CD_3OD) δ 7.00 and 6.68 (AA'BB', $J_{\text{AB}} = 8.5$ Hz, 4H), 4.23 (d, $J = 48.1$ Hz, 2H), 2.37 (tt, $J = 12.3, 2.8$ Hz, 1H), 1.90–1.80 (m, 4H), 1.78–1.59 (m, 2H), 1.52–1.37 (m, 2H), 1.24–1.09 (m, 2H) ppm. ^{13}C NMR (100 MHz, CD_3OD) δ 156.5, 139.7, 128.6, 116.0, 89.4 (d, $J = 166$ Hz), 44.9, 39.6 (d, $J = 17$ Hz), 35.0, 30.0, 29.9 ppm.

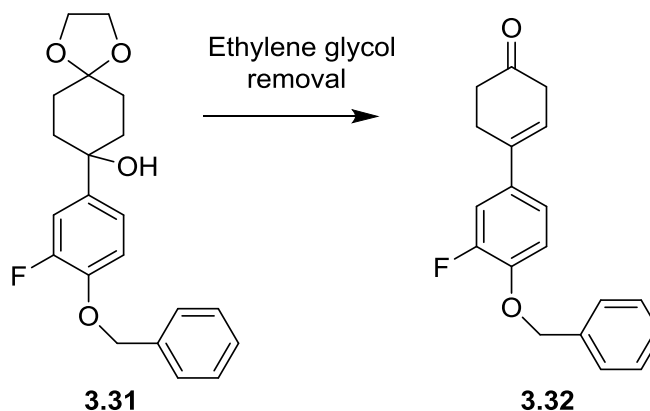


1-(benzyloxy)-4-bromo-2-fluorobenzene (3.3). To a solution of 4-bromo-2-fluorophenol **3.29** (1.00 g, 5.24 mmol) in DMF (8 mL), benzyl bromide (1.16 g, 0.81 mL, 6.81 mmol) and potassium carbonate (0.941 g, 6.81 mmol) were added and the mixture was heated at reflux for 6 h. After cooling to room temperature the mixture was poured into ice-cold water. The resulting mixture was partitioned with ethyl acetate (2 x 20 mL) and washed with brine (2 x 20 mL). The combined organic extracts were dried (Na_2SO_4), concentrated and purified by column chromatography (SiO_2 , hexanes -ethyl acetate = 90:10) to give **3.30** (1.397 g, 95%) as a colorless solid. mp 55-60 °C. ^1H NMR (400 MHz, CDCl_3) δ 7.47-7.32 (m, 5H), 7.26 (dd, $J = 10.6, 2.3$ Hz, 1H), 7.19-7.13 (m, 1H), 6.88 (t, $J = 8.7$ Hz, 1H), 5.13 (s, 2H) ppm. ^{13}C NMR (100 MHz, CDCl_3) δ 152.9 (d, $J_{\text{C-F}} = 250$ Hz), 146.3 (d, $J_{\text{C-F}} = 10$ Hz), 136.2, 128.9, 128.4, 127.6, 127.3, 120.0 (d, $J_{\text{C-F}} = 20$ Hz), 117.1, (d, $J_{\text{C-F}} = 10$ Hz), 112.8 (d, $J_{\text{C-F}} = 10$ Hz), 71.7 ppm. The NMR spectral data for this compound are consistent with the literature values.¹²¹



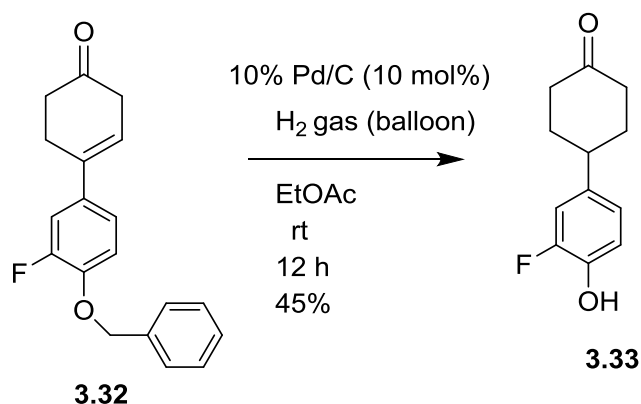
8-(4-(Benzyloxy)-3-fluorophenyl)-8-hydroxy-1,4-dioxaspiro[4.5]decane (3.31). Dry magnesium turnings (0.384 g, 0.016 mol) were placed in a flame dried three-necked flask followed by THF (10 mL). The system was flushed with N₂ and fitted with a REFLUX condenser and an addition funnel. The addition funnel was filled with a solution of **3.30** (0.900 g, 3.20 mmol) in THF (10 mL). A little amount of the bromobenzene solution (3 mL) was added slowly to the magnesium turnings, and the contents were heated at reflux. Once the Grignard formation had started, the remaining bromide solution was added dropwise and the mixture was stirred until most of the magnesium had reacted. A solution of 1,4-cyclohexanedione monoethylene acetal (0.250 g, 1.60 mmol) in THF (10 mL) was added dropwise over 20 min. After stirring overnight at room temperature, a saturated solution of NH₄Cl (15 mL) was slowly added to quench the reaction. The resultant emulsion was stirred for 15 min and the solution was extracted with ether (3 x 20 mL). The combined organic layers were washed with brine (20 mL), dried (MgSO₄) and concentrated. The residue was purified by column chromatography (SiO₂, hexanes-ethyl acetate = 70:30) to give **3.31** (0.470 g, 82%) as a colorless solid. mp 137-143 °C. ¹H NMR (400 MHz, CDCl₃) δ 7.46-7.28 (m, 5H), 7.26 (s, 1H), 7.18-7.12 (m, 1H), 6.95 (t, J = 8.4 Hz, 1H), 5.13 (s, 2H), 4.03-3.93 (m, 4H), 2.16-2.01 (m, 4H), 1.83-1.75 (m, 2H), 1.71-1.63

(m, 2H), ppm. ^{13}C NMR (100 MHz, CDCl_3) δ 152.7 (d, $J_{\text{C-F}} = 245$ Hz), 145.5 (d, $J_{\text{C-F}} = 13$ Hz), 142.6 (d, $J_{\text{C-F}} = 5$ Hz), 136.8, 128.8, 128.3, 127.6, 120.3 (d, $J_{\text{C-F}} = 4$ Hz), 115.4 (d, $J_{\text{C-F}} = 2$ Hz), 113.3 (d, $J_{\text{C-F}} = 20$ Hz), 108.5, 72.1, 71.5, 64.5, 64.4, 36.7, 30.9 ppm.



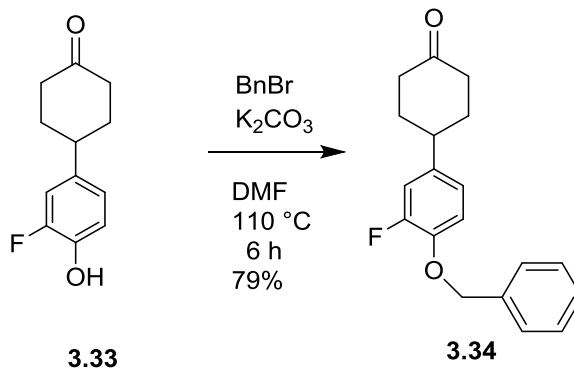
4-(4-Benzyloxy-3-fluorophenyl)-3-cyclohexanone (3.32). Method A: Compound **3.31** (0.100 g, 0.279 mmol) was dissolved in THF: Water-4:1 mixture (10 mL) to give a colorless solution. Then 2-3 drops of Conc sulfuric acid was slowly added and the mixture was heated at reflux for 5 h. After completion, the solution was diluted with brine and extracted with ethyl acetate (2 x 10 mL). The combined organic layers were washed with brine (20 mL), dried (Na_2SO_4) and concentrated. The residue was purified by column chromatography (SiO_2 , hexanes-ethyl acetate = 80:20) to give **3.32** (0.043 g, 52%) as a light yellow solid. mp 74-82 °C. ^1H NMR (400 MHz, CDCl_3) δ 7.50-7.30 (m, 5H), 7.16 (dd, $J = 12.6, 2.1$ Hz, 1H), 7.10-7.03 (m, 1H), 6.96 (t, $J = 8.6$ Hz, 1H), 6.02 (nr t, $J = 3.9$ Hz, 1H), 5.15 (s, 2H), 3.05 (br s, 2H), 2.82 (t, $J = 6.4$ Hz, 2H), 2.67-2.59 (m, 2H) ppm. ^{13}C NMR (100 MHz, CDCl_3) δ 210.0, 152.8 (d, $J_{\text{C-F}} = 245$ Hz), 146.1 (d, $J_{\text{C-F}} = 11$ Hz), 136.6, 136.3 (d, $J_{\text{C-F}} = 2$ Hz), 134.6 (d, $J_{\text{C-F}} = 6$ Hz), 128.8, 128.4, 127.6, 121.0 (d, $J_{\text{C-F}} = 3$ Hz), 120.7, 115.6 (d, $J_{\text{C-F}} = 2$ Hz), 113.4 (d, $J_{\text{C-F}} = 19$ Hz), 71.6, 40.0, 38.8, 27.9 ppm.

Method B: To a solution of **3.31** (1.189 g, 3.317 mmol) was dissolved in dry CH₂Cl₂ (20 mL) was added TFA (3.5 mL, 0.046 mol) and the mixture was stirred at room temperature for 4h while monitoring the reaction by TLC. Once completed, saturated aqueous NaHCO₃ (10 mL) was added and stirred for another 10 minutes. The resulting solution was extracted with CH₂Cl₂, washed with brine (10 mL), dried (Na₂SO₄) and concentrated. Purification of the crude material by column chromatography (SiO₂, hexanes-ethyl acetate = 80:20) gave **3.32** (0.883 g, 90%) as a light yellow solid.

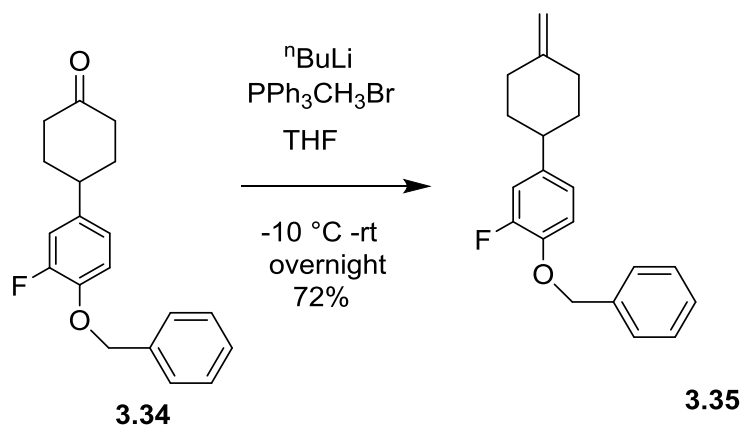


4-(3-Fluoro-4-hydroxyphenyl)cyclohexanone (3.33). To a solution of **3.32** (1.000 g, 3.374 mmol) in ethyl acetate (15 mL), was added 10% Pd/C (0.360 g, 10 mol %) and the mixture was stirred under a balloon of H₂ at room temperature for 12 h. The reaction mixture was filtered through a pad of celite, concentrated, and the residue was purified by column chromatography (SiO₂, hexanes-ethyl acetate = 60:40) to give **3.33** (0.315 g, 45%) as a colorless solid. mp 137-145 °C. ¹H NMR (400 MHz, CD₃OD) δ 6.97 (dd, J = 12.4, 2.1 Hz, 1H), 6.91-6.87 (m, 1H), 6.86-6.79 (m, 1H), 3.00 (tt, J = 12.1, 3.5 Hz, 1H), 2.58 (td, J = 14.0, 6.1 Hz, 2H), 2.41-2.33 (m, 2H), 2.19-2.10 (m, 2H), 1.86 (qd, J = 12.8, 4.2 Hz, 2H) ppm. ¹³C NMR (100 MHz, CD₃OD) δ 214.1, 152.8 (d, J_{C-F} = 240 Hz), 144.5 (d, J_{C-F}

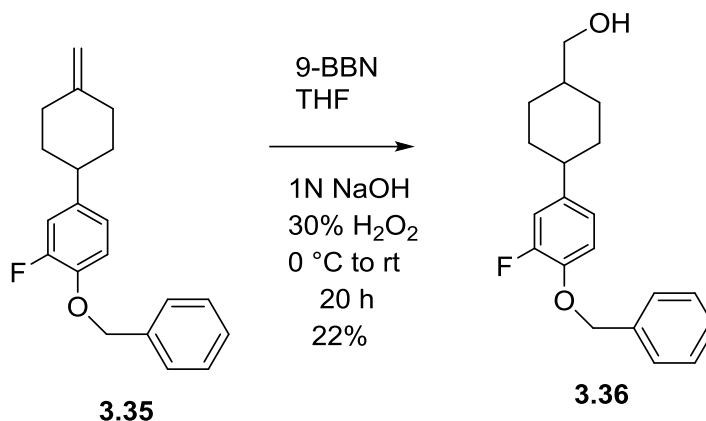
= 20 Hz), 138.6 (d, J_{C-F} = 10 Hz), 123.7 (d, J_{C-F} = 10 Hz), 118.7 (d, J_{C-F} = 10 Hz), 115.2 (d, J_{C-F} = 20 Hz), 42.8, 42.1, 35.3 ppm.



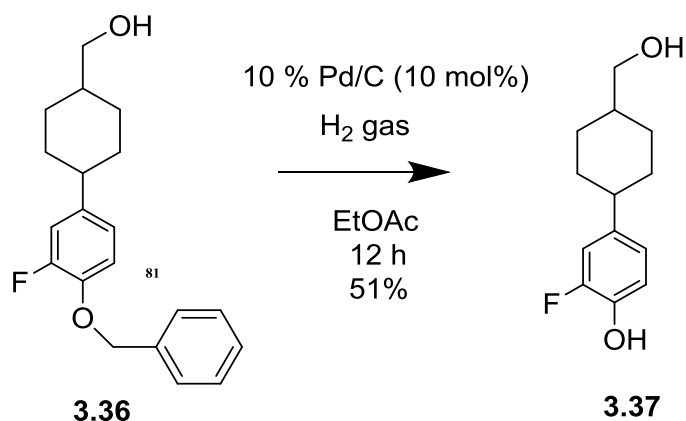
4-(4-(Benzyloxy)-3-fluorophenyl)cyclohexan-1-one (3.34). To a solution of **3.33** (0.205 g, 0.984 mmol) in DMF (10 mL), was added benzyl bromide (0.219 g, 0.15 mL, 1.28 mmol) and potassium carbonate (0.177 g, 1.28 mmol) and the mixture was heated at reflux for 6 h. After cooling to room temperature, the mixture was poured into ice-cold water. The mixture was extracted with ethyl acetate (2 x 15 mL) and the combined extracts were washed with brine (15 mL), dried (Na_2SO_4), and concentrated. Purification of the residue by column chromatography (SiO_2 , hexanes-ethyl acetate = 90:10) gave **3.34** (0.232 g, 79 %) as a colorless solid. mp 81-87 °C. ^1H NMR (400 MHz, CDCl_3) 7.49-7.29 (m, 5H), 7.02-6.88 (m, 3H), 5.11(s, 2H), 2.95 (tt, J = 12.2, 6.9 Hz, 1H), 2.51-2.43 (m, 3H), 2.22-2.13 (m, 2H), 1.92-1.79 (m, 2H) ppm. ^{13}C NMR (100 MHz, CDCl_3) δ 211.0, 152.9 (d, J_{C-F} = 240 Hz), 145.3 (d, J_{C-F} = 10 Hz), 138.7 (d, J_{C-F} = 10 Hz), 136.7, 128.7, 128.2, 127.5, 122.3 (d, J_{C-F} = 10 Hz), 115.9, 114.7 (d, J_{C-F} = 20 Hz), 71.6, 41.8, 41.3, 34.0 ppm



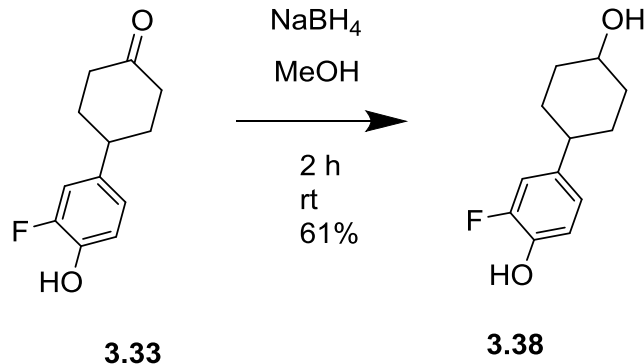
1-(Benzyloxy)-2-fluoro-4-(4-methylenecyclohexyl)benzene (3.35). A solution of n butyllithium in hexane (2.5 M, 0.47 mL, 1.17 mmol) was slowly added to a solution of methyltriphenylphosphonium bromide (0.556 g, 1.56 mmol) in dry THF (20 mL) at $-10\text{ }^\circ\text{C}$. After 20 min, a solution of **3.34** (0.232 g, 0.778 mmol) in dry THF (10 mL) was added dropwise. The reaction mixture was slowly warmed to room temperature and stirred overnight. The mixture was diluted with water (10 mL), extracted with ethyl acetate (2 \times 25 mL), dried (Na_2SO_4) and concentrated. The crude residue was purified by column chromatography (SiO_2 , hexanes-ethyl acetate = 90:10) to give **3.35** (0.165 g, 72 %) as a colorless solid. ^1H NMR (400 MHz, CDCl_3) 7.56-7.29 (m, 5H), 7.02-6.83 (m, 3H), 5.13 (s, 2H), 4.71 (s, 2H), 2.63 (tt, $J = 12.2, 3.3$ Hz, 1H), 2.49-2.37 (m, 2H), 2.27-2.12 (m, 2H), 2.04-1.92 (m, 2H), 1.57-1.43 (m, 2H) ppm. ^{13}C NMR (100 MHz, CDCl_3) δ 153.0 (d, $J_{\text{C-F}} = 250$ Hz), 148.6, 144.9, 141.0, 137.0, 133.9 (d, $J_{\text{C-F}} = 20$ Hz), 128.7, 128.2, 127.6, 122.3, 115.8, 114.9 (d, $J_{\text{C-F}} = 20$ Hz), 107.8, 71.7, 43.3, 35.7, 35.2 ppm.



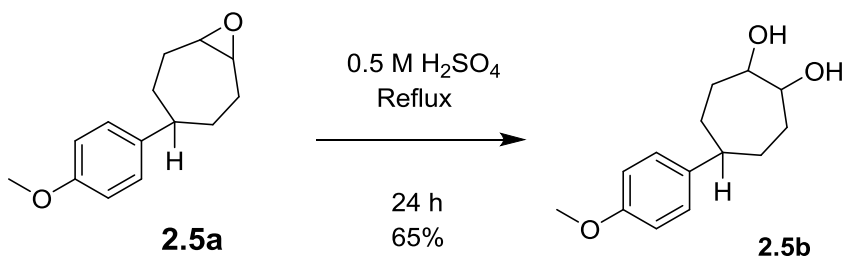
(4-(4-(Benzyloxy)-3-fluorophenyl)cyclohexyl)methanol (3.36). A solution of 9-BBN in THF (0.5 M, 1.46 mL, 0.729 mmol) was added to a solution of **3.35** (0.108 g, 0.364 mmol) in THF (15 mL) at 0 °C. The reaction mixture was slowly warmed to room temperature and stirred for 20 h. The mixture was cooled to 0 °C hydrogen peroxide solution (30% in water, 0.20 mL) and 1N NaOH solution (0.50 mL) was sequentially added. The resulting mixture was warmed to room temperature, stirred for 15 min and extracted with ethyl acetate (2 × 20 mL). The combined organic extracts were dried (Na₂SO₄), and concentrated. The residue was purified by column chromatography (SiO₂, hexanes-ethyl acetate = 60:40) to give **3.36** (0.025 g, 22%) as a colorless solid. This was determined to be a 1:2 mixture of cis- and trans-stereoisomers by ¹H NMR integration. ¹H NMR (400 MHz, CDCl₃) 7.50-7.28 (m, 5H), 7.01-6.80 (m, 3H), 5.11 (s, 2H), 3.67 (d, J = 7.9 Hz, 0.7H), 3.50 (d, J = 6.2 Hz, 1.3H), 2.60-2.50 (m, 0.3H), 2.47-2.36 (m, 0.7H), 1.98-1.33 (m, 8H), 1.17-1.03 (m, 1H) ppm. ¹³C NMR (100 MHz, CDCl₃) δ 154.2, 151.8, 144.8, 141.6, 137.0, 128.8, 128.2, 127.6, 122.4, 122.3, 115.9, 115.1, 114.9, 114.7, 71.8, 68.7, 64.6, 43.7, 42.2, 40.2, 36.2, 33.9, 29.8, 29.3, 26.8 ppm.



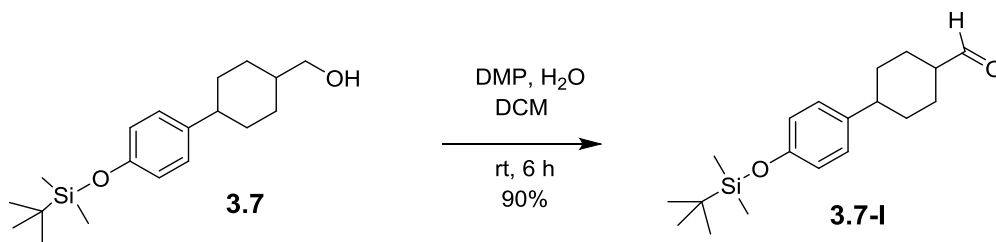
2-Fluoro-4-(4-(hydroxymethyl)cyclohexyl)phenol (3.37). To a solution of **3.36** (0.050 g, 0.159 mmol) in ethyl acetate (10 mL) was added 10% Pd/C (0.017 g, 10 mol %) and mixture was stirred under a balloon of H₂ at room temperature for 12 h. The reaction mixture was filtered through a pad of celite, concentrated, and the residue was purified by column chromatography (SiO₂, hexanes-ethyl acetate = 60:40) to give **3.37** (0.018 g, 51%) as a colorless solid. This was determined to be a 1:2 mixture of *cis*- and *trans*-stereoisomers by ¹H NMR integration. ¹H NMR (400 MHz, CD₃OD) 6.92-6.85 (m, 1H), 6.84-6.76 (m, 2H), 3.60 (d, J = 7.4 Hz, 0.7H), 3.39 (d, J = 6.5 Hz, 1.3H), 2.55-2.33 (m, 1H), 1.94-1.34 (m, 8H), 1.15-1.01 (m, 1H) ppm. ¹³C NMR (100 MHz, CD₃OD) δ 154.0, 151.6, 143.9, 141.1, 123.5, 118.5, 115.0, 68.8, 64.4, 45.0, 41.3, 37.1, 35.2, 31.0, 30.4, 29.5, 27.8 ppm.



2-Fluoro-4-(4-hydroxycyclohexyl)phenol (3.38). To a solution of **3.33** (0.033 g, 0.159 mmol) in anhydrous methanol (10 mL) was added NaBH₄ (0.090 g, 2.38 mmol). The mixture was stirred at room temperature for 2 h and then diluted with water. The resulting mixture was extracted with ethyl acetate (2× 15 mL), combined extracts were dried (Na₂SO₄) and concentrated. Purification of the crude material by column chromatography (SiO₂, hexanes-ethyl acetate = 65:35) gave the **3.38** (0.020 g, 61%) as a colorless solid. mp 179-186 °C. ¹H NMR (400 MHz, CD₃OD) δ 6.91-6.85 (m, 1H), 6.83-6.74 (m, 2H), 3.60-3.52 (m, 1H), 2.39 (tt, J = 12.0, 3.1 Hz, 1H), 2.05-1.96 (m, 2H), 1.88-1.79 (m, 2H), 1.52-1.20 (m, 4H) ppm. ¹³C NMR (100 MHz, CD₃OD) δ 152.8 (d, J_{C-F} = 240 Hz), 144.0 (d, J_{C-F} = 10 Hz), 140.3, 123.6, 118.5, 115.1 (d, J_{C-F} = 10 Hz), 71.1, 44.0, 36.6, 33.8 ppm.

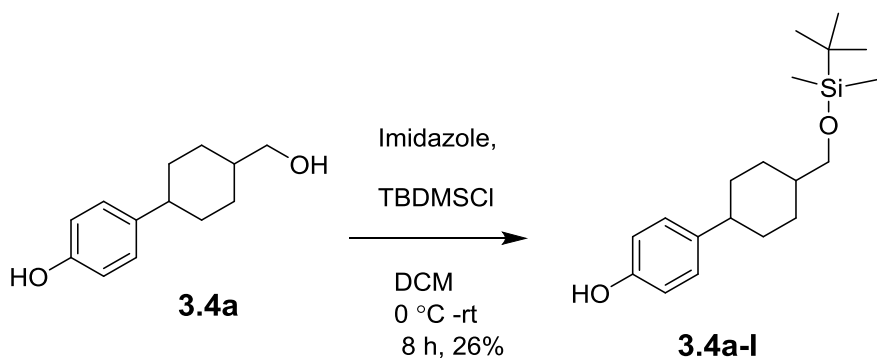


5-(4-Methoxyphenyl)-1,2-cycloheptanediol (2.5b). Epoxide **2.5a** (0.103 g, 0.469 mmol) was dissolved in 0.5 M sulfuric acid solution (50 mL) and heated to reflux for 24 h. The organic oil turned to a brown color and the mixture was allowed to cool and extracted with ether (3 × 30 mL). The combined ethereal extracts were washed with water (2 × 20 mL), dried (MgSO₄) and concentrated to give a crude residue. The residue was purified by column chromatography (SiO₂, ethyl acetate = 100%) to give **2.5b** (0.064g, 65%) as a colorless solid. mp 66-70 °C. ¹H NMR (400 MHz, CDCl₃) δ 7.08 and 6.82 (AA'BB', J_{AB} = 8.5 Hz, 4H), 3.79 (s, 3H), 3.67-3.51 (m, 2H), 2.92 (s, 2H), 2.69-2.60 (m, 1H), 2.02-1.77 (m, 6H), 1.68-1.54 (m, 2H) ppm. ¹³C NMR (400 MHz, CDCl₃) δ 157.8, 141.0, 127.4, 113.8, 78.5, 77.2, 55.3, 44.1, 33.2, 31.9, 30.8, 29.8 ppm



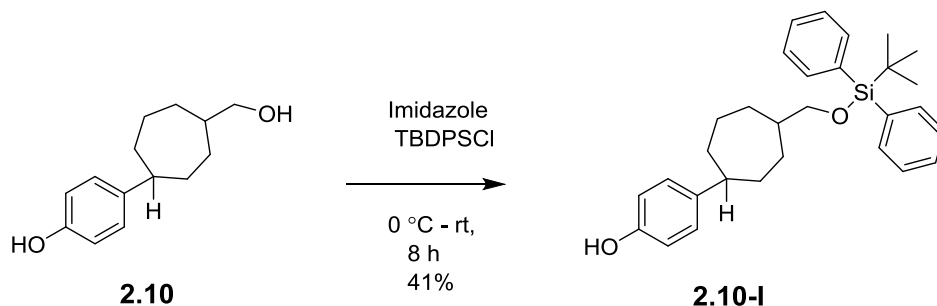
4-(4-((tert-Butyldimethylsilyloxy)phenyl)cyclohexane-1-carboxaldehyde (3.7-I). To a solution of **3.7** (0.315 g, 0.983 mmol) in CH₂Cl₂ (15 mL) at room temperature, was added Dess–Martin periodinane (0.625 g, 1.47 mmol) and water (10 drops) and mixture was

stirred at room temperature for 6 h. The mixture was quenched with 1:1 sodium thiosulfate:sodium bicarbonate solution. The resulting mixture was stirred at room temperature for 30 min, and extracted with ethyl acetate (2 x 20 mL), dried (MgSO₄), and concentrated to give the product **3.7-I** (0.282 g, 90%) as a mixture of stereoisomers. ¹H NMR (400 MHz, CDCl₃) δ 9.78 and 9.67 (2 x s, 1H total), 7.10-6.97 (m, 2H), 6.80-6.71 (m, 2H), 2.56-1.32 (m, 10H), 0.97 (s, 9H), 0.18 (s, 6H) ppm. ¹³C NMR (100 MHz, CDCl₃) δ 205.9, 153.9, 139.9, 127.8, 119.9, 46.5, 42.9, 42.8, 41.6, 33.6, 33.3, 31.1, 30.8, 29.4, 27.6, 26.6, 25.9, 25.2, 18.4, -4.2 ppm.



4-(4-(((tert-Butyldimethylsilyl)oxy)methyl)cyclohexyl)phenol (3.4a-I). To a solution of 4-(4-(hydroxymethyl)cyclohexyl)phenol **3.4a** (0.225 g, 1.09 mmol) in dry CH₂Cl₂ (30 ml) at 0 °C, was added imidazole (0.223 g, 3.27 mmol) and the mixture was stirred for a 30 min. A solution of t- butyldimethylsilyl chloride (0.115 g, 0.764 mmol) was added, and the mixture was slowly warmed to room temperature and stirred for 8 h. The mixture was diluted with water (20 mL) and extracted with CH₂Cl₂ (2 × 20 mL). The combined organic extracts were washed with brine, dried (Na₂SO₄), and concentrated. The residue was purified by column chromatography (SiO₂, hexanes-ethyl acetate = 90: 10) to give the product **3.4a-I** (0.090 g, 26%) as a colorless oil. ¹H NMR (400 MHz, CDCl₃) δ 7.14-7.04

(m, 2H), 6.82-6.73 (m, 2H), 5.14 (s, 1H), 3.67 (d, $J = 7.6$ Hz, 1.2 H), 3.49 (d, $J = 6.2$ Hz, 0.8H), 2.60-2.48 (m, 0.6 H), 2.41 (br t, $J = 11.5$ Hz, 0.4 H), 1.96-1.34 (m, 9H), 0.94 (s, 9H), 0.10 (s, 6H) ppm. ^{13}C NMR (100 MHz, CDCl_3) δ 153.8, 140.0, 139.6, 128.1, 115.3, 69.1, 64.9, 43.9, 42.5, 40.2, 35.8, 34.2, 30.1, 29.6, 26.9, 26.2, 18.6, -5.0 ppm.



4-(4-(((tert-Butyl)diphenylsilyloxy)methyl)cycloheptyl)phenol (2.10-I). To a solution of 4-(4-(hydroxymethyl)cycloheptyl)phenol **2.10** (0.158 g, 0.717 mmol) in dry CH_2Cl_2 (15 mL) at $0\text{ }^\circ\text{C}$, was added imidazole (0.122 g, 1.79 mmol). The mixture was stirred for 30 min and then a solution of *t*-butyldiphenylsilyl chloride (0.15 mL, 0.574 mmol) in CH_2Cl_2 (2 mL) was added. The mixture was slowly warmed to room temperature and stirred overnight. The mixture was diluted with brine (20 mL) and extracted with CH_2Cl_2 (2×20 mL). The combined organic extracts were dried (Na_2SO_4), and concentrated. The residue was purified by column chromatography (SiO_2 , hexanes-ethyl acetate = 80: 20) to give the product **2.10-I** (0.135 g, 41%) as a colorless oil. ^1H NMR (400 MHz, CDCl_3) δ 7.79-7.68 (m, 4H), 7.51-7.38 (m, 6H), 7.13-7.04 (m, 2H), 6.82-6.74 (m, 2H), 5.05 (s, 1H), 3.53 (s, 2H), 2.75-2.50 (m, 1H), 2.02-1.42 (m, 11H), 1.12 (s, 9H) ppm. ^{13}C NMR (100 MHz, CDCl_3) δ 153.4, 142.1, 135.8, 134.2, 129.7, 127.8, 115.3, 69.3, 69.1, 47.4, 46.2, 42.0, 41.1, 39.0, 36.9, 36.5, 33.0, 31.5, 30.6, 30.0, 28.5, 27.4, 24.3, 19.5 ppm.

REFERENCES

1. Bryant, H. U., Selective estrogen receptor modulators. *Rev. Endocr. Metab. Disord.* **2002**, *3* (3), 231-241.
2. Meegan, M. J.; Lloyd, D. G., Advances in the science of estrogen receptor modulation. *Curr. Med. Chem.* **2003**, *10* (3), 181-210.
3. Mueller, S. O.; Korach, K. S., Estrogen receptors and endocrine diseases: lessons from estrogen receptor knockout mice. *Curr. Opin. Pharmacol.* **2001**, *1* (6), 613-619.
4. Dey, P.; Barros, R. P. A.; Warner, M.; Strom, A.; Gustafsson, J.-A., Insight into the mechanisms of action of estrogen receptor β in the breast, prostate, colon, and CNS. *J. Mol. Endocrinol.* **2013**, *51* (3), T61-T74.
5. Jensen, E. V.; Suzuki, T.; Kawashima, T.; Stumpf, W. E.; Jungblut, P. W.; DeSombre, E. R., Two-step mechanism for the interaction of estradiol with rat uterus. *Proc. Nat. Acad. Sci. U. S.* **1968**, *59* (2), 632-8.
6. Nilsson, S.; Makela, S.; Treuter, E.; Tujague, M.; Thomsen, J.; Andersson, G.; Enmark, E.; Pettersson, K.; Warner, M.; Gustafsson, J.-A., Mechanisms of estrogen action. *Physiol. Rev.* **2001**, *81* (4), 1535-1565.
7. Koehler, K. F.; Helguero, L. A.; Haldosen, L.-A.; Warner, M.; Gustafsson, J.-A., Reflections on the discovery and significance of estrogen receptor β . *Endocr. Rev.* **2005**, *26* (3), 465-478.
8. Thomas, C.; Gustafsson, J.-A., The different roles of ER subtypes in cancer biology and therapy. *Nat. Rev. Cancer* **2011**, *11* (8), 597-608.
9. Malamas, M. S.; Manas, E. S.; McDevitt, R. E.; Gunawan, I.; Xu, Z. B.; Collini, M. D.; Miller, C. P.; Dinh, T.; Henderson, R. A.; Keith, J. C., Jr.; Harris, H. A., Design and Synthesis of Aryl Diphenolic Azoles as Potent and Selective Estrogen Receptor- β Ligands. *J. Med. Chem.* **2004**, *47* (21), 5021-5040.
10. De Angelis, M.; Stossi, F.; Carlson, K. A.; Katzenellenbogen, B. S.; Katzenellenbogen, J. A., Indazole Estrogens: Highly Selective Ligands for the Estrogen Receptor β . *J. Med. Chem.* **2005**, *48* (4), 1132-1144.
11. Yonekubo, S.; Fushimi, N.; Miyagi, T.; Nakanishi, O.; Katsuno, K.; Ozawa, M.; Handa, C.; Furuya, N.; Muranaka, H., Synthesis and structure-activity relationships of 1-benzylindane derivatives as selective agonists for estrogen receptor beta. *Bioorg. Med. Chem.* **2016**, *24* (22), 5895-5910.

12. Hartman, J.; Stroem, A.; Gustafsson, J.-A., Estrogen receptor beta in breast cancer-Diagnostic and therapeutic implications. *Steroids* **2009**, *74* (8), 635-641.
13. Nilsson, S.; Gustafsson, J. A., Estrogen Receptors: Therapies Targeted to Receptor Subtypes. *Clin. Pharmacol. Ther. (N. Y., NY, U. S.)* **2011**, *89* (1), 44-55.
14. Warner, M.; Huang, B.; Gustafsson, J.-A., Estrogen Receptor β as a Pharmaceutical Target. *Trends Pharmacol. Sci.* **2017**, *38* (1), 92-99.
15. American Cancer Society. *Cancer Facts & Figures 2009*. Atlanta: American Cancer Society; 2009.; 2009; pp 1-72.
16. Jiang, X.-R.; Wang, P.; Smith, C. L.; Zhu, B. T., Synthesis of Novel Estrogen Receptor Antagonists Using Metal-Catalyzed Coupling Reactions and Characterization of Their Biological Activity. *J. Med. Chem.* **2013**, *56* (7), 2779-2790.
17. Lv, W.; Liu, J.; Lu, D.; Flockhart, D. A.; Cushman, M., Synthesis of Mixed (E,Z)-, (E)-, and (Z)-Norendoxifen with Dual Aromatase Inhibitory and Estrogen Receptor Modulatory Activities. *J. Med. Chem.* **2013**, *56* (11), 4611-4618.
18. Musgrove, E. A.; Sutherland, R. L., Biological determinants of endocrine resistance in breast cancer. *Nat. Rev. Cancer* **2009**, *9* (9), 631-643.
19. Fabian, C.; Tilzer, L.; Sternson, L., Comparative binding affinities of tamoxifen, 4-hydroxytamoxifen, and desmethyltamoxifen for estrogen receptors isolated from human breast carcinoma: correlation with blood levels in patients with metastatic breast cancer. *Biopharm Drug Dispos* **1981**, *2* (4), 381-90.
20. Butt, A. J.; McNeil, C. M.; Musgrove, E. A.; Sutherland, R. L., Downstream targets of growth factor and estrogen signalling and endocrine resistance: the potential roles of c-Myc, cyclin D1 and cyclin E. *Endocr.-Relat. Cancer* **2005**, *12* (Suppl. 1), S47-S59.
21. Nazarali, S. A.; Narod, S. A., Tamoxifen for women at high risk of breast cancer. *Breast Cancer: Targets Ther.* **2014**, *6*, 29-36, 8 pp.
22. Dey, P.; Jonsson, P.; Hartman, J.; Williams, C.; Strom, A.; Gustafsson, J.-A., Estrogen receptors β 1 and β 2 have opposing roles in regulating proliferation and bone metastasis genes in the prostate cancer cell line PC3. *Mol. Endocrinol.* **2012**, *26* (12), 1991-2003.
23. Deroo, B. J.; Korach, K. S., Estrogen receptors and human disease. *J. Clin. Invest.* **2006**, *116* (3), 561-570.
24. Couse, J. F.; Korach, K. S., Estrogen receptor null mice: what have we learned and where will they lead us? *Endocr. Rev.* **1999**, *20* (3), 358-417.

25. Windahl, S. H.; Vidal, O.; Andersson, G.; Gustafsson, J. A.; Ohlsson, C., Increased cortical bone mineral content but unchanged trabecular bone mineral density in female ER β -/- mice. *J. Clin. Invest.* **1999**, *104* (7), 895-901.
26. Vidal, O.; Lindberg, M. K.; Hollberg, K.; Baylink, D. J.; Andersson, G.; Lubahn, D. B.; Mohan, S.; Gustafsson, J.-A.; Ohlsson, C., Estrogen receptor specificity in the regulation of skeletal growth and maturation in male mice. *Proc. Natl. Acad. Sci. U. S. A.* **2000**, *97* (10), 5474-5479.
27. Dubal, D. B.; Zhu, H.; Yu, J.; Rau, S. W.; Shughrue, P. J.; Merchenthaler, I.; Kindy, M. S.; Wise, P. M., Estrogen receptor α , not β , is a critical link in estradiol-mediated protection against brain injury. *Proc. Natl. Acad. Sci. U. S. A.* **2001**, *98* (4), 1952-1957.
28. Sampei, K.; Goto, S.; Alkayed, N. J.; Crain, B. J.; Korach, K. S.; Traystman, R. J.; Demas, G. E.; Nelson, R. J.; Hurn, P. D., Stroke in estrogen receptor- α -deficient mice. *Stroke* **2000**, *31* (3), 738-744.
29. Wang, L.; Andersson, S.; Warner, M.; Gustafsson, J.-A., Morphological abnormalities in the brains of estrogen receptor β knockout mice. *Proc. Natl. Acad. Sci. U. S. A.* **2001**, *98* (5), 2792-2796.
30. Zhao, L.; Woody, S. K.; Chhibber, A., Estrogen receptor β in Alzheimer's disease: From mechanisms to therapeutics. *Ageing Res. Rev.* **2015**, *24* (Part_B), 178-190.
31. Frick, K. M., Building a better hormone therapy?: how understanding the rapid effects of sex steroid hormones could lead to new therapeutics for age-related memory decline. *Behav. Neurosci.* **2012**, *126* (1), 29-53.
32. Liu, F.; Day, M.; Muniz, L. C.; Bitran, D.; Arias, R.; Revilla-Sanchez, R.; Grauer, S.; Zhang, G.; Kelley, C.; Pulito, V.; Sung, A.; Mervis, R. F.; Navarra, R.; Hirst, W. D.; Reinhart, P. H.; Marquis, K. L.; Moss, S. J.; Pangalos, M. N.; Brandon, N. J., Activation of estrogen receptor- β regulates hippocampal synaptic plasticity and improves memory. *Nat. Neurosci.* **2008**, *11* (3), 334-343.
33. Frick, K. M., Molecular mechanisms underlying the memory-enhancing effects of estradiol. *Horm. Behav.* **2015**, *74*, 4-18.
34. Day, M.; Sung, A.; Logue, S.; Bowlby, M.; Arias, R., Beta estrogen receptor knockout (BERKO) mice present attenuated hippocampal CA1 long-term potentiation and related memory deficits in contextual fear conditioning. *Behav. Brain Res.* **2005**, *164* (1), 128-131.
35. Rissman, E. F.; Heck, A. L.; Leonard, J. E.; Shupnik, M. A.; Gustafsson, J.-A., Disruption of estrogen receptor β gene impairs spatial learning in female mice. *Proc. Natl. Acad. Sci. U. S. A.* **2002**, *99* (6), 3996-4001.

36. Fugger, H. N.; Foster, T. C.; Gustafsson, J. A.; Rissman, E. F., Novel effects of estradiol and estrogen receptor α and β on cognitive function. *Brain Res.* **2000**, 883 (2), 258-264.
37. Foster, T. C.; Rani, A.; Kumar, A.; Cui, L.; Semple-Rowland, S. L., Viral vector-mediated delivery of estrogen receptor- α to the hippocampus improves spatial learning in estrogen receptor- α knockout mice. *Mol. Ther.* **2008**, 16 (9), 1587-1593.
38. Walf, A. A.; Koonce, C.; Manley, K.; Frye, C. A., Proestrous compared to diestrous wildtype, but not estrogen receptor beta knockout, mice have better performance in the spontaneous alternation and object recognition tasks and reduced anxiety-like behavior in the elevated plus and mirror maze. *Behav. Brain Res.* **2009**, 196 (2), 254-260.
39. Walf, A. A.; Koonce, C. J.; Frye, C. A., Estradiol or diarylpropionitrile administration to wild type, but not estrogen receptor beta knockout, mice enhances performance in the object recognition and object placement tasks. *Neurobiol. Learn. Mem.* **2008**, 89 (4), 513-521.
40. Gann, P. H.; Morrow, M., Combined hormone therapy and breast cancer: a single-edged sword. *JAMA* **2003**, 289 (24), 3304-6.
41. Stanford, J. L.; Weiss, N. S.; Voigt, L. F.; Daling, J. R.; Habel, L. A.; Rossing, M. A., Combined estrogen and progestin hormone replacement therapy in relation to risk of breast cancer in middle-aged women. *JAMA* **1995**, 274 (2), 137-42.
42. Hermsmeyer, R. K.; Kaski, J. C.; Thompson, T. L., Breast cancer in postmenopausal women after hormone therapy. *JAMA, J. Am. Med. Assoc.* **2011**, 305 (5), 466.
43. Shumaker, S. A.; Legault, C.; Kuller, L.; Rapp, S. R.; Thai, L.; Lane, D. S.; Fillit, H.; Stefanick, M. L.; Hendrix, S. L.; Lewis, C. E.; Masaki, K.; Coker, L. H.; Wassertheil-Smoller, S.; Hays, J.; Manson, J.; Assaf, A. R.; Phillips, L.; Hsia, J.; Chlebowski, R.; Caan, B.; Kotchen, J. M.; Passaro, M.; Van Horn, L.; Powell, L.; Jackson, R.; Bassford, T.; Trevisan, M.; Robbins, J.; Hubbell, A.; Judd, H.; Langer, R. D.; Gass, M.; Limacher, M.; Curb, D.; Wallace, R.; Ockene, J.; Lasser, N.; Margolis, K.; Brunner, R.; Murphy, C.; Royall, D.; Allen, C.; Vitolins, M.; Colenda, C.; Albert, M.; Sherwin, B. B.; Henderson, V.; Birge, S.; Alving, B.; Rossouw, J.; Pottern, L.; Prentice, R.; Anderson, G.; LaCroix, A.; Patterson, R. E.; McTiernan, A.; Rautaharju, P.; Stein, E.; Cummings, S.; Himes, J.; Psaty, B.; Beresford, S.; Ritenbaugh, C.; Howard, B. V.; Black, H.; Wactawski-Wende, J.; O'Sullivan, M. J.; Heiss, G.; Johnson, K. C.; Brzyski, R.; Sarto, G.; Bonds, D., Conjugated equine estrogens and incidence of probable dementia and mild cognitive impairment in postmenopausal women. Women's Health Initiative Memory Study. *JAMA, J. Am. Med. Assoc.* **2004**, 291 (24), 2947-2958.
44. Cavalieri, E.; Chakravarti, D.; Guttenplan, J.; Hart, E.; Ingle, J.; Jankowiak, R.; Muti, P.; Rogan, E.; Russo, J.; Santen, R.; Sutter, T., Catechol estrogen quinones as

initiators of breast and other human cancers: Implications for biomarkers of susceptibility and cancer prevention. *Biochim. Biophys. Acta, Rev. Cancer* **2006**, 1766 (1), 63-78.

45. Sarabia, S. F.; Zhu, B. T.; Kurosawa, T.; Tohma, M.; Liehr, J. G., Mechanism of Cytochrome P450-Catalyzed Aromatic Hydroxylation of Estrogens. *Chem. Res. Toxicol.* **1997**, 10 (7), 767-771.

46. Zhang, F.; Chen, Y.; Pisha, E.; Shen, L.; Xiong, Y.; van Breemen, R. B.; Bolton, J. L., The Major Metabolite of Equilin, 4-Hydroxyequilin, Autoxidizes to an o-Quinone Which Isomerizes to the Potent Cytotoxin 4-Hydroxyequilenin-o-quinone. *Chem. Res. Toxicol.* **1999**, 12 (2), 204-213.

47. Wright, J. S.; Shadnia, H.; Anderson, J. M.; Durst, T.; Asim, M.; El-Salfiti, M.; Choueiri, C.; Pratt, M. A. C.; Ruddy, S. C.; Lau, R.; Carlson, K. E.; Katzenellenbogen, J. A.; O'Brien, P. J.; Wan, L., A-CD Estrogens. I. Substituent Effects, Hormone Potency, and Receptor Subtype Selectivity in a New Family of Flexible Estrogenic Compounds. *J. Med. Chem.* **2011**, 54 (2), 433-448.

48. Michalsen, B. T.; Gherezghiher, T. B.; Choi, J.; Chandrasena, R. E. P.; Qin, Z.; Thatcher, G. R. J.; Bolton, J. L., Selective Estrogen Receptor Modulator (SERM) Lasofoxifene Forms Reactive Quinones Similar to Estradiol. *Chem. Res. Toxicol.* **2012**, 25 (7), 1472-1483.

49. Fan, L.; Zhao, Z.; Orr, P. T.; Chambers, C. H.; Lewis, M. C.; Frick, K. M., Estradiol-induced object memory consolidation in middle-aged female mice requires dorsal hippocampal extracellular signal-regulated kinase and phosphatidylinositol 3-kinase activation. *J. Neurosci.* **2010**, 30 (12), 4390-4400.

50. Fernandez, S. M.; Lewis, M. C.; Pechenino, A. S.; Harburger, L. L.; Orr, P. T.; Gresack, J. E.; Schafe, G. E.; Frick, K. M., Estradiol-induced enhancement of object memory consolidation involves hippocampal extracellular signal-regulated kinase activation and membrane-bound estrogen receptors. *J. Neurosci.* **2008**, 28 (35), 8660-8667.

51. Cano, A., Alsina, J.C., Duenaz-Diez, J. L., *Selective Estrogen Receptor Modulators*. Springer: 2006.

52. Katzenellenbogen, B. S.; Choi, I.; Delage-Mourroux, R.; Ediger, T. R.; Martini, P. G. V.; Montano, M.; Sun, J.; Weis, K.; Katzenellenbogen, J. A., Molecular mechanisms of estrogen action: selective ligands and receptor pharmacology. *J. Steroid Biochem. Mol. Biol.* **2000**, 74 (5), 279-285.

53. Brinton, R. D., Cellular and molecular mechanisms of estrogen regulation of memory function and neuroprotection against Alzheimer's disease: recent insights and remaining challenges. *Learn Mem* **2001**, 8 (3), 121-33.

54. Bjoernstroem, L.; Sjoeborg, M., Mechanisms of estrogen receptor signaling: convergence of genomic and nongenomic actions on target genes. *Mol. Endocrinol.* **2005**, *19* (4), 833-842.
55. Harrington, W. R.; Sheng, S.; Barnett, D. H.; Petz, L. N.; Katzenellenbogen, J. A.; Katzenellenbogen, B. S., Activities of estrogen receptor alpha- and beta-selective ligands at diverse estrogen responsive gene sites mediating transactivation or transrepression. *Mol. Cell. Endocrinol.* **2003**, *206* (1-2), 13-22.
56. Tanenbaum, D. M.; Wang, Y.; Williams, S. P.; Sigler, P. B., Crystallographic comparison of the estrogen and progesterone receptor's ligand binding domains. *Proc. Natl. Acad. Sci. U. S. A.* **1998**, *95* (11), 5998-6003.
57. van Lipzig, M. M. H.; Ter Laak, A. M.; Jongejan, A.; Vermeulen, N. P. E.; Wamelink, M.; Geerke, D.; Meerman, J. H. N., Prediction of ligand binding affinity and orientation of xenoestrogens to the estrogen receptor by molecular dynamics simulations and the linear interaction energy method. *J. Med. Chem.* **2004**, *47* (4), 1018-1030.
58. Bertini, S.; De Cupertinis, A.; Granchi, C.; Bargagli, B.; Tuccinardi, T.; Martinelli, A.; Macchia, M.; Gunther, J. R.; Carlson, K. E.; Katzenellenbogen, J. A.; Minutolo, F., Selective and potent agonists for estrogen receptor beta derived from molecular refinements of salicylaldoximes. *Eur. J. Med. Chem.* **2011**, *46* (6), 2453-2462.
59. Ohta, K.; Ogawa, T.; Oda, A.; Kaise, A.; Endo, Y., Design and synthesis of carborane-containing estrogen receptor-beta (ER β)-selective ligands. *Bioorg. Med. Chem. Lett.* **2015**, *25* (19), 4174-4178.
60. Minutolo, F.; Macchia, M.; Katzenellenbogen, B. S.; Katzenellenbogen, J. A., Estrogen receptor β ligands: Recent advances and biomedical applications. *Med. Res. Rev.* **2011**, *31* (3), 364-442.
61. Dao, K.-L.; Hanson, R. N., Targeting the Estrogen Receptor using Steroid-Therapeutic Drug Conjugates (Hybrids). *Bioconjugate Chem.* **2012**, *23* (11), 2139-2158.
62. Brzozowski, A. M.; Pike, A. C. W.; Dauter, Z.; Hubbard, R. E.; Bonn, T.; Engstrom, O.; Ohman, L.; Greene, G. L.; Gustafsson, J.-A.; Carlquist, M., Molecular basis of agonism and antagonism in the estrogen receptor. *Nature (London)* **1997**, *389* (6652), 753-758.
63. Maximov, P. Y.; Lee, T. M.; Jordan, V. C., The discovery and development of selective estrogen receptor modulators (SERMs) for clinical practice. *Curr. Clin. Pharmacol.* **2013**, *8* (2), 135-155.
64. Pike, A. C. W.; Brzozowski, A. M.; Hubbard, R. E.; Bonn, T.; Thorsell, A.-G.; Engstrom, O.; Ljunggren, J.; Gustafsson, J.-A.; Carlquist, M., Structure of the ligand-

binding domain of oestrogen receptor beta in the presence of a partial agonist and a full antagonist. *EMBO J.* **1999**, *18* (17), 4608-4618.

65. Kuiper, G. G. J. M.; Lemmen, J. G.; Carlsson, B.; Corton, J. C.; Safe, S. H.; Van Der Saag, P. T.; Van Der Burg, B.; Gustafsson, J.-A., Interaction of estrogenic chemicals and phytoestrogens with estrogen receptor β . *Endocrinology* **1998**, *139* (10), 4252-4263.

66. Mersereau, J. E.; Levy, N.; Staub, R. E.; Baggett, S.; Zogric, T.; Chow, S.; Ricke, W. A.; Tagliaferri, M.; Cohen, I.; Bjeldanes, L. F.; Leitman, D. C., Liguiritigenin is a plant-derived highly selective estrogen receptor β agonist. *Mol. Cell. Endocrinol.* **2008**, *283* (1-2), 49-57.

67. Mallavadhani, U. V.; Narasimhan, K.; Sudhakar, A. V. S.; Mahapatra, A.; Li, W.; van Breemen, R. B., Three new pentacyclic triterpenes and some flavonoids from the fruits of an Indian ayurvedic plant *Dendrophthoe falcata* and their estrogen receptor binding activity. *Chem. Pharm. Bull.* **2006**, *54* (5), 740-744.

68. Meyers, M. J.; Sun, J.; Carlson, K. E.; Marriner, G. A.; Katzenellenbogen, B. S.; Katzenellenbogen, J. A., Estrogen Receptor- β Potency-Selective Ligands: Structure-Activity Relationship Studies of Diarylpropionitriles and Their Acetylene and Polar Analogues. *J. Med. Chem.* **2001**, *44* (24), 4230-4251.

69. Boulware, M. I.; Heisler, J. D.; Frick, K. M., The memory-enhancing effects of hippocampal estrogen receptor activation involve metabotropic glutamate receptor signaling. *J. Neurosci.* **2013**, *33* (38), 15184-15194.

70. Pereira, L. M.; Bastos, C. P.; de Souza, J. M.; Ribeiro, F. M.; Pereira, G. S., Estradiol enhances object recognition memory in Swiss female mice by activating hippocampal estrogen receptor α . *Neurobiol. Learn. Mem.* **2014**, *114*, 1-9.

71. Weiser, M. J.; Wu, T. J.; Handa, R. J., Estrogen receptor- β agonist diarylpropionitrile: biological activities of R- and S-enantiomers on behavior and hormonal response to stress. *Endocrinology* **2009**, *150* (4), 1817-1825.

72. Carroll, V. M.; Jeyakumar, M.; Carlson, K. E.; Katzenellenbogen, J. A., Diarylpropionitrile (DPN) Enantiomers: Synthesis and Evaluation of Estrogen Receptor β -Selective Ligands. *J. Med. Chem.* **2012**, *55* (1), 528-537.

73. Sun, J.; Baudry, J.; Katzenellenbogen, J. A.; Katzenellenbogen, B. S., Molecular basis for the subtype discrimination of the estrogen receptor- β -selective ligand, diarylpropionitrile. *Mol. Endocrinol.* **2003**, *17* (2), 247-258.

74. Manas, E. S.; Unwalla, R. J.; Xu, Z. B.; Malamas, M. S.; Miller, C. P.; Harris, H. A.; Hsiao, C.; Akopian, T.; Hum, W.-T.; Malakian, K.; Wolfrom, S.; Bapat, A.; Bhat, R. A.; Stahl, M. L.; Somers, W. S.; Alvarez, J. C., Structure-Based Design of Estrogen Receptor- β Selective Ligands. *J. Am. Chem. Soc.* **2004**, *126* (46), 15106-15119.

75. Harris, H. A.; Albert, L. M.; Leathurby, Y.; Malamas, M. S.; Mewshaw, R. E.; Miller, C. P.; Kharode, Y. P.; Marzolf, J.; Komm, B. S.; Winneker, R. C.; Frail, D. E.; Henderson, R. A.; Zhu, Y.; Keith, J. C., Jr., Evaluation of an estrogen receptor- β agonist in animal models of human disease. *Endocrinology* **2003**, *144* (10), 4241-4249.
76. Richardson, T. I.; Norman, B. H.; Lugar, C. W.; Jones, S. A.; Wang, Y.; Durbin, J. D.; Krishnan, V.; Dodge, J. A., Benzopyrans as sladitudinarianeective estrogen receptor β agonists (SERBAs). Part 2: Structure-activity relationship studies on the benzopyran scaffold. *Bioorg. Med. Chem. Lett.* **2007**, *17* (13), 3570-3574.
77. Norman, B. H.; Dodge, J. A.; Richardson, T. I.; Borromeo, P. S.; Lugar, C. W.; Jones, S. A.; Chen, K.; Wang, Y.; Durst, G. L.; Barr, R. J.; Montrose-Rafizadeh, C.; Osborne, H. E.; Amos, R. M.; Guo, S.; Boodhoo, A.; Krishnan, V., Benzopyrans Are Selective Estrogen Receptor β Agonists with Novel Activity in Models of Benign Prostatic Hyperplasia. *J. Med. Chem.* **2006**, *49* (21), 6155-6157.
78. Asim, M.; El-Salfiti, M.; Qian, Y.; Choueiri, C.; Salari, S.; Cheng, J.; Shadnia, H.; Bal, M.; Christine Pratt, M. A.; Carlson, K. E.; Katzenellenbogen, J. A.; Wright, J. S.; Durst, T., Deconstructing estradiol: Removal of B-ring generates compounds which are potent and subtype-selective estrogen receptor agonists. *Bioorg. Med. Chem. Lett.* **2009**, *19* (4), 1250-1253.
79. Asim, M.; El-Salfiti, M.; Qian, Y.; Choueiri, C.; Salari, S.; Cheng, J.; Shadnia, H.; Bal, M.; Christine Pratt, M. A.; Carlson, K. E.; Katzenellenbogen, J. A.; Wright, J. S.; Durst, T., Deconstructing estradiol: Removal of B-ring generates compounds which are potent and subtype-selective estrogen receptor agonists. [Erratum to document cited in CA150:423383]. *Bioorg. Med. Chem. Lett.* **2010**, *20* (22), 6861-6862.
80. Dabrota, C.; Asim, M.; Choueiri, C.; Gargaun, A.; Korobkov, I.; Butt, A.; Carlson, K. E.; Katzenellenbogen, J. A.; Wright, J. S.; Durst, T., Synthesis and receptor binding in trans-CD ring-fused A-CD estrogens: Comparison with the cis-fused isomers. *Bioorg. Med. Chem. Lett.* **2014**, *24* (16), 3841-3844.
81. McCullough, C.; Neumann, T. S.; Gone, J. R.; He, Z.; Herrild, C.; Wondergem, J.; Pandey, R. K.; Donaldson, W. A.; Sem, D. S., Probing the human estrogen receptor- α binding requirements for phenolic mono- and di-hydroxyl compounds: A combined synthesis, binding and docking study. *Bioorg. Med. Chem.* **2014**, *22* (1), 303-310.
82. Pandey, R. K.; Wang, L.; Wallock, N. J.; Lindeman, S.; Donaldson, W. A., Reactivity of (2-Alkenyl-3-pentene-1,5-diyl)iron Complexes: Preparation of Functionalized Vinylcyclopropanes and Cycloheptadienes. *J. Org. Chem.* **2008**, *73* (18), 7236-7245.
83. Wallock, N. J.; Donaldson, W. A., Synthesis of Cyclopropanes via Organoiron Methodology: Preparation and Rearrangement of Divinylcyclopropanes. *Org. Lett.* **2005**, *7* (10), 2047-2049.

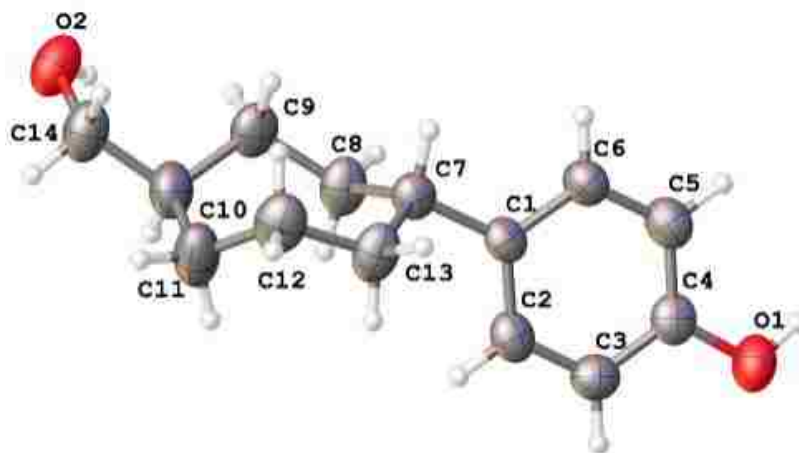
84. Tao, C.; Donaldson, W. A., Reactivity of tricarbonyl(pentadienyl)iron(1+) cations: enantioselective synthesis of 5-HETE methyl ester. *J. Org. Chem.* **1993**, *58* (8), 2134-43.
85. Desai, K. G.; Desai, K. R., Esterification and hydrolysis under microwave irradiation. *Molbank* **2006**, M477/1-M477/2.
86. Luo, G.; Chen, L.; Conway, C. M.; Denton, R.; Keavy, D.; Gulianello, M.; Huang, Y.; Kostich, W.; Lentz, K. A.; Mercer, S. E.; Schartman, R.; Signor, L.; Browning, M.; Macor, J. E.; Dubowchik, G. M., Discovery of BMS-846372, a Potent and Orally Active Human CGRP Receptor Antagonist for the Treatment of Migraine. *ACS Med. Chem. Lett.* **2012**, *3* (4), 337-341.
87. Hashimoto, T.; Isobe, S.; Callens, C. K. A.; Maruoka, K., Axially chiral dicarboxylic acid catalyzed asymmetric semipinacol rearrangement of cyclic β -hydroxy- α -diazo esters. *Tetrahedron* **2012**, *68* (37), 7630-7635.
88. Narasaka, K.; Morikawa, A.; Saigo, K.; Mukaiyama, T., Efficient methods for oxidation of alcohols. *Bull. Chem. Soc. Jpn.* **1977**, *50* (10), 2773-6.
89. Liu, H.-J.; Yeh, W.-L.; Browne, E. N. C., Activated cycloheptenone dienophiles. A versatile approach to 6,7-fused ring targets. *Can. J. Chem.* **1995**, *73* (7), 1135-47.
90. Friese, A.; Hell-Momeni, K.; Zuendorf, I.; Winckler, T.; Dingermann, T.; Dannhardt, G., Synthesis and Biological Evaluation of Cycloalkylidene Carboxylic Acids as Novel Effectors of Ras/Raf Interaction. *J. Med. Chem.* **2002**, *45* (7), 1535-1542.
91. Stefane, B.; Brozic, P.; Vehovec, M.; Rizner, T. L.; Gobec, S., New cyclopentane derivatives as inhibitors of steroid metabolizing enzymes AKR1C1 and AKR1C3. *Eur. J. Med. Chem.* **2009**, *44* (6), 2563-2571.
92. Ye, Q.; Grunewald, G. L., Conformationally defined adrenergic agents. 15. Conformationally restricted and conformationally defined tyramine analogs as inhibitors of phenylethanolamine N-methyltransferase. *J. Med. Chem.* **1989**, *32* (2), 478-86.
93. Kobayashi, S.; Kawamoto, T.; Uehara, S.; Fukuyama, T.; Ryu, I., Black-Light-Induced Radical/Ionic Hydroxymethylation of Alkyl Iodides with Atmospheric CO in the Presence of Tetrabutylammonium Borohydride. *Org. Lett.* **2010**, *12* (7), 1548-1551.
94. Buszek, K. R.; Brown, N., Improved Method for the Diimide Reduction of Multiple Bonds on Solid-Supported Substrates. *J. Org. Chem.* **2007**, *72* (8), 3125-3128.
95. Shaikh, N. S.; Junge, K.; Beller, M., A Convenient and General Iron-Catalyzed Hydrosilylation of Aldehydes. *Org. Lett.* **2007**, *9* (26), 5429-5432.

96. Hou, X.-L.; Xie, Q.-C.; Dai, L.-X., Stereoselective metal catalyzed hydroboration of 4-substituted 1-methylenecyclohexanes. *J. Chem. Res., Synop.* **1997**, (12), 436.
97. Moon, N. G.; Harned, A. M., A Concise Synthetic Route to the Stereotetrad Core of the Briarane Diterpenoids. *Org. Lett.* **2015**, *17* (9), 2218-2221.
98. Paterni, I.; Bertini, S.; Granchi, C.; Tuccinardi, T.; Macchia, M.; Martinelli, A.; Caligiuri, I.; Toffoli, G.; Rizzolio, F.; Carlson, K. E.; Katzenellenbogen, B. S.; Katzenellenbogen, J. A.; Minutolo, F., Highly Selective Salicylketoxime-Based Estrogen Receptor β Agonists Display Antiproliferative Activities in a Glioma Model. *J. Med. Chem.* **2015**, *58* (3), 1184-1194.
99. Lal, G. S.; Pez, G. P.; Pesaresi, R. J.; Prozonic, F. M.; Cheng, H., Bis(2-methoxyethyl)aminosulfur trifluoride: A new broad-spectrum deoxofluorinating agent with enhanced thermal stability. *J. Org. Chem.* **1999**, *64* (19), 7048-7054.
100. Filler, R.; Kobayashi, Y.; Yagupolskii, L. M.; Editors, *Organofluorine Compounds in Medicinal Chemistry and Biomedical Applications. [In: Stud. Org. Chem. (Amsterdam), 1993; 48]*. Elsevier: 1993; p 386 pp.
101. Sladojevich, F.; Arlow, S. I.; Tang, P.; Ritter, T., Late-Stage Deoxyfluorination of Alcohols with PhenoFluor. *J. Am. Chem. Soc.* **2013**, *135* (7), 2470-2473.
102. Singh, R. P.; Shreeve, J. n. M., Recent advances in nucleophilic fluorination reactions of organic compounds using deoxofluor and DAST. *Synthesis* **2002**, (17), 2561-2578.
103. Heravi, M. R. P., Fluorination of activated aromatic systems with Selectfluor F-TEDA-BF₄ in ionic liquids. *J. Fluorine Chem.* **2008**, *129* (3), 217-221.
104. Bogautdinov, R. P.; Fidarov, A. F.; Morozkina, S. N.; Zolotarev, A. A.; Starova, G. L.; Selivanov, S. I.; Shavva, A. G., Fluorination of steroid estrogens with Selectfluor: Elucidation of regio- and stereoselectivity. *J. Fluorine Chem.* **2014**, *168*, 218-222.
105. Andreev, R. V.; Borodkin, G. I.; Shubin, V. G., Fluorination of aromatic compounds with N-fluorobenzenesulfonimide under solvent-free conditions. *Russ. J. Org. Chem.* **2009**, *45* (10), 1468-1473.
106. Nikov, G. N.; Eshete, M.; Rajnarayanan, R. V.; Alworth, W. L., Interactions of synthetic estrogens with human estrogen receptors. *J. Endocrinol.* **2001**, *170* (1), 137-145.
107. Ogu, C. C.; Maxa, J. L., Drug interactions due to cytochrome P450. *Proc (Bayl Univ Med Cent)* **2000**, *13* (4), 421-3.
108. Priest, B. T.; Bell, I. M.; Garcia, M. L., Role of hERG potassium channel assays in drug development. *Channels (Austin)* **2008**, *2* (2), 87-93.

109. Kim, J.; Szinte, J. S.; Boulware, M. I.; Frick, K. M., 17 β -estradiol and agonism of G-protein-coupled estrogen receptor enhance hippocampal memory via different cell-signaling mechanisms. *J. Neurosci.* **2016**, *36* (11), 3309-3321.
110. Tuscher, J. J.; Fortress, A. M.; Kim, J.; Frick, K. M., Regulation of object recognition and object placement by ovarian sex steroid hormones. *Behav. Brain Res.* **2015**, *285*, 140-157.
111. Pajouhesh, H.; Lenz, G. R., Medicinal chemical properties of successful central nervous system drugs. *NeuroRx* **2005**, *2* (4), 541-53.
112. Lipinski, C. A., Lead- and drug-like compounds: the rule-of-five revolution. *Drug Discovery Today: Technol.* **2004**, *1* (4), 337-341.
113. Artursson, P.; Karlsson, J., Correlation between oral drug absorption in humans and apparent drug permeability coefficients in human intestinal epithelial (Caco-2) cells. *Biochem. Biophys. Res. Commun.* **1991**, *175* (3), 880-5.
114. van Breemen, R. B.; Li, Y., Caco-2 cell permeability assays to measure drug absorption. *Expert Opin. Drug Metab. Toxicol.* **2005**, *1* (2), 175-185.
115. Gao, H.-Y.; Ha, C.-Y., Total synthesis of aristogin C in aqueous systems. *Synth. Commun.* **2006**, *36* (22), 3283-3286.
116. Yeom, C.-E.; Kim, Y. J.; Lee, S. Y.; Shin, Y. J.; Kim, B. M., Efficient chemoselective deprotection of silyl ethers using catalytic 1-chloroethyl chloroformate in methanol. *Tetrahedron* **2005**, *61* (52), 12227-12237.
117. Danishefsky, S.; Yan, C.-F.; Singh, R. K.; Gammill, R. B.; McCurry, P. M., Jr.; Fritsch, N.; Clardy, J., Derivatives of 1-methoxy-3-trimethylsilyloxy-1,3-butadiene for Diels-Alder reactions. *J. Am. Chem. Soc.* **1979**, *101* (23), 7001-8.
118. Payne, R. J.; Toscano, M. D.; Bulloch, E. M. M.; Abell, A. D.; Abell, C., Design and synthesis of aromatic inhibitors of anthranilate synthase. *Org. Biomol. Chem.* **2005**, *3* (12), 2271-2281.
119. Hockett, R. C., Chemistry of the tetrose sugars. II. The degradation of d-xylose by the method of Wohl. The rotation of d-threose. *J. Am. Chem. Soc.* **1935**, *57*, 2265-8.
120. Nishimura, T.; Ohtaka, S.; Kimura, A.; Hayama, E.; Haseba, Y.; Takeuchi, H.; Uemura, S., Metal cation-exchanged montmorillonite(Mn⁺-mont)-catalyzed reductive alkylation of phenol and 1-naphthol with cyclohexanones. *Appl. Catal., A* **2000**, *194-195*, 415-425.

121. Givens, R. S.; Stensrud, K.; Conrad, P. G.; Yousef, A. L.; Perera, C.; Senadheera, S. N.; Heger, D.; Wirz, J., p-Hydroxyphenacyl photoremovable protecting groups - Robust photochemistry despite substituent diversity. *Can. J. Chem.* **2011**, *89* (3), 364-384.

APPENDIX

**Table 1 Crystal data and structure refinement for ISP163-PK1**

Identification code	ISP163PK-1 (don2e)
Empirical formula	C ₁₄ H ₂₀ O ₂
Formula weight	220.30
Temperature/K	99.90(14)
Crystal system	orthorhombic
Space group	P2 ₁ 2 ₁ 2 ₁
a/Å	9.9579(5)
b/Å	10.1803(8)
c/Å	24.0251(12)
α/°	90.00
β/°	90.00
γ/°	90.00
Volume/Å ³	2435.5(3)
Z	8
ρ _{calc} /cm ³	1.202
μ/mm ⁻¹	0.617
F(000)	960.0
Crystal size/mm ³	0.3986 × 0.202 × 0.0143
Radiation	Cu Kα (λ = 1.54184)
2θ range for data collection/°	7.36 to 148.1
Index ranges	-9 ≤ h ≤ 12, -10 ≤ k ≤ 12, -29 ≤ l ≤ 27
Reflections collected	12560
Independent reflections	4845 [R _{int} = 0.0642, R _{sigma} = 0.0740]
Data/restraints/parameters	4845/0/293
Goodness-of-fit on F ²	1.052
Final R indexes [I ≥ 2σ (I)]	R ₁ = 0.0807, wR ₂ = 0.1991

Final R indexes [all data] $R_1 = 0.1259$, $wR_2 = 0.2335$
 Largest diff. peak/hole / e \AA^{-3} 0.34/-0.31
 Flack parameter -1.1(5)

Table 2 Fractional Atomic Coordinates ($\times 10^4$) and Equivalent Isotropic Displacement Parameters ($\text{\AA}^2 \times 10^3$) for don2e. U_{eq} is defined as 1/3 of the trace of the orthogonalised U_{ij} tensor.

Atom	<i>x</i>	<i>y</i>	<i>z</i>	U_{eq}
O1	1257 (4)	1630 (3)	813.4 (12)	52.5 (8)
O2	3907 (3)	358 (4)	5117.3 (13)	59.1 (9)
C1	1195 (4)	854 (4)	2522.1 (16)	37.3 (9)
C2	1216 (4)	2128 (5)	2308.6 (18)	44.1 (10)
C3	1228 (4)	2376 (5)	1742.0 (18)	44.4 (10)
C4	1263 (4)	1325 (5)	1370.9 (17)	43 (1)
C5	1255 (5)	56 (5)	1570.3 (18)	47.4 (10)
C6	1227 (4)	-190 (5)	2138.3 (17)	42.8 (9)
C7	1205 (4)	595 (5)	3144.6 (17)	40.8 (9)
C8	2613 (4)	837 (6)	3378.8 (19)	50.9 (12)
C9	2777 (4)	415 (6)	3985.6 (19)	51.3 (12)
C10	2505 (5)	1489 (6)	4415 (2)	55.6 (13)
C11	1114 (6)	2141 (7)	4353 (2)	72.2 (17)
C12	21 (5)	1331 (6)	4067 (2)	59.9 (14)
C13	73 (4)	1388 (6)	3436.0 (18)	51.2 (12)
C14	2660 (4)	1019 (6)	5005 (2)	57.4 (13)
O1A	3775 (3)	5782 (4)	587.8 (12)	50.2 (8)
O2A	2794 (4)	6197 (4)	5279.3 (14)	63 (1)
C1A	3762 (4)	6250 (4)	2321.7 (17)	40.8 (9)
C2A	3683 (4)	4998 (5)	2084.0 (18)	43.2 (10)
C3A	3678 (4)	4818 (5)	1513.4 (17)	41.2 (9)
C4A	3766 (4)	5923 (4)	1159.4 (18)	41.8 (9)
C5A	3875 (5)	7157 (5)	1385 (2)	47.8 (10)
C6A	3867 (5)	7312 (5)	1957 (2)	46.3 (10)
C7A	3723 (4)	6485 (5)	2944.2 (18)	46.8 (10)
C8A	2439 (5)	6014 (11)	3195 (2)	109 (3)
C9A	2148 (5)	6604 (11)	3763 (2)	127 (4)
C10A	2678 (5)	5945 (7)	4266 (2)	71.9 (18)
C11A	4048 (7)	5372 (7)	4195 (3)	80 (2)
C12A	5045 (4)	6139 (9)	3868 (2)	82 (2)
C13A	4968 (4)	6014 (8)	3225 (2)	69.7 (19)
C14A	2565 (6)	6837 (7)	4755 (2)	73.8 (18)

Table 3 Anisotropic Displacement Parameters ($\text{\AA}^2 \times 10^3$) for don2e. The Anisotropic displacement factor exponent takes the form: $-2\pi^2[h^2a^{*2}U_{11}+2hka^*b^*U_{12}+\dots]$.

Atom	U_{11}	U_{22}	U_{33}	U_{23}	U_{13}	U_{12}
O1	49.1 (16)	69 (2)	39.9 (16)	-0.5 (15)	3.0 (14)	-11.0 (18)
O2	39.9 (15)	87 (3)	50.0 (19)	11.3 (18)	-3.4 (14)	-4.1 (18)
C1	26.1 (15)	41 (2)	45 (2)	-4.6 (17)	0.6 (16)	-6.3 (18)
C2	31.1 (17)	52 (3)	49 (2)	-8 (2)	1.0 (19)	-6 (2)
C3	34.3 (18)	45 (2)	54 (3)	2 (2)	1.5 (19)	-2 (2)
C4	26.5 (16)	55 (3)	47 (2)	-2 (2)	2.1 (17)	-7 (2)
C5	38.2 (19)	52 (3)	52 (3)	-8 (2)	7 (2)	-3 (2)
C6	37.2 (18)	44 (2)	48 (2)	-4.4 (19)	3.5 (19)	1 (2)
C7	28.4 (16)	48 (2)	46 (2)	-2.7 (18)	-1.1 (17)	1.2 (19)
C8	27.0 (18)	76 (4)	49 (3)	-5 (2)	-0.6 (17)	2 (2)
C9	32.5 (18)	69 (3)	53 (3)	-3 (2)	-6.2 (18)	9 (2)
C10	48 (2)	68 (4)	50 (3)	-7 (2)	-9 (2)	-5 (2)
C11	68 (3)	92 (4)	57 (3)	-20 (3)	-16 (3)	26 (4)
C12	39 (2)	81 (4)	59 (3)	-3 (3)	5 (2)	14 (2)
C13	26.2 (17)	80 (4)	47 (3)	0 (2)	1.8 (17)	6 (2)
C14	41 (2)	85 (4)	46 (3)	-3 (3)	-2.3 (19)	4 (2)
O1A	41.1 (14)	66 (2)	43.4 (17)	2.6 (14)	0.9 (13)	-11.1 (17)
O2A	73 (2)	73 (3)	43.3 (19)	1.9 (17)	-2.3 (16)	-24 (2)
C1A	30.4 (16)	42 (2)	50 (2)	-2.5 (19)	-1.4 (17)	1.5 (19)
C2A	31.2 (18)	53 (3)	45 (2)	5.8 (19)	4.1 (17)	-4.0 (19)
C3A	32.4 (18)	41 (2)	50 (2)	-1.7 (19)	0.9 (17)	0.3 (18)
C4A	26.3 (15)	50 (3)	50 (2)	6.7 (19)	-1.6 (17)	-5.7 (19)
C5A	39 (2)	45 (3)	60 (3)	11 (2)	-4 (2)	-7 (2)
C6A	39 (2)	36 (2)	65 (3)	-2 (2)	-7 (2)	0 (2)
C7A	35.7 (19)	58 (3)	46 (2)	-8 (2)	-5.8 (18)	5 (2)
C8A	36 (2)	253 (11)	39 (3)	-31 (4)	3 (2)	-25 (4)
C9A	38 (2)	303 (14)	40 (3)	-34 (5)	-10 (2)	42 (5)
C10A	59 (3)	111 (5)	46 (3)	-21 (3)	18 (2)	-36 (3)
C11A	107 (5)	69 (4)	63 (4)	12 (3)	4 (3)	31 (4)
C12A	30 (2)	170 (7)	46 (3)	18 (4)	-8 (2)	-8 (3)
C13A	30 (2)	138 (6)	42 (3)	3 (3)	0.8 (18)	4 (3)
C14A	75 (4)	111 (5)	35 (3)	-7 (3)	-8 (2)	21 (3)

Table 4 Bond Lengths for don2e.

Atom	Atom	Length/Å	Atom	Atom	Length/Å
O1	C4	1.375 (5)	O1A	C4A	1.381 (5)
O2	C14	1.437 (6)	O2A	C14A	1.436 (7)
C1	C2	1.395 (7)	C1A	C2A	1.398 (6)
C1	C6	1.408 (6)	C1A	C6A	1.395 (6)
C1	C7	1.519 (6)	C1A	C7A	1.515 (6)
C2	C3	1.384 (6)	C2A	C3A	1.383 (6)
C3	C4	1.393 (6)	C3A	C4A	1.413 (6)
C4	C5	1.378 (7)	C4A	C5A	1.372 (7)
C5	C6	1.388 (6)	C5A	C6A	1.384 (7)
C7	C8	1.530 (5)	C7A	C8A	1.493 (7)
C7	C13	1.553 (6)	C7A	C13A	1.490 (6)
C8	C9	1.529 (7)	C8A	C9A	1.519 (8)
C9	C10	1.528 (7)	C9A	C10A	1.479 (10)
C10	C11	1.544 (7)	C10A	C11A	1.494 (8)
C10	C14	1.505 (7)	C10A	C14A	1.490 (8)
C11	C12	1.528 (8)	C11A	C12A	1.489 (9)
C12	C13	1.517 (7)	C12A	C13A	1.551 (7)

Table 5 Bond Angles for don2e.

Atom	Atom	Atom	Angle/°	Atom	Atom	Atom	Angle/°
C2	C1	C6	117.4 (4)	C2A	C1A	C7A	123.1 (4)
C2	C1	C7	121.6 (4)	C6A	C1A	C2A	117.0 (4)
C6	C1	C7	120.9 (4)	C6A	C1A	C7A	119.9 (4)
C3	C2	C1	122.1 (4)	C3A	C2A	C1A	121.7 (4)
C2	C3	C4	119.3 (4)	C2A	C3A	C4A	119.4 (4)
O1	C4	C3	116.7 (4)	O1A	C4A	C3A	121.1 (4)
O1	C4	C5	123.4 (4)	C5A	C4A	O1A	119.2 (4)
C5	C4	C3	119.8 (4)	C5A	C4A	C3A	119.7 (4)
C4	C5	C6	120.7 (4)	C4A	C5A	C6A	119.8 (4)
C5	C6	C1	120.6 (4)	C5A	C6A	C1A	122.4 (4)
C1	C7	C8	109.9 (3)	C8A	C7A	C1A	111.7 (4)
C1	C7	C13	110.4 (4)	C13A	C7A	C1A	112.0 (4)
C8	C7	C13	114.6 (4)	C13A	C7A	C8A	115.2 (5)
C9	C8	C7	113.8 (4)	C7A	C8A	C9A	113.5 (6)
C10	C9	C8	115.1 (5)	C10A	C9A	C8A	119.2 (8)
C9	C10	C11	113.6 (4)	C9A	C10A	C11A	114.1 (4)
C14	C10	C9	113.0 (5)	C9A	C10A	C14A	109.9 (6)
C14	C10	C11	108.7 (4)	C14A	C10A	C11A	113.4 (5)

C12	C11	C10	116.8 (5)	C12AC11AC10A	117.7 (6)
C13	C12	C11	113.9 (5)	C11AC12AC13A	116.7 (6)
C12	C13	C7	117.1 (4)	C7A C13AC12A	117.8 (4)
O2	C14	C10	114.4 (4)	O2A C14AC10A	113.7 (6)

Table 6 Hydrogen Bonds for don2e.

D	H	A	d(D-H)/Å	d(H-A)/Å	d(D-A)/Å	D-H-A/°
O1	H1	O2 ¹	0.84	1.80	2.631 (5)	167.6
O2	H2	O1A ²	0.84	2.11	2.896 (5)	156.0
O1AH1A	O2A ³		0.84	1.82	2.655 (5)	175.7
O2AH2AA	O1 ⁴		0.84	1.93	2.726 (5)	158.1

¹1/2-X,-Y,-1/2+Z; ²1-X,-1/2+Y,1/2-Z; ³1/2-X,1-Y,-1/2+Z; ⁴1/2-X,1-Y,1/2+Z

Table 7 Hydrogen Atom Coordinates (Å×10⁴) and Isotropic Displacement Parameters (Å²×10³) for don2e.

Atom	x	y	z	U(eq)
H1	1276	935	625	79
H2	4412	420	4839	89
H2A	1221	2849	2560	53
H3	1213	3254	1608	53
H5	1270	-659	1316	57
H6	1229	-1071	2269	51
H7	999	-357	3199	49
H8A	3273	354	3148	61
H8B	2822	1785	3348	61
H9A	2160	-328	4059	62
H9B	3705	90	4039	62
H10	3193	2191	4355	67
H11A	789	2380	4729	87
H11B	1230	2967	4141	87
H12A	107	404	4186	72
H12B	-868	1652	4192	72
H13A	164	2320	3325	61
H13B	-800	1072	3291	61
H14A	2584	1783	5258	69
H14B	1911	413	5092	69
H1A	3305	5130	498	75
H2AA	3190	6716	5496	95

H2AB	3632	4252	2321	52
H3A	3615	3960	1361	49
H5A	3956	7902	1150	57
H6A	3935	8172	2108	56
H7A	3721	7461	2992	56
H8AA	2474	5046	3230	131
H8AB	1690	6234	2940	131
H9AA	2497	7514	3763	153
H9AB	1161	6662	3804	153
H10A	2063	5189	4342	86
H11C	4429	5219	4570	96
H11D	3947	4502	4015	96
H12C	5955	5867	3987	98
H12D	4941	7078	3966	98
H13C	5737	6500	3065	84
H13D	5091	5076	3129	84
H14C	3221	7560	4713	89
H14D	1656	7231	4759	89

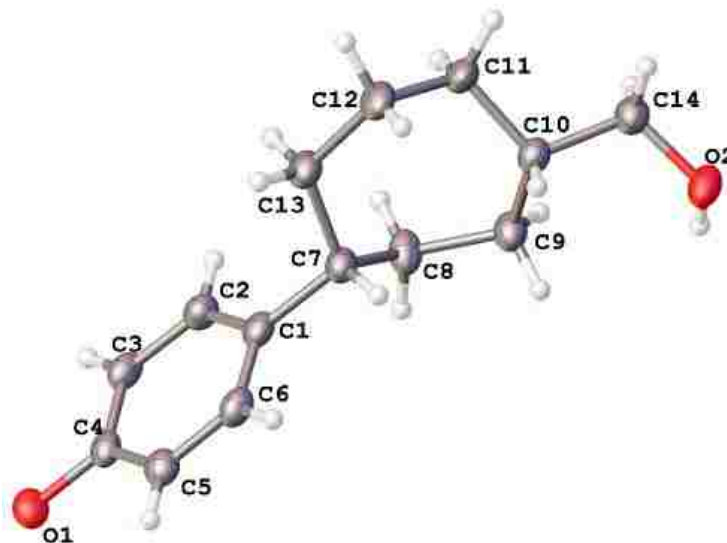


Table 1 Crystal data and structure refinement for ISP163-PK3.

Identification code	ISP163-PK3 (don2d)
Empirical formula	C ₁₄ H ₂₀ O ₂
Formula weight	220.30
Temperature/K	100.00(10)
Crystal system	monoclinic
Space group	P2 ₁
a/Å	10.0103(7)
b/Å	10.1468(8)
c/Å	12.2271(9)
α/°	90.00
β/°	103.012(8)
γ/°	90.00
Volume/Å ³	1210.05(16)
Z	4
ρ _{calc} /cm ³	1.209
μ/mm ⁻¹	0.621
F(000)	480.0
Crystal size/mm ³	0.2462 × 0.1633 × 0.0221
Radiation	Cu Kα (λ = 1.54184)
2θ range for data collection/°	7.42 to 148.44
Index ranges	-12 ≤ h ≤ 11, -12 ≤ k ≤ 12, -14 ≤ l ≤ 15
Reflections collected	15025
Independent reflections	4596 [R _{int} = 0.0583, R _{sigma} = 0.0618]
Data/restraints/parameters	4596/1/305
Goodness-of-fit on F ²	1.029

Final R indexes [$I \geq 2\sigma(I)$] $R_1 = 0.0528$, $wR_2 = 0.1256$
 Final R indexes [all data] $R_1 = 0.0730$, $wR_2 = 0.1399$
 Largest diff. peak/hole / $e \text{ \AA}^{-3}$ 0.28/-0.25
 Flack parameter 0.0(3)

Table 2 Fractional Atomic Coordinates ($\times 10^4$) and Equivalent Isotropic Displacement Parameters ($\text{\AA}^2 \times 10^3$) for don2d. U_{eq} is defined as 1/3 of the trace of the orthogonalised U_{ij} tensor.

Atom	x	y	z	U(eq)
O1	3964 (2)	4063 (2)	1458.7 (16)	30.5 (4)
O2	7030 (2)	6822 (2)	10051.0 (17)	33.9 (5)
C1	5101 (3)	4152 (3)	4982 (2)	26.6 (5)
C2	3716 (3)	4102 (3)	4424 (2)	29.8 (6)
C3	3325 (3)	4072 (3)	3253 (2)	28.0 (6)
C4	4309 (3)	4102 (3)	2620 (2)	25.5 (5)
C5	5691 (3)	4153 (3)	3157 (2)	28.8 (6)
C6	6061 (3)	4162 (3)	4325 (2)	28.4 (6)
C7	5523 (3)	4186 (3)	6257 (2)	26.7 (6)
C8	4760 (3)	5290 (3)	6723 (2)	33.7 (7)
C9	5481 (3)	5899 (3)	7855 (2)	31.7 (6)
C10	6122 (3)	4950 (3)	8812 (2)	27.5 (6)
C11	5385 (3)	3632 (3)	8797 (2)	31.3 (6)
C12	5806 (4)	2622 (3)	8006 (3)	34.2 (7)
C13	5262 (3)	2835 (3)	6748 (2)	32.1 (6)
C14	6212 (3)	5645 (3)	9938 (2)	32.9 (7)
O1A	-429 (2)	6584 (2)	1371.8 (17)	33.8 (5)
O2A	1553 (2)	5163 (3)	10642.6 (17)	41.3 (6)
C1A	-226 (3)	6766 (3)	4824 (2)	27.8 (6)
C2A	954 (3)	6672 (3)	4404 (2)	30.8 (6)
C3A	872 (3)	6620 (3)	3249 (2)	32.7 (6)
C4A	-399 (3)	6647 (3)	2508 (2)	28.2 (6)
C5A	-1590 (3)	6727 (3)	2902 (2)	30.6 (6)
C6A	-1484 (3)	6790 (3)	4059 (2)	29.8 (6)
C7A	-183 (3)	6805 (3)	6074 (2)	30.4 (6)
C8A	32 (3)	5426 (3)	6601 (2)	31.3 (6)
C9A	-555 (3)	5270 (4)	7643 (2)	35.8 (7)
C10A	261 (3)	5862 (3)	8769 (2)	29.9 (6)
C11A	1373 (3)	6864 (4)	8679 (2)	34.3 (6)
C12A	863 (4)	8053 (3)	7923 (3)	36.7 (7)
C13A	820 (4)	7856 (4)	6671 (3)	38.7 (7)
C14A	866 (4)	4736 (4)	9545 (2)	37.8 (7)

Table 3 Anisotropic Displacement Parameters ($\text{\AA}^2 \times 10^3$) for don2d. The Anisotropic displacement factor exponent takes the form: $-2\pi^2[h^2a^{*2}U_{11}+2hka^*b^*U_{12}+\dots]$.

Atom	U_{11}	U_{22}	U_{33}	U_{23}	U_{13}	U_{12}
O1	34.0 (11)	26.7 (12)	27 (1)	2.2 (9)	-0.8 (8)	5.1 (9)
O2	39.7 (11)	22.1 (11)	34.2 (10)	-0.4 (9)	-3.4 (9)	-1.1 (9)
C1	29.8 (13)	17.6 (13)	30.1 (12)	-0.3 (11)	1.7 (10)	-1.7 (11)
C2	29.6 (13)	26.9 (15)	32.4 (14)	-1.0 (13)	6.1 (11)	-3.7 (12)
C3	24.3 (12)	22.4 (14)	32.7 (14)	3.2 (12)	-3.1 (10)	-1.1 (11)
C4	30.6 (13)	16.3 (13)	26.7 (12)	-1.0 (11)	0.4 (10)	0.8 (11)
C5	31.7 (14)	21.9 (14)	31.3 (13)	0.4 (12)	3.6 (11)	2.0 (12)
C6	24.2 (12)	22.1 (14)	35.2 (14)	-0.5 (13)	-1.4 (11)	-0.2 (11)
C7	31.2 (14)	21.0 (14)	26.2 (13)	-0.7 (11)	3.0 (11)	-0.7 (11)
C8	39.1 (16)	27.0 (17)	29.4 (14)	-3.0 (12)	-4.2 (12)	6.6 (13)
C9	40.8 (16)	23.6 (15)	27.7 (15)	-0.5 (12)	1.5 (12)	1.4 (13)
C10	29.3 (14)	22.8 (15)	28.7 (13)	-1.0 (11)	3.1 (11)	-1.4 (11)
C11	39.4 (15)	22.5 (15)	31.3 (14)	-0.7 (12)	6.8 (12)	-7.5 (12)
C12	48.4 (18)	18.6 (15)	33.5 (16)	0.5 (11)	4.5 (13)	-1.9 (12)
C13	41.8 (16)	21.5 (15)	30.7 (15)	0.0 (12)	3.7 (12)	-1.8 (12)
C14	40.4 (16)	26.6 (17)	29.9 (15)	-0.9 (11)	4.3 (12)	-2.6 (12)
O1A	38.3 (12)	37.7 (14)	23.8 (10)	1.8 (9)	3.7 (9)	5.7 (10)
O2A	44.2 (13)	47.9 (15)	27 (1)	1.1 (10)	-2.4 (9)	16.2 (11)
C1A	33.8 (14)	22.7 (14)	25.4 (13)	-0.6 (12)	3.3 (11)	-1.0 (12)
C2A	26.3 (13)	30.9 (16)	30.6 (13)	0.5 (12)	-3.4 (10)	-1.4 (12)
C3A	30.0 (14)	37.0 (19)	31.0 (14)	1.8 (13)	7.1 (11)	-0.4 (13)
C4A	34.8 (14)	21.9 (15)	26.1 (13)	1.1 (11)	3.4 (11)	1.0 (12)
C5A	27.2 (13)	30.5 (16)	30.5 (14)	0.3 (13)	-1 (1)	1.4 (12)
C6A	29.4 (13)	28.7 (16)	30.7 (13)	-1.3 (12)	5.5 (11)	0.3 (12)
C7A	31.8 (13)	31.4 (17)	25.9 (13)	-3.5 (12)	2.4 (11)	1.5 (13)
C8A	36.8 (15)	28.8 (16)	26.7 (13)	-2.4 (12)	3.5 (11)	-3.5 (12)
C9A	37.0 (15)	38.0 (19)	29.7 (14)	-0.4 (13)	1.5 (12)	-10.9 (14)
C10A	31.0 (14)	31.6 (17)	24.8 (13)	-0.9 (11)	1.4 (11)	2.2 (13)
C11A	32.6 (14)	36.4 (18)	29.9 (14)	-2.6 (13)	-1.2 (11)	-4.7 (14)
C12A	50.0 (19)	27.0 (17)	30.9 (15)	-8.0 (12)	4.4 (13)	-9.9 (14)
C13A	54.3 (19)	27.5 (17)	33.1 (16)	-3.2 (13)	7.3 (14)	-9.9 (15)
C14A	45.1 (18)	37.3 (19)	28.1 (15)	-1.3 (13)	2.3 (13)	7.5 (14)

Table 4 Bond Lengths for don2d.

Atom	Atom	Length/Å	Atom	Atom	Length/Å
O1	C4	1.384 (3)	O1A	C4A	1.384 (3)
O2	C14	1.438 (4)	O2A	C14A	1.430 (4)
C1	C2	1.402 (4)	C1A	C2A	1.394 (4)
C1	C6	1.384 (4)	C1A	C6A	1.389 (4)
C1	C7	1.521 (4)	C1A	C7A	1.520 (4)
C2	C3	1.397 (4)	C2A	C3A	1.396 (4)
C3	C4	1.384 (4)	C3A	C4A	1.387 (4)
C4	C5	1.392 (4)	C4A	C5A	1.384 (4)
C5	C6	1.393 (4)	C5A	C6A	1.397 (4)
C7	C8	1.537 (4)	C7A	C8A	1.535 (5)
C7	C13	1.542 (4)	C7A	C13A	1.532 (4)
C8	C9	1.539 (4)	C8A	C9A	1.527 (4)
C9	C10	1.539 (4)	C9A	C10A	1.555 (4)
C10	C11	1.526 (4)	C10A	C11A	1.530 (4)
C10	C14	1.531 (4)	C10A	C14A	1.521 (4)
C11	C12	1.532 (4)	C11A	C12A	1.536 (5)
C12	C13	1.528 (4)	C12A	C13A	1.535 (4)

Table 5 Bond Angles for don2d.

Atom	Atom	Atom	Angle/°	Atom	Atom	Atom	Angle/°
C2	C1	C7	121.0 (3)	C2A	C1A	C7A	122.5 (2)
C6	C1	C2	117.2 (3)	C6A	C1A	C2A	117.9 (2)
C6	C1	C7	121.7 (3)	C6A	C1A	C7A	119.5 (2)
C3	C2	C1	121.2 (3)	C1A	C2A	C3A	120.9 (3)
C4	C3	C2	120.1 (2)	C4A	C3A	C2A	119.8 (3)
O1	C4	C5	118.5 (2)	O1A	C4A	C3A	117.7 (3)
C3	C4	O1	121.9 (2)	C5A	C4A	O1A	121.7 (3)
C3	C4	C5	119.6 (2)	C5A	C4A	C3A	120.6 (2)
C4	C5	C6	119.4 (3)	C4A	C5A	C6A	118.7 (3)
C1	C6	C5	122.4 (3)	C1A	C6A	C5A	122.1 (3)
C1	C7	C8	110.5 (2)	C1A	C7A	C8A	111.6 (3)
C1	C7	C13	110.3 (2)	C1A	C7A	C13A	111.4 (3)
C8	C7	C13	111.2 (2)	C13A	C7A	C8A	114.8 (3)
C7	C8	C9	117.0 (2)	C9A	C8A	C7A	113.6 (3)
C8	C9	C10	117.6 (3)	C8A	C9A	C10A	118.4 (3)
C11	C10	C9	114.9 (3)	C11A	C10A	C9A	116.0 (2)
C11	C10	C14	110.1 (2)	C14A	C10A	C9A	108.6 (3)
C14	C10	C9	109.0 (2)	C14A	C10A	C11A	110.5 (3)

C10	C11	C12	113.1(2)	C10A	C11A	C12A	114.6(2)
C13	C12	C11	117.0(3)	C13A	C12A	C11A	115.4(3)
C12	C13	C7	117.7(2)	C7A	C13A	C12A	115.7(3)
O2	C14	C10	112.7(2)	O2A	C14A	C10A	113.4(3)

Table 6 Torsion Angles for don2d.

A	B	C	D	Angle/°	A	B	C	D	Angle/°
O1	C4	C5	C6	-178.6(3)	O1A	C4A	C5A	C6A	-179.9(3)
C1	C2	C3	C4	-0.5(5)	C1A	C2A	C3A	C4A	-0.7(5)
C1	C7	C8	C9	-152.1(3)	C1A	C7A	C8A	C9A	-153.1(2)
C1	C7	C13	C12	171.7(3)	C1A	C7A	C13A	C12A	175.5(3)
C2	C1	C6	C5	1.4(5)	C2A	C1A	C6A	C5A	-0.2(5)
C2	C1	C7	C8	-52.0(4)	C2A	C1A	C7A	C8A	-78.5(4)
C2	C1	C7	C13	71.3(4)	C2A	C1A	C7A	C13A	51.2(4)
C2	C3	C4	O1	179.4(3)	C2A	C3A	C4A	O1A	-179.6(3)
C2	C3	C4	C5	0.4(5)	C2A	C3A	C4A	C5A	0.1(5)
C3	C4	C5	C6	0.5(5)	C3A	C4A	C5A	C6A	0.4(5)
C4	C5	C6	C1	-1.5(5)	C4A	C5A	C6A	C1A	-0.4(5)
C6	C1	C2	C3	-0.4(5)	C6A	C1A	C2A	C3A	0.8(5)
C6	C1	C7	C8	128.3(3)	C6A	C1A	C7A	C8A	99.7(3)
C6	C1	C7	C13	-108.4(3)	C6A	C1A	C7A	C13A	-130.5(3)
C7	C1	C2	C3	179.9(3)	C7A	C1A	C2A	C3A	179.0(3)
C7	C1	C6	C5	-178.9(3)	C7A	C1A	C6A	C5A	-178.5(3)
C7	C8	C9	C10	-46.7(4)	C7A	C8A	C9A	C10A	-77.5(4)
C8	C7	C13	C12	-65.4(3)	C8A	C7A	C13A	C12A	-56.5(4)
C8	C9	C10	C11	-31.4(4)	C8A	C9A	C10A	C11A	16.0(4)
C8	C9	C10	C14	-155.6(3)	C8A	C9A	C10A	C14A	-109.1(3)
C9	C10	C11	C12	83.1(3)	C9A	C10A	C11A	C12A	56.6(4)
C9	C10	C14	O2	-59.6(3)	C9A	C10A	C14A	O2A	-175.4(3)
C10	C11	C12	C13	-73.8(4)	C10A	C11A	C12A	C13A	-86.4(3)
C11	C10	C14	O2	173.4(2)	C11A	C10A	C14A	O2A	56.3(3)
C11	C12	C13	C7	53.9(4)	C11A	C12A	C13A	C7A	64.3(4)
C13	C7	C8	C9	85.1(3)	C13A	C7A	C8A	C9A	79.0(3)
C14	C10	C11	C12	-153.3(3)	C14A	C10A	C11A	C12A	-179.3(3)

Table 7 Hydrogen Atom Coordinates ($\text{\AA}\times 10^4$) and Isotropic Displacement Parameters ($\text{\AA}^2\times 10^3$) for don2d.

Atom	<i>x</i>	<i>y</i>	<i>z</i>	U(eq)
H1	3290 (40)	4440 (40)	1220 (30)	23 (9)
H2	6610 (40)	7460 (50)	9600 (40)	52 (12)
H2A	3031	4088	4850	36
H3	2381	4032	2890	34
H5	6375	4181	2730	35
H6	7007	4176	4685	34
H7	6529	4375	6479	32
H8A	3864	4938	6802	40
H8B	4570	6006	6159	40
H9A	4807	6457	8120	38
H9B	6215	6488	7719	38
H10	7081	4760	8744	33
H11A	4383	3781	8563	38
H11B	5582	3266	9567	38
H12A	6820	2605	8158	41
H12B	5502	1741	8200	41
H13A	4259	2685	6576	38
H13B	5667	2149	6346	38
H14A	5275	5874	10012	39
H14B	6610	5030	10554	39
H1A	-1140 (50)	6720 (50)	1020 (30)	57 (13)
H2AA	900 (50)	5610 (60)	10900 (40)	79 (16)
H2AB	1826	6643	4910	37
H3A	1685	6566	2973	39
H5A	-2461	6739	2394	37
H6A	-2298	6850	4332	36
H7A	-1115	7095	6145	36
H8AA	-403	4768	6034	38
H8AB	1027	5235	6806	38
H9AA	-674	4316	7761	43
H9AB	-1481	5671	7476	43
H10A	-415	6324	9125	36
H11C	2095	6410	8387	41
H11D	1798	7189	9442	41
H12C	-71	8281	8005	44
H12D	1464	8815	8196	44
H13C	577	8707	6282	46
H13D	1752	7618	6592	46
H14C	120	4122	9614	45

H14D

1523

4245

9203

45

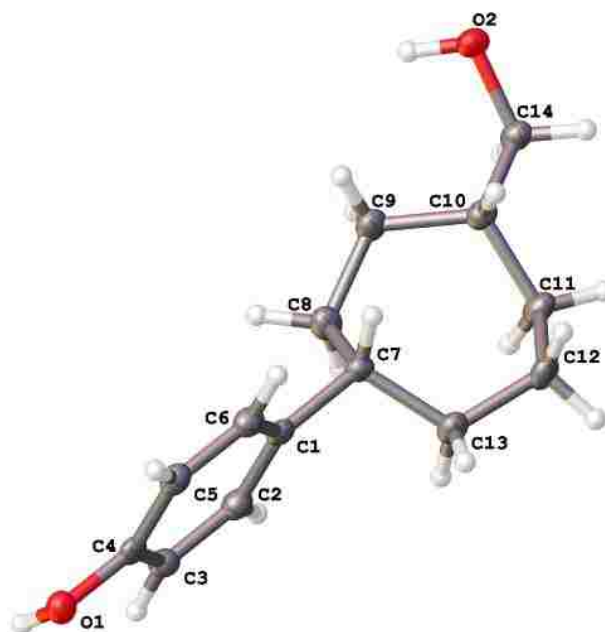


Table 1 Crystal data and structure refinement for ISP163-PK4.

Identification code	ISP163-PK4 (don2c)
Empirical formula	C ₁₄ H ₂₀ O ₂
Formula weight	220.30
Temperature/K	99.90(14)
Crystal system	monoclinic
Space group	P2 ₁
a/Å	10.0043(3)
b/Å	10.1405(4)
c/Å	12.2188(3)
α/°	90.00
β/°	103.121(3)
γ/°	90.00
Volume/Å ³	1207.22(6)
Z	4
ρ _{calc} /cm ³	1.212
μ/mm ⁻¹	0.623
F(000)	480.0
Crystal size/mm ³	0.8254 × 0.4513 × 0.0546
Radiation	CuKα (λ = 1.54184)
2θ range for data collection/°	7.42 to 148.64
Index ranges	-12 ≤ h ≤ 12, -12 ≤ k ≤ 12, -15 ≤ l ≤ 14
Reflections collected	7992
Independent reflections	7992 [R _{int} = 0.0000, R _{sigma} = 0.0091]
Data/restraints/parameters	7992/1/306

Goodness-of-fit on F^2	1.062
Final R indexes [$I \geq 2\sigma(I)$]	$R_1 = 0.0688$, $wR_2 = 0.1938$
Final R indexes [all data]	$R_1 = 0.0696$, $wR_2 = 0.1948$
Largest diff. peak/hole / $e \text{ \AA}^{-3}$	0.48/-0.25
Flack parameter	-0.1(2)

Table 2 Fractional Atomic Coordinates ($\times 10^4$) and Equivalent Isotropic Displacement Parameters ($\text{\AA}^2 \times 10^3$) for don2c. U_{eq} is defined as 1/3 of the trace of the orthogonalised U_{ij} tensor.

Atom	x	y	z	U(eq)
O1	6036.6 (17)	5934.1 (17)	8540.7 (12)	24.9 (3)
O2	2970.2 (16)	3174.2 (18)	-54.6 (13)	27.7 (4)
C1	4897 (2)	5849 (2)	5011.7 (18)	21.2 (4)
C2	6281 (2)	5899 (2)	5572.3 (18)	23.3 (4)
C3	6675 (2)	5927 (2)	6742.1 (18)	23.8 (4)
C4	5689 (2)	5899 (2)	7383.4 (17)	21.3 (4)
C5	4305 (2)	5854 (2)	6841.0 (17)	23.2 (4)
C6	3924 (2)	5837 (2)	5673.1 (18)	23.1 (4)
C7	4475 (2)	5811 (2)	3739.4 (17)	21.4 (4)
C8	5250 (3)	4704 (3)	3278.6 (19)	28.7 (5)
C9	4522 (2)	4099 (2)	2145.5 (19)	26.1 (5)
C10	3877 (2)	5049 (2)	1185.7 (18)	22.2 (4)
C11	4614 (2)	6376 (2)	1204.0 (19)	26.3 (5)
C12	4188 (3)	7377 (2)	1996 (2)	28.6 (5)
C13	4737 (3)	7167 (2)	3257.9 (19)	26.8 (5)
C14	3795 (2)	4357 (2)	61.7 (18)	25.3 (5)
O1A	426.7 (18)	3417.3 (18)	8623.7 (13)	27.1 (4)
O2A	-1557 (2)	4841 (2)	-642.8 (14)	34.3 (4)
C1A	231 (2)	3231 (2)	5173.3 (17)	22.8 (4)
C2A	-958 (2)	3335 (3)	5590.8 (18)	26.2 (5)
C3A	-870 (2)	3392 (3)	6746.1 (18)	25.5 (5)
C4A	402 (2)	3353 (2)	7495.6 (18)	23.4 (4)
C5A	1600 (2)	3268 (3)	7099.3 (18)	25.3 (5)
C6A	1490 (2)	3208 (2)	5941.9 (19)	24.6 (5)
C7A	195 (2)	3181 (2)	3924.1 (18)	24.2 (5)
C8A	-34 (2)	4575 (2)	3395.9 (17)	24.6 (5)
C9A	555 (2)	4725 (3)	2352.1 (18)	27.8 (5)
C10A	-258 (2)	4136 (3)	1229.4 (18)	25.9 (5)
C11A	-1378 (2)	3137 (3)	1319.4 (19)	29.3 (5)
C12A	-863 (3)	1944 (3)	2073.4 (19)	30.9 (5)
C13A	-837 (3)	2150 (3)	3320.6 (19)	30.7 (5)
C14A	-863 (3)	5270 (3)	452.9 (19)	30.9 (5)

Table 3 Anisotropic Displacement Parameters ($\text{\AA}^2 \times 10^3$) for don2c. The Anisotropic displacement factor exponent takes the form: $-2\pi^2[h^2a^{*2}U_{11}+2hka^*b^*U_{12}+\dots]$.

Atom	U_{11}	U_{22}	U_{33}	U_{23}	U_{13}	U_{12}
O1	31.0 (8)	18.9 (9)	22.6 (7)	0.7 (6)	1.2 (6)	2.3 (7)
O2	33.2 (8)	16.8 (9)	28.5 (8)	-1.0 (6)	-2.3 (6)	-2.8 (7)
C1	26.4 (10)	11.0 (9)	23.4 (9)	0.3 (8)	0.0 (7)	-2.0 (8)
C2	25.4 (10)	16.9 (11)	26.8 (10)	1.1 (9)	4.1 (8)	-1.3 (9)
C3	22.6 (10)	17.9 (12)	27.6 (10)	0.8 (9)	-1.2 (8)	-2.1 (9)
C4	28.4 (11)	9.7 (10)	23.4 (9)	0.1 (8)	0.9 (8)	1.3 (8)
C5	26.5 (10)	16.0 (11)	26.5 (10)	1.1 (9)	4.9 (8)	0.3 (9)
C6	21.7 (10)	16.3 (11)	28.6 (10)	1.2 (9)	0.6 (8)	0.5 (8)
C7	24.6 (10)	14.6 (10)	22.2 (9)	-0.7 (8)	-0.6 (7)	-1.7 (8)
C8	37.4 (13)	19.3 (12)	25.3 (10)	-1.5 (9)	-1.6 (9)	4.4 (10)
C9	34.8 (12)	14.6 (12)	26.4 (10)	-0.4 (9)	2.0 (8)	2.6 (10)
C10	25.3 (10)	16.5 (12)	23.9 (9)	0.2 (8)	3.5 (8)	-1.2 (8)
C11	35.2 (11)	16.5 (11)	26.7 (10)	0.5 (8)	6.3 (9)	-5.4 (10)
C12	44.0 (14)	12.9 (12)	26.9 (11)	2.3 (8)	4 (1)	0.8 (10)
C13	38.0 (12)	15.0 (11)	25.2 (10)	0.1 (8)	2.6 (9)	-0.9 (9)
C14	32.5 (12)	17.6 (12)	24.1 (10)	-0.6 (8)	2.8 (8)	-3.7 (9)
O1A	31.3 (9)	27.7 (10)	21.2 (7)	0.4 (7)	3.8 (6)	4.3 (7)
O2A	37.8 (10)	37.4 (11)	23.4 (8)	-1.3 (7)	-2.0 (7)	14.4 (9)
C1A	29.6 (11)	14.5 (11)	22.7 (10)	0.1 (8)	2.5 (8)	-0.1 (9)
C2A	25 (1)	22.9 (12)	27.6 (10)	1.2 (9)	-0.2 (8)	1.3 (9)
C3A	24.6 (11)	24.2 (13)	27.3 (10)	1.4 (10)	5.2 (8)	2.6 (9)
C4A	29.4 (11)	16.3 (11)	23.5 (10)	-0.1 (9)	4.2 (8)	1.7 (9)
C5A	26.1 (10)	21.6 (12)	26.2 (10)	-1.7 (9)	1.6 (8)	1.4 (9)
C6A	25.1 (10)	21.1 (12)	27 (1)	-1.1 (9)	4.4 (8)	0.1 (9)
C7A	27.5 (10)	20.4 (12)	23.3 (10)	-1.0 (8)	2.6 (8)	0.1 (9)
C8A	29.4 (11)	19.3 (12)	22.6 (9)	-1.1 (8)	0.9 (8)	-2.1 (9)
C9A	30.3 (11)	27.9 (13)	22.5 (9)	0.9 (9)	0.4 (8)	-6.7 (10)
C10A	29.0 (11)	25.1 (13)	21.4 (9)	-1.4 (9)	1.2 (8)	0.3 (10)
C11A	29.1 (11)	29.2 (14)	26.3 (10)	-3.2 (10)	-0.8 (8)	-4.9 (10)
C12A	43.7 (14)	20.7 (13)	26.2 (10)	-4.3 (9)	3.3 (9)	-7.3 (10)
C13A	43.7 (13)	20.1 (12)	27.3 (11)	-1.9 (9)	6.1 (9)	-6.4 (10)
C14A	41.6 (13)	25.0 (13)	22.8 (10)	0.7 (9)	0.8 (9)	6.6 (11)

Table 4 Bond Lengths for don2c.

Atom	Atom	Length/Å	Atom	Atom	Length/Å
O1	C4	1.378 (2)	O1A	C4A	1.374 (3)
O2	C14	1.445 (3)	O2A	C14A	1.429 (3)
C1	C2	1.399 (3)	C1A	C2A	1.400 (3)
C1	C6	1.399 (3)	C1A	C6A	1.390 (3)
C1	C7	1.516 (3)	C1A	C7A	1.519 (3)
C2	C3	1.394 (3)	C2A	C3A	1.395 (3)
C3	C4	1.392 (3)	C3A	C4A	1.389 (3)
C4	C5	1.394 (3)	C4A	C5A	1.394 (3)
C5	C6	1.391 (3)	C5A	C6A	1.395 (3)
C7	C8	1.541 (3)	C7A	C8A	1.549 (3)
C7	C13	1.542 (3)	C7A	C13A	1.535 (3)
C8	C9	1.539 (3)	C8A	C9A	1.529 (3)
C9	C10	1.542 (3)	C9A	C10A	1.547 (3)
C10	C11	1.532 (3)	C10A	C11A	1.533 (3)
C10	C14	1.528 (3)	C10A	C14A	1.526 (3)
C11	C12	1.529 (3)	C11A	C12A	1.537 (4)
C12	C13	1.530 (3)	C12A	C13A	1.533 (3)

Table 5 Bond Angles for don2c.

Atom	Atom	Atom	Angle/°	Atom	Atom	Atom	Angle/°
C2	C1	C6	117.27 (19)	C2A	C1A	C7A	122.69 (18)
C2	C1	C7	121.2 (2)	C6A	C1A	C2A	118.0 (2)
C6	C1	C7	121.6 (2)	C6A	C1A	C7A	119.3 (2)
C3	C2	C1	121.4 (2)	C3A	C2A	C1A	120.51 (19)
C4	C3	C2	120.35 (19)	C4A	C3A	C2A	120.3 (2)
O1	C4	C3	122.08 (19)	O1A	C4A	C3A	117.7 (2)
O1	C4	C5	118.74 (19)	O1A	C4A	C5A	122.00 (19)
C3	C4	C5	119.17 (19)	C3A	C4A	C5A	120.2 (2)
C6	C5	C4	119.9 (2)	C4A	C5A	C6A	118.6 (2)
C5	C6	C1	121.9 (2)	C1A	C6A	C5A	122.3 (2)
C1	C7	C8	110.28 (19)	C1A	C7A	C8A	110.80 (19)
C1	C7	C13	109.68 (18)	C1A	C7A	C13A	111.45 (19)
C8	C7	C13	111.50 (19)	C13A	C7A	C8A	113.69 (19)
C9	C8	C7	116.41 (19)	C9A	C8A	C7A	113.0 (2)
C8	C9	C10	117.8 (2)	C8A	C9A	C10A	118.4 (2)
C11	C10	C9	114.86 (19)	C11A	C10A	C9A	115.93 (19)
C14	C10	C9	108.95 (19)	C14A	C10A	C9A	108.4 (2)
C14	C10	C11	110.07 (18)	C14A	C10A	C11A	110.43 (19)

C12	C11	C10	112.95 (19)	C10A C11A C12A	114.32 (19)
C11	C12	C13	117.2 (2)	C13A C12A C11A	114.6 (2)
C12	C13	C7	117.11 (19)	C12A C13A C7A	115.3 (2)
O2	C14	C10	112.46 (18)	O2A C14A C10A	113.1 (2)

Table 6 Hydrogen Bonds for don2c.

D	H	A	d(D-H)/Å	d(H-A)/Å	d(D-A)/Å	D-H-A/°
O1	H1	O2A ¹	0.90 (4)	1.74 (4)	2.632 (2)	172 (3)
O2	H2	O1 ²	0.91 (4)	2.08 (4)	2.955 (2)	161 (4)
O1A	H1A	O2 ³	0.79 (4)	1.91 (4)	2.698 (2)	172 (5)
O2A	H2A	O1A ⁴	0.80 (4)	1.96 (5)	2.763 (3)	177 (4)

¹1+X,+Y,1+Z; ²1-X,-1/2+Y,1-Z; ³+X,+Y,1+Z; ⁴+X,+Y,-1+Z

Table 7 Torsion Angles for don2c.

A	B	C	D	Angle/°	A	B	C	D	Angle/°
O1	C4	C5	C6	179.0 (2)	O1A	C4A	C5A	C6A	-179.9 (2)
C1	C2	C3	C4	0.3 (4)	C1A	C2A	C3A	C4A	0.3 (4)
C1	C7	C8	C9	152.3 (2)	C1A	C7A	C8A	C9A	153.47 (19)
C1	C7	C13	C12	-171.6 (2)	C1A	C7A	C13A	C12A	-175.2 (2)
C2	C1	C6	C5	-1.0 (3)	C2A	C1A	C6A	C5A	0.8 (4)
C2	C1	C7	C8	51.7 (3)	C2A	C1A	C7A	C8A	77.9 (3)
C2	C1	C7	C13	-71.5 (3)	C2A	C1A	C7A	C13A	-49.8 (3)
C2	C3	C4	O1	-179.5 (2)	C2A	C3A	C4A	O1A	179.8 (2)
C2	C3	C4	C5	-0.6 (3)	C2A	C3A	C4A	C5A	0.6 (4)
C3	C4	C5	C6	0.0 (3)	C3A	C4A	C5A	C6A	-0.7 (4)
C4	C5	C6	C1	0.8 (4)	C4A	C5A	C6A	C1A	0.0 (4)
C6	C1	C2	C3	0.4 (4)	C6A	C1A	C2A	C3A	-0.9 (4)
C6	C1	C7	C8	-128.5 (2)	C6A	C1A	C7A	C8A	-100.5 (3)
C6	C1	C7	C13	108.4 (2)	C6A	C1A	C7A	C13A	131.8 (3)
C7	C1	C2	C3	-179.7 (2)	C7A	C1A	C2A	C3A	-179.3 (2)
C7	C1	C6	C5	179.1 (2)	C7A	C1A	C6A	C5A	179.2 (2)
C7	C8	C9	C10	46.8 (3)	C7A	C8A	C9A	C10A	77.8 (3)
C8	C7	C13	C12	65.9 (3)	C8A	C7A	C13A	C12A	58.7 (3)
C8	C9	C10	C11	31.0 (3)	C8A	C9A	C10A	C11A	-15.9 (3)
C8	C9	C10	C14	155.0 (2)	C8A	C9A	C10A	C14A	108.9 (3)
C9	C10	C11	C12	-83.0 (2)	C9A	C10A	C11A	C12A	-57.1 (3)
C9	C10	C14	O2	60.0 (2)	C9A	C10A	C14A	O2A	175.8 (2)
C10	C11	C12	C13	74.1 (3)	C10A	C11A	C12A	C13A	87.4 (3)

C11C10C14O2	173.22 (18)	⁻ C11AC10AC14AO2A	-56.2 (3)
C11C12C13C7	-54.2 (3)	C11AC12AC13AC7A	-66.4 (3)
C13C7 C8 C9	-85.6 (3)	C13AC7A C8A C9A	-80.1 (3)
C14C10C11C12	153.6 (2)	C14AC10AC11AC12A	179.2 (2)

Table 8 Hydrogen Atom Coordinates ($\text{\AA}\times 10^4$) and Isotropic Displacement Parameters ($\text{\AA}^2\times 10^3$) for don2c.

Atom	x	y	z	U(eq)
H1	6860 (40)	5540 (40)	8760 (30)	39 (9)
H2	3360 (40)	2640 (40)	530 (30)	48 (10)
H2A	6966	5915	5147	28
H3	7621	5966	7104	29
H5	3621	5834	7269	28
H6	2977	5818	5314	28
H7	3469	5619	3514	26
H8A	6145	5059	3200	34
H8B	5441	3989	3844	34
H9A	3787	3510	2282	31
H9B	5194	3539	1879	31
H10	2916	5235	1250	27
H11A	5617	6229	1440	32
H11B	4415	6744	434	32
H12A	3173	7386	1844	34
H12B	4483	8262	1802	34
H13A	4330	7850	3661	32
H13B	5741	7319	3432	32
H14A	3400	4972	-556	30
H14B	4734	4127	-8	30
H1A	1180 (40)	3290 (50)	8980 (40)	61 (12)
H2AB	-970 (40)	4420 (50)	-830 (30)	59 (12)
H2AA	-1831	3365	5084	31
H3A	-1682	3458	7021	31
H5A	2473	3251	7607	30
H6A	2305	3150	5669	30
H7A	1124	2884	3851	29
H8AA	-1031	4762	3190	29
H8AB	400	5235	3963	29
H9AA	1481	4322	2521	33
H9AB	677	5679	2233	33

H10A	417	3671	874	31
H11C	-1810	2815	556	35
H11D	-2096	3594	1617	35
H12C	-1457	1178	1797	37
H12D	77	1724	2000	37
H13C	-625	1295	3713	37
H13D	-1767	2416	3388	37
H14C	-1517	5764	797	37
H14D	-115	5881	382	37

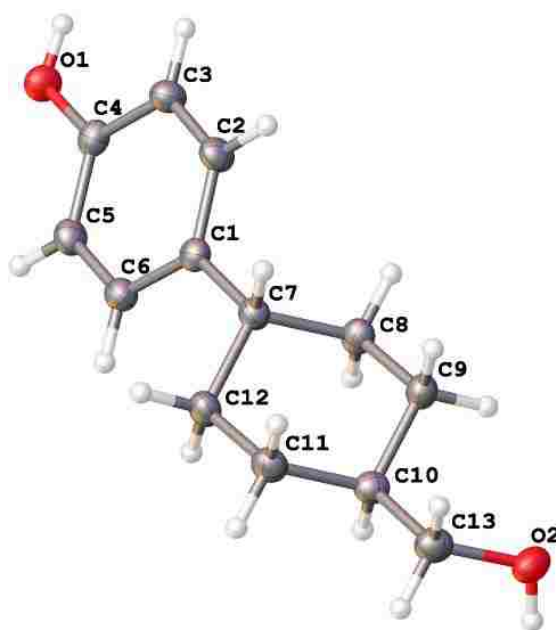


Table 1 Crystal data and structure refinement for ISP358-2.

Identification code	ISP358-2 (don2f)
Empirical formula	C ₁₃ H ₁₈ O ₂
Formula weight	206.27
Temperature/K	100.00(10)
Crystal system	orthorhombic
Space group	Pbca
a/Å	12.0669(2)
b/Å	8.09601(18)
c/Å	22.4321(4)
α/°	90.00
β/°	90.00
γ/°	90.00
Volume/Å ³	2191.46(7)
Z	8
ρ _{calc} /cm ³	1.250
μ/mm ⁻¹	0.653
F(000)	896.0
Crystal size/mm ³	0.25 × 0.15 × 0.01
Radiation	Cu Kα (λ = 1.54184)
2θ range for data collection/°	7.88 to 148.36
Index ranges	-10 ≤ h ≤ 14, -9 ≤ k ≤ 8, -19 ≤ l ≤ 27
Reflections collected	9115
Independent reflections	2181 [R _{int} = 0.0318, R _{sigma} = 0.0235]

Data/restraints/parameters 2181/0/138
 Goodness-of-fit on F^2 1.043
 Final R indexes [$I \geq 2\sigma(I)$] $R_1 = 0.0414$, $wR_2 = 0.1109$
 Final R indexes [all data] $R_1 = 0.0503$, $wR_2 = 0.1190$
 Largest diff. peak/hole / $e \text{ \AA}^{-3}$ 0.23/-0.20

Table 2 Fractional Atomic Coordinates ($\times 10^4$) and Equivalent Isotropic Displacement Parameters ($\text{\AA}^2 \times 10^3$) for don2f. U_{eq} is defined as 1/3 of the trace of the orthogonalised U_{ij} tensor.

Atom	x	y	z	U(eq)
O1	6398.2 (8)	5568.4 (12)	5152.2 (4)	27.0 (2)
O2	6894.3 (8)	2635.2 (13)	9776.1 (4)	30.9 (3)
C1	6163.1 (10)	5414.5 (15)	7017.2 (5)	21.2 (3)
C2	6978.5 (11)	6355.0 (17)	6734.5 (6)	25.2 (3)
C3	7075.8 (11)	6425.1 (17)	6119.5 (6)	25.5 (3)
C4	6335.5 (11)	5541.8 (15)	5766.6 (6)	22.5 (3)
C5	5517.3 (11)	4598.7 (16)	6031.9 (6)	24.9 (3)
C6	5437.1 (11)	4537.3 (16)	6652.7 (6)	24.0 (3)
C7	6135.1 (10)	5371.5 (15)	7694.9 (5)	21.4 (3)
C8	7066.4 (11)	4283.3 (17)	7941.1 (6)	24.6 (3)
C9	7105.2 (11)	4268.6 (17)	8619.6 (5)	23.8 (3)
C10	5996.7 (11)	3692.7 (16)	8874.8 (6)	23.5 (3)
C11	5066.9 (11)	4813.0 (18)	8648.1 (6)	26.6 (3)
C12	5026.6 (10)	4848.1 (18)	7965.8 (6)	25.7 (3)
C13	6009.6 (12)	3638.7 (18)	9550.2 (6)	28.0 (3)

Table 3 Anisotropic Displacement Parameters ($\text{\AA}^2 \times 10^3$) for don2f. The Anisotropic displacement factor exponent takes the form: $-2\pi^2[h^2a^2U_{11}+2hka*b*U_{12}+...]$.

Atom	U_{11}	U_{22}	U_{33}	U_{23}	U_{13}	U_{12}
O1	30.6 (5)	30.7 (5)	19.9 (5)	-1.3 (4)	-0.7 (4)	-3.2 (4)
O2	37.5 (6)	28.1 (5)	27.0 (5)	5.6 (4)	-5.5 (4)	-3.4 (4)
C1	20.6 (6)	20.6 (6)	22.4 (6)	-0.1 (5)	-0.7 (5)	2.8 (5)
C2	24.5 (6)	27.4 (7)	23.7 (7)	-2.7 (5)	-2.6 (5)	-5.7 (5)
C3	25.5 (6)	26.7 (7)	24.4 (7)	0.5 (5)	1.3 (5)	-4.5 (5)
C4	25.0 (6)	22.4 (6)	20.0 (6)	-1.6 (5)	-1.5 (5)	4.8 (5)
C5	25.0 (7)	23.8 (6)	26.1 (7)	-2.6 (5)	-4.4 (5)	-1.7 (5)
C6	22.1 (6)	23.7 (6)	26.1 (7)	1.1 (5)	-0.9 (5)	-1.3 (5)
C7	20.0 (6)	22.9 (6)	21.2 (6)	-0.1 (5)	-0.7 (5)	-1.3 (5)
C8	21.9 (6)	29.4 (7)	22.6 (6)	1.0 (5)	2.4 (5)	4.0 (5)

C9	22.7 (6)	26.6 (7)	22.1 (6)	1.8 (5)	-1.7 (5)	1.8 (5)
C10	26.2 (7)	22.2 (6)	22.2 (6)	-0.7 (5)	0.4 (5)	-2.5 (5)
C11	22.9 (7)	31.3 (7)	25.5 (7)	0.9 (5)	3.4 (5)	-0.7 (5)
C12	19.7 (6)	32.2 (7)	25.1 (7)	1.5 (5)	-0.5 (5)	-0.4 (5)
C13	30.4 (7)	29.3 (7)	24.1 (7)	0.5 (5)	1.4 (5)	-2.6 (6)

Table 4 Bond Lengths for don2f.

Atom	Atom	Length/Å	Atom	Atom	Length/Å
O1	C4	1.3805 (15)	C5	C6	1.3967 (18)
O2	C13	1.4340 (17)	C7	C8	1.5310 (17)
C1	C2	1.3964 (18)	C7	C12	1.5291 (17)
C1	C6	1.3931 (18)	C8	C9	1.5226 (17)
C1	C7	1.5209 (16)	C9	C10	1.5279 (18)
C2	C3	1.3858 (18)	C10	C11	1.5297 (18)
C3	C4	1.3915 (18)	C10	C13	1.5159 (17)
C4	C5	1.3827 (19)	C11	C12	1.5315 (17)

Table 5 Bond Angles for don2f.

Atom	Atom	Atom	Angle/°	Atom	Atom	Atom	Angle/°
C2	C1	C7	118.82 (11)	C1	C7	C12	115.03 (11)
C6	C1	C2	117.03 (12)	C12	C7	C8	109.83 (10)
C6	C1	C7	124.13 (12)	C9	C8	C7	112.81 (10)
C3	C2	C1	122.29 (12)	C8	C9	C10	110.49 (11)
C2	C3	C4	119.40 (12)	C9	C10	C11	109.67 (11)
O1	C4	C3	121.65 (12)	C13	C10	C9	111.98 (11)
O1	C4	C5	118.52 (11)	C13	C10	C11	110.91 (11)
C5	C4	C3	119.83 (12)	C10	C11	C12	111.50 (11)
C4	C5	C6	119.88 (12)	C7	C12	C11	111.99 (11)
C1	C6	C5	121.57 (12)	O2	C13	C10	112.15 (11)
C1	C7	C8	110.94 (10)				

Table 6 Hydrogen Bonds for don2f.

D	H	A	d(D-H)/Å	d(H-A)/Å	d(D-A)/Å	D-H-A/°
O1	H1	O2 ¹	0.84	1.82	2.6594 (14)	172.7
O2	H2	O1 ²	0.84	1.97	2.7924 (14)	165.1

¹3/2-X,1-Y,-1/2+Z; ²X,1/2-Y,1/2+Z

Table 7 Hydrogen Atom Coordinates ($\text{\AA}\times 10^4$) and Isotropic Displacement Parameters ($\text{\AA}^2\times 10^3$) for don2f.

Atom	<i>x</i>	<i>y</i>	<i>z</i>	U(eq)
H1	6910	6208	5046	41
H2	6660	1674	9839	46
H2A	7484	6968	6972	30
H3	7643	7070	5940	31
H5	5011	3994	5792	30
H6	4874	3882	6830	29
H7	6284	6522	7836	26
H8A	6962	3139	7796	30
H8B	7785	4688	7786	30
H9A	7274	5393	8768	29
H9B	7702	3519	8755	29
H10	5852	2549	8726	28
H11A	5184	5948	8800	32
H11B	4348	4412	8804	32
H12A	4828	3736	7816	31
H12B	4442	5627	7836	31
H13A	6090	4776	9707	34
H13B	5294	3195	9695	34

VITA

Karannagoda Liyanage Iresha Sampathi Perera was born in Colombo, Sri Lanka. She received her primary and secondary education at Anula Vidyalaya, Colombo. She entered the University of Colombo to study Physical Sciences in year 2004 and was selected for a Major in chemistry in 2006. She received her Bachelor of Science degree majoring in chemistry in 2008 with honors. After working for one year as a teaching assistant at the Department of Chemistry of University of Colombo, she enrolled in the master's program in the Department of Chemistry at Louisiana State University in fall 2009. She completed her master's degree in summer 2012 in Analytical and Material chemistry under Prof. Robin L. McCarley. In the Fall of 2012, she was accepted to the doctoral program at Department of Chemistry in Marquette University. In spring 2014 she joined to Prof. William Donaldson's research group and involved in Medicinal chemistry research. She is currently a candidate for the Doctor of Philosophy in Organic and Medicinal chemistry, which will be awarded to her at the Summer 2017 Commencement at Marquette University in Milwaukee Wisconsin.

